# Interim Draft Report

## METEOROLOGICAL MODELING

## Development of Base Case Photochemical Modeling to Address 1-Hour and 8-Hour Ozone Attainment in the Dallas/Fort Worth Area

Prepared for

Texas Commission on Environmental Quality
12118 Park 35 Circle
Austin, Texas 78753

Prepared by

ENVIRON International Corporation
101 Rowland Way, Suite 220
Novato, CA

June 30, 2003

# TABLE OF CONTENTS



## APPENDICES



## TABLES

## FIGURES

# EXECUTIVE SUMMARY

This report describes meteorological modeling for the Dallas/Fort Worth (DFW) 4-county nonattainment area. Meteorological modeling was performed to support air quality modeling with the goals of developing ozone control strategies and demonstrating attainment of the 1-hour and 8-hour standard in the DFW area.

The Fifth Generation NCAR/Penn State Mesoscale Model (MM5) version 3.6 was used to simulate the August 13-22, 1999 episode. The grid configuration includes four two-way nested grids with the 4-km grid spacing covering the DFW 4-county nonattainment area. The 36-km and 12-km grids are sufficiently large to better simulate the dominant regional and local flow and weather patterns, thus to address more properly the multi-day transport of ozone and precursors from significant source areas outside of Texas. Unlike the previous modeling practices (with one-way nesting for the finest grid), all four grids were utilized with two-way nesting. We think that two-way nesting can better represent the interaction between the finest grid and outer domains. The boundary inconsistency can also be restricted.

The quality of meteorological simulations plays a crucial role in determining the accuracy of air quality modeling. Thus, the statistical and qualitative evaluations were conducted to carefully assess the performance of MM5 model results. The results from four configured MM5 runs focusing DFW area during August 13-22, 1999 are presented in this report. The MM5 model results of wind, temperature and humidity from all runs in this study showed rather good performance in replicating the large- and meso-scale meteorology in the DFW area. The overall pressure and flow patterns covering south central U.S. and the placement of clouds and precipitations were replicated well. Statistical results on the 12-km grid suggest better performance overall than on the 4-km grid, but this is partially due to the small number of prediction-observation pairings on the 4-km grid, which permits a larger contribution to hourly "noise" (i.e., stochastic fluctuation). Some noted features about the results of four runs are summarized as follows:

- The performance for wind speed and direction is rather good in all four runs with the best performance in Run3. The hourly and daily statistical results for wind show that smaller prediction-observation bias, no "spike" abnormity during August 15-16, and overall better performance parameters (such as RMSE and IOA) in Run3. The simulated vertical wind profiles from Rub3 are also better matched with the 12-hourly sounding at Dallas Fort Worth.

- A slight under-prediction of humidity on the 4-km grid during almost the whole episode remains throughout all runs. But the humidity bias in Run1a is much smaller comparing to those of other runs. In fact, Run1a is the only one that meets benchmark standard in all three categories (RMSE, Bias, and IOA) for the daily statistics at 4-km grid.

- The temperature performances on the 4km and 12-km grid for all runs are pretty good with the replication of the observed diurnal variation. The amplitude of diurnal change of Run3 and Run1 on the 4-km domain are well reproduced, while the daytime maximum temperatures in Run2 are slightly over predicted. The strength of the diurnal variation in Run1a is relatively weaker, that is, the daytime maximum are relative lower than the observed and the nighttime minimum temperatures are slightly over estimated.

Comparing the results from all four runs, the MM5 Run3 is recommended for the photochemical modeling of the Dallas Forth Worth Area. In Run3, the wind performance is the best among the all four runs. From previous CAMx and other photochemical modeling experience, the performance of wind direction and speed is proved to be essential to the air quality modeling. The overall performance of temperature and humidity in Run3 is comparable or better than the other runs, except that the humidity performance of Run1a is the best among all runs. Therefore, we believe that Run3 is our best choice and Run1a is also usable given its best performance in humidity and acceptable performance in wind and temperature.

A brief introduction is given in Section 1. In Section 2, the MM5 model configuration, data sources, and the model horizontal and vertical structure definitions are described. The results from Run3 are discussed in details in Section 3. Then the conclusion is presented in Section 4.

# 1. INTRODUCTION

## BACKGROUND

The US Environmental Protection Agency (EPA) currently enforces a 1-hour ozone National Ambient Air Quality Standard (NAAQS) that simply stated, says no monitor can measure more than three exceedances (0.12 ppm or 124 ppb) in a three-year period. With complete data capture compliance with the 1-hour ozone NAAQS requires that the fourth highest daily maximum 1-hour ozone concentration in three years at every ozone monitor in the area be less than or equal to 0.12 ppm. However, the standard is defined in terms of an expected exceedance rate (to compensate for inadequate data capture) which allows no more than one expected exceedance per year calculated over three consecutive years. Areas that have more than three exceedances violate the 1-hour ozone NAAQS and are classified as ozone nonattainment areas. Ozone nonattainment areas must develop an ozone emissions control plan and demonstrate that they will attain the ozone NAAQS by the date specified in the Clean Air Act Amendments (CAAA) in a State Implementation Plan (SIP). The SIP ozone attainment demonstration is usually accomplished using air quality modeling.

In 1997, EPA promulgated a new ozone NAAQS that is potentially much more stringent than the old 1-hour standard. The new form is based on ozone measurements averaged over eight hours; violations of the 8-hour ozone standard occur when the fourth highest 8-hour ozone concentration each year, averaged over three consecutive years, at an individual monitor exceeds 0.08 ppm (84 ppb). The actual nonattainment designations are likely to be based on ambient measurements taken during the three years between 2001-2003. Regions that are currently designated as nonattainment of the 1-hour ozone NAAQS must still attain the 1-hour standard (i.e., have three consecutive years over which the fourth highest hourly ozone concentrations at all monitors are 124 ppb or less). Once an ozone nonattainment region attains the 1-hour ozone NAAQS, then the 1-hour standard can be revoked by EPA and the area would be required to meet only the 8-hour standard.

On May 14, 1999, the D.C. District Court declared that EPA exceeded their authority in setting the 8-hour ozone standard and remanded it back to EPA. EPA appealed the decision to the US Supreme Court who upheld the new 8-hour ozone standard in February 2001 but remanded implementation issues back to the lower court. The lower court issued a ruling in March 2002 that required EPA to develop a new 8-hour ozone implementation approach and EPA plans to propose such an implementation rulemaking soon. Although EPA has not officially proposed a new implementation schedule, it would likely require states to recommend to EPA their 8-hour ozone nonattainment areas and boundaries by mid-2003. EPA would likely then make 8-hour ozone nonattainment designations by April 2004 based on 2001-2003 ambient air quality data.

## OBJECTIVES

In order for Dallas/Fort Worth (DFW) and the state of Texas to develop 1-hour and 8-hour ozone plans by 2004, new emissions and photochemical modeling databases need to be developed quickly. This interim report describes the meteorological modeling, one of the key procedures in developing the new photochemical modeling database for the DFW area. In this study, the Fifth Generation NCAR/Penn State Mesoscale Model (MM5) version 3.6 was used to simulate the August 13-22, 1999 episode. The grid configuration includes four two-way nested grids with the 4-km grid spacing covering the DFW 4-county nonattainment area. The 36-km and 12-km grids are sufficiently large to better simulate the dominant regional and local flow and weather patterns, thus to address more properly the multi-day transport of ozone and precursors from significant source areas outside of Texas.

In Section two of this report, the MM5 model configuration (including physics and FDDA), initial data sources, and the MM5 horizontal and vertical grid definitions are described. The MM5 model results and performance evaluation are discussed in detail in Section 3. Ancillary graphical presentations are grouped in Appendix A, B and C.

# 2. MODEL CONFIGURATION

ENVIRON has conducted a series of meteorological modeling runs of an August 1999 episode for northeast Texas (Emery et al 2002, 2003) using the 5th Generation PSU/NCAR Mesoscale Model (MM5). From this MM5 meteorological modeling we have learned that:

1. The use of three-hourly EDAS (NCEP Eta Data Assimilation System) Analysis data instead of the Initialization data for developing initial/boundary conditions and inputs for the MM5 Four-Dimensional Data Assimilation (FDDA) package has proven to be more beneficial to the MM5 modeling. Although the EDAS Initialization data may be more dynamically balanced via pre-forecast spinup cycles of the Eta model, they can deviate from observed conditions due to the numerical errors of Eta model simulation. The EDAS Analysis data are generated strictly by diagnostic objective analysis procedures so they more faithfully reflect the meteorological observations. Currently, the EDAS Analysis data are widely used by the MM5 community and are recommended for use by the NCAR Data Support Section.
2. An expanded regional-scale 36-km grid can better simulate the dominant synoptic scale flow and pressure patterns and eliminate boundary effects in the finer resolution domains (12/4 km grids). This results in improved meteorological fields for the 12-km and 4-km grids.
3. Incorporation of routine surface and upper air station observation data obtained from NCAR archives can improve the EDAS analysis fields by better characterizing the mesoscale and local meteorological features.
4. A more sophisticated Pleim-Xiu Land Surface Model, which replaces the simple Five-layer Soil model, results in MM5 meteorological model estimates that better match the observed values.

Combing the knowledge we have gained from previous studies with analyses of the Dallas Fort Worth (DFW) August 1999 episode, we have developed the model configurations described below.

## HORIZONTAL AND VERTICAL GRID DEFINITION

The MM5 grids for the Texas DFW application are displayed in Figure 2-1. The four-domain nested mesh with 108/36/12/4-km resolutions was adopted. The coarse domain spans 53 by 43 grid points with a resolution of 108-km covering the continental United States. The coverage of 36-km grid is 85 by 61 grids (3024 km east-west by 2160 km north-south); the 12-km resolution domain has 100 by 100 grid points; and the 4-km-resolution domain covers Dallas Fort Worth area with 85 by 76 grid points.

In the vertical, the MM5 is configured to run with 28 layers, with a minimum surface layer depth of ~20m. Ten layers resolve the typical depth of the daytime boundary layer. The model extends to a pressure altitude of 50 mb (~20-km). The vertical structure is shown on Table 2-1. A subset of layers is used for CAMx vertical grid structure (shown on the right side of the table matching the height figures in bold). More recently, discussions among the MM5 community are tending toward using higher resolution (more than 30 layers) in the vertical direction. In recent tests with MM5 applied to the Texas Near Nonattainment Areas (and elsewhere), we investigated the impact of using 40 layers in MM5 as opposed to the 28 used in many previous simulations. The effects of this change were so minimal that we do not believe that significantly more layers is critical for ozone modeling in Texas. We suggest that adding more vertical levels might be considered for future model applications depending upon issues associated with topography and mesoscale forcings. However, 28 vertical layers were considered sufficient for the MM5 modeling of the DFW region.

**Table 2-1.** MM5 vertical grid structure based on 28 sigma-p levels. Heights (m) are above sea level according to a standard atmosphere; pressure is in millibars.

| k | sigma | pressure | height | thickness | CAMx Layers |
|---|---|---|---|---|---|
| 28 | 0.0000 | 50.00 | 18874.41 | 1706.76 | |
| 27 | 0.0250 | 73.75 | 17167.65 | 1362.47 | |
| 26 | 0.0500 | 97.50 | 15805.17 | 2133.42 | |
| 25 | 0.1000 | 145.00 | 13671.75 | 1664.35 | |
| 24 | 0.1500 | 192.50 | 12007.40 | 1376.75 | |
| 23 | 0.2000 | 240.00 | 10630.65 | 1180.35 | |
| 22 | 0.2500 | 287.50 | 9450.30 | 1036.79 | |
| 21 | 0.3000 | 335.00 | 8413.52 | 926.80 | |
| 20 | 0.3500 | 382.50 | 7486.72 | 839.57 | |
| 19 | 0.4000 | 430.00 | 6647.15 | 768.53 | |
| 18 | 0.4500 | 477.50 | 5878.62 | 709.45 | |
| 17 | 0.5000 | 525.00 | 5169.17 | 659.47 | |
| 16 | 0.5500 | 572.50 | 4509.70 | 616.58 | |
| 15 | 0.6000 | 620.00 | **3893.12** | 579.34 | --15--- |
| 14 | 0.6500 | 667.50 | **3313.78** | 546.67 | --14--- |
| 13 | 0.7000 | 715.00 | **2767.11** | 517.77 | --13--- |
| 12 | 0.7500 | 762.50 | **2249.35** | 491.99 | --12--- |
| 11 | 0.8000 | 810.00 | **1757.36** | 376.81 | --11--- |
| 10 | 0.8400 | 848.00 | **1380.55** | 273.60 | --10--- |
| 9 | 0.8700 | 876.50 | **1106.95** | 266.37 | ---9--- |
| 8 | 0.9000 | 905.00 | **840.58** | 259.54 | ---8--- |
| 7 | 0.9300 | 933.50 | **581.04** | 169.41 | ---7--- |
| 6 | 0.9500 | 952.50 | **411.63** | 166.65 | ---6--- |
| 5 | 0.9700 | 971.50 | **244.98** | 82.31 | ---5--- |
| 4 | 0.9800 | 981.00 | **162.67** | 65.38 | ---4--- |
| 3 | 0.9880 | 988.60 | **97.29** | 56.87 | ---3--- |
| 2 | 0.9950 | 995.25 | **40.43** | 20.23 | ---2--- |
| 1 | 0.9975 | 997.62 | **20.19** | 20.19 | ---1--- |
| 0 | 1.0000 | 1000.00 | 0.00 | | ============Surface====== |

## MODEL INPUT AND INITIALIZATION

In this MM5 meteorological model application, the Pleim-Xiu Land-Surface Model, which will be discussed in the section of Model Physics Configuration below, was employed. Therefore, additional datasets, such as soil and vegetation category, deep soil temperature and vegetation fraction, were needed and processed by the MM5 TERRAIN pre-processing program. These datasets are all archived at NCAR.

The EDAS Analysis fields were used as the first-guess initialization fields. Currently, the EDAS Analysis data are widely used by the MM5 community and are recommended by the NCAR Data Support Section.

To further enhance the mesoscale and localized meteorological features of the EDAS analysis initial input, surface and upper-air station meteorological observation data were obtained from NCAR/NCEP. The analysis fields were improved by blending these observation data into the analyses using the RAWINS program. This program not only improves the EDAS analysis data for 3D analysis nudging, but it also generates an additional dataset for each domain for 2-D surface analysis nudging. The surface analysis nudging will be discussed in detail in the section below.

## MODEL PHYSICS CONFIGURATION

Since the revised MM5 meteorological modeling for the northeast Texas (Emery et al 2003) is proved to be successful for the air quality simulations, such as the use of RRTM radiation scheme dramatically improved the nighttime and morning minimum temperature, we adopted most of the configurations from that study. The MM5 model physics configuration for the Texas DFW August 1999 episode application is summarized as follows:

- Simple-ice microphysics is employed for all domains
- Kain-Fritsch cumulus parameterization scheme is invoked for 108/36/12-km grids. No cumulus parameterization scheme is invoked for the 4-km domain as convection is explicitly fully resolved at this resolution scale.
- The RRTM radiation scheme is used for all the grids.
- Two-way interactive 108/36/12/4-km grids are used.

It was realized in the MM5 meteorological modeling study of an August 1999 episode for northeast Texas (Emery et al 2002, 2003) that the relatively simple MM5 “Five-Layer Soil Model” used previously does not adequately handle complex land-surface interaction processes, and that a more sophisticated Land-Surface Model (LSM) may be important for mesoscale meteorology modeling. Land-surface processes control the surface sensible and latent heat fluxes, which in turn strongly influence ground level air temperature, humidity and PBL development. As these parameters are especially critical for successful air pollution modeling, a more sophisticated LSM is used in this application. Currently, two new LSM models are available in MM5, the Oregon State University LSM and Pleim-Xiu LSM models, are available in the MM5 version 3.5. In the revised MM5 meteorological modeling for the northeast Texas (Emery et al 2003), the use of Pleim-Xiu LSM coupled with its own PBL scheme is proved to have the impact of dramatically different PBL depths, thus result in noticeable improvements in the air quality simulations. Therefore,

- The Pleim-Xiu LSM, coupled with its own (mandatory) Planetary Boundary Layer (PBL) scheme, was employed in this work. In the sensitivity Run 1 and Run 1a, the soil moisture nudging techniques in this scheme were also tested and the soil moisture was initialized by the EDAS data through REGRID program.

As mentioned previously, FDDA has proven to be a powerful tool to limit the growth of numerical errors in MM5 and its benefits are widely recognized in the air pollution modeling community. In order to compare the effects of different FDDA configurations and find the best performance simulation, 4 MM5 runs were designed to have the same physics but different FDDA configurations. The major differences between each run are summarized in Table 2-2.

**Table 2-2.** The major configuration differences between each run.

| | | Analysis Nudging (3D & SFC) Coefficient (*E-04) | | | | Obs Nudging Coefficient (*E-04) | | Modified Obs Nudging File | Soil Moisture Nudging |
|---|---|---|---|---|---|---|---|---|---|
| Run | | 108 | 36 | 12 | 4 | 12 | 4 | | |
| 1 | Wind | 4.0 | 2.5 | 1.0 | 1.0 | 10.0 | 10.0 | No | Yes |
| | Temp | 4.0 | 2.5 | 1.0 | 1.0 | 4.0 | 4.0 | | |
| | Humi | 0.1 | 0.1 | 0.1 | 0.1 | 4.0 | 4.0 | | |
| 1a | Wind | 4.0 | 2.5 | 1.0 | --- | 4.0 | 4.0 | Yes | Yes |
| | Temp | 4.0 | 2.5 | 1.0 | --- | --- | 4.0 | | |
| | Humi | 0.2 | 0.2 | 0.2 | --- | --- | 4.0 | | |
| 2 | Wind | 4.0 | 2.5 | 1.0 | --- | 5.0 | 5.0 | No | No |
| | Temp | 4.0 | 2.5 | 1.0 | --- | 5.0 | 5.0 | | |
| | Humi | 0.1 | 0.1 | 0.1 | --- | 5.0 | 5.0 | | |
| 3 | Wind | 4.0 | 2.5 | 1.0 | --- | 10.0 | 10.0 | No | No |
| | Temp | 4.0 | 2.5 | 1.0 | --- | --- | --- | | |
| | Humi | 0.1 | 0.1 | 0.1 | --- | --- | --- | | |

Starting with Run 1, the strongest FDDA configuration is designed. The surface and 3D analysis nudging of wind, temperature and humidity are employed on all four domains. The observation nudging of wind, temperature and humidity are turned on for the 12-km and 4-km grids with very strong nudging coefficient for wind. Soil moisture nudging is also used. Compared to Run 1, a relative weaker FDDA design is applied in Run 1a, with no surface and 3D analysis nudging on the 4 km domain, no observation nudging of temperature and humidity on 12 km grid, and weaker wind nudging on 12 km and 4 km domains. Also, part of the data (surface observations from AIRS stations) in the observation nudging file are withheld since a dense cluster of the observations in a small area (here DFW) might have disadvantageous effects on the FDDA nudging. The method of withholding (or "sequestering") portions of an observation data set for model verification is a common practice in model simulations with FDDA. In Run 2, no surface or 3D analysis nudging is used on the 4-km grid, nor is there any soil moisture nudging.

After reviewing the MM5 results of the above three runs, we found that the wind fields were relatively noisy. The observational nudging of moisture and temperature on the 4-km grid might have caused a surface heat budget imbalance, thus resulting in the abnormal fluctuations in wind performance. Therefore, observational nudging of moisture and temperature were removed in the Run 3 configuration. Following are the configurations of FDDA technique used in Run 3:

- FDDA analysis nudging on the 108/36/12-km grids:

  - o 3D analysis nudging above the boundary layer -- MM5 is nudged toward 3-hourly EDAS analysis of wind, temperature, and humidity, which are improved by the surface and upper-air station observation data.
  - o Surface analysis nudging within the boundary layer -- MM5 is nudged toward 3-hourly gridded surface analysis data generated by RAWINS program
- FDDA observation nudging of wind on the 12-km and 4-km grids from routine and special measurement data set available from NCAR that includes data from NOAA profiler, NWS Surface and Upper Air stations over most of the 12-km domain.

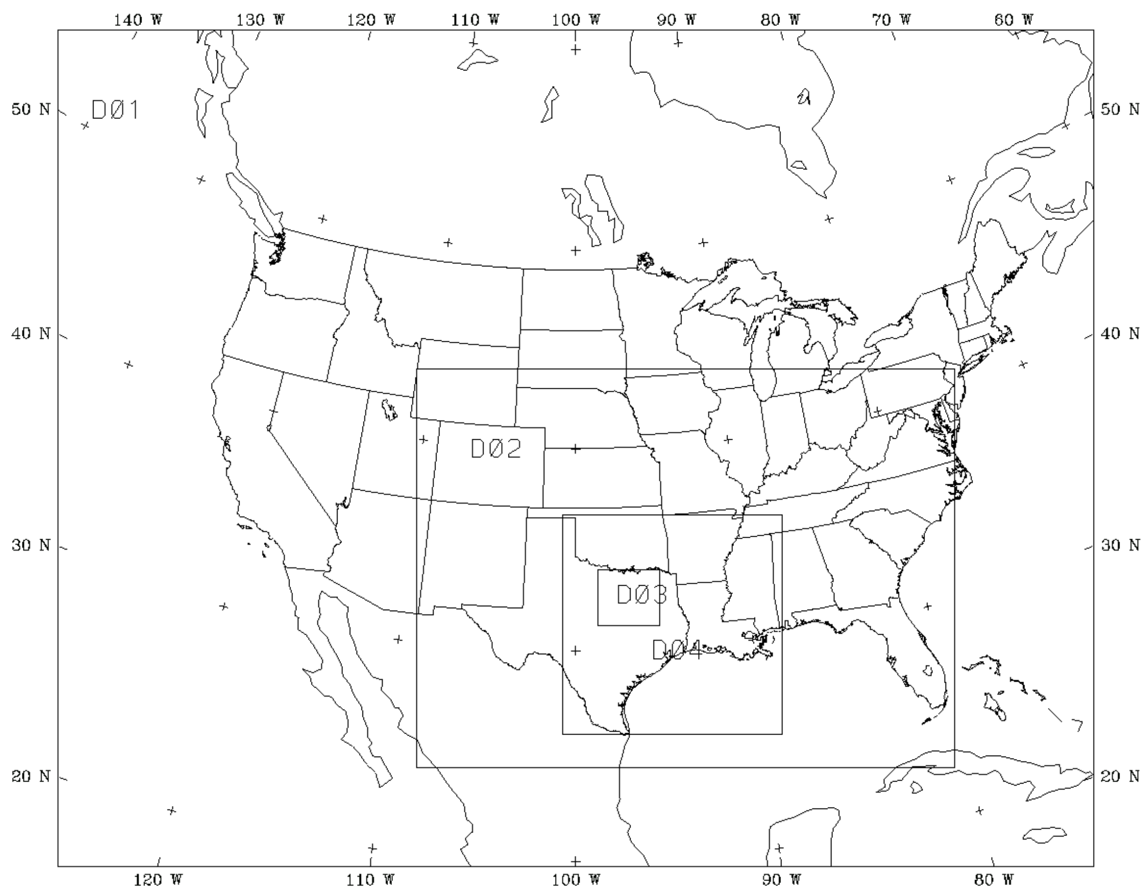


**Figure 2-1.** MM5 domain configuration (108/36/12/4-km) for the August 13 – 22, 1999 Texas Dallas Fort Worth episode.

# 3. MM5 APPLICATION AND RESULTS

The MM5 version 3.6 was used to simulate regional and local meteorology for the 13-22 August 1999 Episode in the Dallas Fort Worth Area. The model physics and FDDA configurations were discussed in Section 2. MM5 results from four simulations, especially results from Run 3, and comparisons between each run are presented in this section. Model performance is evaluated using quantitative analysis (statistical evaluation) and qualitative (graphical) review of surface and vertical profiles of wind, temperature, and humidity.

## STATISTICAL EVALUATION

A quantitative assessment of MM5 performance in replicating surface-level wind, temperature, and humidity is undertaken by calculating the statistical parameters (such as Bias, Gross error, RMSE, etc.) discussed in a 2001 study (Emery et al, 2001). Statistics are calculated for both hourly and daily time scales, and for the 12-km and 4-km grids. The meteorological observation data from NOAA profilers, NWS Surface and Upper Air stations, and other local stations are used to evaluate the model performance. There are about 133 observation stations in the 12-km domain and 18 stations in the 4-km domain. The site locations by station type in the 12-km and 4-km domains are displayed in Figure 3-1 and 3-2, respectively. Performance is discussed relative to the proposed statistical benchmarks developed in the Emery et al (2001) report.

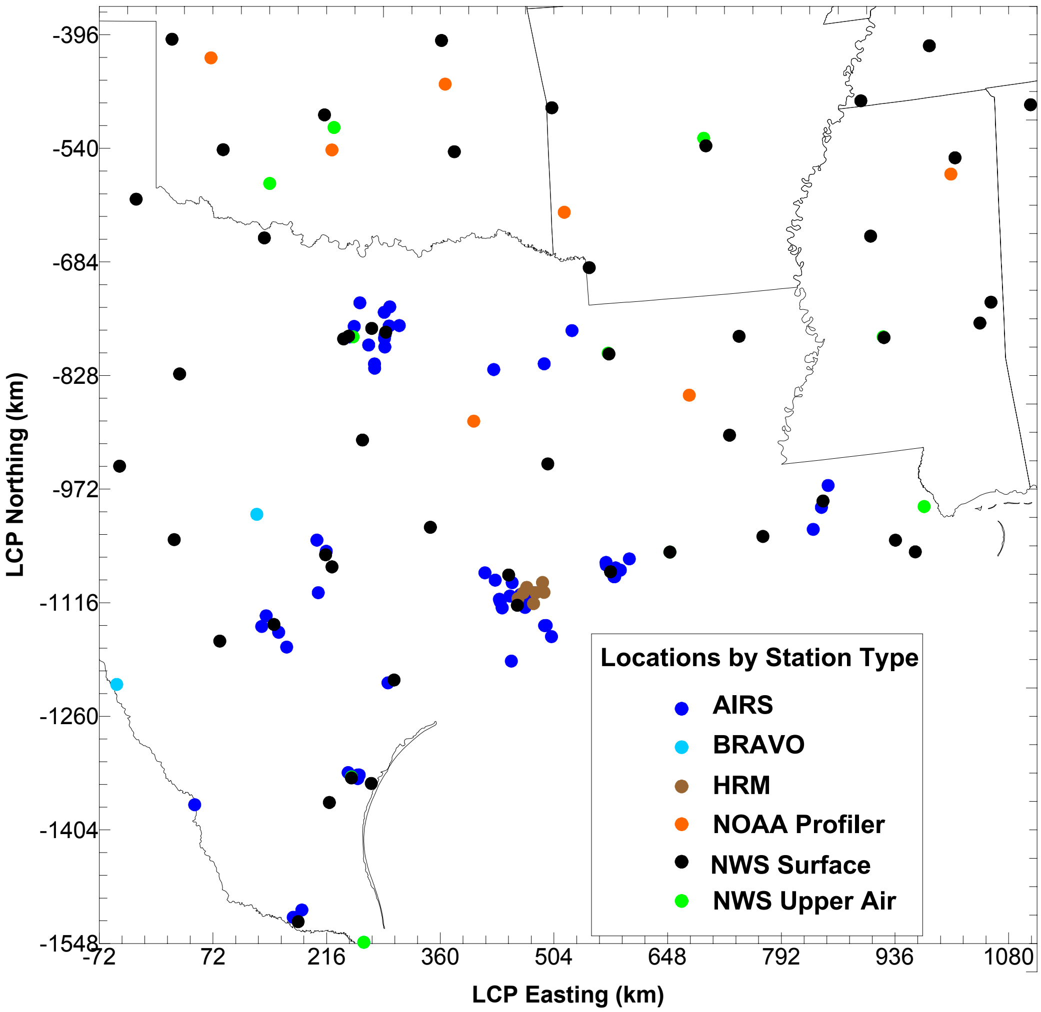


**Figure 3-1.** Locations of meteorological observation stations by station type.

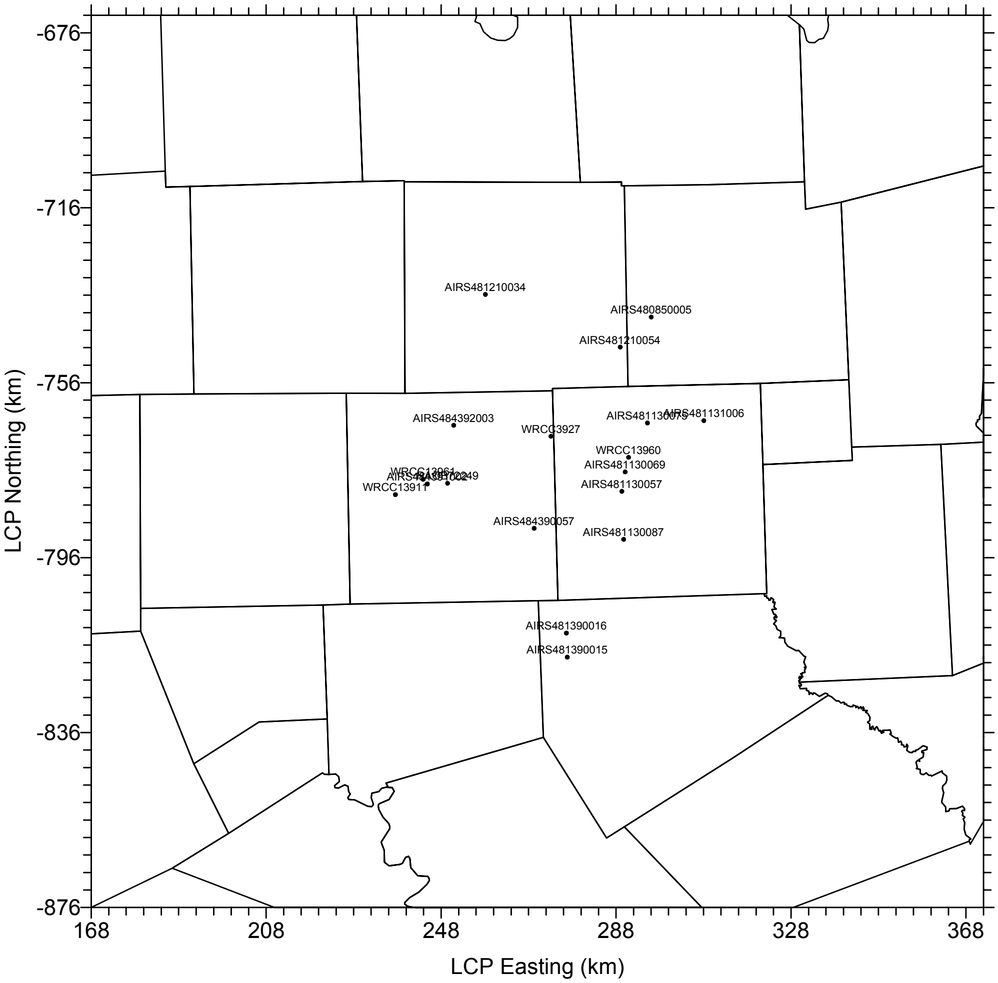


**Figure 3-2.** Locations of meteorological observation stations over the 4-km DFW area.

## Results on the 12-km Domain

### *Hourly Statistics*

Hourly statistical results for Run 3 on the 12-km grid are presented in Figure 3-3 for wind, temperature, and humidity. Starting with surface wind (Figure 3-3a), the diurnal variation of wind speed and the light wind conditions during the whole episode are replicated well, with the wind speed bias restricted between −1.0 m/s and 1.5 m/s. The slight over-prediction of the wind speeds, especially during the daytime, is dominant during the episode. The IOA for wind speed varies around 0.7, which is considered to be quite good. The wind direction is well simulated with bias within 30 degrees during all episode days.

The hourly temperature time series (Figure 3-3b) shows a nice agreement with observations. The diurnal variation and its amplitude of each are replicated pretty well. The nighttime temperatures are simulated better than during the daytime. The daily maximum temperatures are slightly over predicted. The IOA for temperature ranges around 0.8, which is very good.

The hourly humidity time series is displayed in Figure 3-3c. Though the humidity is under-estimated overall, the pattern and trend of the humidity change during the episode is well reproduced by the model. The IOA for humidity ranges from 0.5 to 0.9 with IOA around 0.8 during most of episode days.

Hourly statistical results for Run 1, Run 1a, and Run 2 on the 12-km grid are attached in Appendix A. Some noticeable features are summarized as follows:

1. Humidity is also under-estimated during the episode in Run2, as in Run 3, where the soil moisture nudging is not employed in both runs. The simulated dry condition is apparently a major cause for the over-prediction of daytime temperature.
2. In Run 1 and Run 1a, where soil moisture nudging is adopted, the model results for humidity are "mixed", with a relatively dominant over-prediction for Run 1a. As a result, the simulated temperatures in these two runs are lower than observations due to the wet conditions.
3. Wind directions in these three runs (Run 1, Run 1a, and Run 2) are reproduced pretty well as in Run 3. However, the wind speed biases in these three runs are abnormally higher during August 15 and 16. The reason for this remains unknown.

*Daily Statistics*

Daily statistics for Run 3 on the 12-km grid are presented in Figure 3-4 for wind, temperature, and humidity. Starting with the surface wind performance (Figure 3-4a), the trend for subsiding wind speed to August 18, and then subsequent increase is well replicated. The daily wind speed bias during all episode days is well within 0.5 m/s, the wind speed gross error is well below 1.5 m/s, and the RMSE is below 1.5 m/s. The systematic RMSE is lower and more consistent than the unsystematic one. The IOA of wind speed is consistently high during all episode days, ranging from 0.75 to 0.87. The predicted wind directions are in good agreement with the observed, except on August 19. The bias of wind direction is close to zero and the gross error is restricted well within 30 degrees.

The daily performance for temperature is shown in Figure 3-4b. The day-to-day trends throughout the episode are simulated well by MM5. The slight over-prediction is obvious during the whole episode. The unsystematic RMSE is more dominant while the systematic RMSE remains relatively low. The IOA ranges from 0.88 to 0.96.

The daily performance for humidity is shown in Figure 3-4c. MM5 under estimates the humidity consistently during this episode. The mean bias (-1.83 g/kg) and mean gross error (2.45 g/kg) are the only two parameters that do not meet the benchmark standard (summarized in Table 3-1). The systematic and unsystematic RMSE are comparable with no dominant component during the episode. The IOA of humidity remains fairly good with a mean of 0.83.

A comparison of the daily performance among all four runs (Run 3 and the three sensitivity runs) is displayed graphically in Figure 3-5. For wind (Figure 3-5a), the difference in bias and gross error between each run is relatively small with slightly higher errors in Run 2 during all episode days. The performance for wind direction in all runs is especially good, with wind direction bias restricted to within 15 degrees.

The performance for temperature and humidity among these runs is very interesting. The under-estimation of temperature (Figure 3-5b) from Run 1 and Run 1a, which have soil moisture nudging turned on, is noticeably larger than that from Run 2 and Run 3, which have no soil moisture nudging. As for humidity (Figure 3-5c), the smaller under-estimation (or even over-estimation) is obvious in Run 1 and Run 1a while the higher under-estimation occurs in Run2 and Run3. The soil moisture nudging in the MM5 model configuration does have a distinct impact on the simulation of temperature and humidity. The soil moisture nudging tends to bring more humidity into the surface air, thus resulting cooler surface layer temperature through the surface heat flux process.

In order to more clearly show the performance difference between all runs, a comparison of the daily statistics from each run with the benchmarks (Emery et al, 2001) is summarized in Table 3-1. The overall performance of these four runs is pretty good, especially that of wind speed. The wind direction gross error in Run 1, Run 1a and Run 2 exceeds the benchmark, and the temperature bias of Run 1 and Run 1a does meet the benchmark. It is noticeable that the humidity performance of Run 1 and Run 1a is much better than that of Run 2 and Run 3 for all three parameters: bias, gross error and IOA.

**Table 3-1.** Comparison of the daily statistics on the 12-km grid for each run against benchmarks.

| | | Run3 | | | Run1 | | | Run1a | | | Run2 | | |
|---|---|---|---|---|---|---|---|---|---|---|---|---|---|
| **Parameter** | **Bench mark** | **Range** | | **Mean** | **Range** | | **Mean** | **Range** | | **Mean** | **Range** | | **Mean** |
| Wind Spd Bias | < ±0.5 | 0.21 | 0.5 | 0.36 | 0.13 | 0.65 | 0.34 | 0.15 | 0.51 | 0.32 | 0.28 | 0.77 | 0.53 |
| Wind Spd RMSE | < 2.0 | 0.93 | 1.5 | 1.28 | 1.11 | 1.83 | 1.42 | 1.06 | 1.6 | 1.40 | 1.29 | 1.81 | 1.55 |
| Wind Spd IOA | ≥ 0.60 | 0.75 | 0.87 | 0.80 | 0.66 | 0.81 | 0.75 | 0.68 | 0.8 | 0.74 | 0.66 | 0.78 | 0.72 |
| Wind Dir Bias | < ±10 | -10.77 | 7.36 | -2.43 | -9.51 | 7.5 | -2.26 | -12.23 | 8.93 | -3.12 | -7.55 | 12.86 | -1.58 |
| Wind Dir Gross Error | < 30 | 23.67 | 38.83 | 29.87 | 23.62 | 43.64 | 33.64 | 27.21 | 46.45 | 35.47 | 26.97 | 47.1 | 37.23 |
| Temp Bias | < ±0.5 | -0.85 | 0.06 | -0.36 | -1.52 | -0.43 | -0.81 | -1.56 | -0.39 | -0.80 | -1.2 | 0.03 | -0.35 |
| Temp Gross Error | < 2.0 | 1.24 | 2.03 | 1.64 | 1.28 | 2.27 | 1.74 | 1.1 | 2.39 | 1.76 | 1.52 | 2.08 | 1.72 |
| Temp IOA | ≥ 0.80 | 0.88 | 0.96 | 0.94 | 0.86 | 0.95 | 0.91 | 0.84 | 0.94 | 0.90 | 0.82 | 0.96 | 0.93 |
| Humidity Bias | < ±1.0 | -2.28 | -1.13 | -1.83 | -1.1 | 0.4 | -0.26 | 0.13 | 1.09 | 0.66 | -3.2 | -1.66 | -2.44 |
| Humidity Gross Error | < 2.0 | 2.12 | 2.66 | 2.45 | 1.48 | 2.45 | 1.98 | 1.01 | 2.33 | 1.81 | 2.54 | 3.47 | 3.04 |
| Humidity IOA | ≥ 0.60 | 0.71 | 0.89 | 0.83 | 0.74 | 0.92 | 0.84 | 0.75 | 0.96 | 0.86 | 0.64 | 0.81 | 0.74 |

## Results on the 4-km Domain

*Hourly Statistics*

Hourly statistical results for Run 3 on the 4-km grid are presented in Figure 3-6 for wind, temperature, and humidity. Performance for wind direction (Figure 3-6a) is generally pretty good with predicted wind directions in good agreement with the observed and the wind direction bias within ±30 degrees during most of the episode days. As expected with less prediction-observation pairings comprising these statistics, the performance for wind speed is relatively worse than that of 12-km grid, but is still quite good. The diurnal variation of wind speed is not that obvious and the wind speeds fluctuate more (“noisy”) in the 4-km grid. The over-prediction of wind speed is relatively dominant during the episode, like on the 12-km grid. While the systematic and unsystematic RMSEs are comparable on the 12-km grid, the unsystematic RMSE is generally much lower than systematic error in the 4-km grid. The IOA fluctuates around 0.6 with several lower points.

The performance for temperature (Figure 3-6b) on the 4-km grid is comparable to that of 12-km. The warmer prediction during the daytime is relatively stronger in the 4-km grid. The unsystematic RMSE remains much lower than the systematic error. The IOA is slightly lower and it fluctuates more in the 4-km grid.

Though the under-estimation of humidity (Figure 3-6c) is relatively larger, the overall predicted humidity pattern follows the observation well during the episode. The humidity bias is relatively larger on the 4-km grid. Like the temperature performance, the unsystematic RMSE remains much lower than systematic one. The IOA of humidity is extremely unstable during the episode, with as high as 0.9 in some days and as low as 0 in the other days.

Hourly statistical results for Run 1, Run 1a, and Run 2 on the 4-km grid are presented in Appendix A. The wind performance from these three runs is comparable to that of Run 3, especially the wind direction, except that the wind speed “spike” from these three runs during August 15 to 16 occurs on the 4-km grid as well. It is worth mentioning that the humidity performance of Run 1a is relatively better than that of Run1, Run2, and Run3 with much lower bias (under-prediction). But the better performance for humidity is at the sacrifice of worse performance for temperature. The amplitude of the diurnal temperature variation from Run 1a is smaller than that of the other three runs. That is, there are cooler predicted daytime temperatures and warmer predicted nighttime temperatures.

*Daily Statistics*

Daily statistical results for Run 3 on the 4-km grid are presented in Figure 3-7 for wind, temperature, and humidity. The daily trend in wind speed (Figure 3-7a) is well replicated through the episode. The performance for the wind direction is very good. Though the over-prediction of wind speed is relatively higher on the 4-km grid with wind speed bias exceeding the benchmark, the overall wind speed performance meets the standard with IOA close to 0.6.

Daily temperature performance (Figure 3-7b) on the 4-km grid is fairly good and comparable to that on the 12-km grid. The temperature bias, gross error and IOA are all meet the benchmark standard.

Similarly to the hourly results, daily humidity performance (Figure3-7c) is not that good. The statistics exceed all three benchmarks for bias, gross error, and IOA. The under-estimation of humidity is even worse on the 4-km grid.

Figure 3-8 displays graphically the comparison of the daily statistical results for wind, temperature, and humidity from all four runs. The wind speed and direction (Figure 3-8a) are well replicated in all runs. The temperature performance (Figure 3-8b) from all runs is generally very good. However, the humidity performance (Figure 3-8c) of all runs except Run 1a is relatively worse comparing to that of wind and temperature.

The performance differences can be clearly shown by a comparison of the daily statistics from each run with the proposed benchmarks (Emery et al, 2001) in Table 3-2.

**Table 3-2.** Comparison of the daily statistics on the 4-km grid for each run against benchmarks.

| | | Run3 | | | Run1 | | | Run1a | | | Run2 | | |
|---|---|---|---|---|---|---|---|---|---|---|---|---|---|
| **Parameter** | **Bench mark** | **Range** | | **Mean** | **Range** | | **Mean** | **Range** | | **Mean** | **Range** | | **Mean** |
| Wind Spd Bias | < ±0.5 | 0.13 | 1.26 | 0.69 | 0.08 | 0.84 | 0.50 | -0.28 | 0.76 | 0.37 | 0.35 | 1.03 | 0.79 |
| Wind Spd RMSE | < 2.0 | 1.08 | 2.10 | 1.55 | 1.20 | 2.10 | 1.49 | 1.13 | 1.85 | 1.47 | 1.32 | 2.11 | 1.73 |
| Wind Spd IOA | ≥ 0.60 | 0.42 | 0.70 | 0.59 | 0.33 | 0.67 | 0.57 | 0.43 | 0.66 | 0.54 | 0.41 | 0.62 | 0.52 |
| Wind Dir Bias | < ±10 | -13.10 | 8.40 | -0.56 | -13.26 | 13.24 | 0.35 | -4.80 | 11.98 | 2.17 | -7.65 | 14.72 | 2.66 |
| Wind Dir Gross Error | < 30 | 14.95 | 51.23 | 27.61 | 14.41 | 46.55 | 28.49 | 20.52 | 53.16 | 34.60 | 19.61 | 53.04 | 33.35 |
| Temp Bias | < ±0.5 | -1.50 | 1.23 | 0.01 | -1.42 | 0.99 | -0.20 | -0.98 | 0.03 | -0.35 | -2.15 | 0.61 | -0.04 |
| Temp Gross Error | < 2.0 | 1.48 | 2.93 | 1.74 | 1.32 | 2.21 | 1.67 | 0.81 | 2.02 | 1.65 | 1.24 | 2.28 | 1.82 |
| Temp IOA | ≥ 0.80 | 0.61 | 0.97 | 0.90 | 0.59 | 0.97 | 0.91 | 0.62 | 0.93 | 0.87 | 0.48 | 0.97 | 0.90 |
| Humidity Bias | < ±1.0 | -4.45 | -0.18 | -2.87 | -3.01 | -0.26 | -1.57 | -1.11 | 0.13 | -0.52 | -4.85 | -1.93 | -3.70 |
| Humidity Gross Error | < 2.0 | 1.79 | 4.48 | 3.22 | 1.12 | 3.55 | 2.41 | 0.87 | 1.90 | 1.52 | 2.33 | 4.85 | 3.79 |
| Humidity IOA | ≥ 0.60 | 0.37 | 0.71 | 0.52 | 0.36 | 0.82 | 0.54 | 0.59 | 0.94 | 0.69 | 0.36 | 0.57 | 0.46 |

## QUALITATIVE ASSESSMENT OF MM5 RESULTS

The plots of surface wind and sea level pressure in the 12-km domain on each episode day at 1800 CST are presented in Appendix C. The regional major weather events and flow pattern are reproduced well by the MM5 simulation. On August 15, MM5 simulated a surface high pressure moving eastward over Great Lakes. The strength and propagation speed of this high pressure system was simulated fairly well by Run 3. The predicted weak pressure gradients and clear skies agreed well with the observed on August 16. Pressure gradients remained weak until August 18. The weak wind speed and a local high near the Arkansas/Mississippi border were simulated correctly during August 17. The position and propagation speed of a cold front pushing south from northern Texas was replicated well from August 19. The pressure was slightly over predicted (about 1 mb) over northern Texas and Oklahoma during August 20 and 21.

A comparison of MM5 vertical profiles of temperature, humidity and wind speed/direction at DFW from Run 3 and Run 1 against the routine 12-hourly soundings is provided in Appendix B. The MM5 replicated upper air profiles for wind and temperature fairly well in both runs, especially in the boundary layer. The performance for wind speed and direction is slightly better in Run 3 (e.g. at 6 LST August 16). The humidity performance from both runs is acceptable but worse compared to that of wind and temperature. The humidity performance of Run 1 is relatively better than that of Run 3 since the FDDA nudging of humidity is stronger.

The plots of PBL depth on the 4-km CAMx domain at 1000 and 1400 CST of each episode day are provided in Appendix C. The simulated PBL depth of 2100 to 2300 meters at 1400 CST and 1000 to 1500 meters at 1000 CST around DFW area is reasonable during most episode days, except that relatively higher PBL depths are estimated on August 18 and 19. Notice that there are spotty areas of extremely low PBL depth (“holes”) occurring consistently in the same areas during all episode days. Further investigation into the landuse data reveals that these “holes” are coincident with the locations of lakes. It is known that this kind of problem is related to the adoption of Pleim-Xiu LSM and PBL scheme in the model configuration.

*Evaluation of Cloud Fields*

The predicted distribution of clouds is most easily accomplished via qualitative comparison to satellite imagery. The most common format is available from the Geostationary Environmental Operational Satellite (GOES) system, and these data are archived and disseminated by several entities at some cost. A comparison between model output and actual photographic imagery is complicated by several factors, however. These include parallax introduced by the sight angle from the satellite to specific areas on the Earth, inaccurate placement of geographic boundaries on the images for reference, and the resolution differences between model and image (e.g., explicitly modeled clouds at coarse grid resolution versus ~1 km image pixels), which usually results in the perception that the model under predicts the amount of cloudiness.

We believe that a more fair assessment is to represent the "observed" cloud fields on the same modeling grid as the predicted cloud fields. Furthermore, this is consistent with our approach to use satellite-derived information to develop sunlight-sensitive biogenic emission estimates on the modeling grid. A data set containing the distribution of photosynthetically active radiation (PAR) from GOES imagery was obtained from the University of Maryland and processed to the 36, 12, and 4-km CAMx modeling grids for use in the GLOBEIS model (Yarwood et al., 2001). When plotted, the gridded PAR fields clearly show the distribution of clouds as patterns of significantly attenuated radiative flux at the surface relative to clear-sky areas, especially around midday.

Still, a comparison of gridded PAR fields with MM5 predicted cloud fields that have been processed for input to CAMx is not entirely straight forward. We need to represent the three-dimensional distribution and optical thickness of the CAMx cloud fields as a two-dimensional (vertically integrated) field similar to the PAR distribution at the surface. Therefore, the CAMx cloud fields are translated to a total vertical "optical depth" using the approach contained within CAMx (described by ENVIRON, 2000). A clear sky has a cloud optical depth of zero, while very thick cloudy columns can have optical depths of more than 1000. Our qualitative cloud evaluation, which again focuses on the location and relative thickness of clouds, is reduced to a comparison of PAR fluxes and model-resolved cloud optical depths on a consistent grid system. In the future, the optical depth calculation could be expanded to include a simple radiative transfer calculation for a visible wavelength band from which to derive an estimate of radiative fluxes at the ground.

Raw PAR data are reported on a 0.5 degree (~50 km) equal-angle grid, and spatially interpolated to the various CAMx grids for use in GLOBEIS. Since the PAR distribution cannot be refined any better for grid resolutions finer than about 50 km, only the 36-km PAR fields were used to evaluate the placement of MM5 cloud fields on the CAMx 36-km grid.

Clouds are present in fairly large amounts at the beginning of the episode over the regional domain as a frontal system extends into Texas. Over the next few days, high pressure builds and cloudiness is reduced. The core period remains only partly cloudy over Texas until near the end of the episode when disturbances skirt across the plains states (Kansas and Missouri) and a tropical disturbance moves into southern Texas. Overall, the MM5 appears to perform admirably in placing the major cloud features in the regional domain. The locations of clouds associated with synoptic-scale phenomena such as fronts, troughs, and mesoscale low pressure areas are all well replicated, as would be expected with a model of this sophistication.

Specific examples of the comparison on the 36-km domain are shown in Figures D-1 to D-4 for midday on August 13, 17, 20, and 22. On August 13 (Figure D-1) cloudiness is associated with a frontal band extending from the Ohio Valley through northeast Texas, and miscellaneous cloud patterns are seen over Missouri and the southeast U.S. The DFW area remained mostly cloud-free during the rest of episode days as observed. Particularly good agreement is seen on August 17 (Figure D-2), with variable cloudiness along the gulf coast. On August 20 (Figure D-3), MM5 properly picks up frontal cloudiness extending from the southeast U.S. into central Texas, and cloud masses in the Gulf and the Ohio Valley. However, it misses a cloud mass in central Kansas. On August 22 (Figure D-4), MM5 replicates the large rotating tropical storm entering into southern Texas. Also scattered cloudiness throughout Texas is well replicated at 36-km resolution. A large cloud mass over eastern Kansas is under estimated by MM5, and too much cloud cover is produced over the northeast Gulf. Miscellaneous cloud cover appears to be well replicated over the southeast U.S. The cloud band over Louisiana and Mississippi is slightly overestimated.

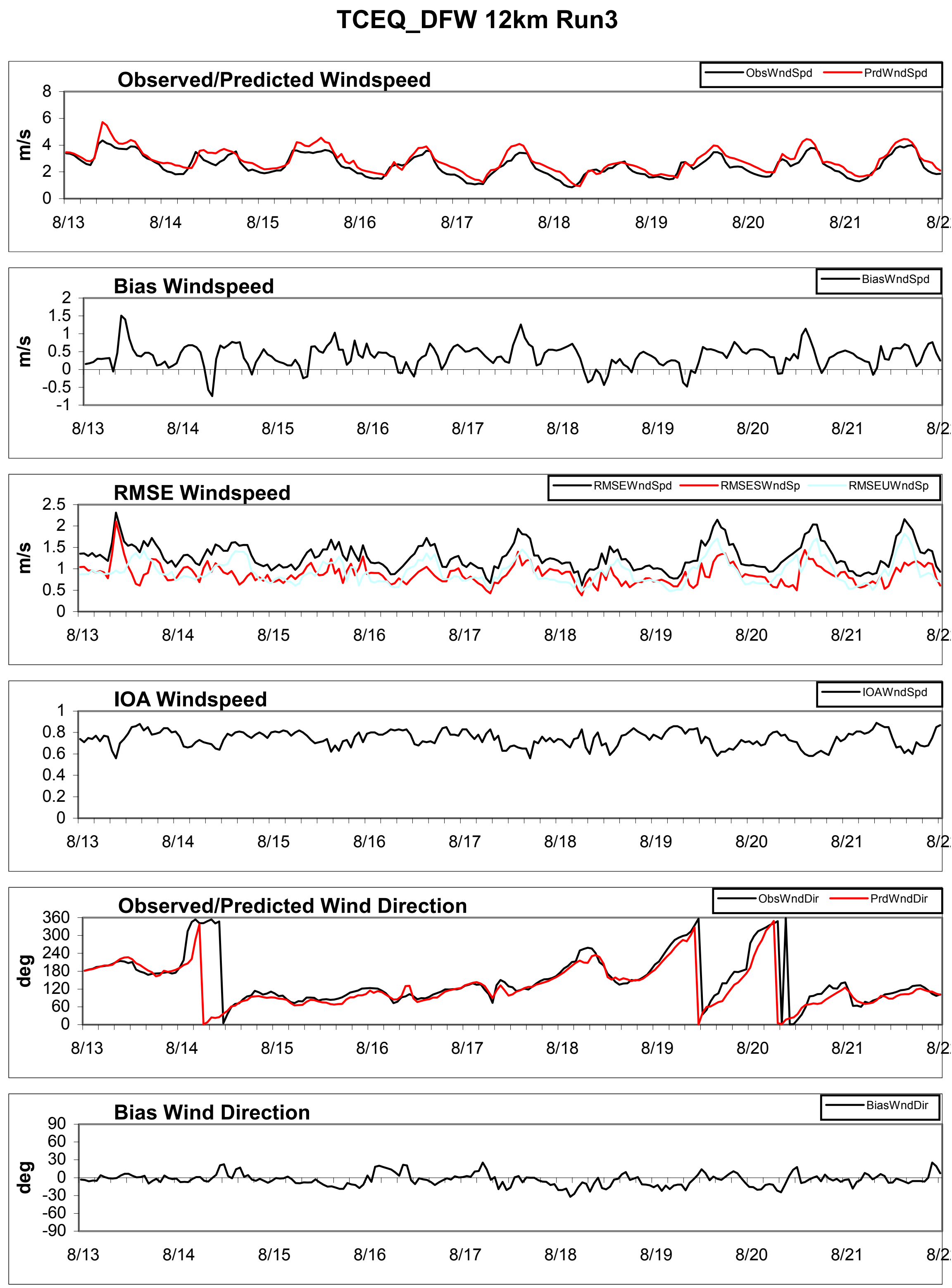


**Figure 3-3a.** Hourly time series of region-average observed and predicted (Run 3) surface-layer winds and performance statistics in the 12-km MM5 domain. RMSE is shown for total, systematic (RMSES) and unsystematic (RMSEU) components.

## TCEQ_DFW 12km Run3

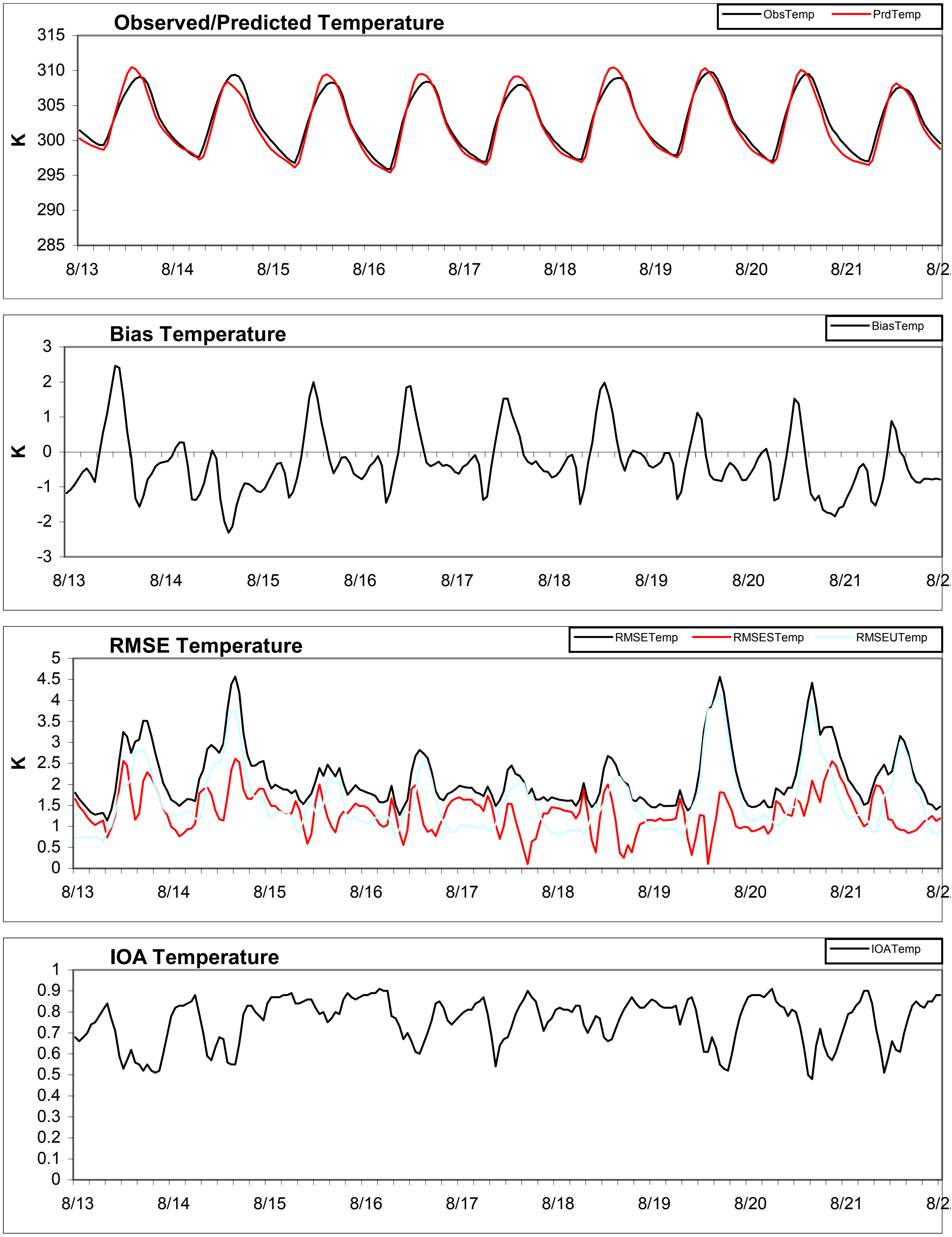


**Figure 3-3b.** Hourly time series of region-average observed and predicted (Run 3) surface-layer temperature and performance statistics in the 12-km MM5 domain. RMSE is shown for total, systematic (RMSES) and unsystematic (RMSEU) components.

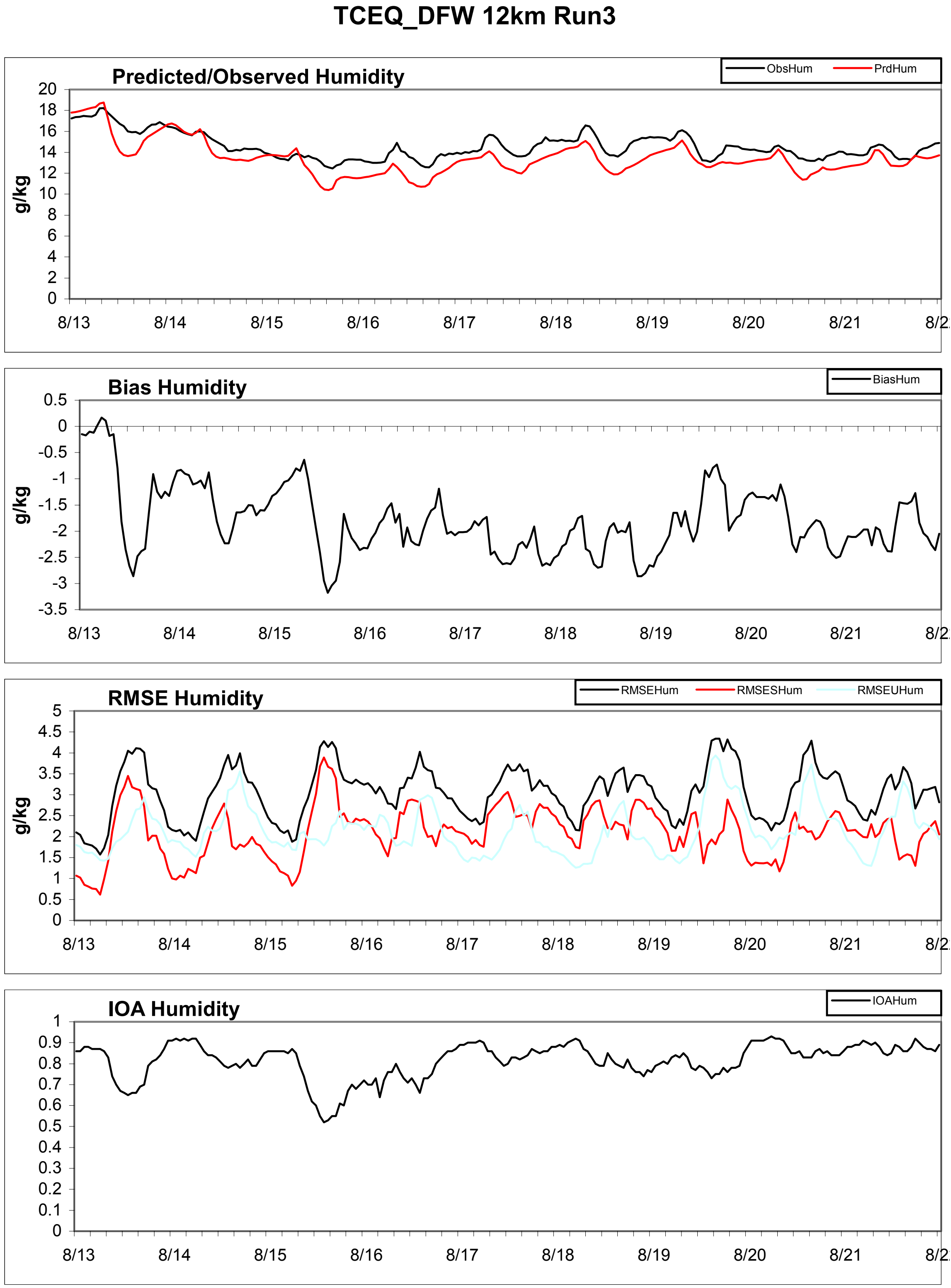


**Figure 3-3c.** Hourly time series of region-average observed and predicted (Run 3) surface-layer humidity and performance statistics in the 12-km MM5 domain. RMSE is shown for total, systematic (RMSES) and unsystematic (RMSEU) components.

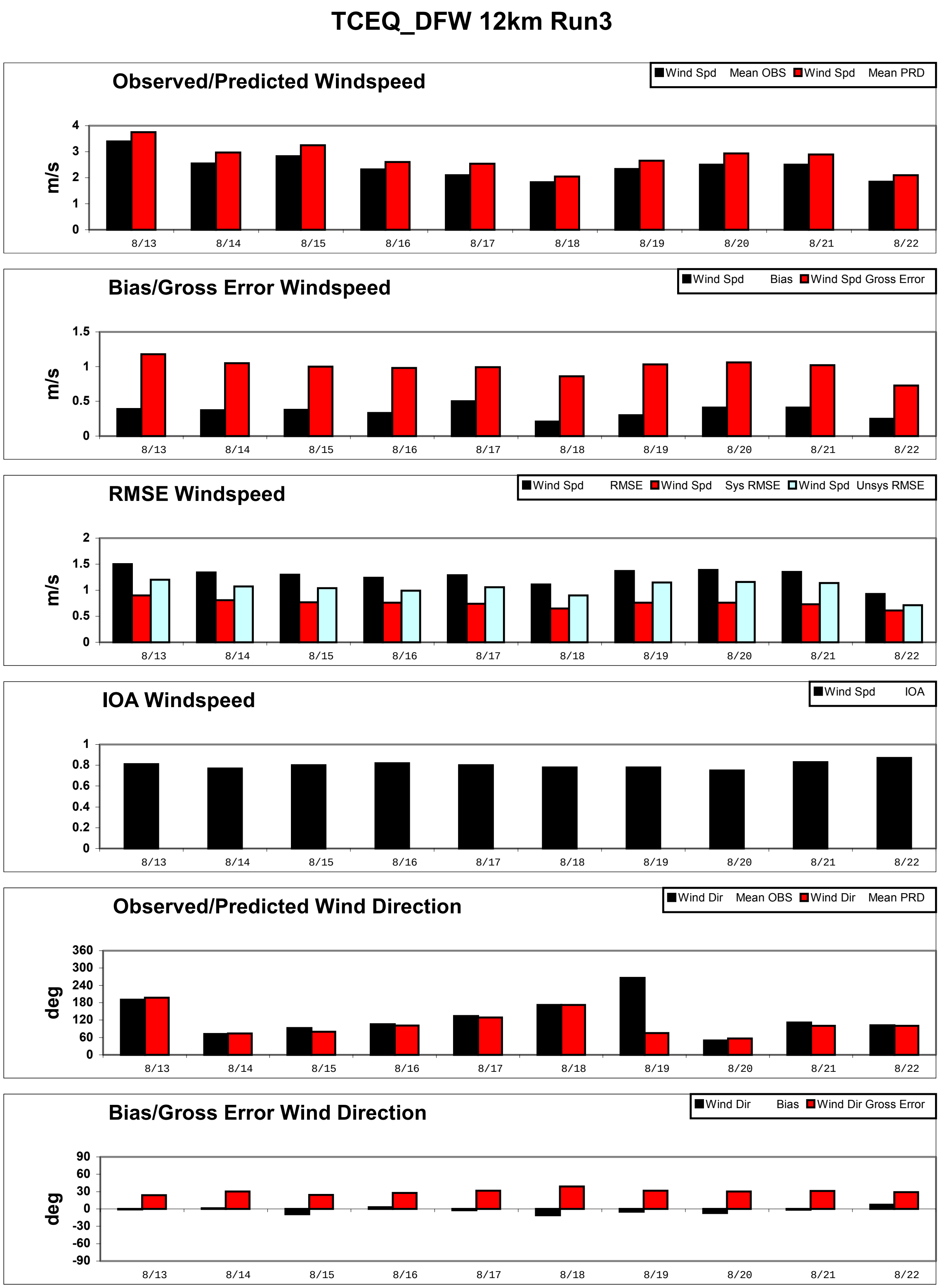


**Figure 3-4a.** Daily region-average observed and predicted (Run 3) surface-layer winds and performance statistics in the 12-km MM5 domain. RMSE is shown for total, systematic (RMSES) and unsystematic (RMSEU) components.

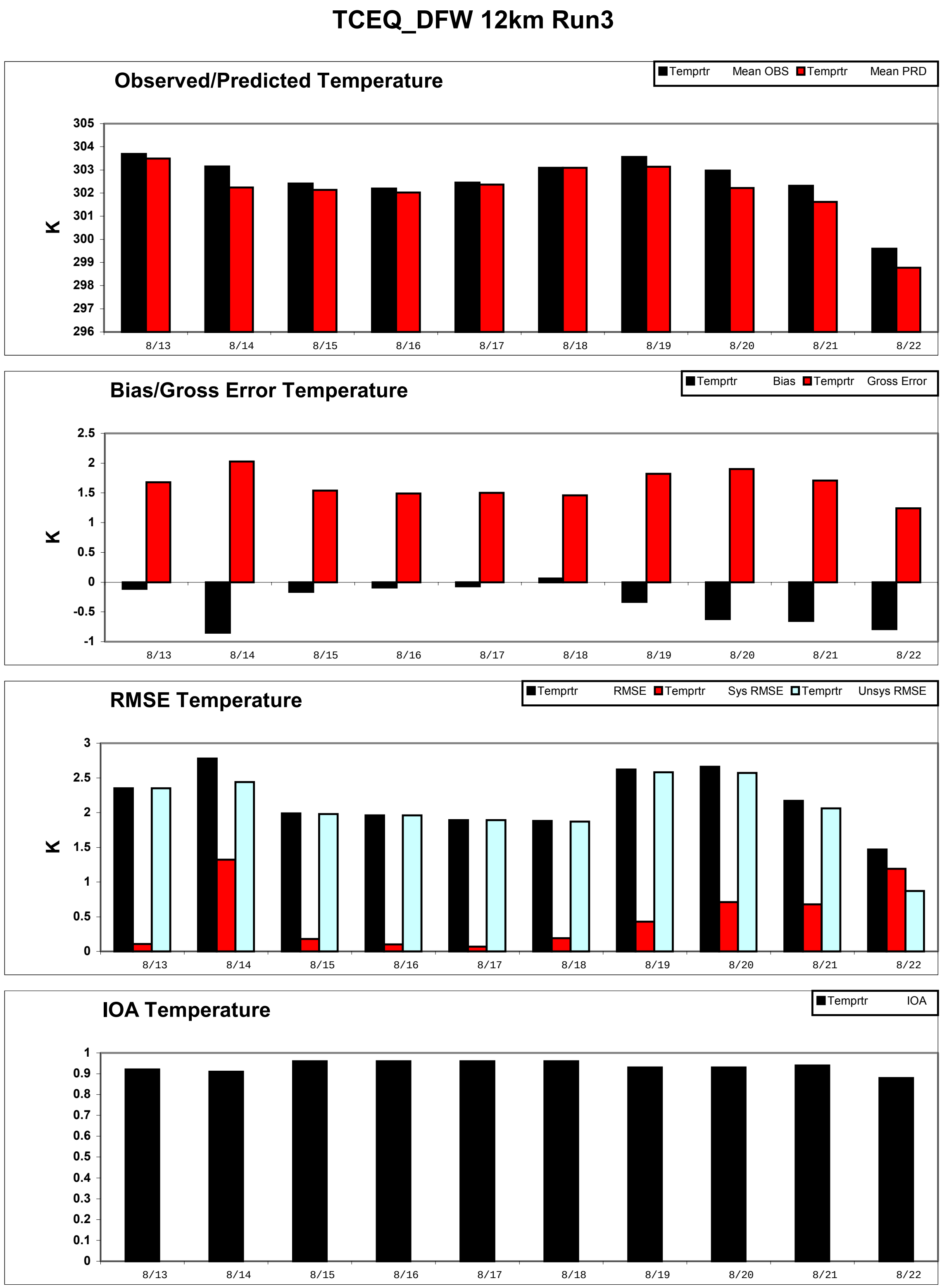


**Figure 3-4b.** Daily region-average observed and predicted (Run 3) surface-layer temperature and performance statistics in the 12-km MM5 domain. RMSE is shown for total, systematic (RMSES) and unsystematic (RMSEU) components.

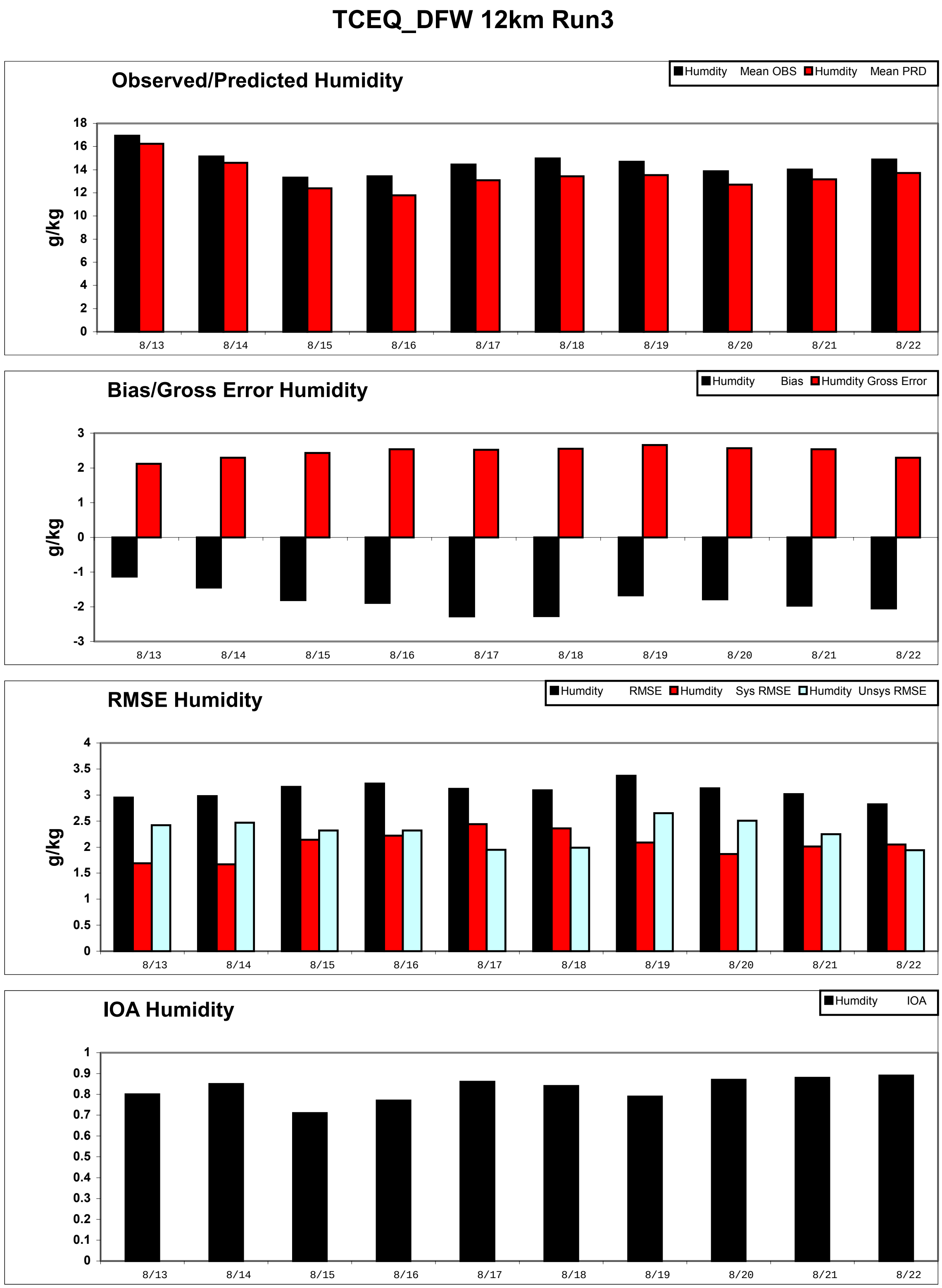


**Figure 3-4c.** Daily region-average observed and predicted (Run 3) surface-layer humidity and performance statistics in the 12-km MM5 domain. RMSE is shown for total, systematic (RMSES) and unsystematic (RMSEU) components.

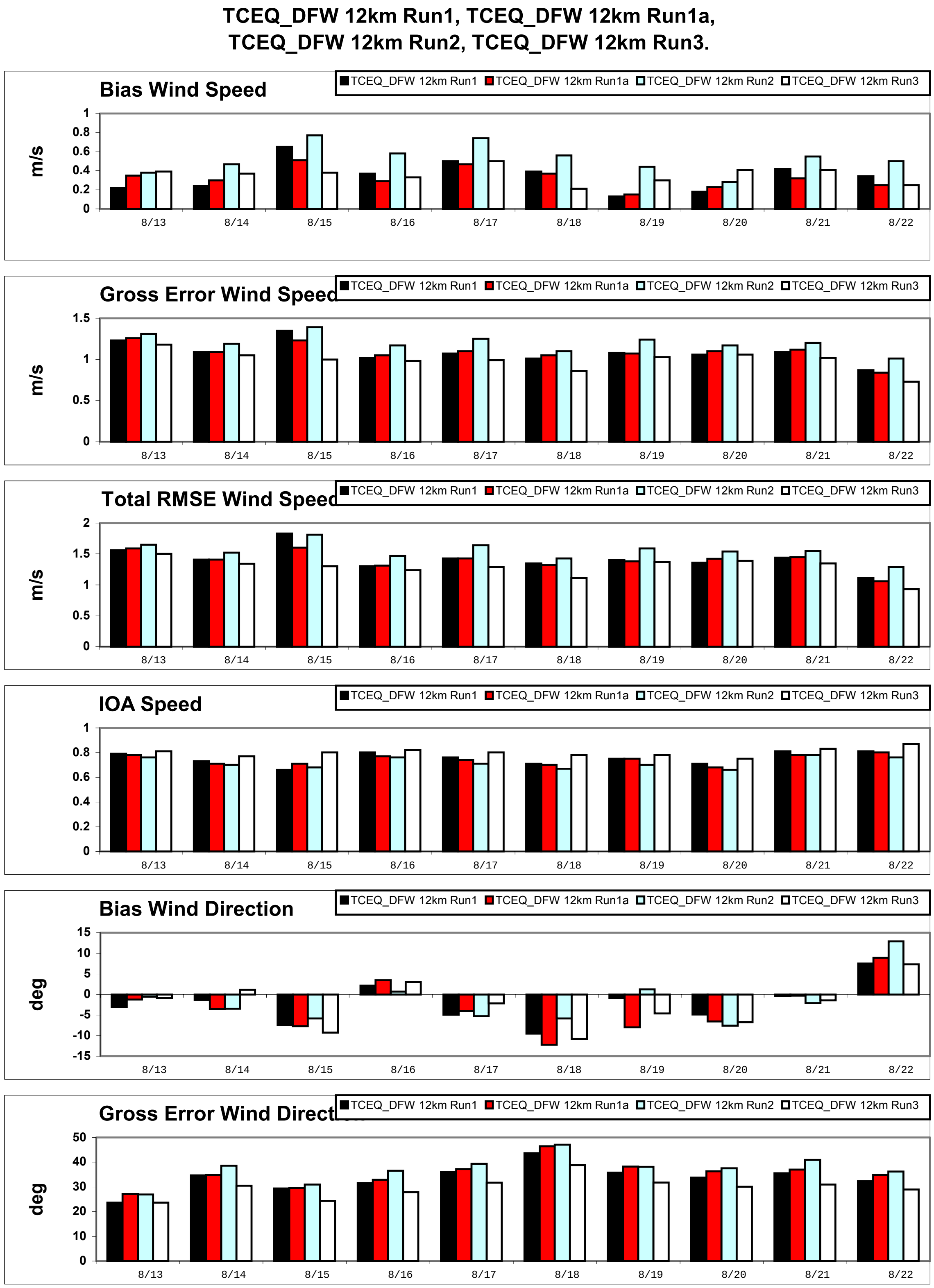


**Figure 3-5a.** Comparison of Run 1, Run 1a, Run 2, and Run 3 daily regional-average performance statistics for wind in the 12-km MM5 domain.

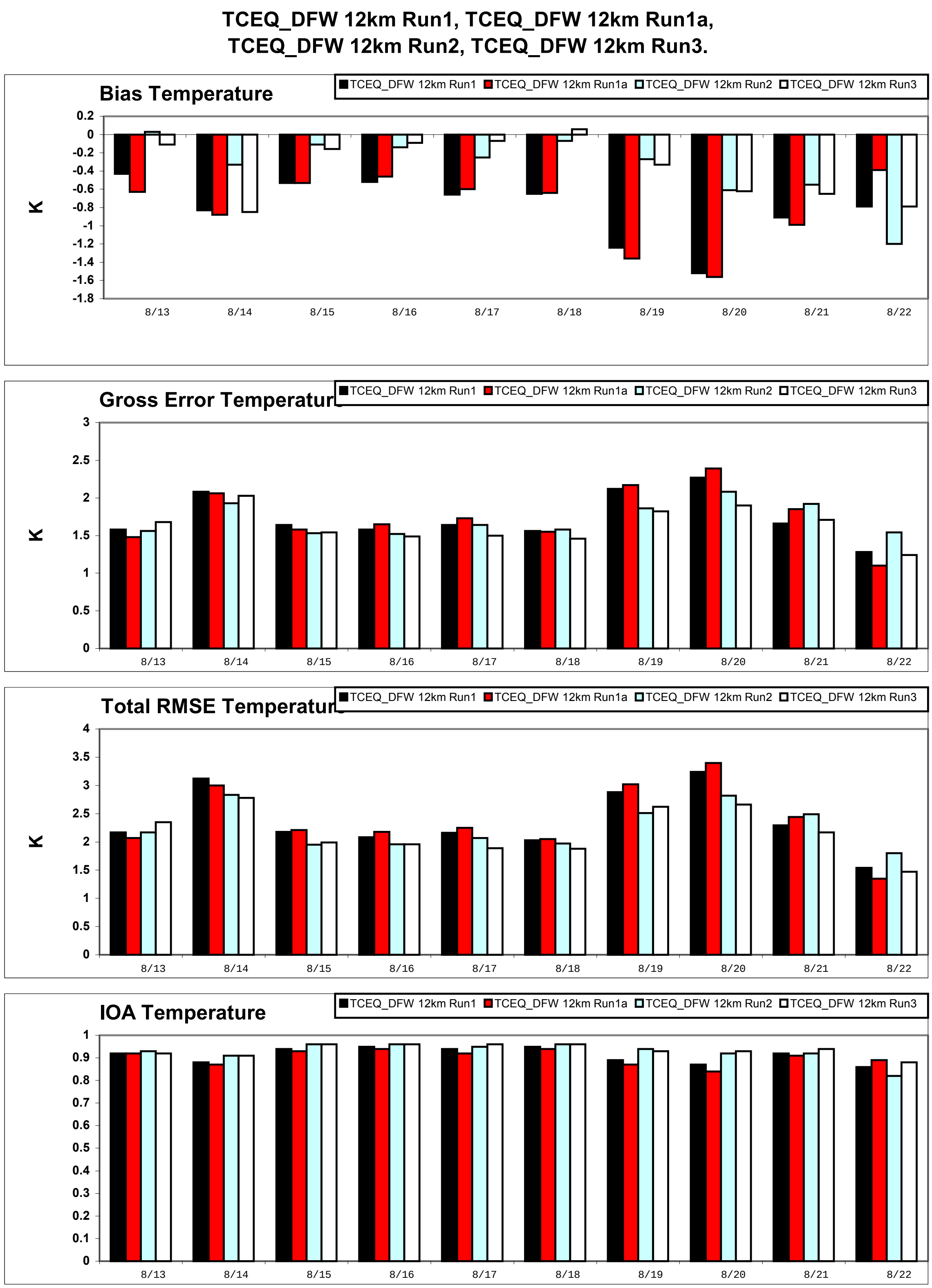


**Figure 3-5b.** Comparison of Run 1, Run 1a, Run 2, and Run 3 daily regional-average performance statistics for temperature in the 12-km MM5 domain.

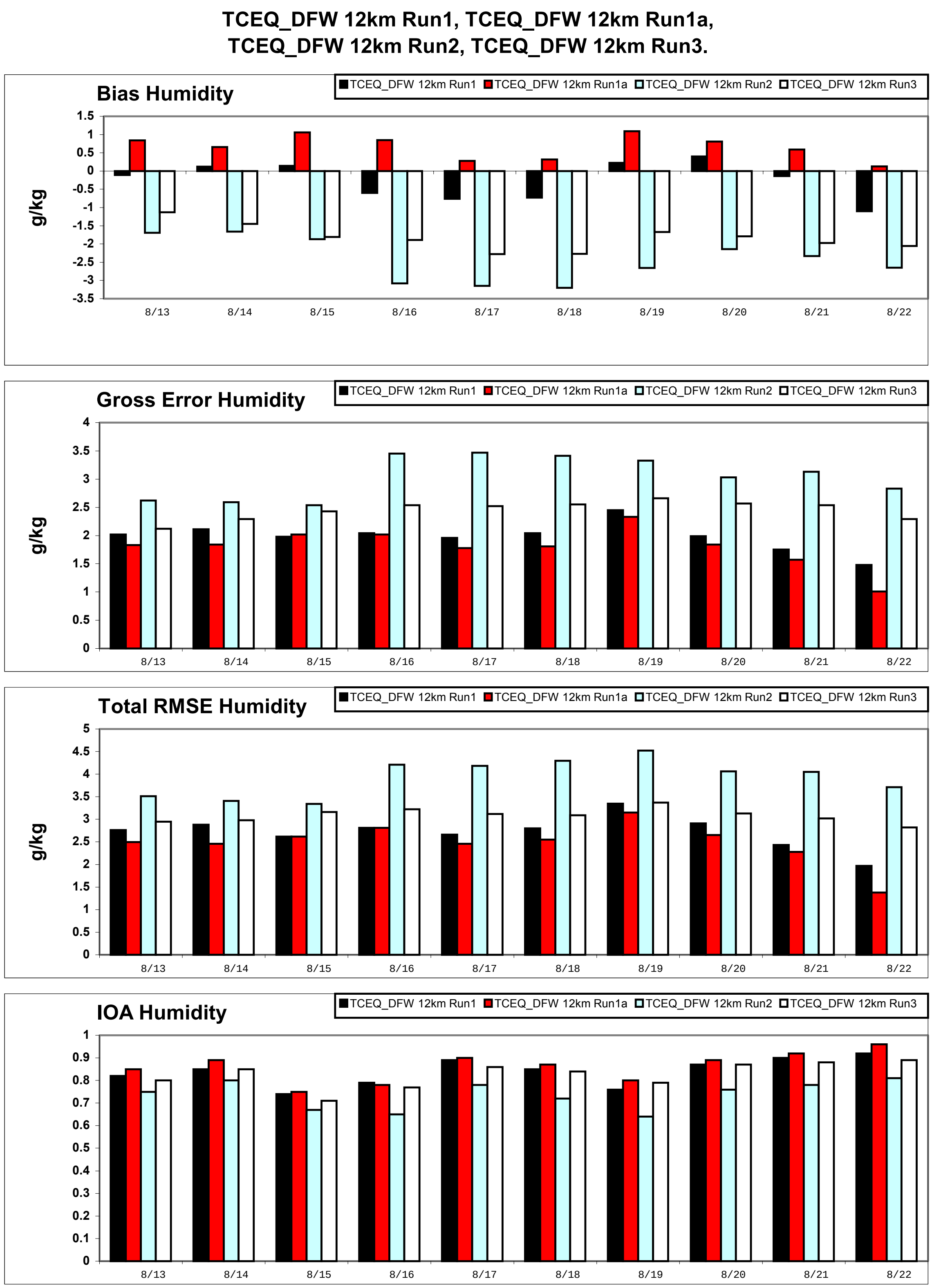


**Figure 3-5c**. Comparison of Run 1, Run 1a, Run 2, and Run 3 daily regional-average performance statistics for humidity in the 12-km MM5 domain.

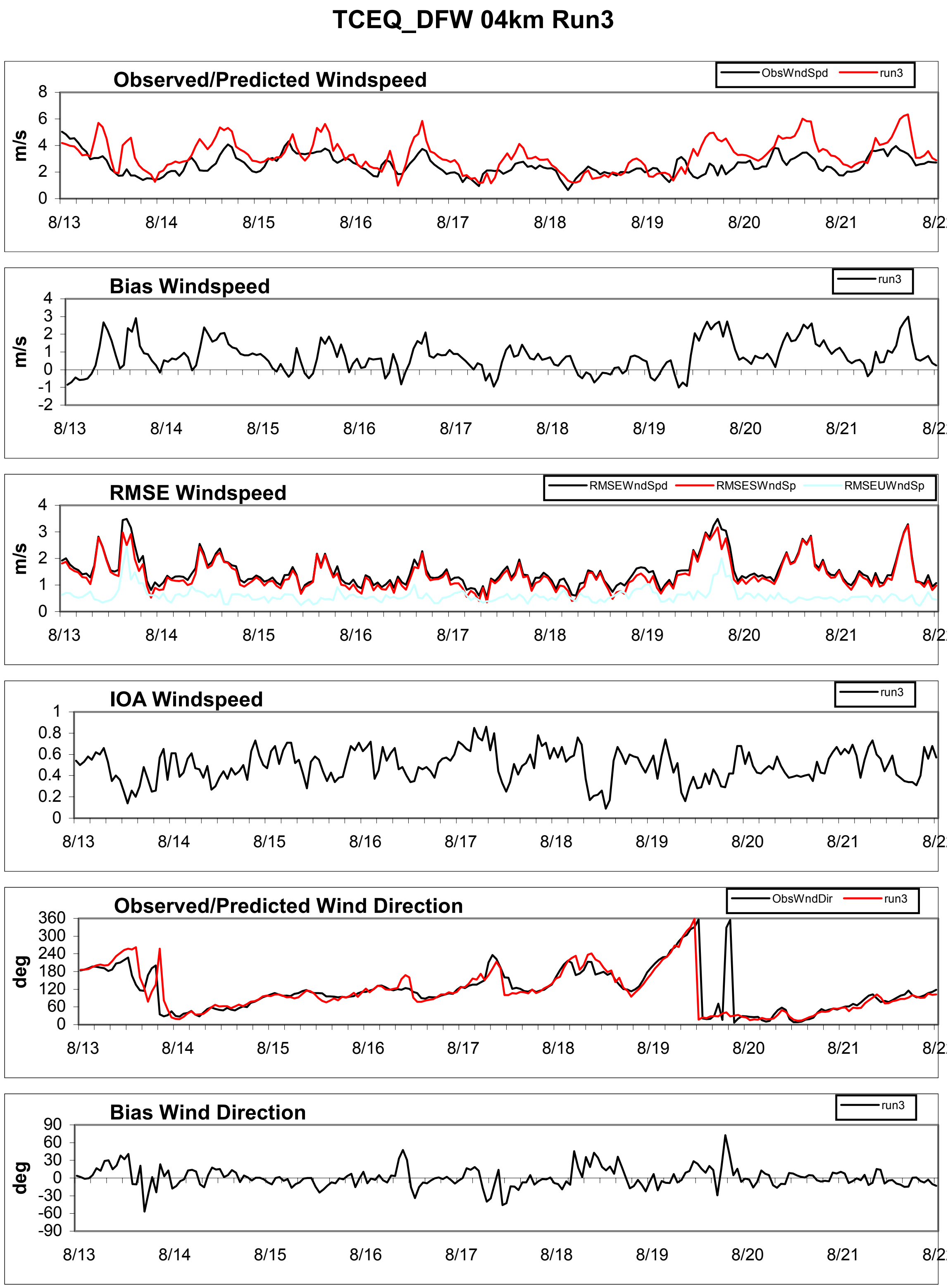


**Figure 3-6a.** Hourly time series of region-average observed and predicted (Run 3) surface-layer winds and performance statistics in the 4-km MM5 domain. RMSE is shown for total, systematic (RMSES) and unsystematic (RMSEU) components.

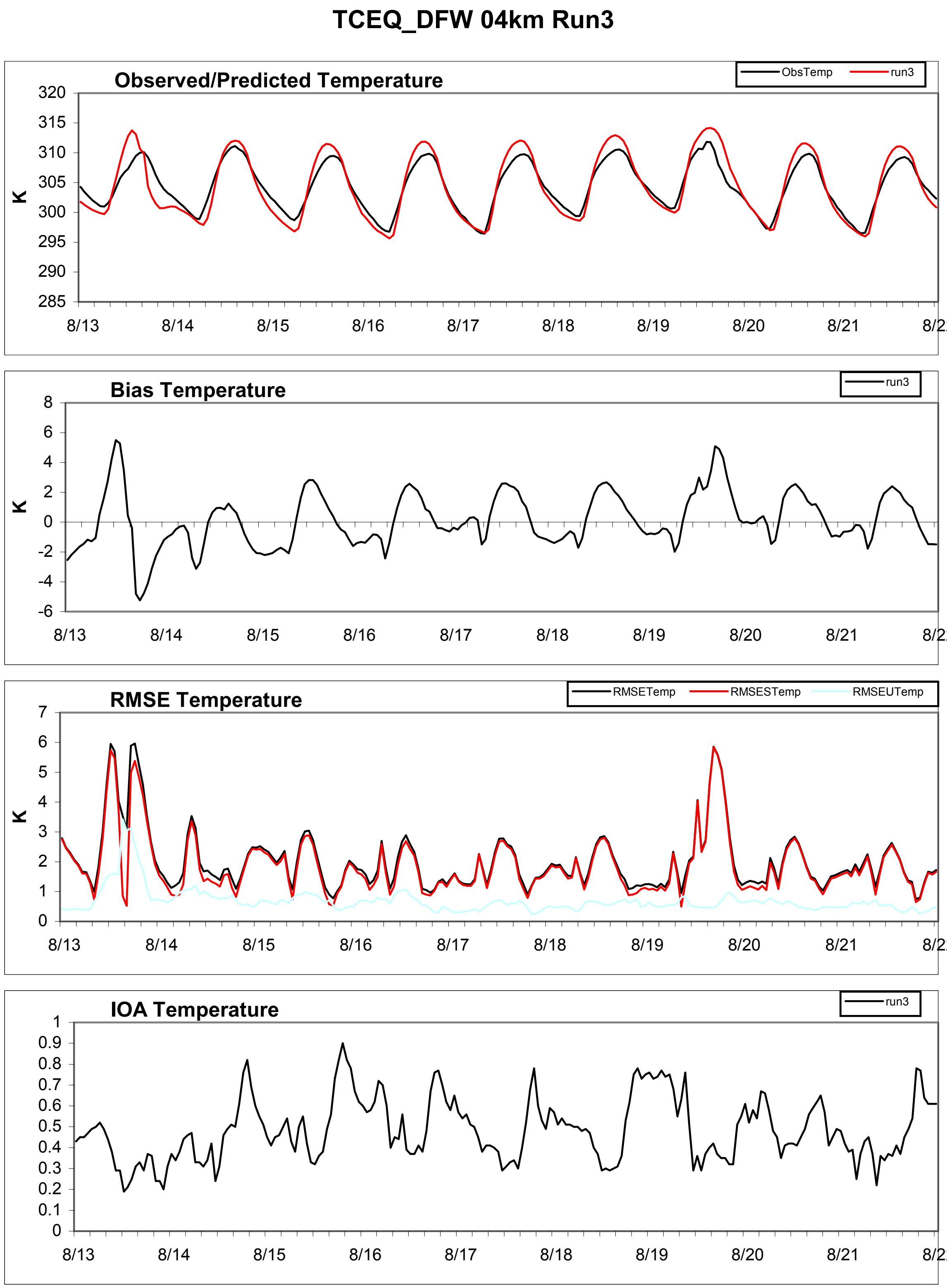


**Figure 3-6b.** Hourly time series of region-average observed and predicted (Run 3) surface-layer temperature and performance statistics in the 4-km MM5 domain. RMSE is shown for total, systematic (RMSES) and unsystematic (RMSEU) components.

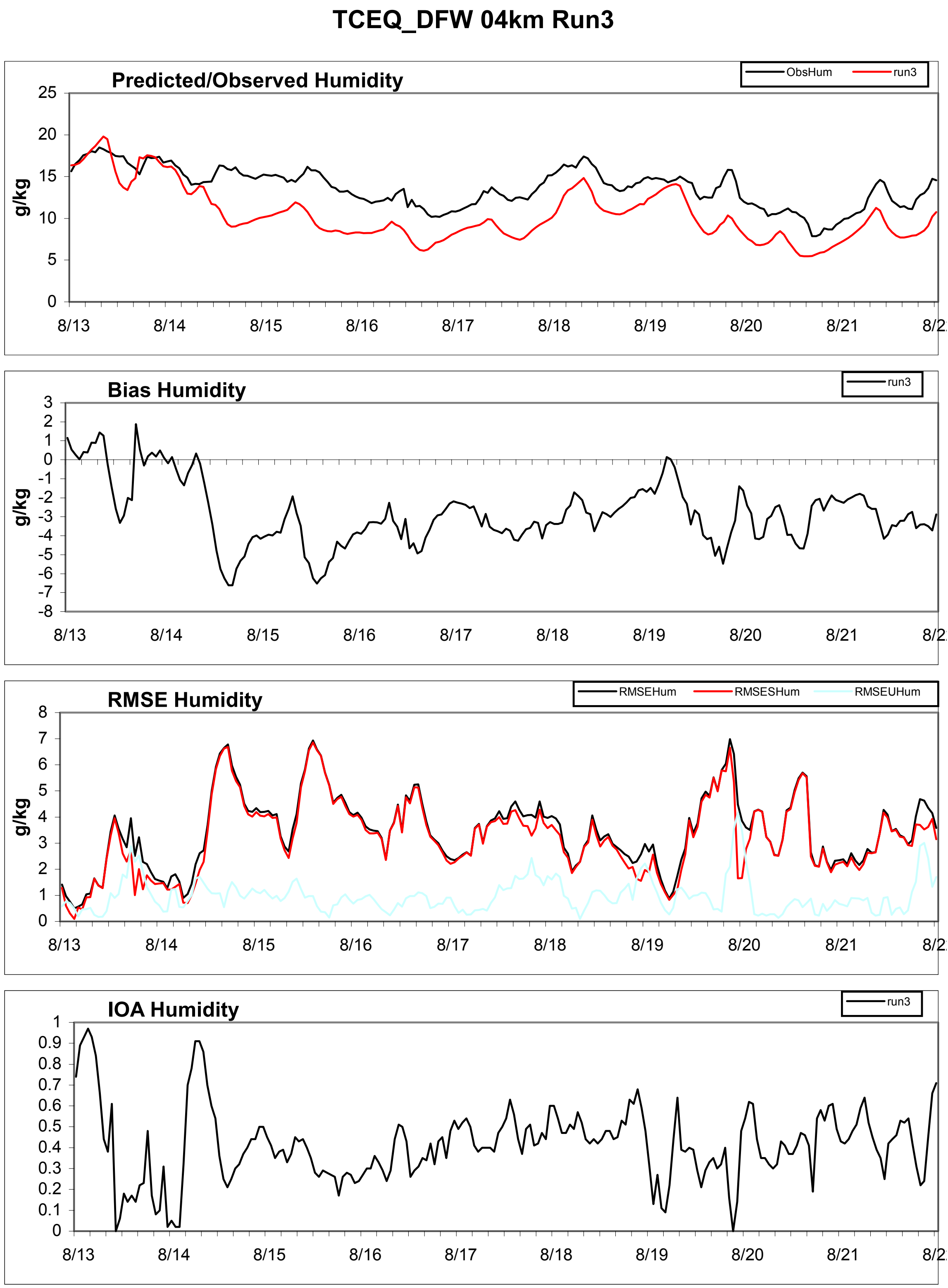


**Figure 3-6c.** Hourly time series of region-average observed and predicted (Run 3) surface-layer humidity and performance statistics in the 4-km MM5 domain. RMSE is shown for total, systematic (RMSES) and unsystematic (RMSEU) components.

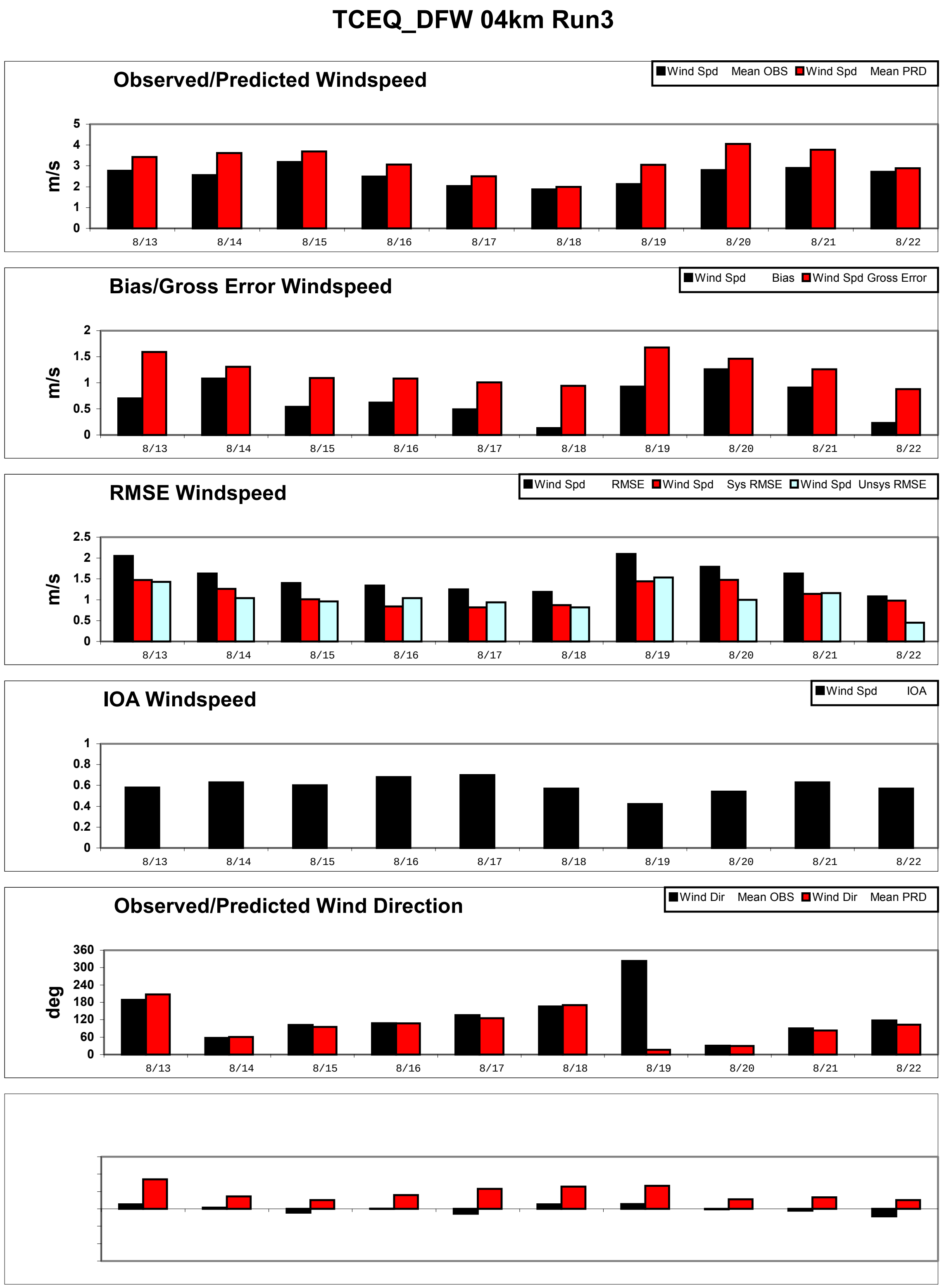


**Figure 3-7a.** Daily region-average observed and predicted (Run 3) surface-layer winds and performance statistics in the 4-km MM5 domain. RMSE is shown for total, systematic (RMSES) and unsystematic (RMSEU) components.

# 4. CONCLUSIONS

This report describes meteorological modeling for the Dallas/Fort Worth (DFW) 4-county nonattainment area. Meteorological modeling was performed to support air quality modeling with the goals of developing ozone control strategies and demonstrating attainment of the 1-hour and 8-hour standard in the DFW area.

The Fifth Generation NCAR/Penn State Mesoscale Model (MM5) version 3.6 was used to simulate the August 13-22, 1999 episode. The grid configuration includes four two-way nested grids with the 4-km grid spacing covering the DFW 4-county nonattainment area. The 36-km and 12-km grids are sufficiently large to better simulate the dominant regional and local flow and weather patterns, thus to address more properly the multi-day transport of ozone and precursors from significant source areas outside of Texas.

The following were the objectives of this study:

- To define a meteorological modeling domain on a Lambert Conformal projection that meshes with the CAMx 36/12/4-km grid system, with the finest resolution over the Dallas Forth Worth area;

- To produce refined meteorological fields for the entire domain using MM5 version 3, while optimizing performance in the subdomain containing DFW via numerous sensitivity runs and a rigorous statistical evaluation.

Four MM5 runs were configured with the same physics but different FDDA techniques. The quality of meteorological simulations plays a crucial role in determining the accuracy of air quality modeling. Thus, the statistical and qualitative evaluations were conducted to carefully assess the performance of MM5 model results. The results from four configured MM5 runs focusing DFW area during August 13-22, 1999 are presented in this report. The MM5 model results of wind, temperature and humidity from all runs in this study showed rather good performance in replicating the large- and meso-scale meteorology in the DFW area. The overall pressure and flow patterns covering south central U.S. and the placement of clouds and precipitations were replicated well. Some noted features about the results of four runs are summarized as follows:

- The performance for wind speed and direction is rather good in all four runs with the best performance in Run3. The hourly and daily statistical results for wind show that smaller prediction-observation bias, no "spike" abnormity during August 15-16, and overall better performance parameters (such as RMSE and IOA) in Run3. The simulated vertical wind profiles from Rub3 are also better matched with the 12-hourly sounding at Dallas Fort Worth.

- A slight under-prediction of humidity on the 4-km grid during almost the whole episode remains throughout all runs. But the humidity bias in Run1a is much smaller comparing to those of other runs. In fact, Run1a is the only one that meets benchmark standard in all three categories (RMSE, Bias, and IOA) for the daily statistics at 4-km grid.

- The temperature performances on the 4km and 12-km grid for all runs are pretty good with the replication of the observed diurnal variation. The amplitude of diurnal change of Run3 and Run1 on the 4-km domain are well reproduced, while the daytime maximum temperatures in Run2 are slightly over predicted. The strength of the diurnal variation in Run1a is relatively weaker, that is, the daytime maximum temperatures are relative lower than the observed and the nighttime minimum temperatures are slightly over estimated.

Table 4-1 presents a recap of the episode-mean daily statistics determined for MM5 Run3, Run1, Run1a, and Run2 in the entire 12-km grid over August 13-22, 1999. Similar statistics are shown in Table 4-2 for the 4-km DFW area.

**Table 4-1.** Episode-mean daily statistics on the 12-km grid for each run against benchmarks.

| | | Run3 | Run1 | Run1a | Run2 |
|---|---|---|---|---|---|
| **Parameter** | **Benchmark** | **Mean** | **Mean** | **Mean** | **Mean** |
| Wind Spd Bias | < ±0.5 | 0.36 | 0.34 | 0.32 | 0.53 |
| Wind Spd RMSE | < 2.0 | 1.28 | 1.42 | 1.40 | 1.55 |
| Wind Spd IOA | ≥ 0.60 | 0.80 | 0.75 | 0.74 | 0.72 |
| Wind Dir Bias | < ±10 | -2.43 | -2.26 | -3.12 | -1.58 |
| Wind Dir Gross Error | < 30 | 29.87 | 33.64 | 35.47 | 37.23 |
| Temp Bias | < ±0.5 | -0.36 | -0.81 | -0.80 | -0.35 |
| Temp Gross Error | < 2.0 | 1.64 | 1.74 | 1.76 | 1.72 |
| Temp IOA | ≥ 0.80 | 0.94 | 0.91 | 0.90 | 0.93 |
| Humidity Bias | < ±1.0 | -1.83 | -0.26 | 0.66 | -2.44 |
| Humidity Gross Error | < 2.0 | 2.45 | 1.98 | 1.81 | 3.04 |
| Humidity IOA | ≥ 0.60 | 0.83 | 0.84 | 0.86 | 0.74 |

**Table 4-2.** Episode-mean daily statistics on the 4-km grid for each run against benchmarks.

| | | Run3 | Run1 | Run1a | Run2 |
|---|---|---|---|---|---|
| **Parameter** | **Benchmark** | **Mean** | **Mean** | **Mean** | **Mean** |
| Wind Spd Bias | < ±0.5 | 0.69 | 0.50 | 0.37 | 0.79 |
| Wind Spd RMSE | < 2.0 | 1.55 | 1.49 | 1.47 | 1.73 |
| Wind Spd IOA | ≥ 0.60 | 0.59 | 0.57 | 0.54 | 0.52 |
| Wind Dir Bias | < ±10 | -0.56 | 0.35 | 2.17 | 2.66 |
| Wind Dir Gross Error | < 30 | 27.61 | 28.49 | 34.60 | 33.35 |
| Temp Bias | < ±0.5 | 0.01 | -0.20 | -0.35 | -0.04 |
| Temp Gross Error | < 2.0 | 1.74 | 1.67 | 1.65 | 1.82 |
| Temp IOA | ≥ 0.80 | 0.90 | 0.91 | 0.87 | 0.90 |
| Humidity Bias | < ±1.0 | -2.87 | -1.57 | -0.52 | -3.70 |
| Humidity Gross Error | < 2.0 | 3.22 | 2.41 | 1.52 | 3.79 |
| Humidity IOA | ≥ 0.60 | 0.52 | 0.54 | 0.69 | 0.46 |

Comparing the results from all four runs, the MM5 Run3 is recommended for the photochemical modeling of the Dallas Forth Worth Area. In Run3, the wind performance is the best among the all four runs. From previous CAMx and other photochemical modeling experience, the performance of wind direction and speed is proved to be essential to the air quality modeling. The overall performance of temperature and humidity in Run3 is comparable or better than the other runs, except that the humidity performance of Run1a is the best among all runs. Therefore, we believe that Run3 is our best choice and Run1a is also usable given its best performance in humidity and acceptable performance in wind and temperature.

# REFERENCES


Anthes, R.A., E.Y. Hsie, Y.H.Kao. 1987. "Description of the Penn State/NCAR Mesoscale Model Version 4 (MM4)." NCAR Technical Note 282, National Center for Atmospheric Research, Boulder, CO.

Anthes, R.A. and T.T. Warner. 1978. The development of mesoscale models suitable for air pollution and other mesometeorological studies. *Mon. Wea. Rev.*, Vol. 106, pp.1045-1078.

Dudhia, J. 1993. A non-hydrostatic version of the Penn State/NCAR mesoscale model: validation tests and simulation of an atlantic cyclone and cold front. *Mon. Wea. Rev.*, Vol. pp. 121, 1493-1513.

Emery, C.A. and E. Tai. 2002. "Meteorological Modeling and Performance Evaluation Of the August 13-22, 1999 Ozone Episodes". Prepared for the East Texas Council of Governments, Kilgore, TX, by ENVIRON, Novato, CA.

Emery, C.A., E. Tai, G. Yarwood. 2001. "Enhanced Meteorological Modeling and Performance Evaluation for Two Texas Ozone Episodes". Prepared for the Texas Natural Resource Conservation Commission, Austin, TX, by ENVIRON, Novato, CA.

ENVIRON. 2001b. "Development of a Joint CAMx Photochemical Modeling Database for the Four Southern Texas Near Non-Attainment Areas." Prepared for the Texas Near Non-Attainment Areas through the Alamo Area Council of Governments, by ENVIRON, Novato, CA.

ENVIRON. 2001a. "Ozone Modeling Protocol for FY 2000/2001 Projects in the Tyler/Longview/Marshall Area of East Texas." Prepared for the East Texas Council of Governments, Kilgore, TX, by ENVIRON, Novato, CA.

ENVIRON. 2000. "User's Guide: Comprehensive Air quality Model with extensions (CAMx), Version 3.00". Prepared by ENVIRON International Corp., Novato, CA.

EPA. 1999. "Draft Guidance on the Use of Models and Other Analyses in Attainment Demonstrations for the 8-Hour Ozone NAAQS." Prepared by the U.S. Environmental Protection Agency, Office of Air Quality Planning and Standards, Research Triangle Park, NC.

Grell, G.A., J. Dudhia, and D.R. Stauffer. 1994. "A Description of the Fifth Generation Penn State/NCAR Mesoscale Model (MM5)." NCAR Tech. Note, NCAR TN-398-STR, pp. 138.

Seaman, N.L. 2000. Meteorological modeling for air quality assessments. *Atmos. Environ.*, Vol. 34, pp. 2231-2259.

Yarwood, G., G. Mansell, G. McGaughey, and W. Vizuete. 2001. "Biogenic Emission Inventories for Regional Modeling of 1999 Ozone Episodes in Texas". Prepared for the Texas Natural Resource Conservation Commission, Austin, TX, by ENVIRON, Novato, CA.

# Appendix A

## Hourly and Daily Statistics of Wind, Temperature and Humidity for Run1, Run1a, and Run2

## TCEQ_DFW 12km Run1

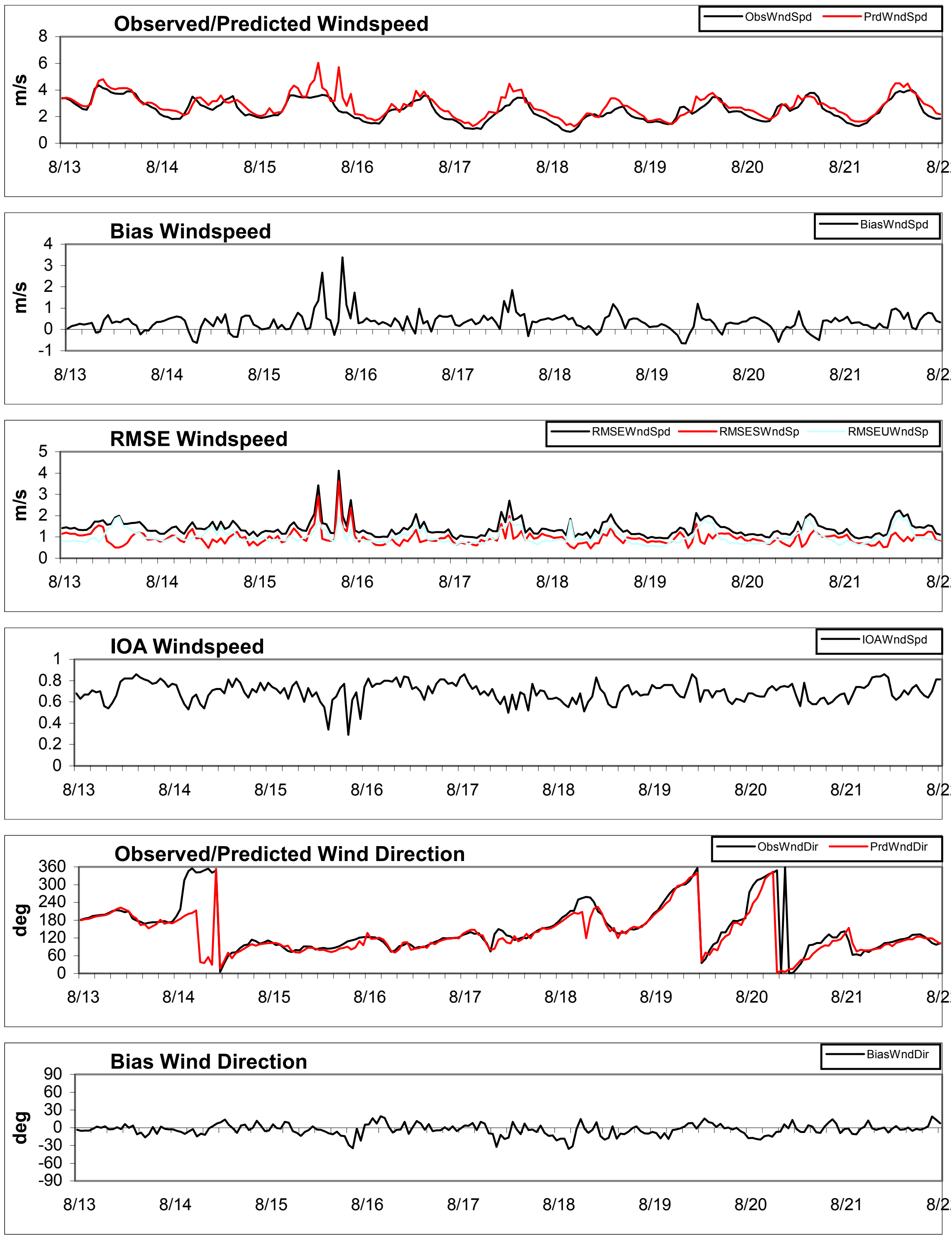


**Figure A-1a.** Hourly time series of region-average observed and predicted (Run1) surface-layer winds and performance statistics in the 12-km MM5 domain. RMSE is shown for total, systematic (RMSES) and unsystematic (RMSEU) components.

**TCEQ_DFW 12km Run1**

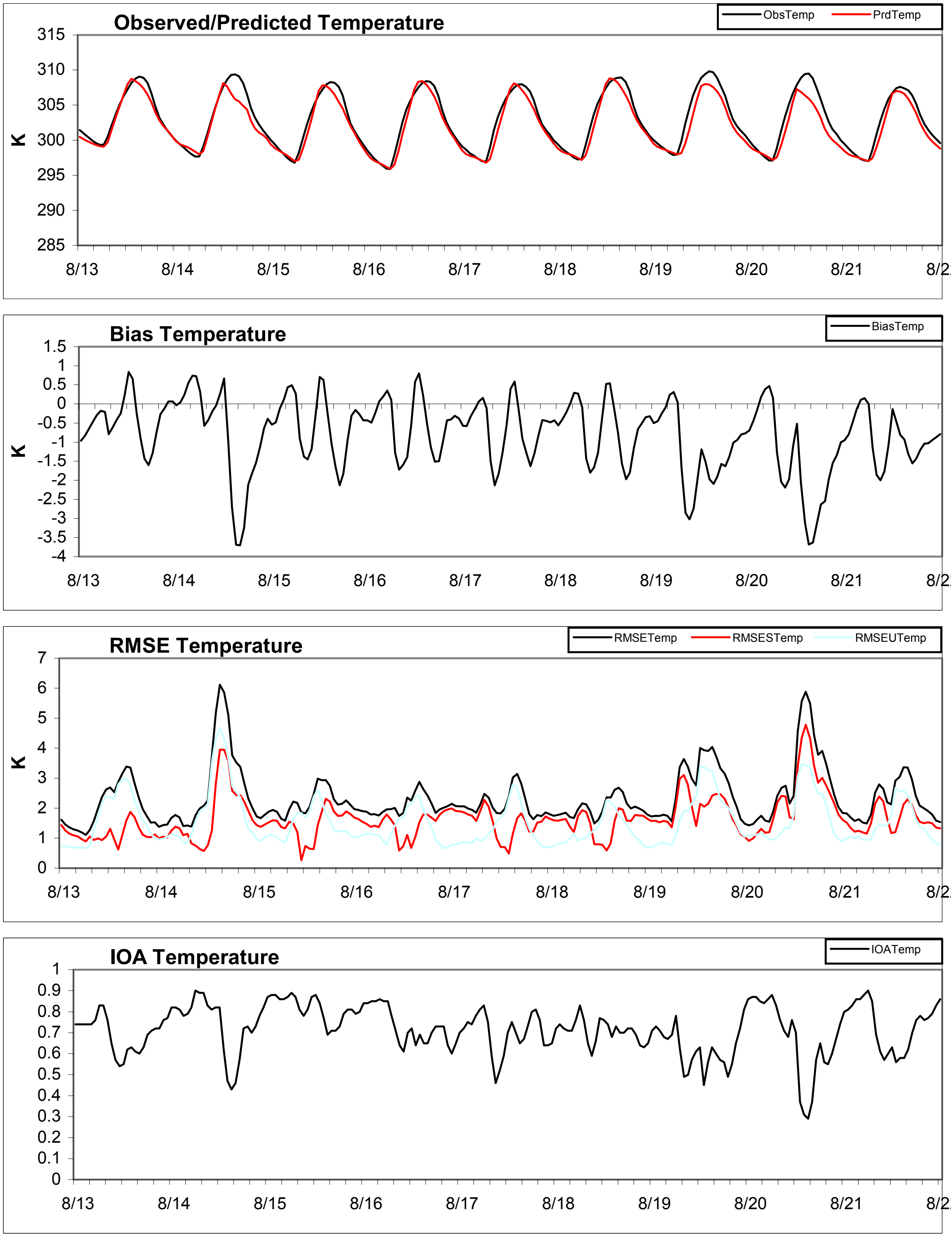


**Figure A-1b.** Hourly time series of region-average observed and predicted (Run1) surface-layer temperature and performance statistics in the 12-km MM5 domain. RMSE is shown for total, systematic (RMSES) and unsystematic (RMSEU) components.

**TCEQ_DFW 12km Run1**

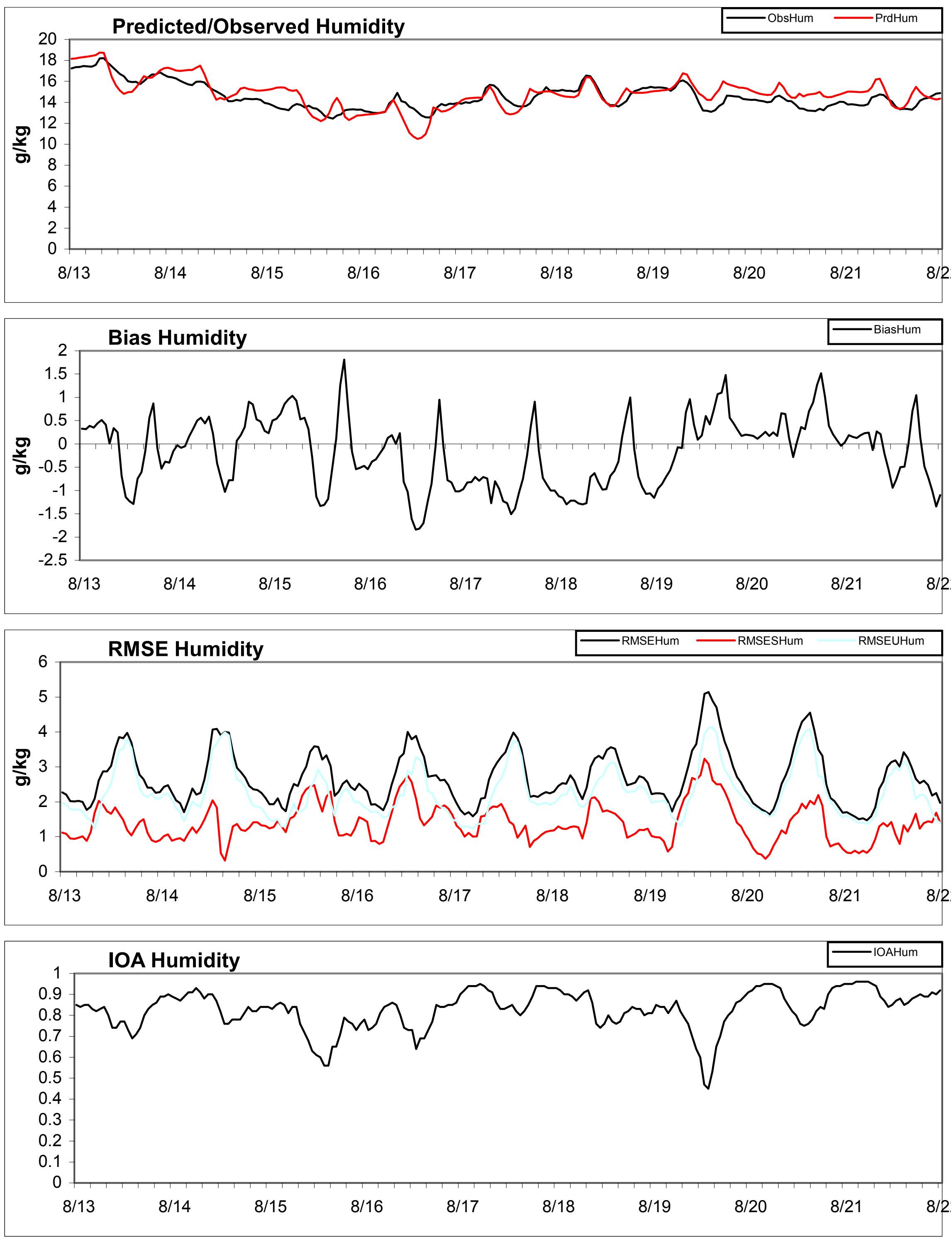


**Figure A-1c**. Hourly time series of region-average observed and predicted (Run1) surface-layer humidity and performance statistics in the 12-km MM5 domain. RMSE is shown for total, systematic (RMSES) and unsystematic (RMSEU) components.

## TCEQ_DFW 12km Run1a

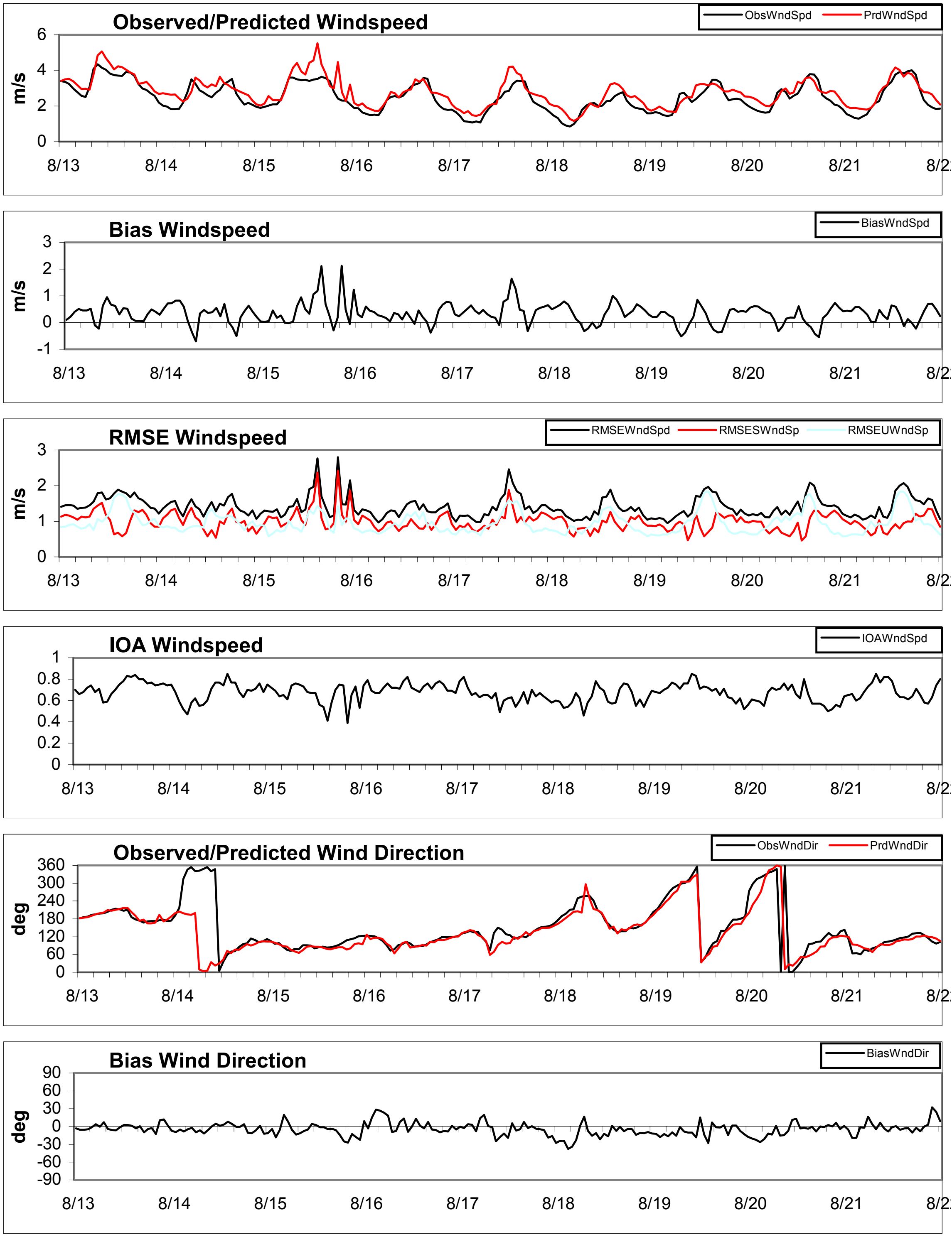


**Figure A-2a.** Hourly time series of region-average observed and predicted (Run1a) surface-layer winds and performance statistics in the 12-km MM5 domain. RMSE is shown for total, systematic (RMSES) and unsystematic (RMSEU) components.

## TCEQ_DFW 12km Run1a

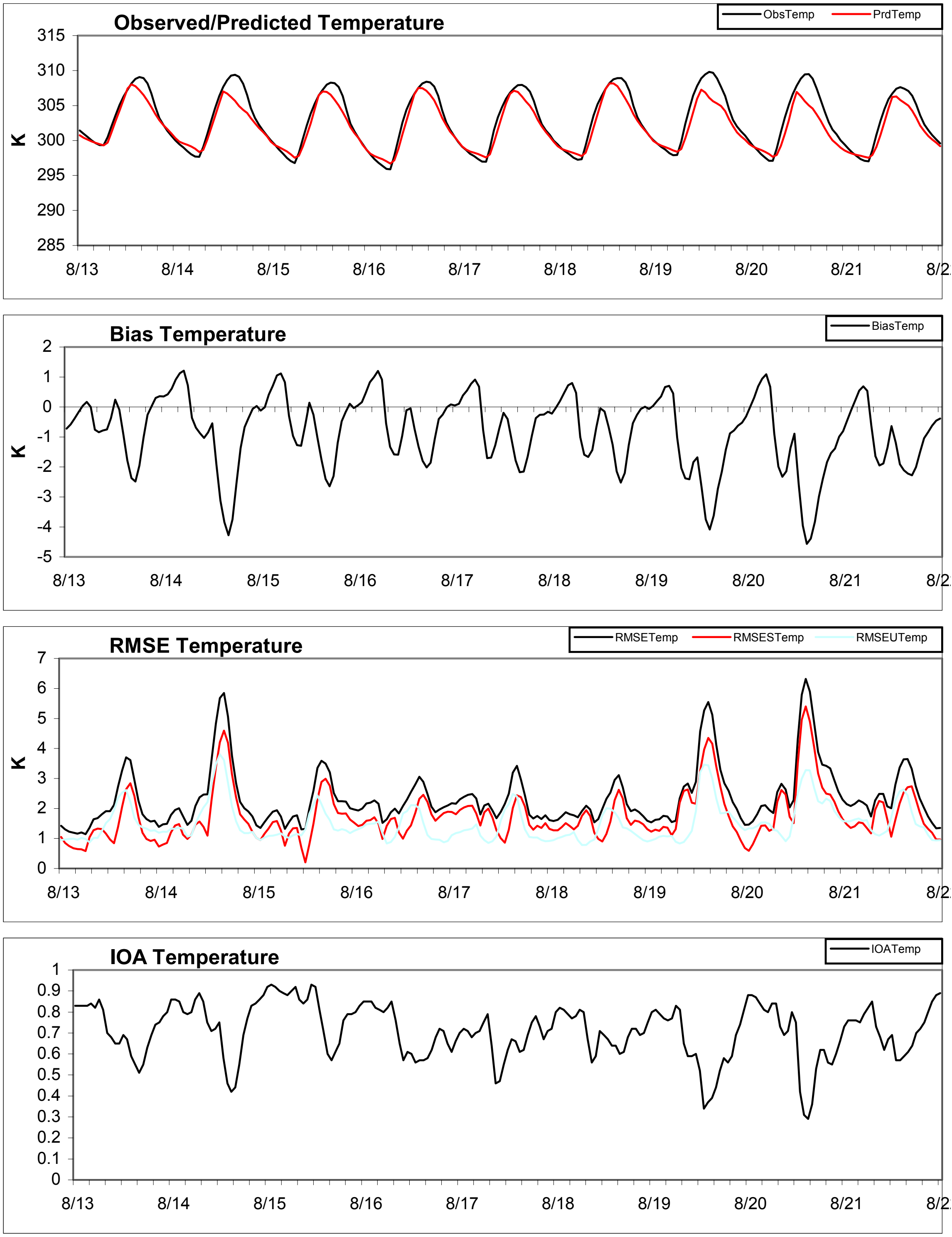


**Figure A-2b.** Hourly time series of region-average observed and predicted (Run1a) surface-layer temperature and performance statistics in the 12-km MM5 domain. RMSE is shown for total, systematic (RMSES) and unsystematic (RMSEU) components.

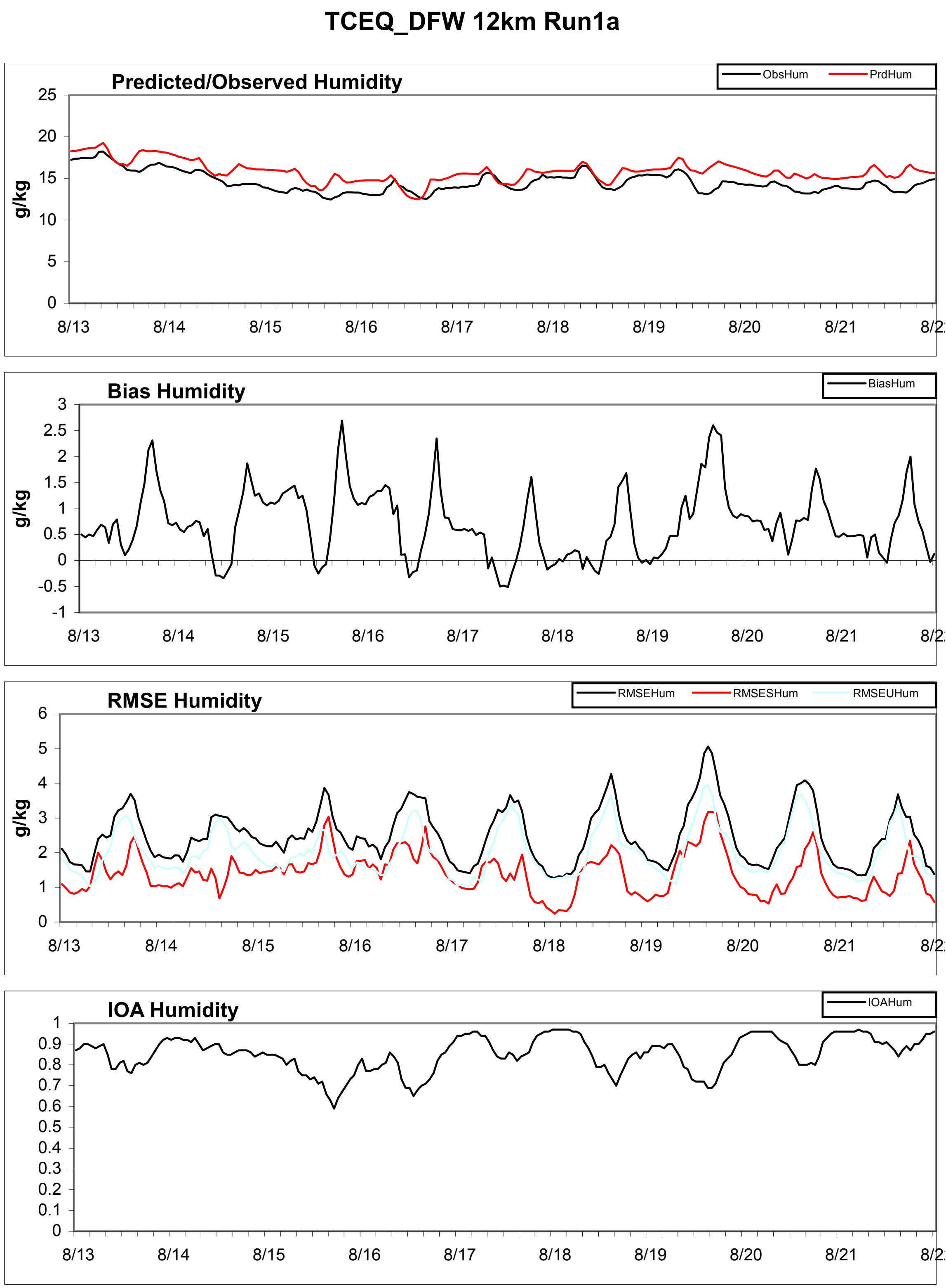


**Figure A-2c.** Hourly time series of region-average observed and predicted (Run1a) surface-layer humidity and performance statistics in the 12-km MM5 domain. RMSE is shown for total, systematic (RMSES) and unsystematic (RMSEU) components.

# TCEQ_DFW 12km Run2

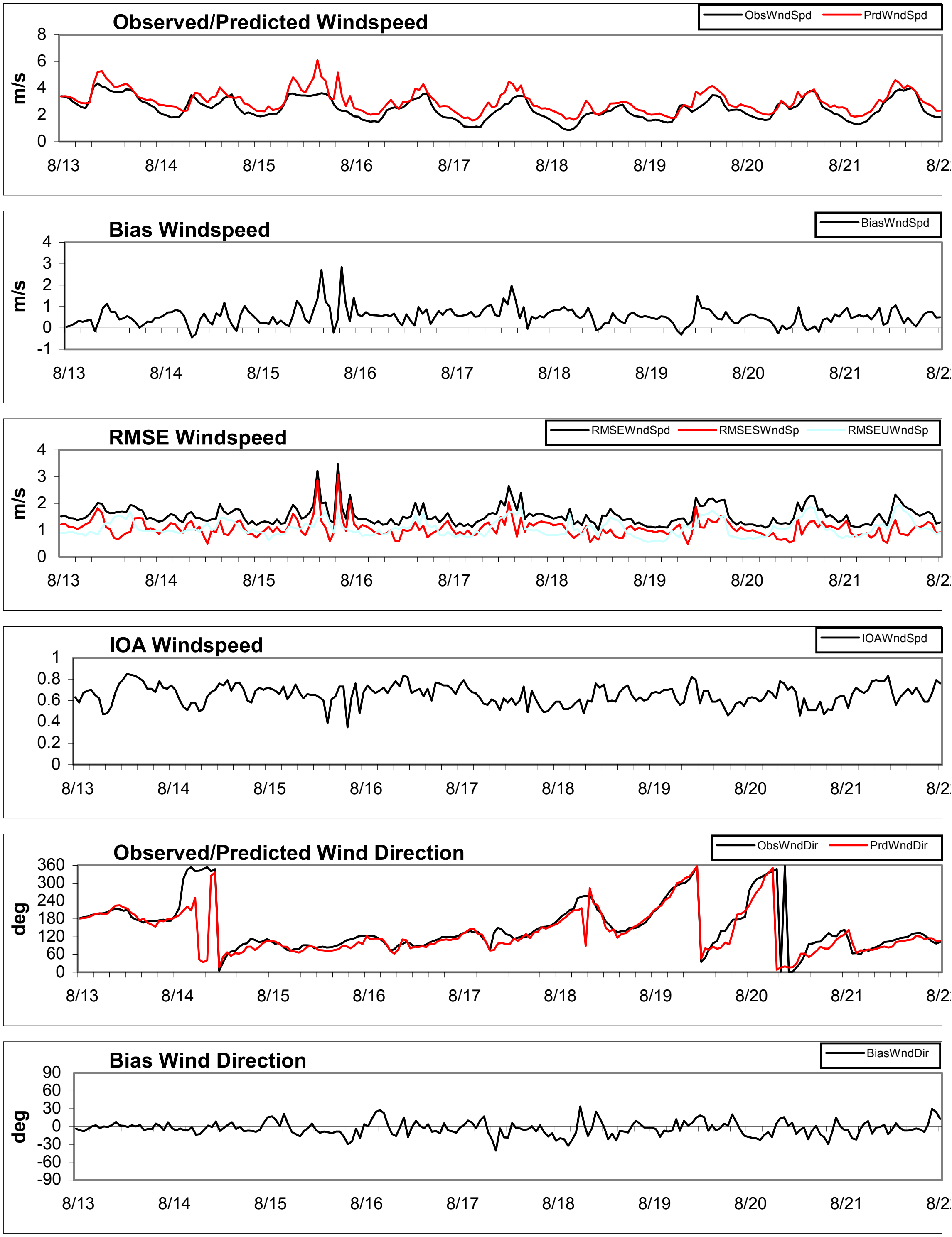


**Figure A-3a.** Hourly time series of region-average observed and predicted (Run2) surface-layer winds and performance statistics in the 12-km MM5 domain. RMSE is shown for total, systematic (RMSES) and unsystematic (RMSEU) components.

TCEQ_DFW 12km Run2

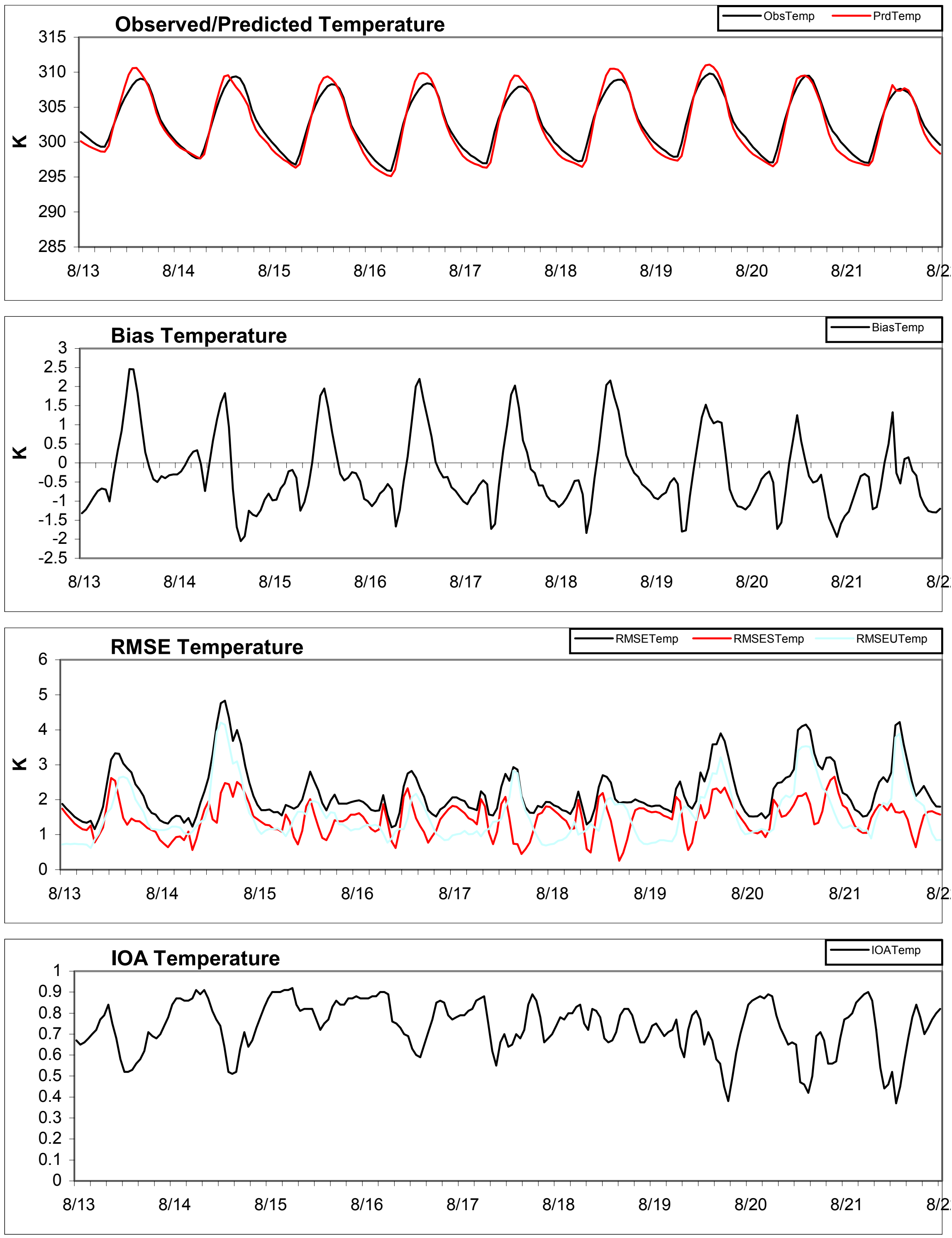


**Figure A-3b.** Hourly time series of region-average observed and predicted (Run2) surface-layer temperature and performance statistics in the 12-km MM5 domain. RMSE is shown for total, systematic (RMSES) and unsystematic (RMSEU) components.

TCEQ_DFW 12km Run2

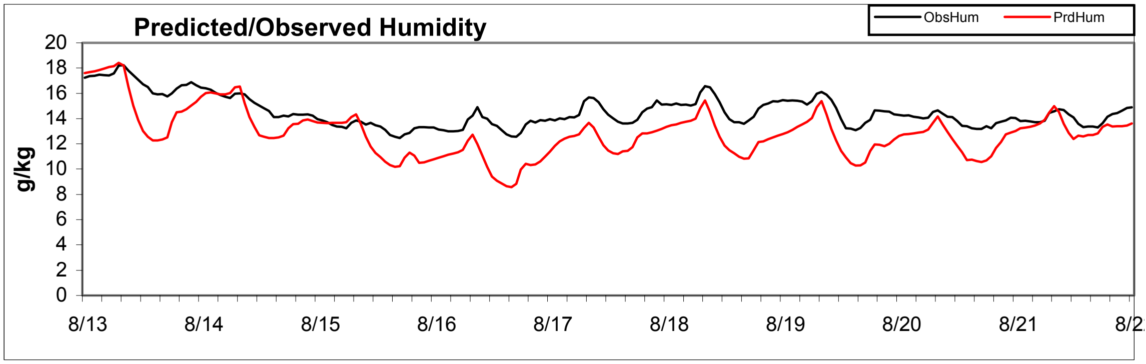


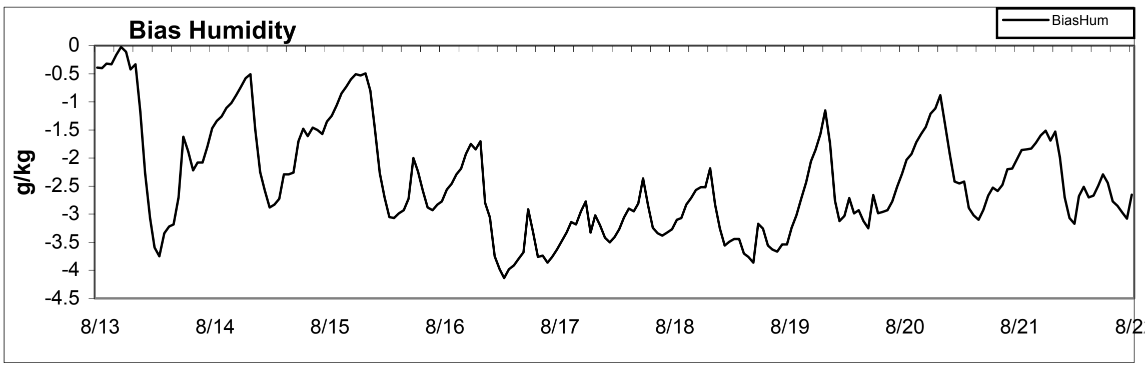


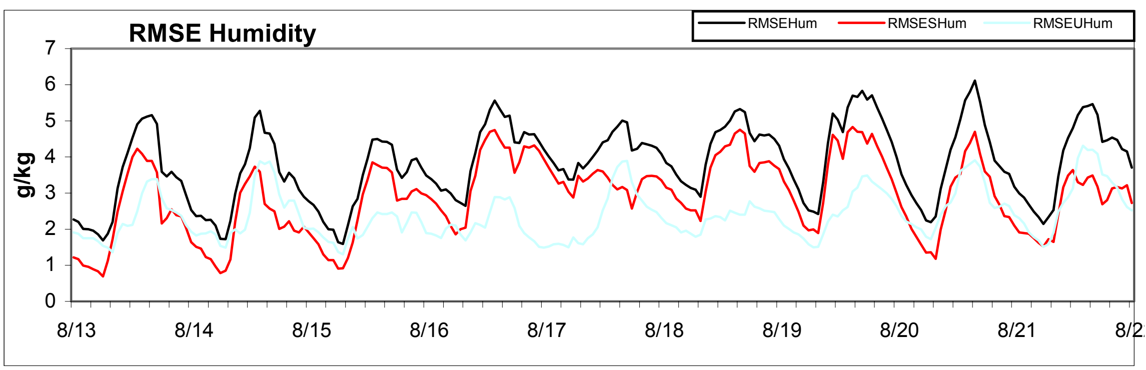


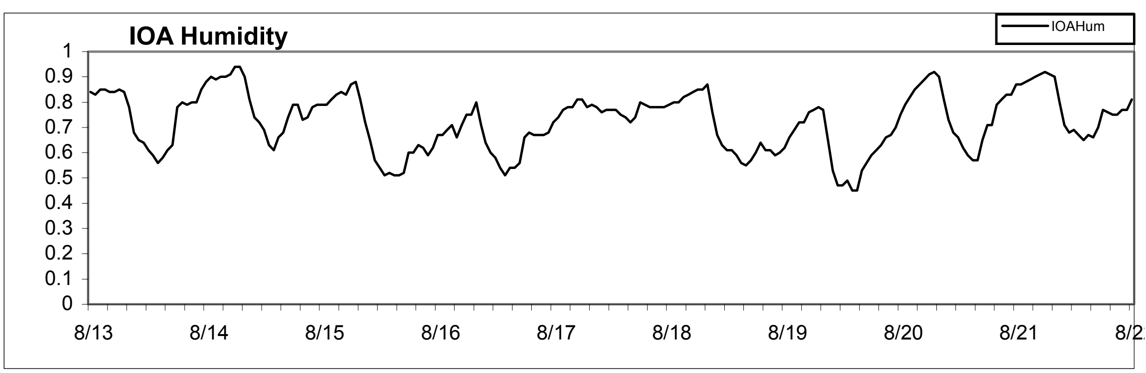


**Figure A-3c**. Hourly time series of region-average observed and predicted (Run2) surface-layer humidity and performance statistics in the 12-km MM5 domain. RMSE is shown for total, systematic (RMSES) and unsystematic (RMSEU) components.

**TCEQ_DFW 04km Run1**

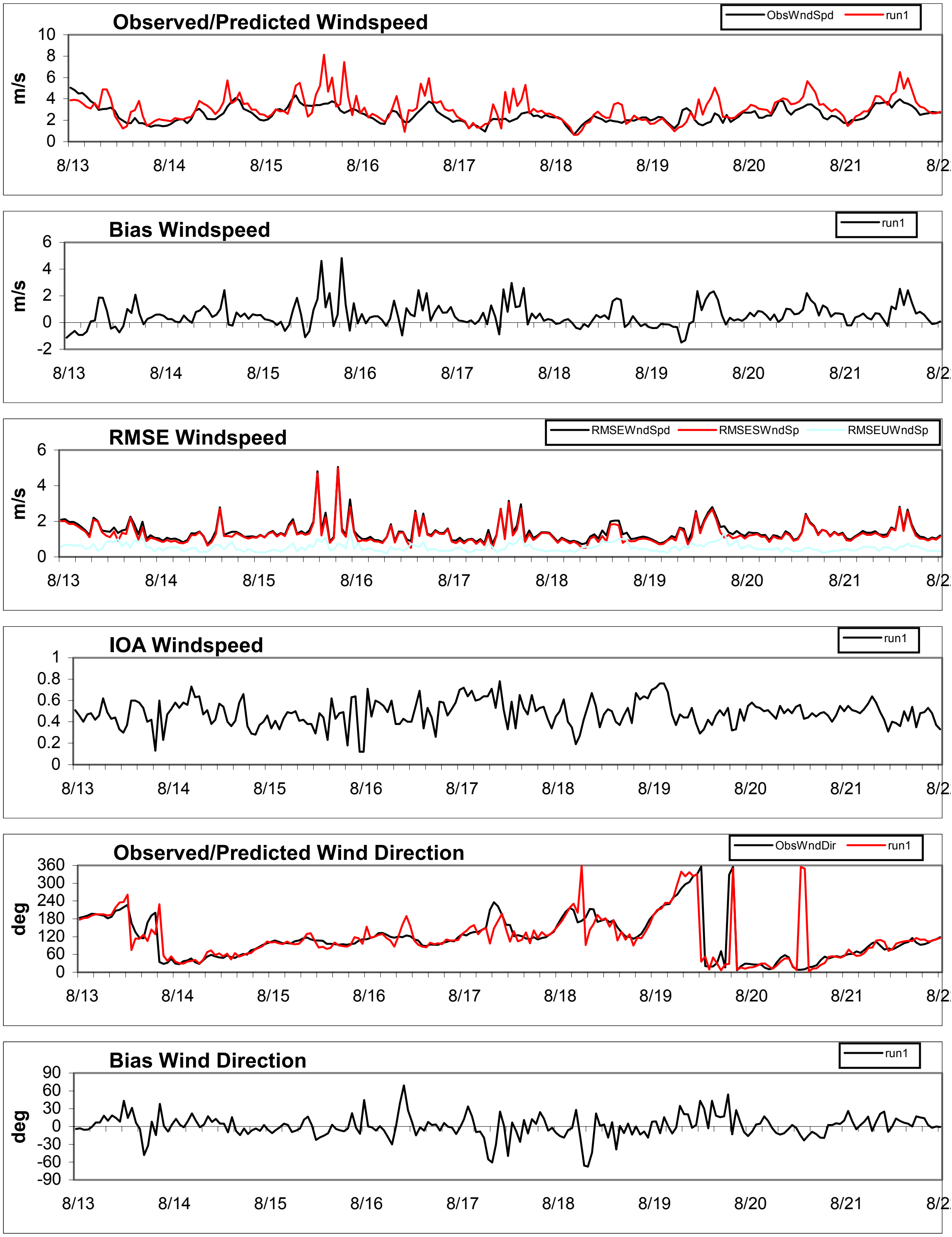


**Figure A-4a.** Hourly time series of region-average observed and predicted (Run1) surface-layer winds and performance statistics in the 4-km DFW MM5 domain. RMSE is shown for total, systematic (RMSES) and unsystematic (RMSEU) components.

**TCEQ_DFW 04km Run1**

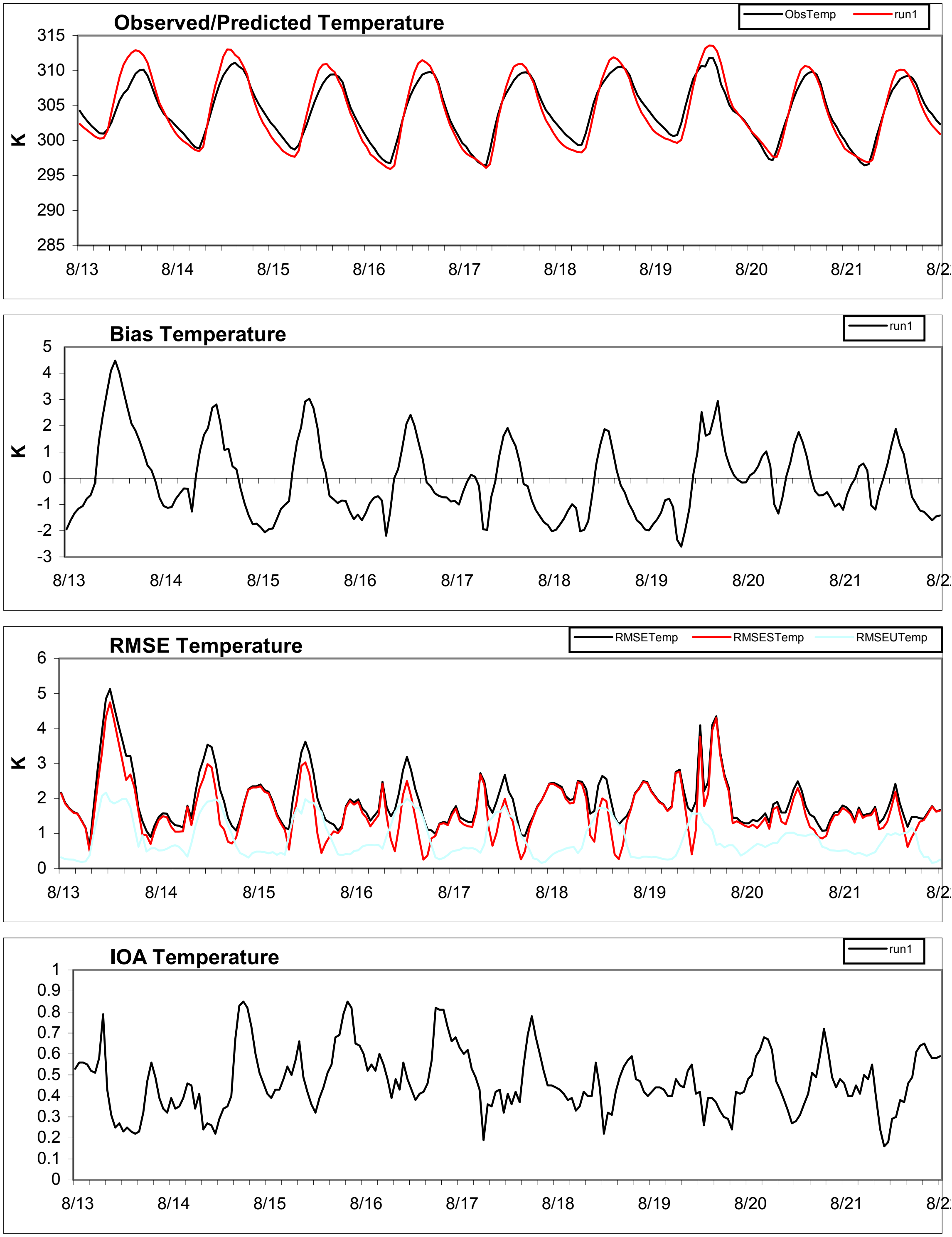


**Figure A-4b.** Hourly time series of region-average observed and predicted (Run1) surface-layer temperature and performance statistics in the 4-km DFW MM5 domain. RMSE is shown for total, systematic (RMSES) and unsystematic (RMSEU) components.

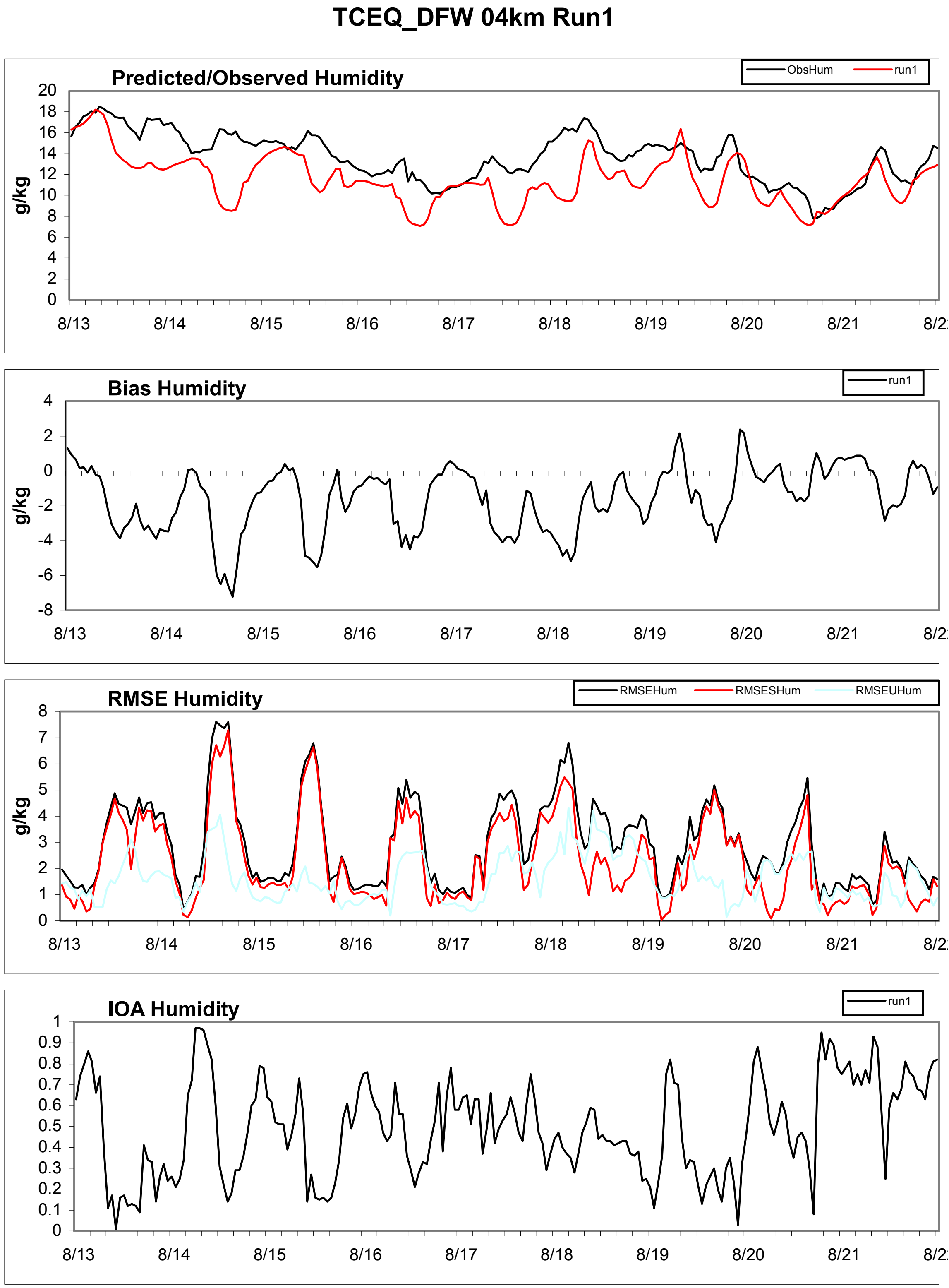


**Figure A-4c.** Hourly time series of region-average observed and predicted (Run1) surface-layer humidity and performance statistics in the 4-km DFW MM5 domain. RMSE is shown for total, systematic (RMSES) and unsystematic (RMSEU) components.

**TCEQ_DFW 04km Run1a**

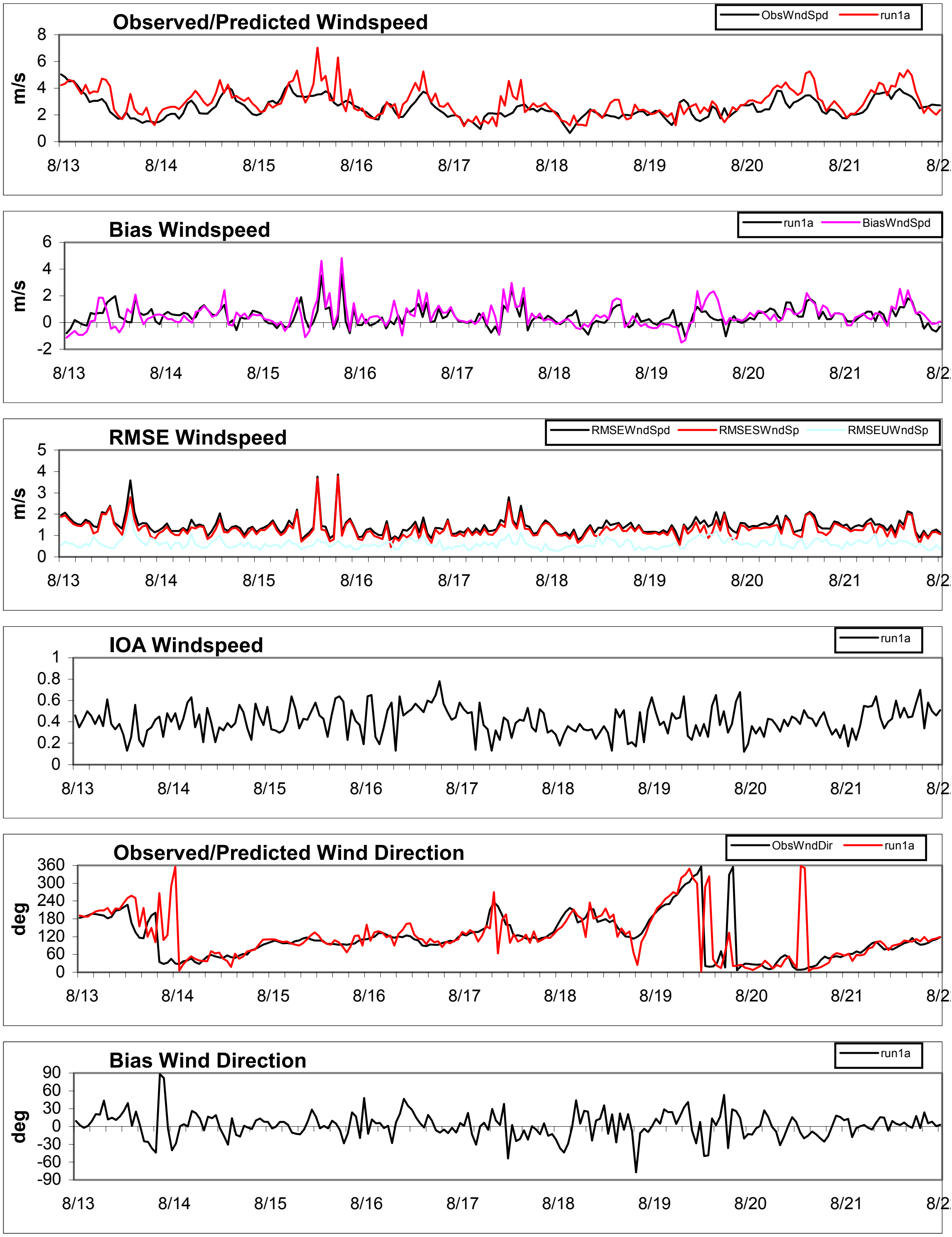


**Figure A-5a.** Hourly time series of region-average observed and predicted (Run1a) surface-layer winds and performance statistics in the 4-km DFW MM5 domain. RMSE is shown for total, systematic (RMSES) and unsystematic (RMSEU) components.

## TCEQ_DFW 04km Run1a

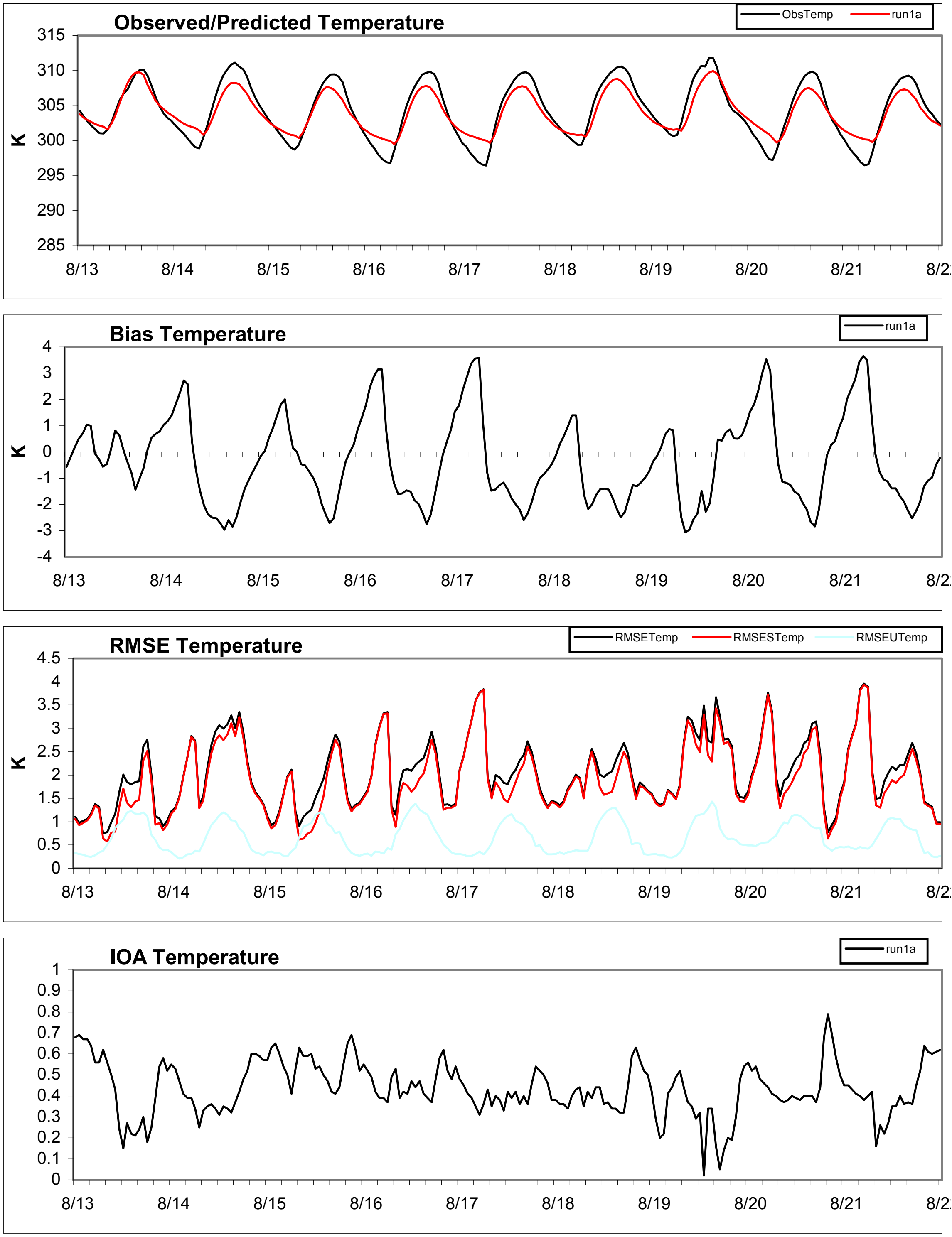


**Figure A-5b.** Hourly time series of region-average observed and predicted (Run1a) surface-layer temperature and performance statistics in the 4-km DFW MM5 domain. RMSE is shown for total, systematic (RMSES) and unsystematic (RMSEU) components.

## TCEQ_DFW 04km Run1a

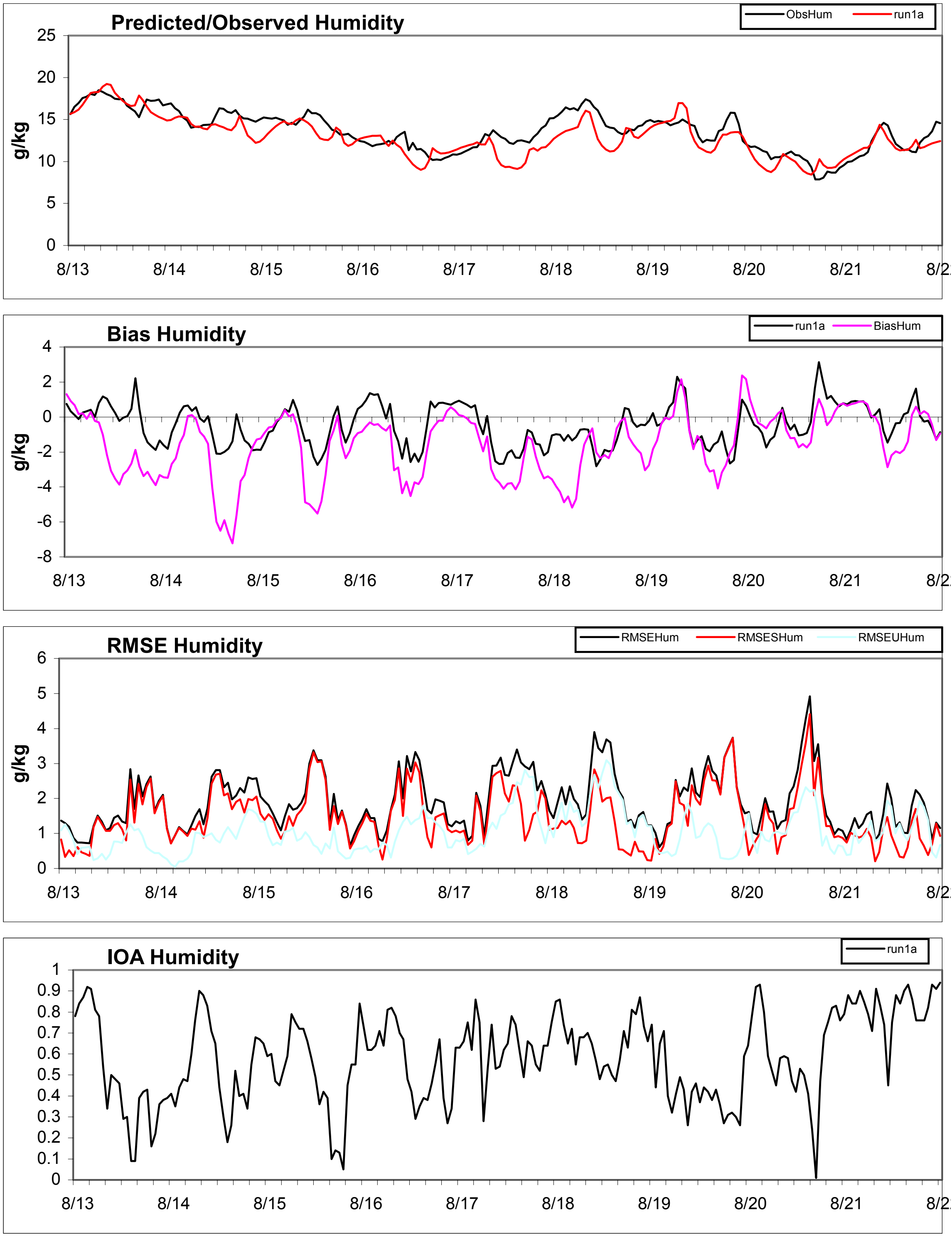


**Figure A-5c.** Hourly time series of region-average observed and predicted (Run1a) surface-layer humidity and performance statistics in the 4-km DFW MM5 domain. RMSE is shown for total, systematic (RMSES) and unsystematic (RMSEU) components.

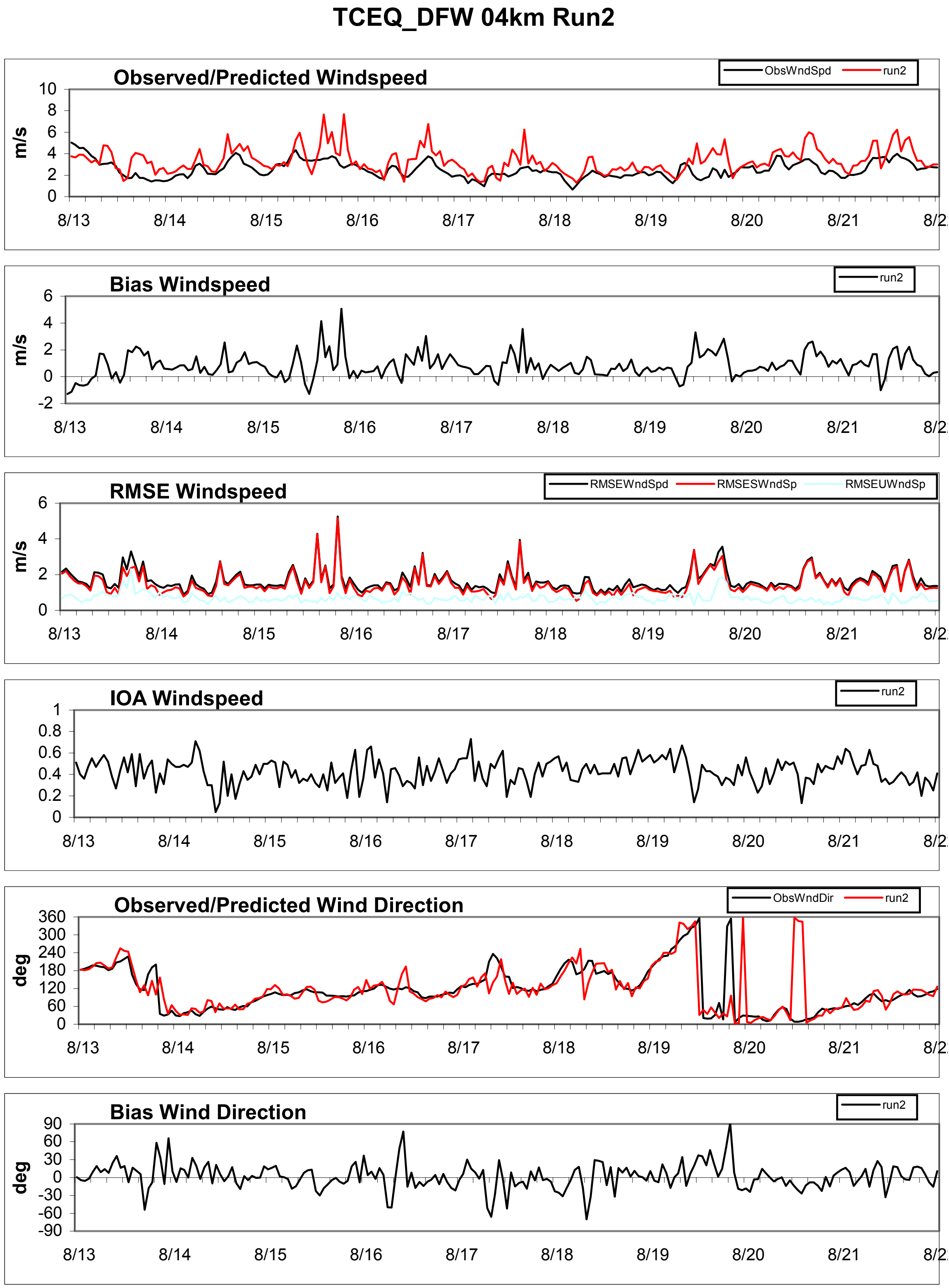


**Figure A-6a.** Hourly time series of region-average observed and predicted (Run2) surface-layer winds and performance statistics in the 4-km DFW MM5 domain. RMSE is shown for total, systematic (RMSES) and unsystematic (RMSEU) components.

**TCEQ_DFW 04km Run2**

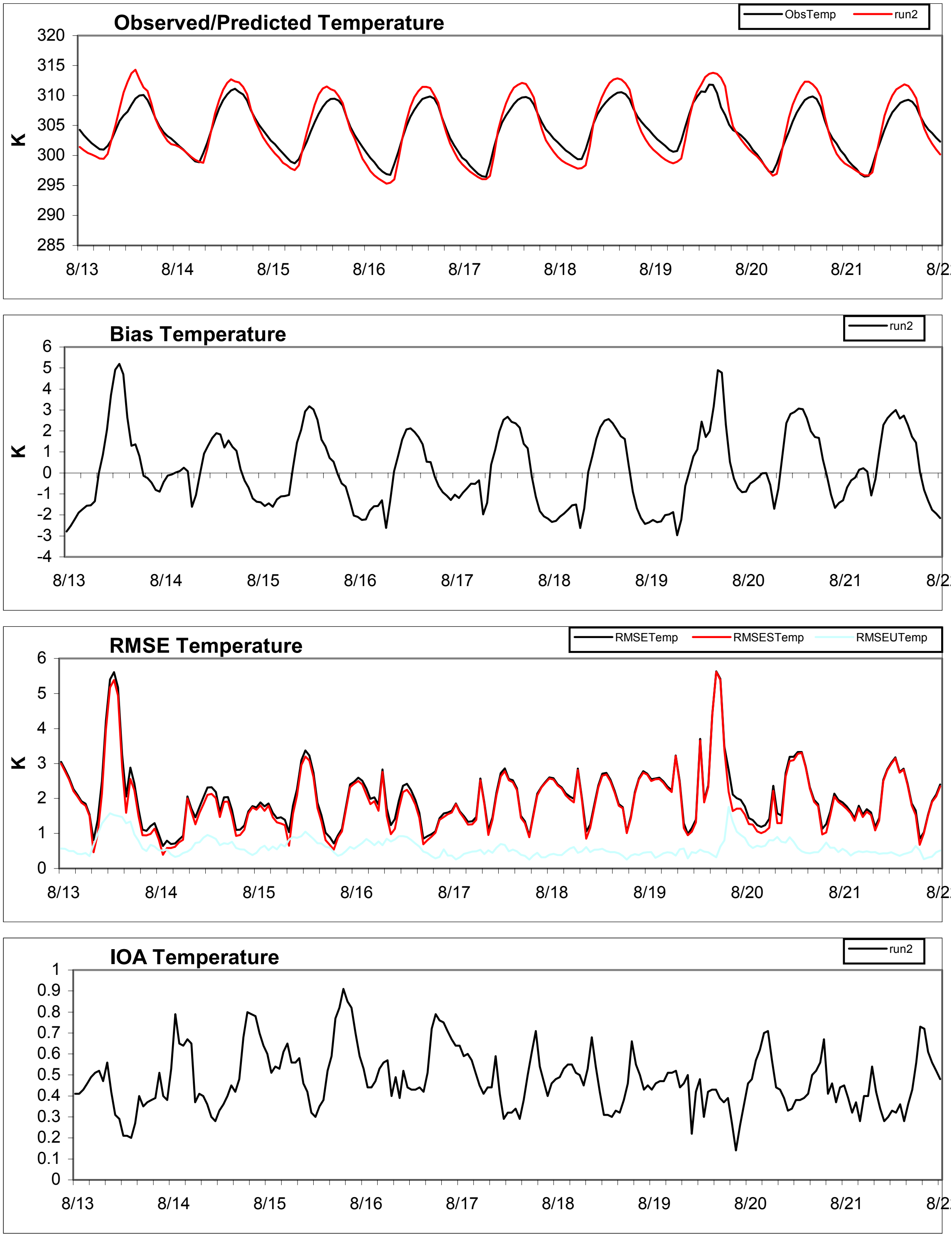


**Figure A-6b.** Hourly time series of region-average observed and predicted (Run2) surface-layer temperature and performance statistics in the 4-km DFW MM5 domain. RMSE is shown for total, systematic (RMSES) and unsystematic (RMSEU) components.

## TCEQ_DFW 04km Run2

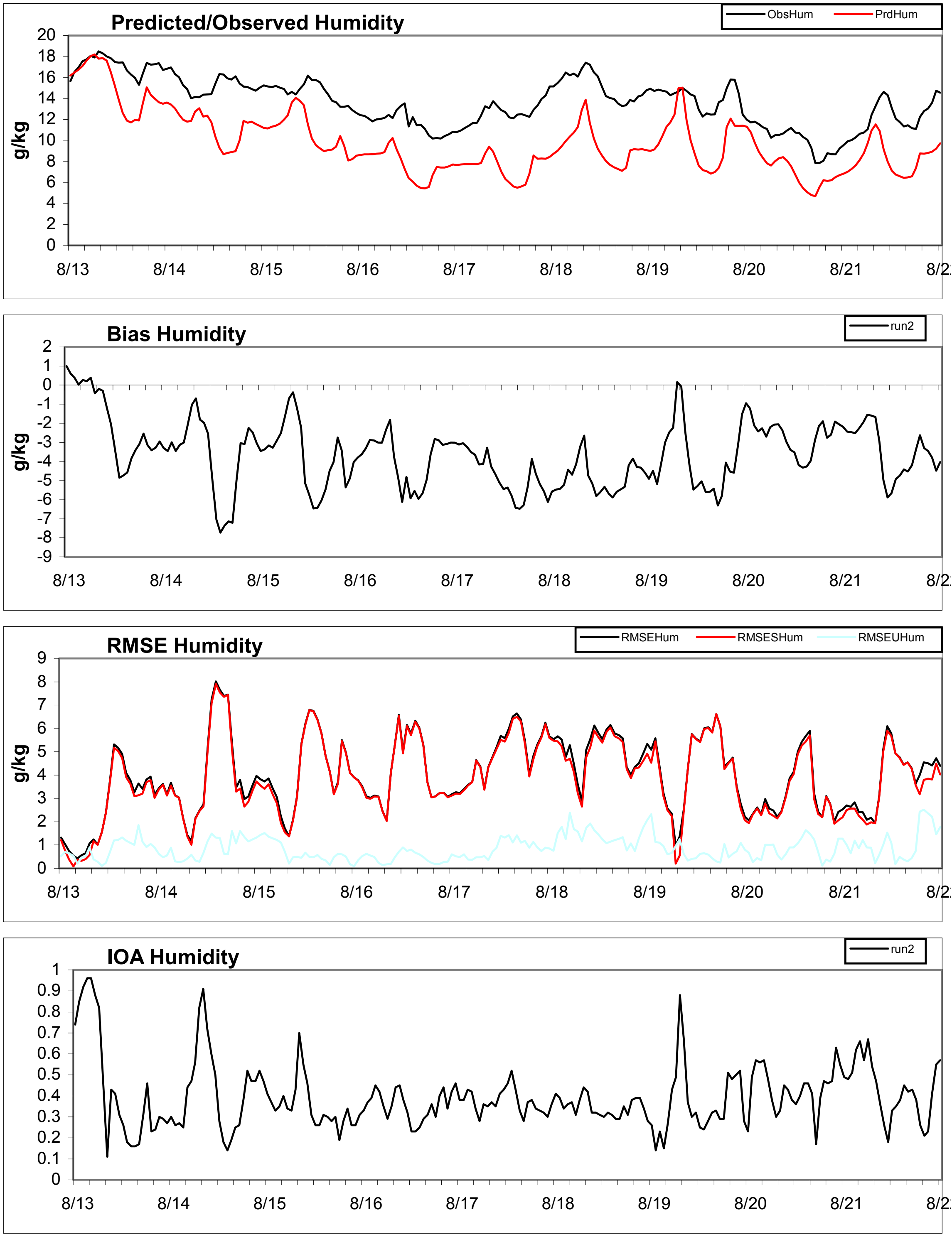


**Figure A-6c.** Hourly time series of region-average observed and predicted (Run2) surface-layer humidity and performance statistics in the 4-km DFW MM5 domain. RMSE is shown for total, systematic (RMSES) and unsystematic (RMSEU) components.

## TCEQ_DFW 12km Run1

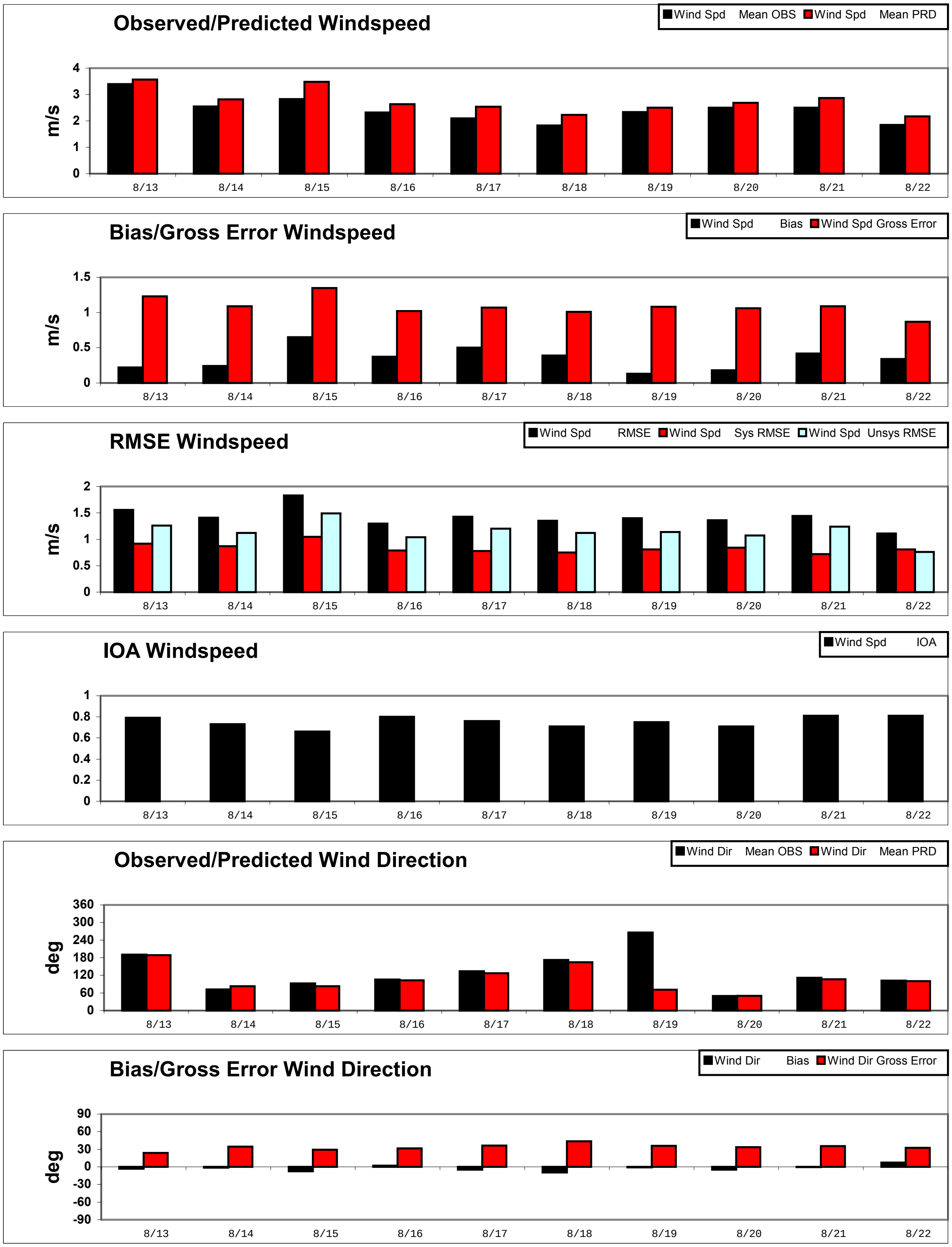


**Figure A-7a.** Daily time series of region-average observed and predicted (Run1) surface-layer winds and performance statistics in the 12-km MM5 domain. RMSE is shown for total, systematic (RMSES) and unsystematic (RMSEU) components.

TCEQ_DFW 12km Run1

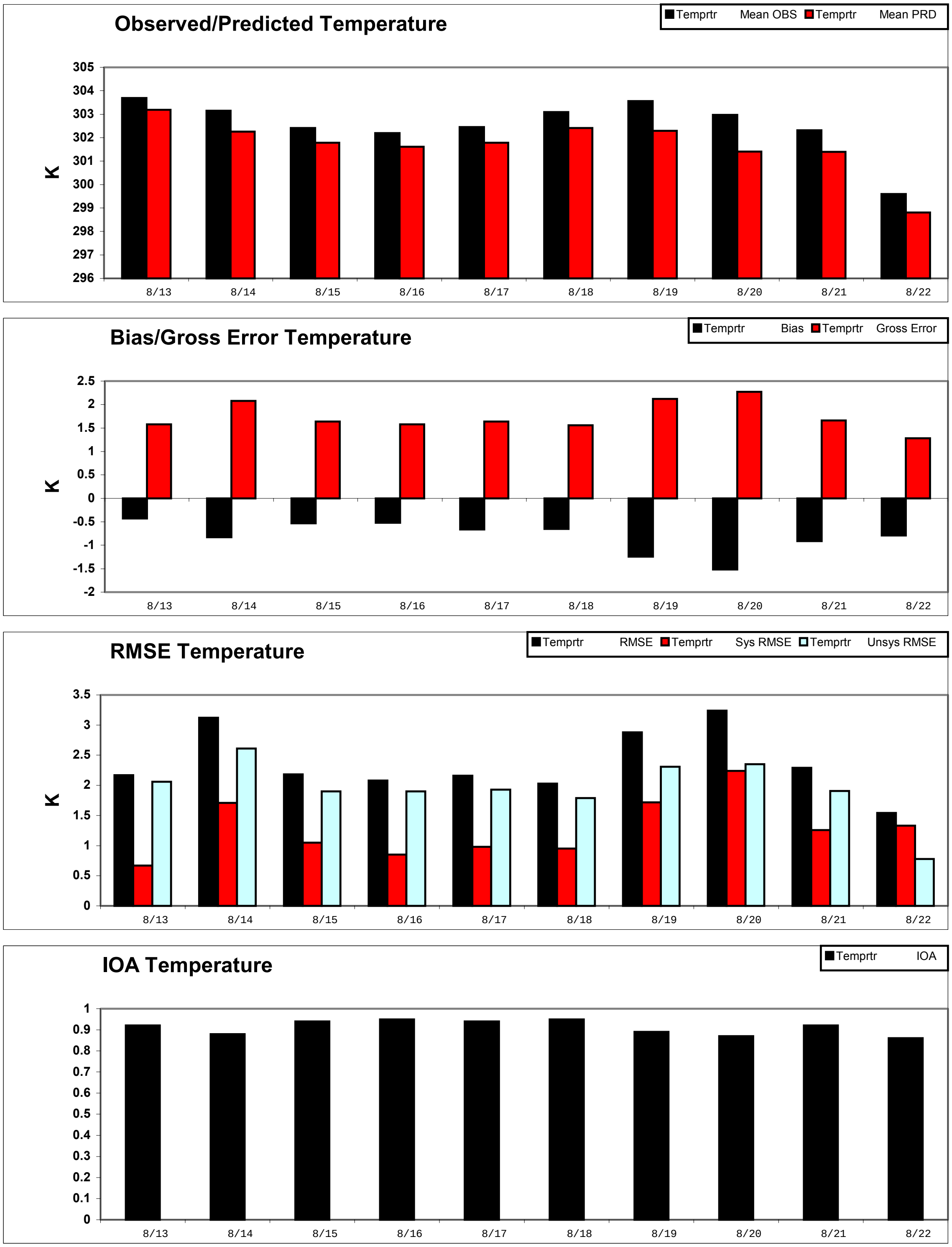


**Figure A-7b.** Daily time series of region-average observed and predicted (Run1) surface-layer temperature and performance statistics in the 12-km MM5 domain. RMSE is shown for total, systematic (RMSES) and unsystematic (RMSEU) components.

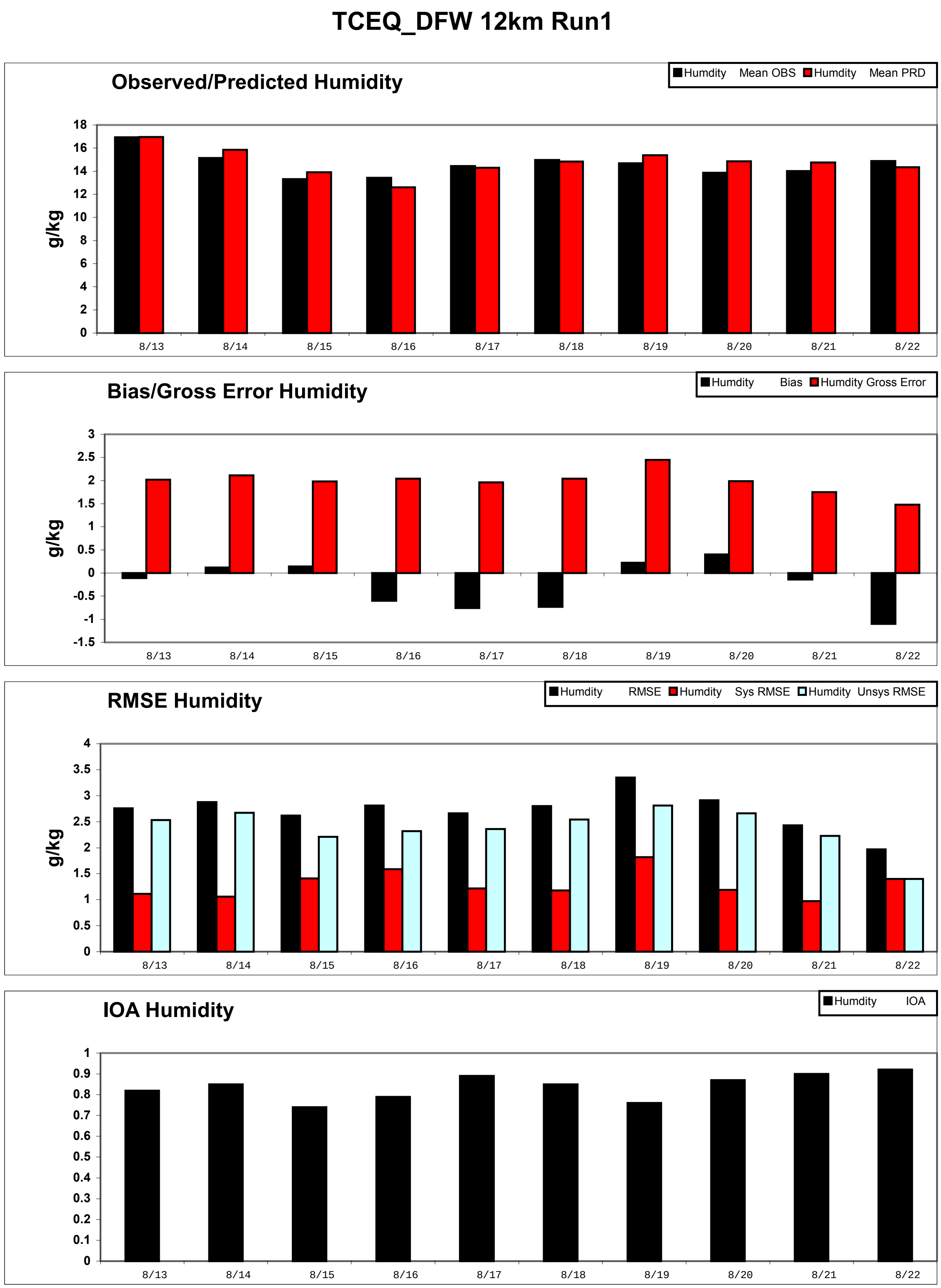


**Figure A-7c.** Daily time series of region-average observed and predicted (Run1) surface-layer humidity and performance statistics in the 12-km MM5 domain. RMSE is shown for total, systematic (RMSES) and unsystematic (RMSEU) components.

# TCEQ_DFW 12km Run1a

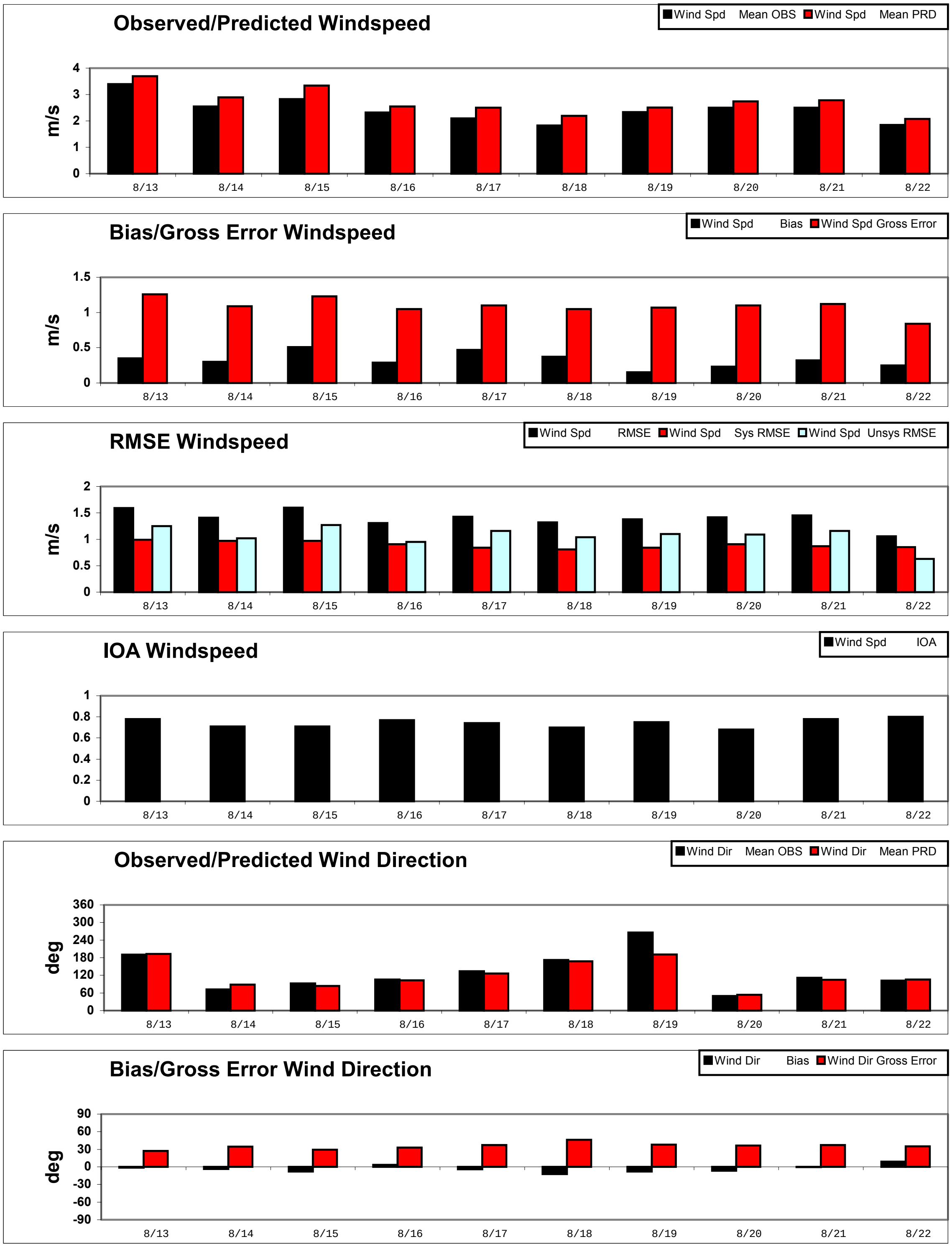


**Figure A-8a.** Daily time series of region-average observed and predicted (Run1a) surface-layer winds and performance statistics in the 12-km MM5 domain. RMSE is shown for total, systematic (RMSES) and unsystematic (RMSEU) components.

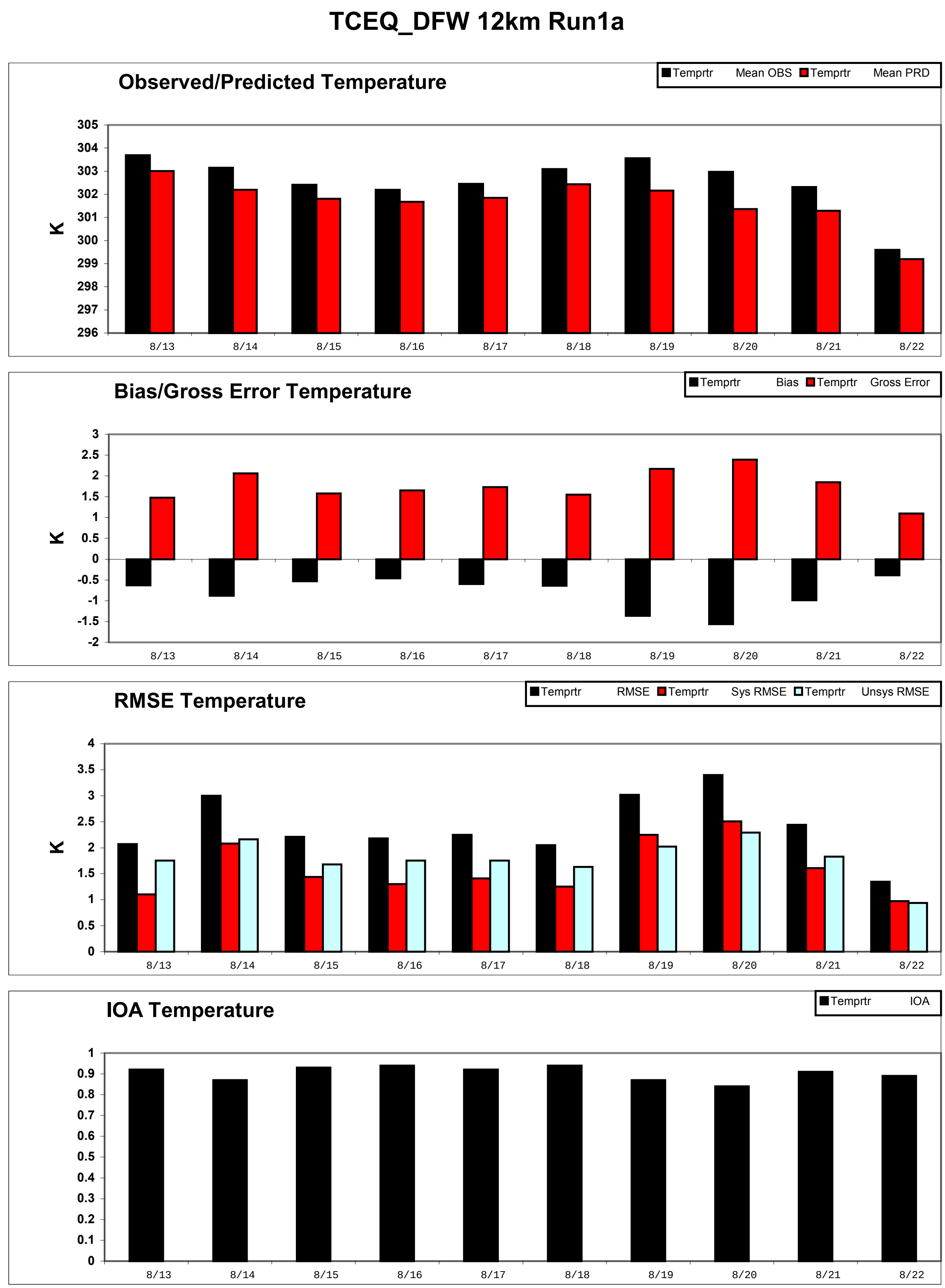


**Figure A-8b.** Daily time series of region-average observed and predicted (Run1a) surface-layer temperature and performance statistics in the 12-km MM5 domain. RMSE is shown for total, systematic (RMSES) and unsystematic (RMSEU) components.

## TCEQ_DFW 12km Run1a

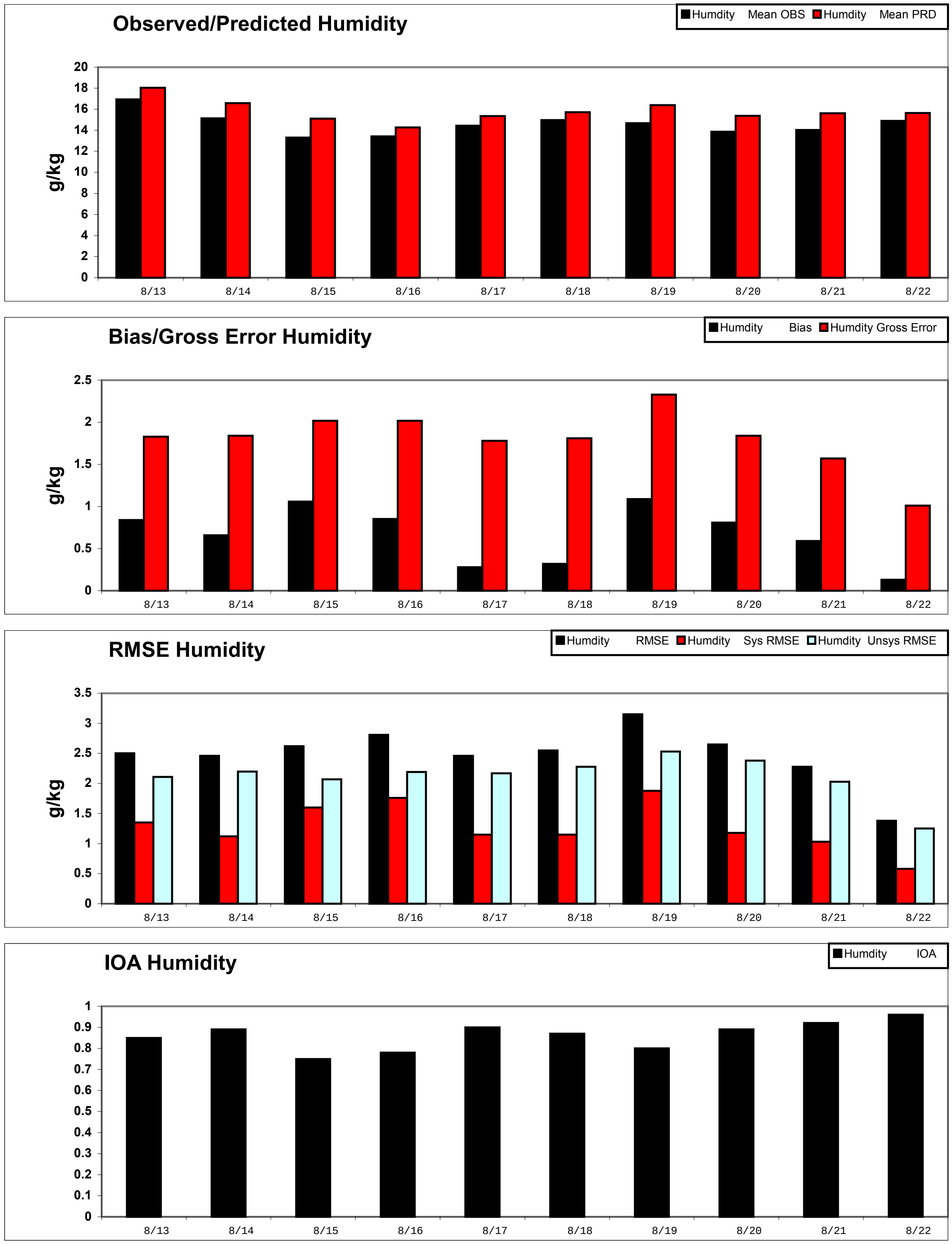


**Figure A-8c.** Daily time series of region-average observed and predicted (Run1a) surface-layer humidity and performance statistics in the 12-km MM5 domain. RMSE is shown for total, systematic (RMSES) and unsystematic (RMSEU) components.

# TCEQ_DFW 12km Run2

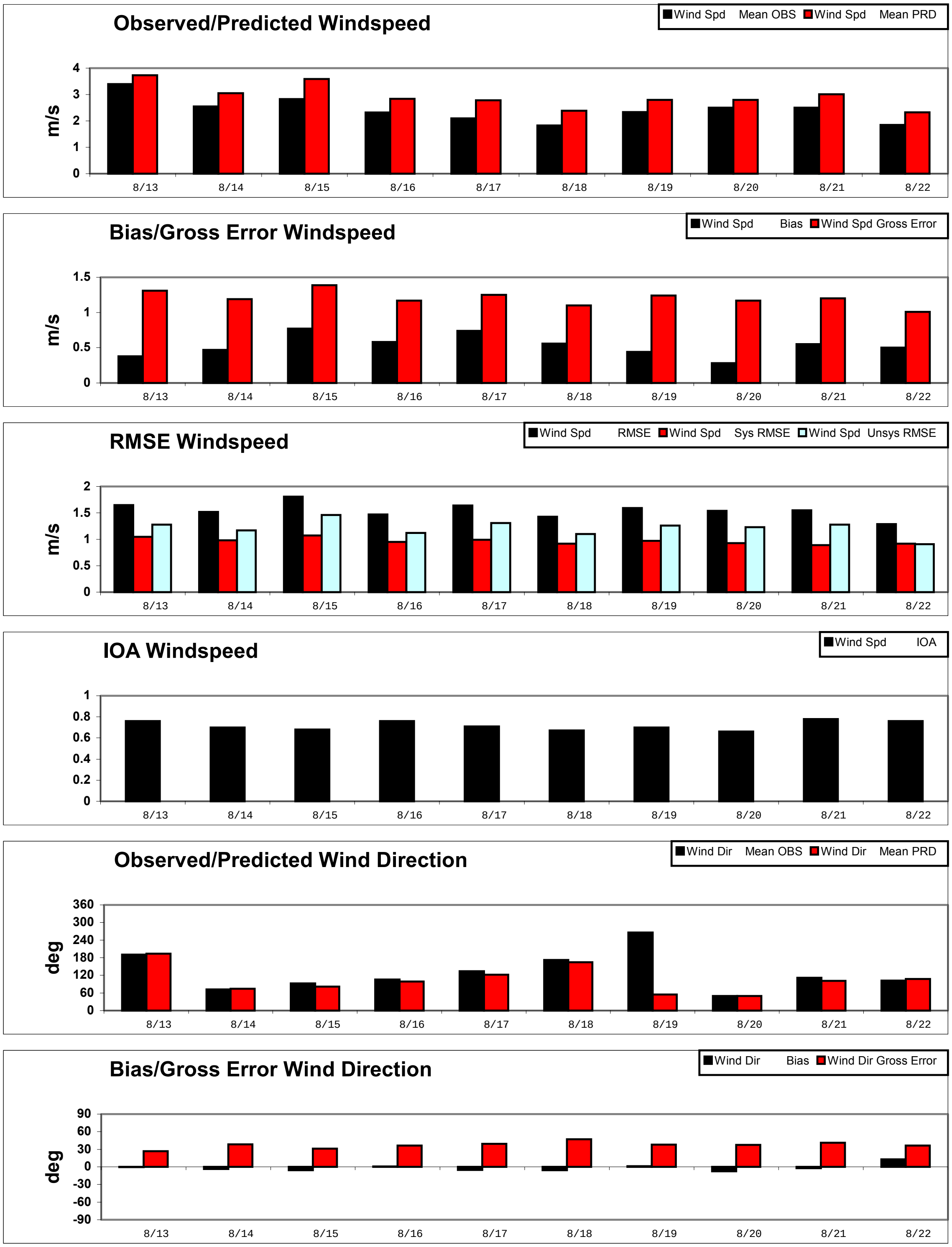


**Figure A-9a.** Daily time series of region-average observed and predicted (Run2) surface-layer winds and performance statistics in the 12-km MM5 domain. RMSE is shown for total, systematic (RMSES) and unsystematic (RMSEU) components.

## TCEQ_DFW 12km Run2

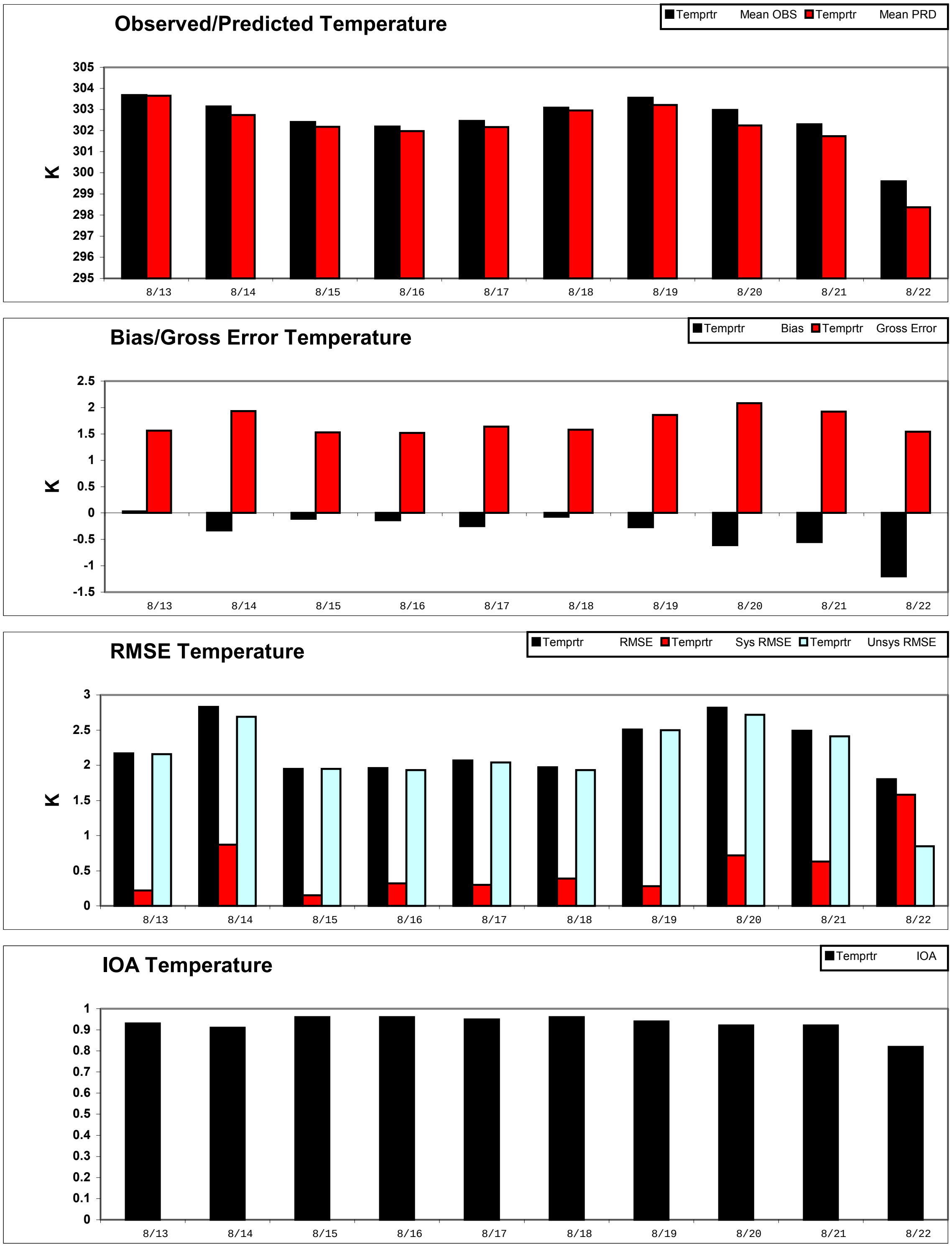


**Figure A-9b.** Daily time series of region-average observed and predicted (Run2) surface-layer temperature and performance statistics in the 12-km MM5 domain. RMSE is shown for total, systematic (RMSES) and unsystematic (RMSEU) components.

## TCEQ_DFW 12km Run2

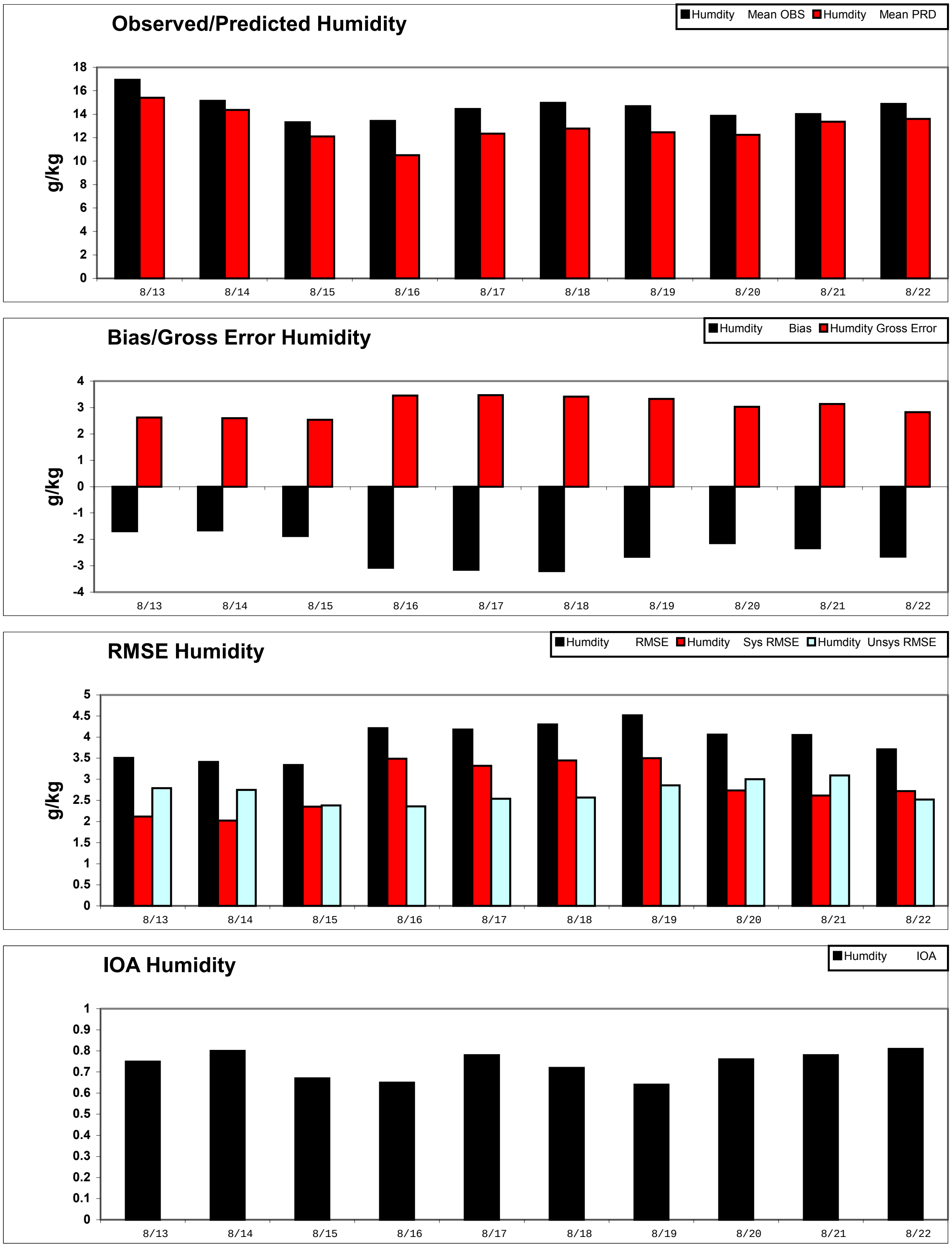


**Figure A-9c.** Daily time series of region-average observed and predicted (Run2) surface-layer humidity and performance statistics in the 12-km MM5 domain. RMSE is shown for total, systematic (RMSES) and unsystematic (RMSEU) components.

## TCEQ_DFW 04km Run1

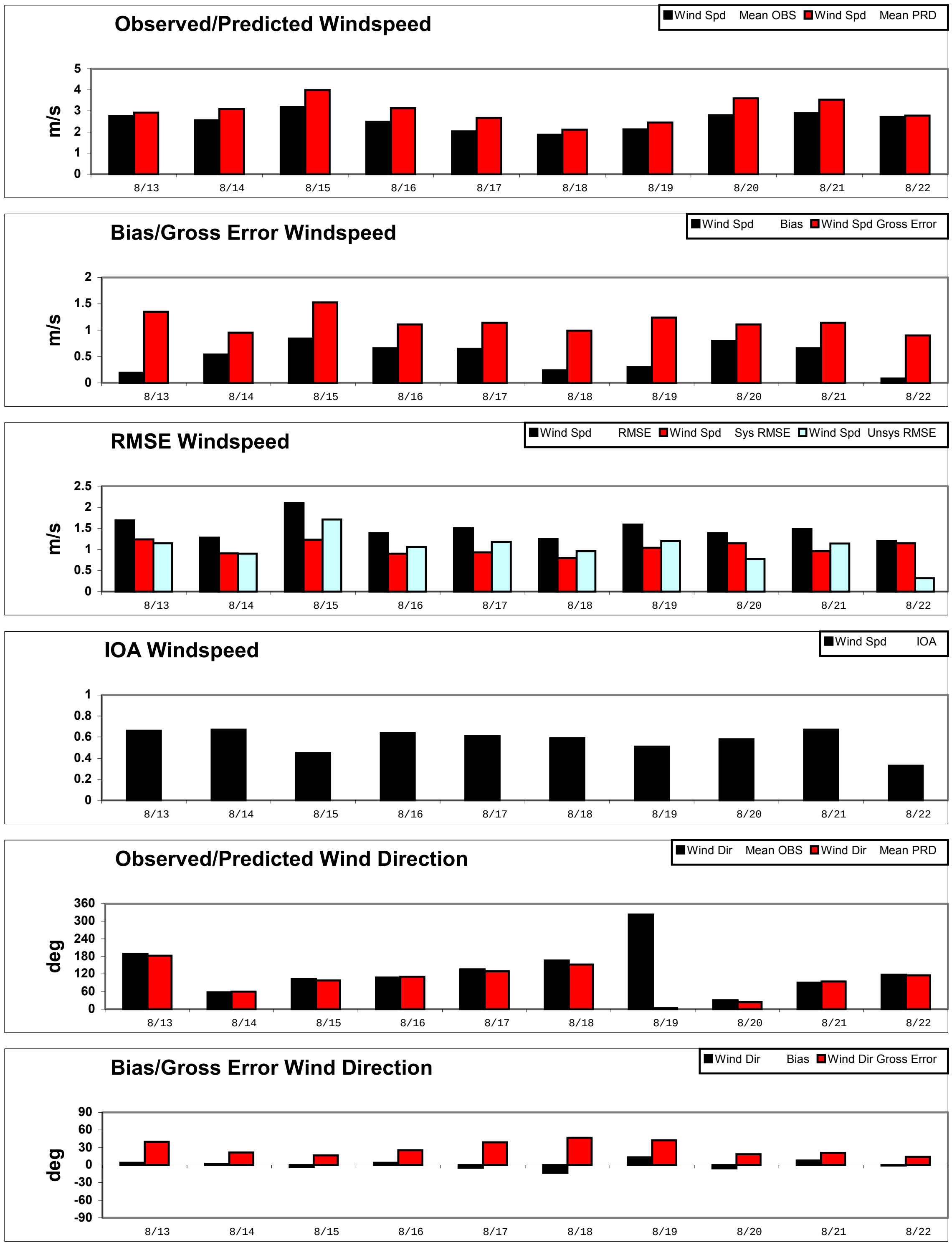


**Figure A-10a**. Daily time series of region-average observed and predicted (Run1) surface-layer winds and performance statistics in the 4-km DFW MM5 domain. RMSE is shown for total, systematic (RMSES) and unsystematic (RMSEU) components.

## TCEQ_DFW 04km Run1

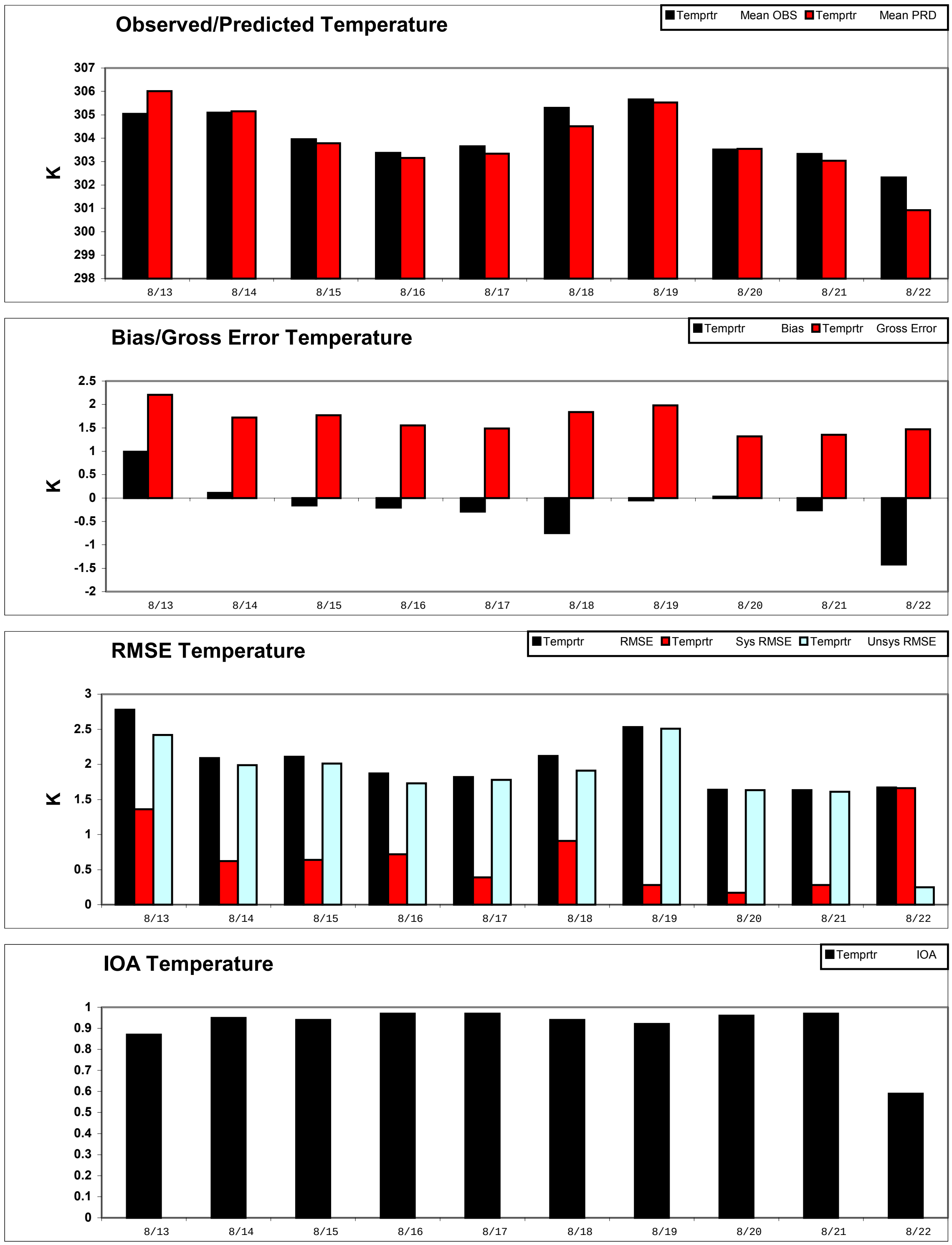


**Figure A-10b.** Daily time series of region-average observed and predicted (Run1) surface-layer temperature and performance statistics in the 4-km DFW MM5 domain. RMSE is shown for total, systematic (RMSES) and unsystematic (RMSEU) components.

## TCEQ_DFW 04km Run1

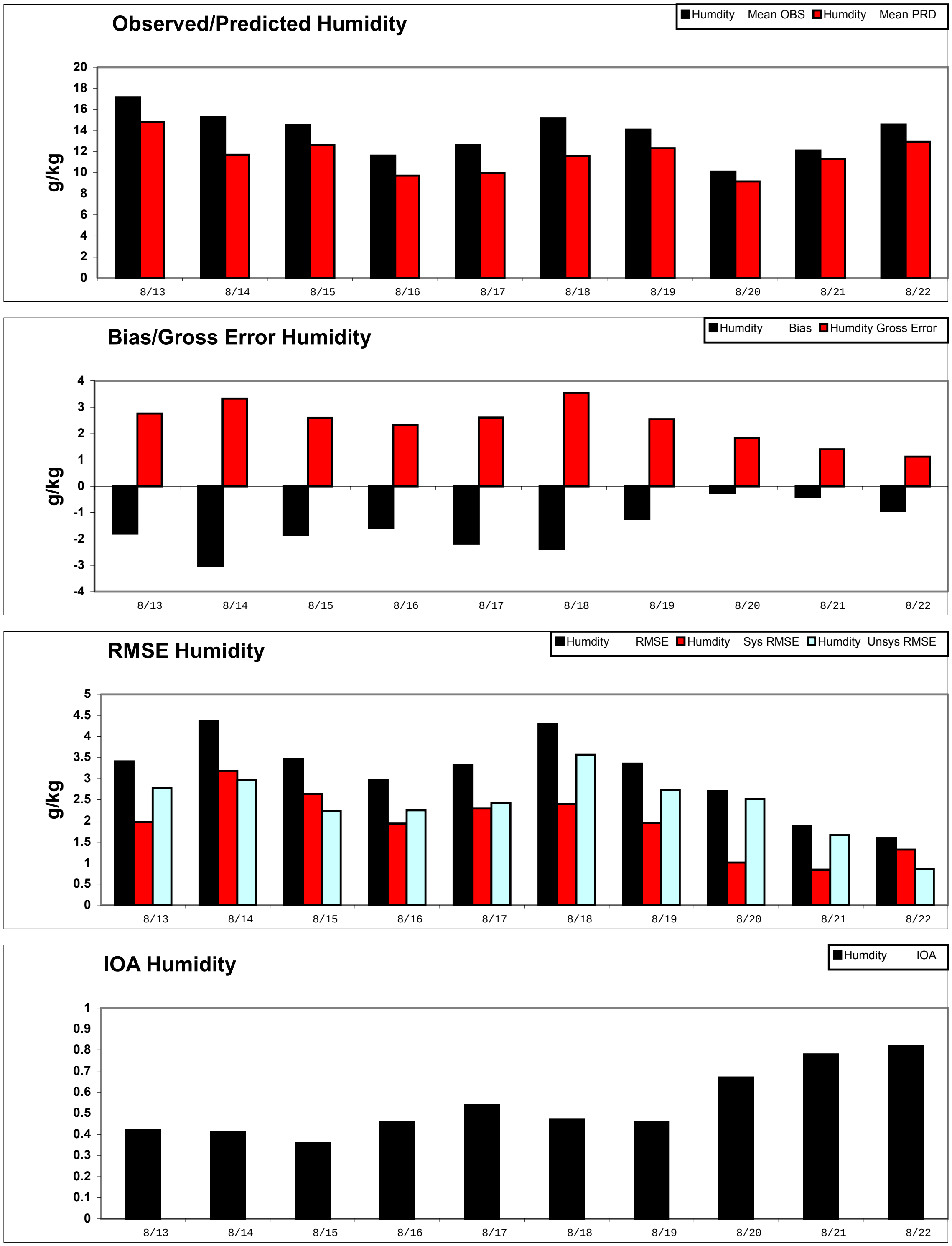


**Figure A-10c.** Daily time series of region-average observed and predicted (Run1) surface-layer humidity and performance statistics in the 4-km DFW MM5 domain. RMSE is shown for total, systematic (RMSES) and unsystematic (RMSEU) components.

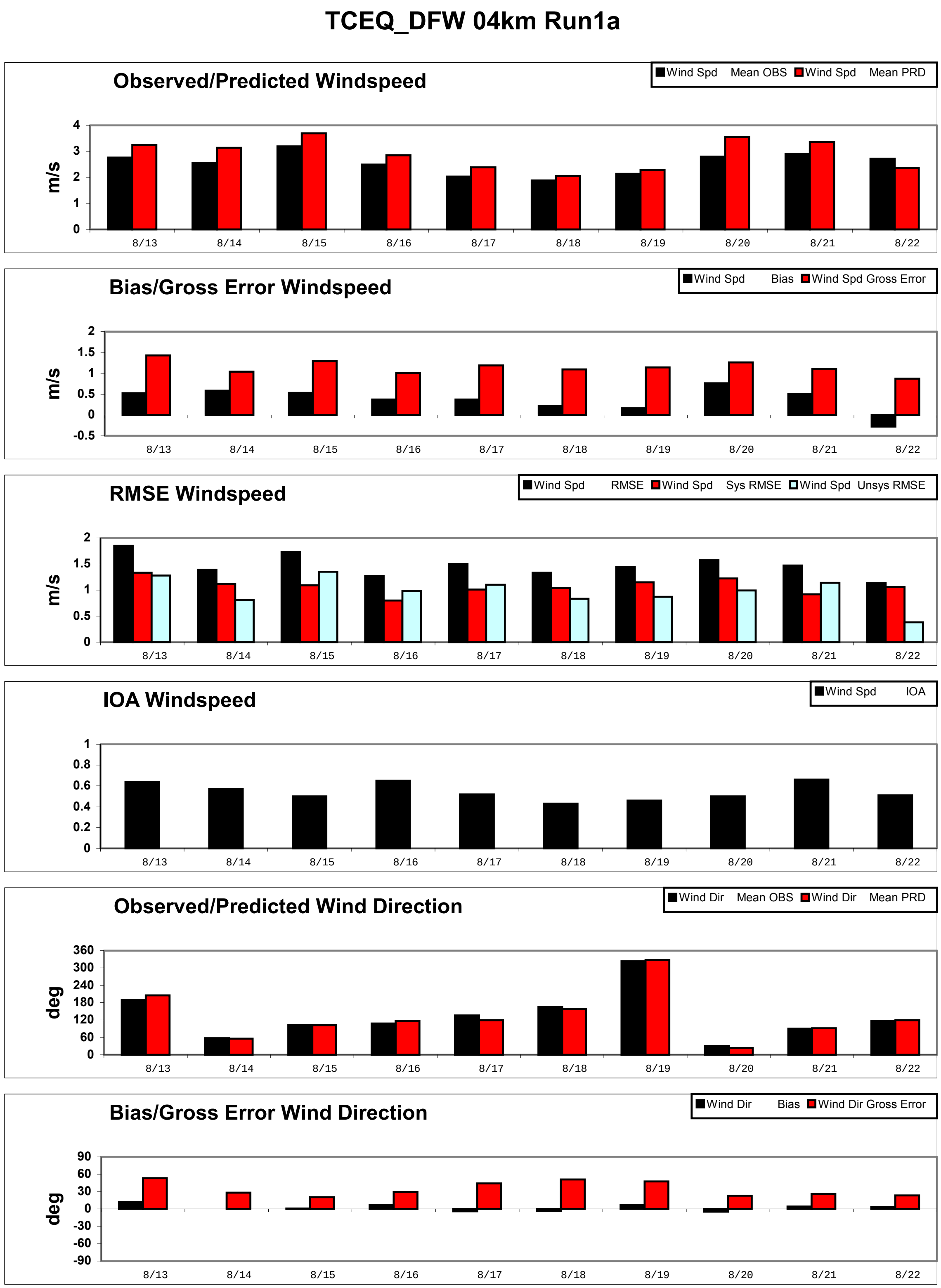


**Figure A-11a.** Daily time series of region-average observed and predicted (Run1a) surface-layer winds and performance statistics in the 4-km DFW MM5 domain. RMSE is shown for total, systematic (RMSES) and unsystematic (RMSEU) components.

## TCEQ_DFW 04km Run1a

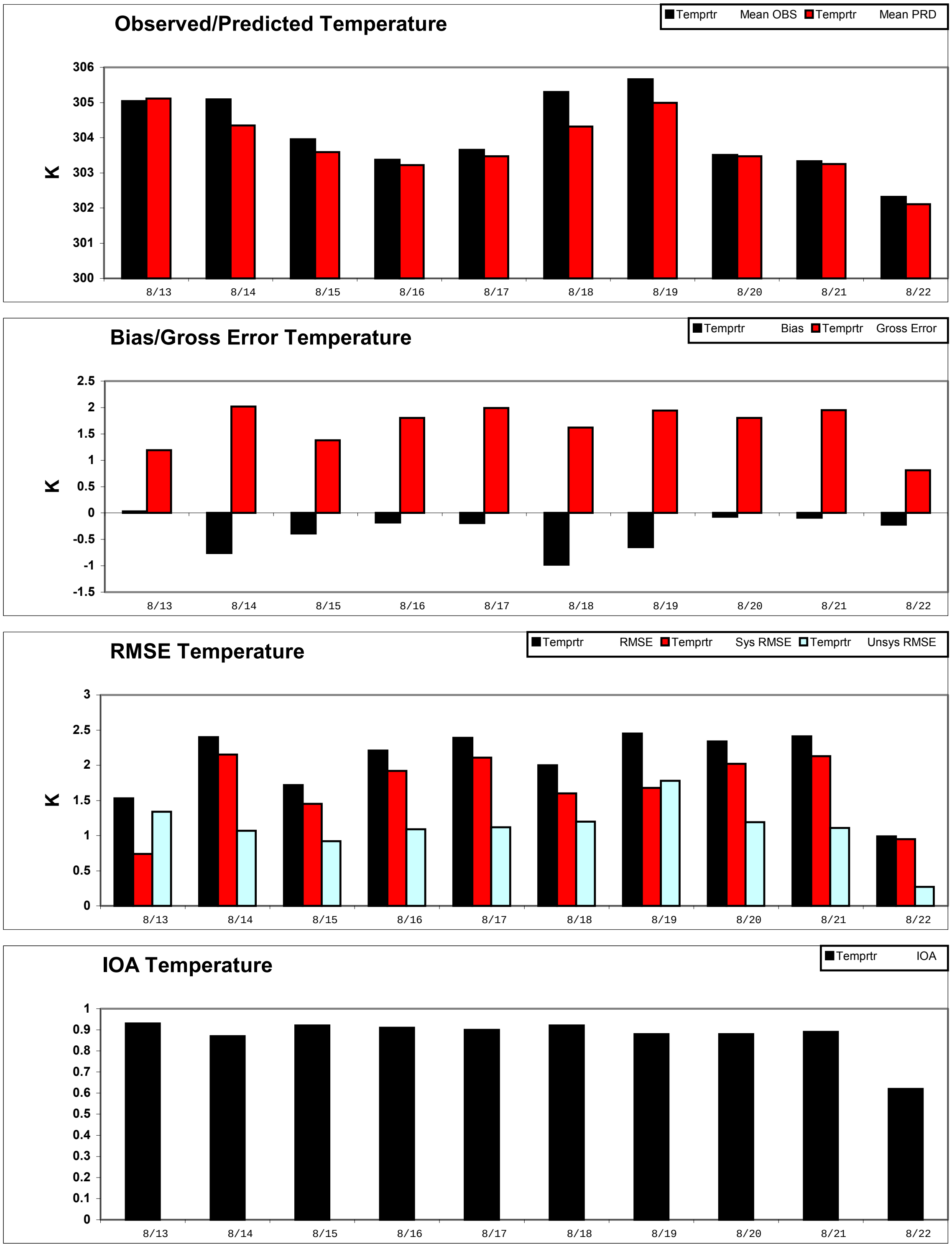


**Figure A-11b.** Daily time series of region-average observed and predicted (Run1a) surface-layer temperature and performance statistics in the 4-km DFW MM5 domain. RMSE is shown for total, systematic (RMSES) and unsystematic (RMSEU) components.

# TCEQ_DFW 04km Run1a

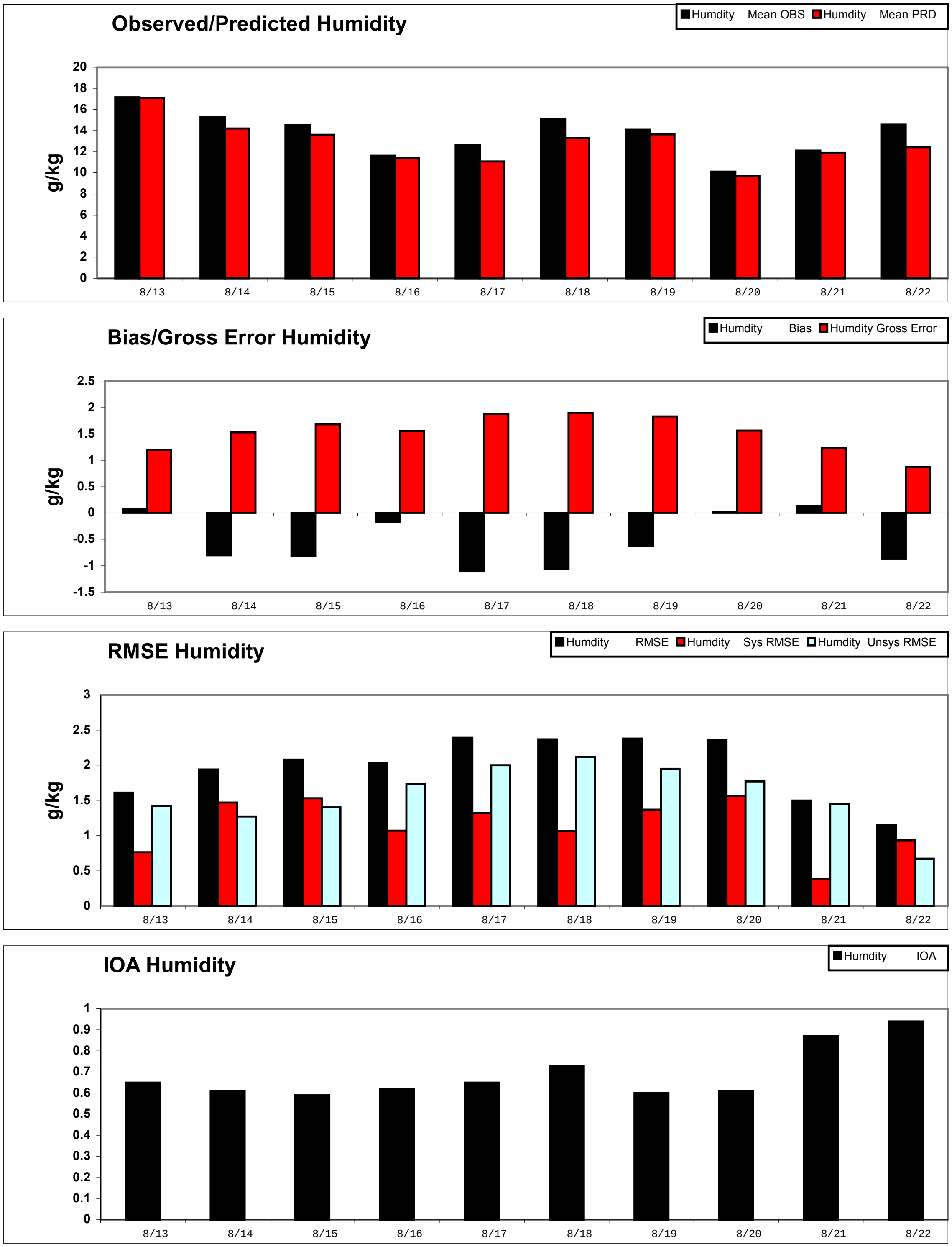


**Figure A-11c.** Daily time series of region-average observed and predicted (Run1a) surface-layer humidity and performance statistics in the 4-km DFW MM5 domain. RMSE is shown for total, systematic (RMSES) and unsystematic (RMSEU) components.

## TCEQ_DFW 04km Run2

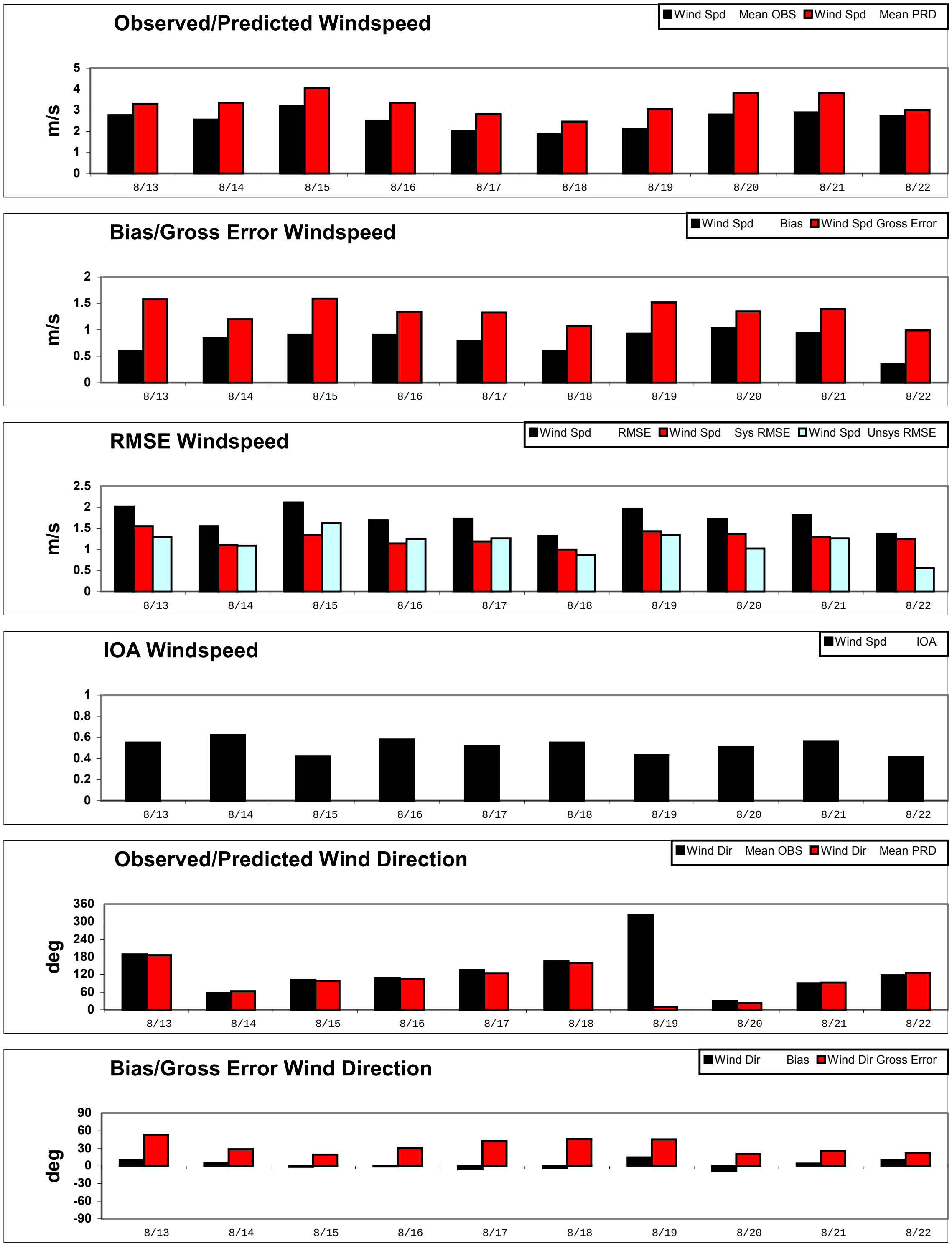


**Figure A-12a.** Daily time series of region-average observed and predicted (Run2) surface-layer winds and performance statistics in the 4-km DFW MM5 domain. RMSE is shown for total, systematic (RMSES) and unsystematic (RMSEU) components.

## TCEQ_DFW 04km Run2

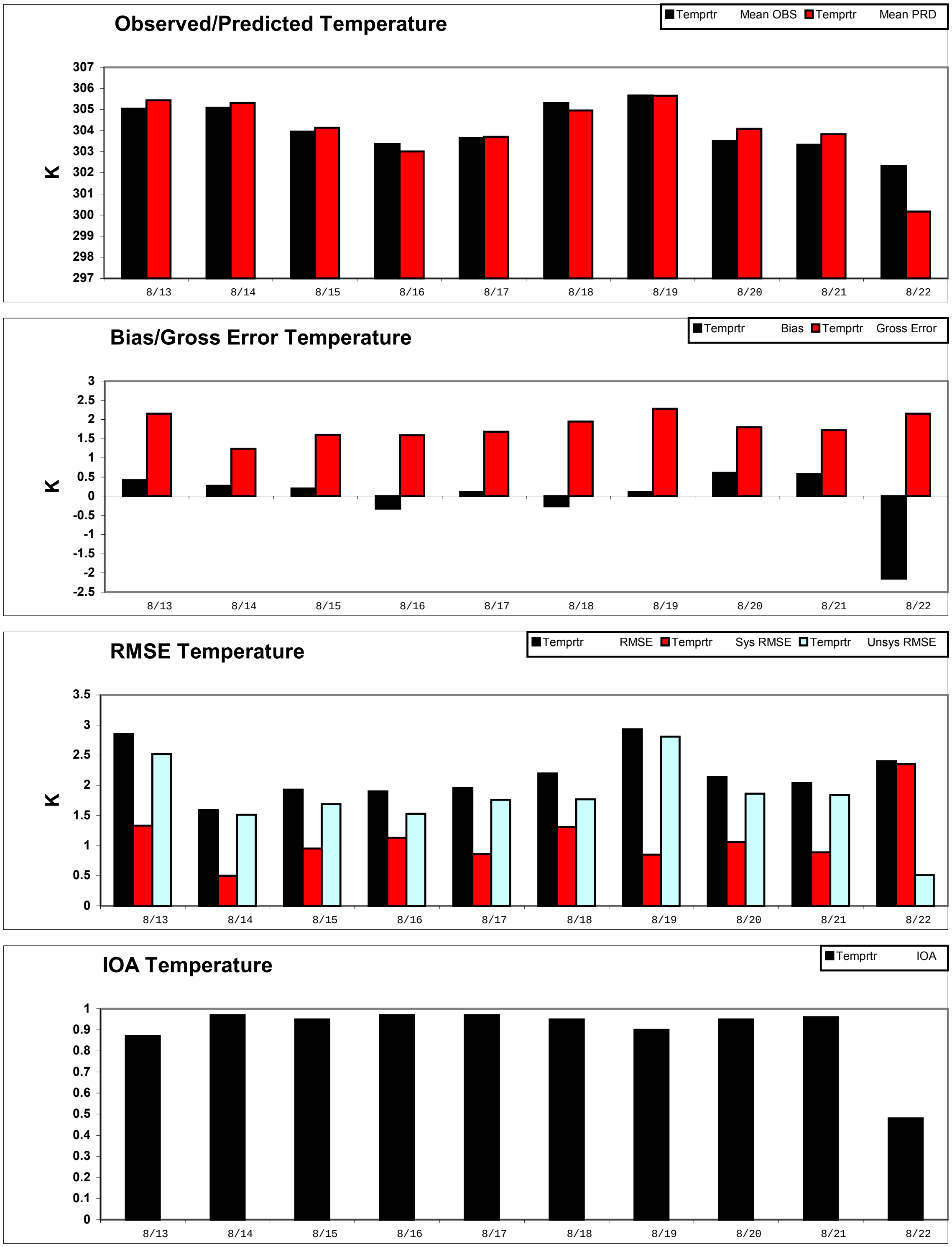


**Figure A-12b.** Daily time series of region-average observed and predicted (Run2) surface-layer temperature and performance statistics in the 4-km DFW MM5 domain. RMSE is shown for total, systematic (RMSES) and unsystematic (RMSEU) components.

TCEQ_DFW 04km Run2

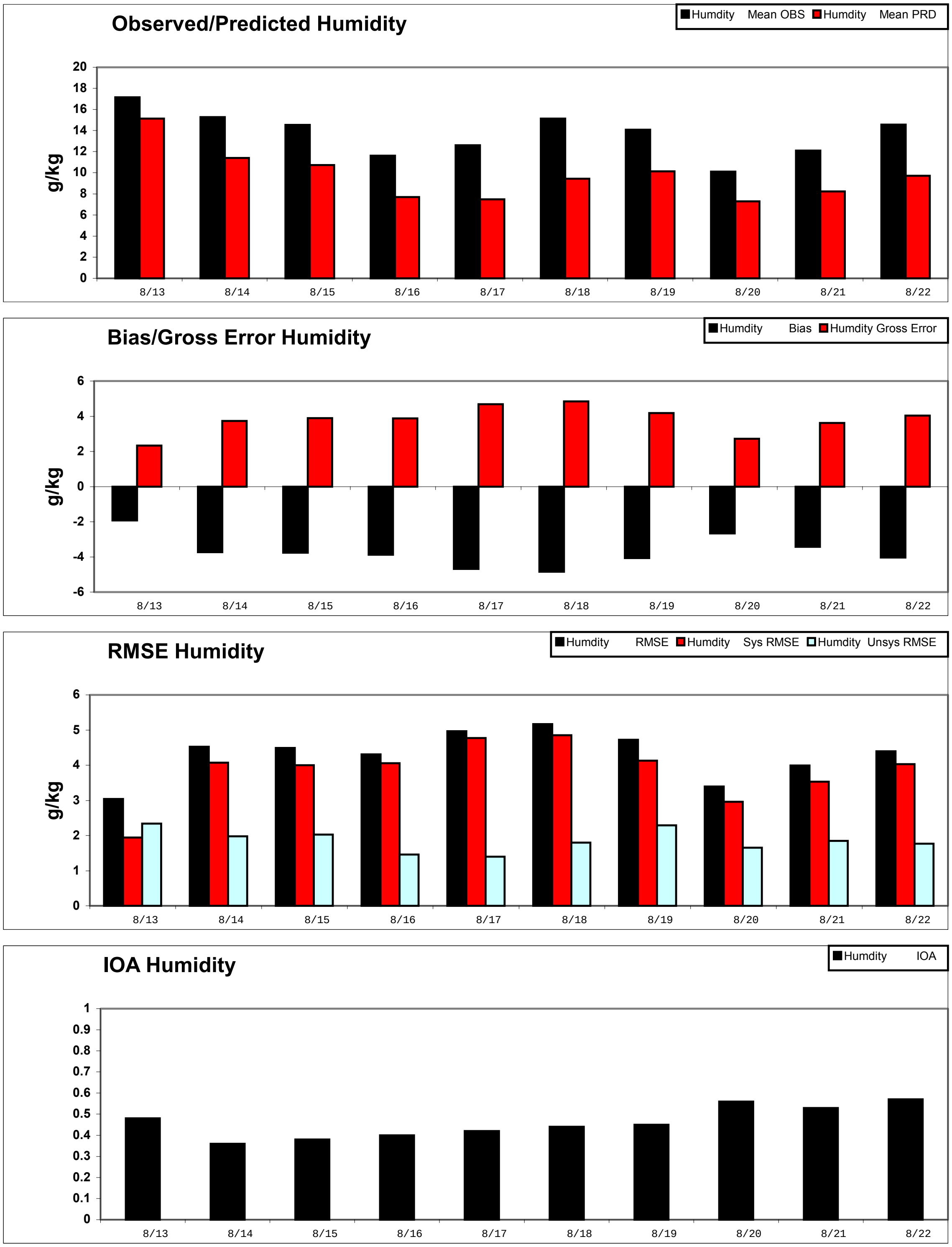


**Figure A-12c.** Daily time series of region-average observed and predicted (Run2) surface-layer humidity and performance statistics in the 4-km DFW MM5 domain. RMSE is shown for total, systematic (RMSES) and unsystematic (RMSEU) components.

# Appendix B

# Comparison of MM5 Results Against Soundings

**MM5 Results of Run3**

RAOB72249 RAOB72249 1999081306 (run3)

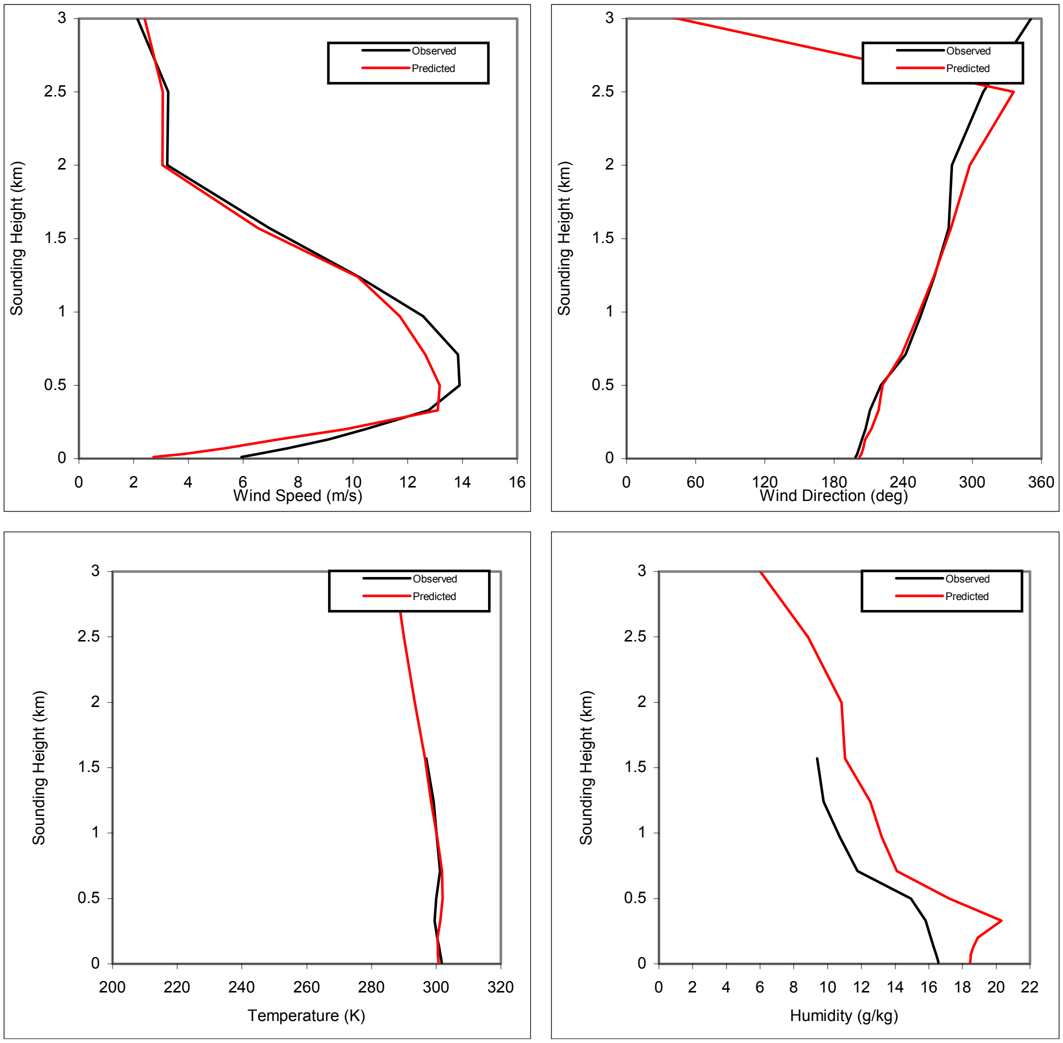

RAOB72249 RAOB72249 1999081318 (run3)

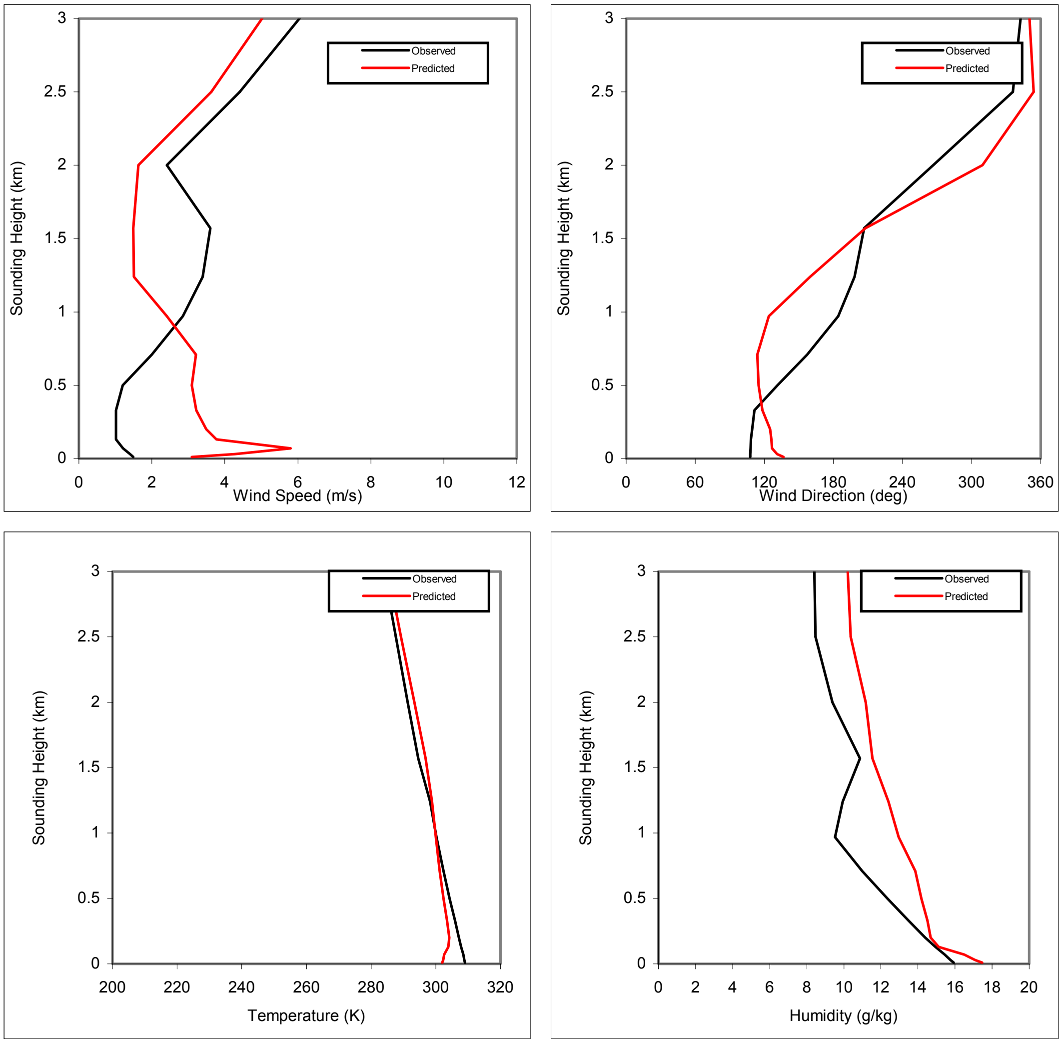

RAOB72249 RAOB72249 1999081406 (run3)

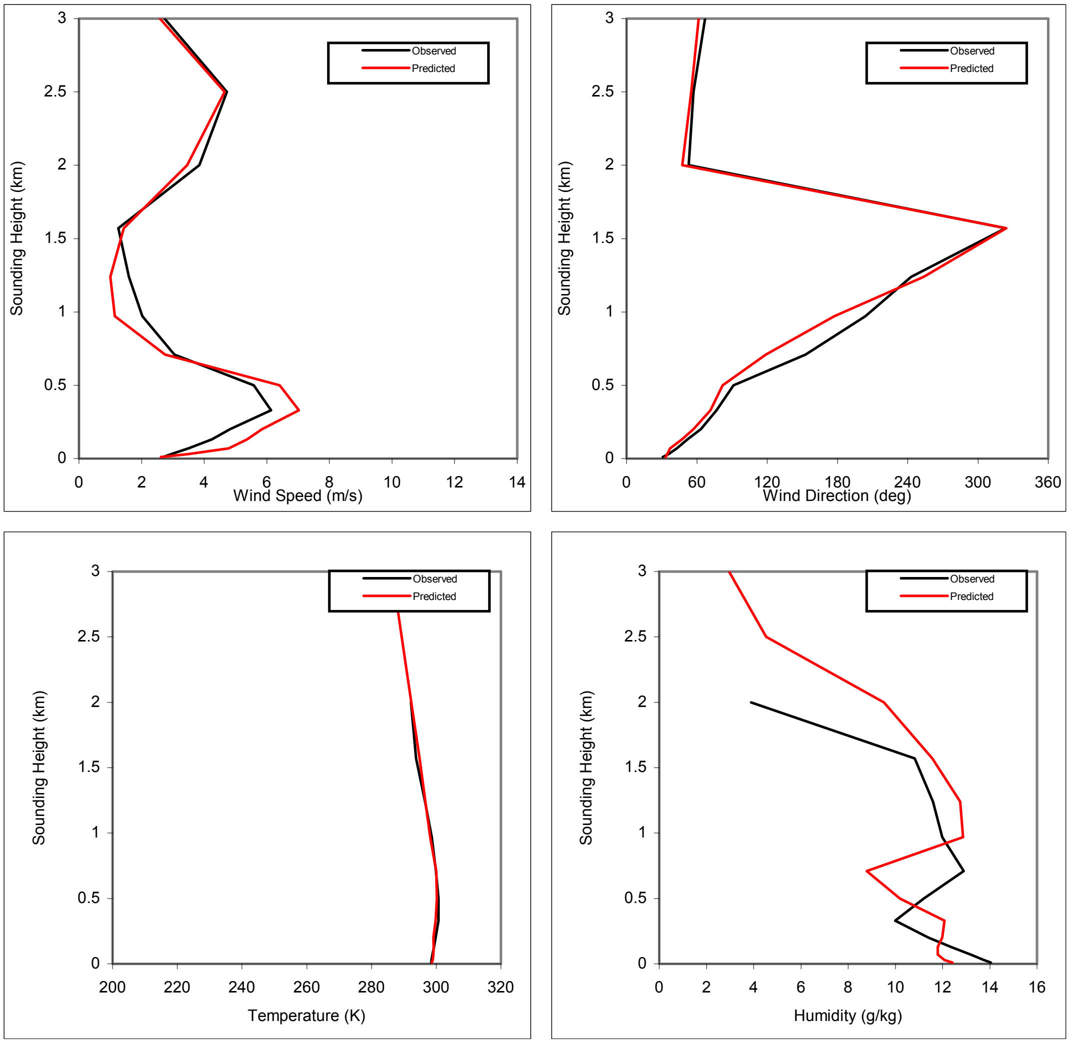

RAOB72249 RAOB72249 1999081418 (run3)

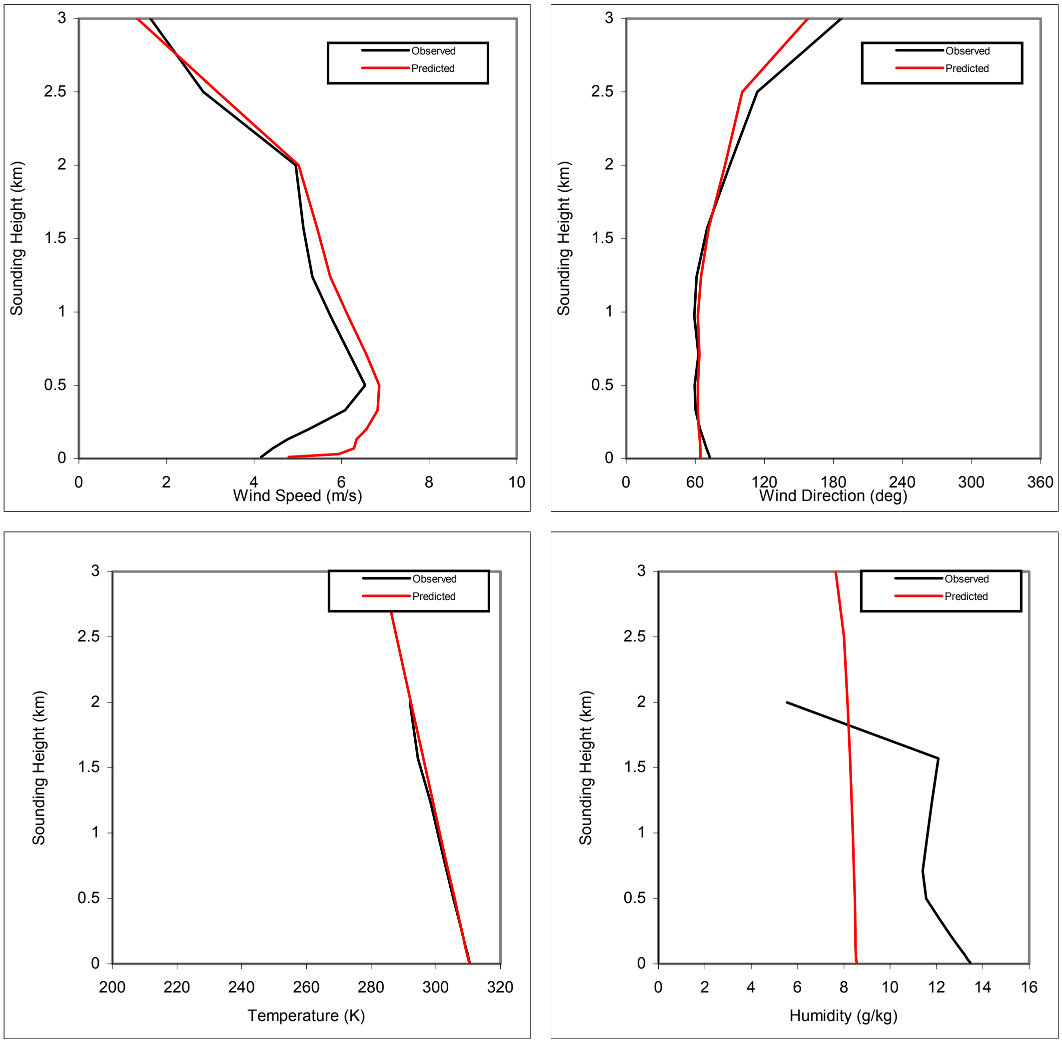

RAOB72249 RAOB72249 1999081506 (run3)

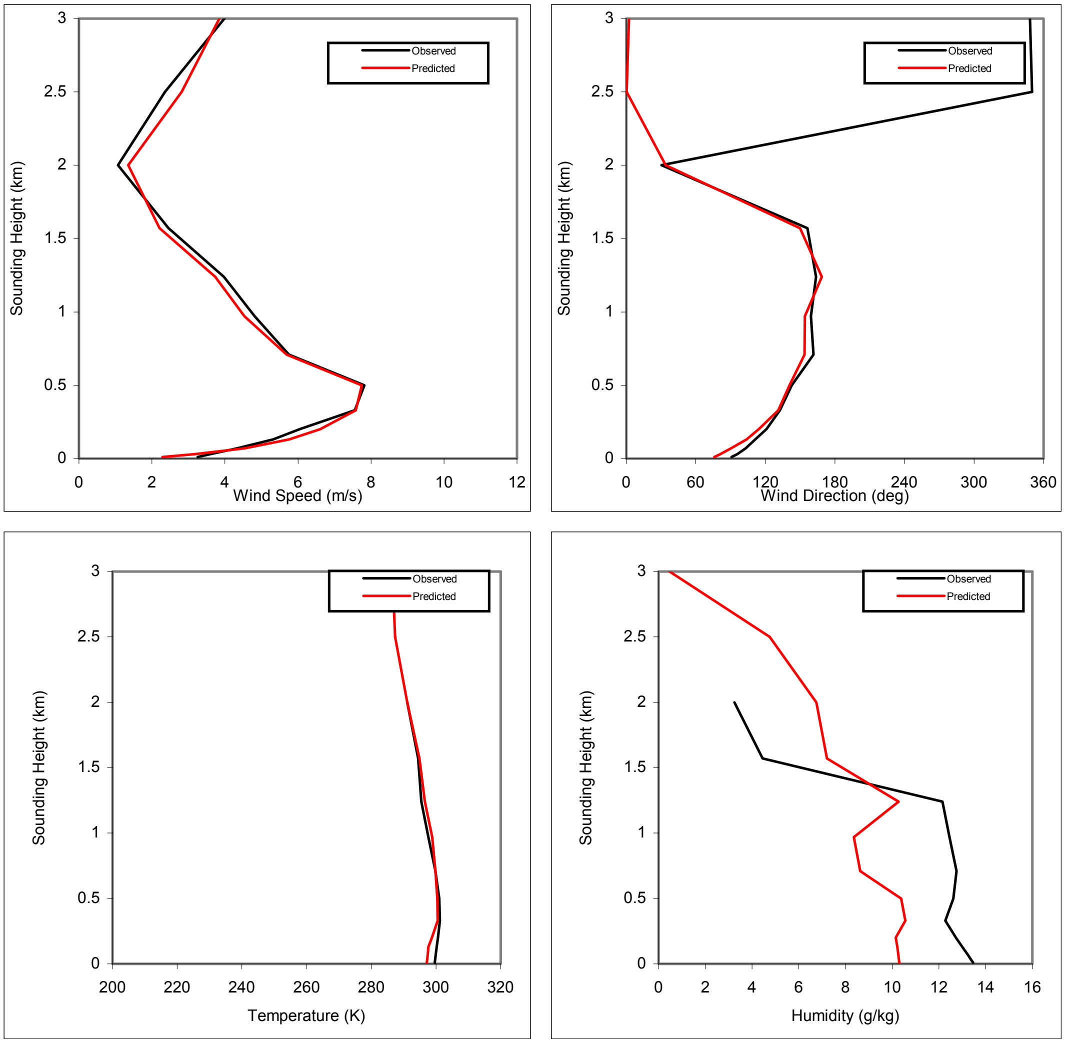

RAOB72249 RAOB72249 1999081518 (run3)

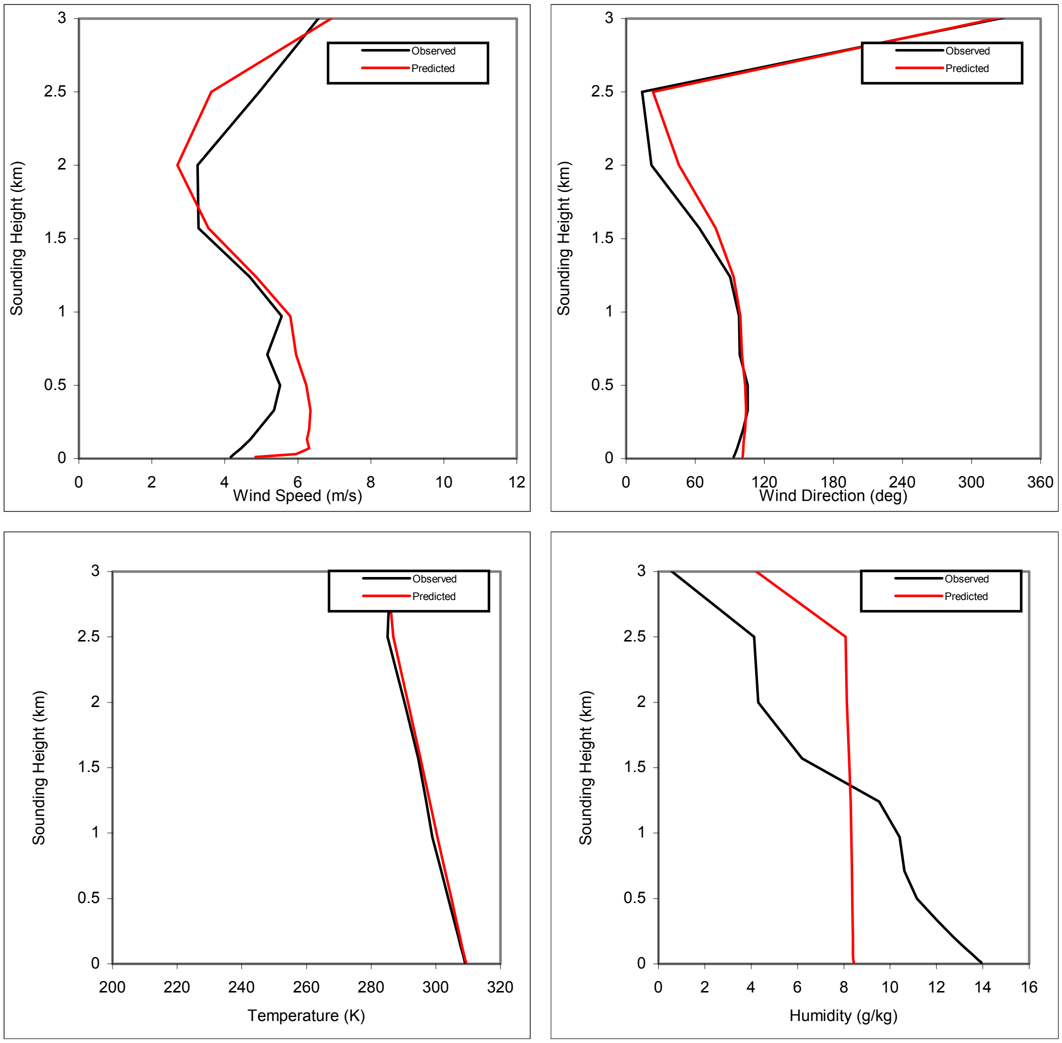

RAOB72249 RAOB72249 1999081606 (run3)

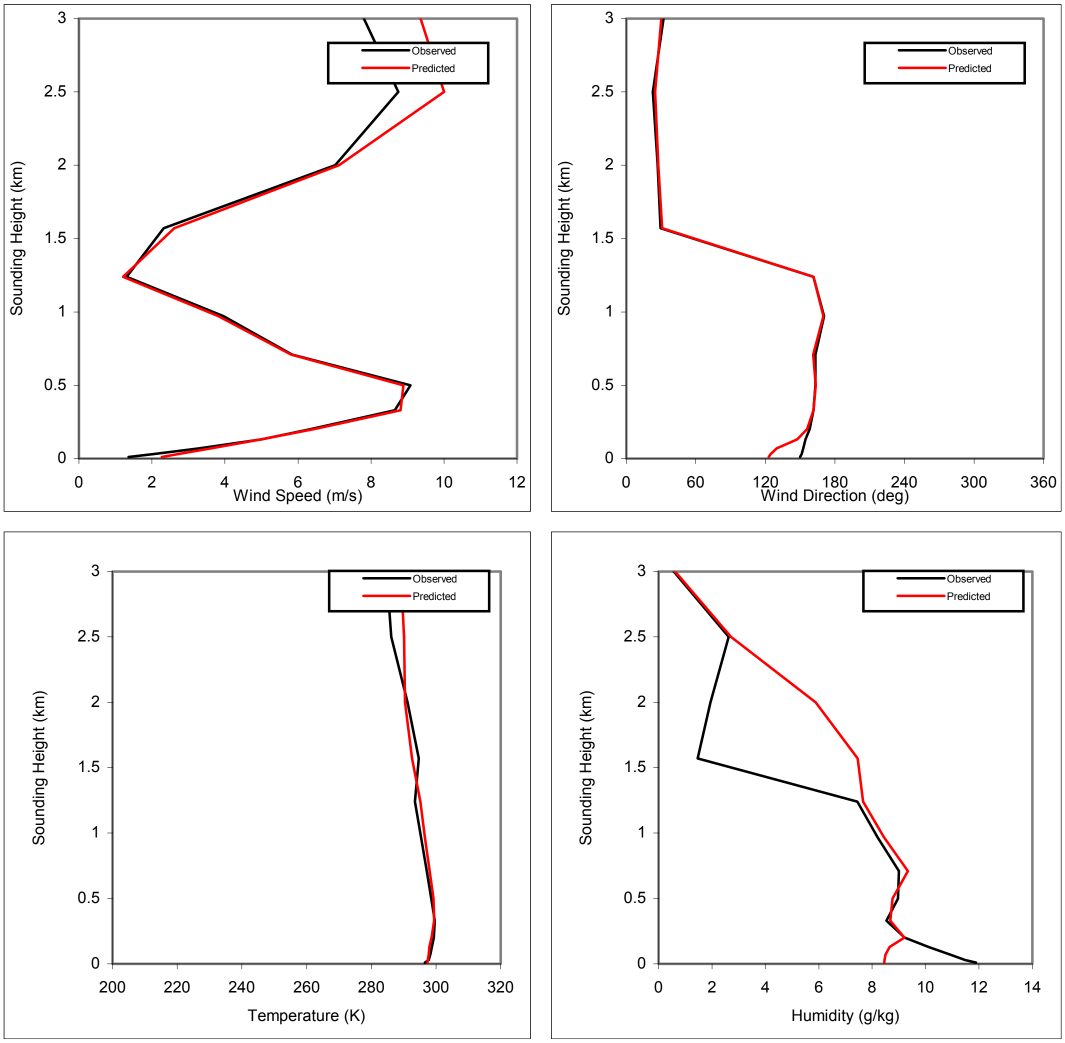

RAOB72249 RAOB72249 1999081618 (run3)

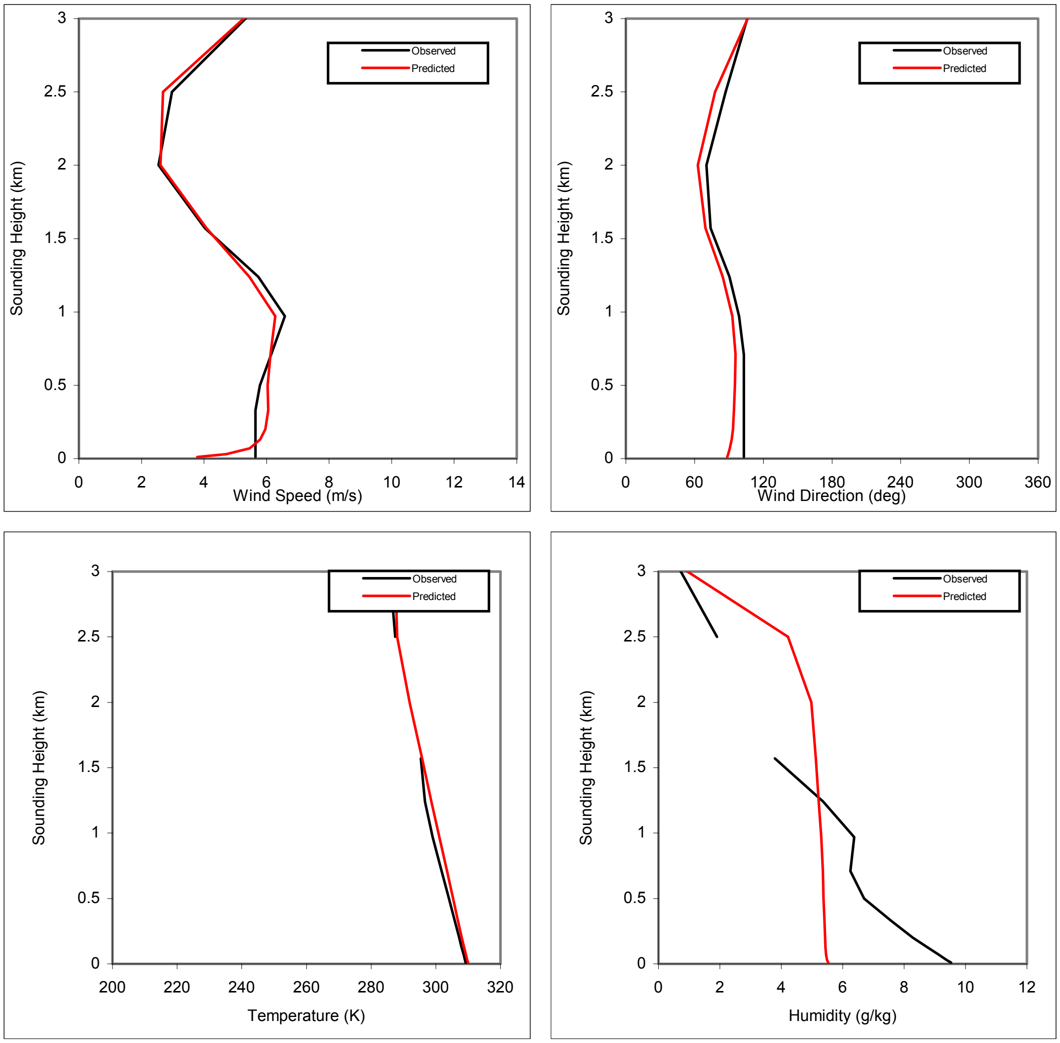

RAOB72249 RAOB72249 1999081706 (run3)

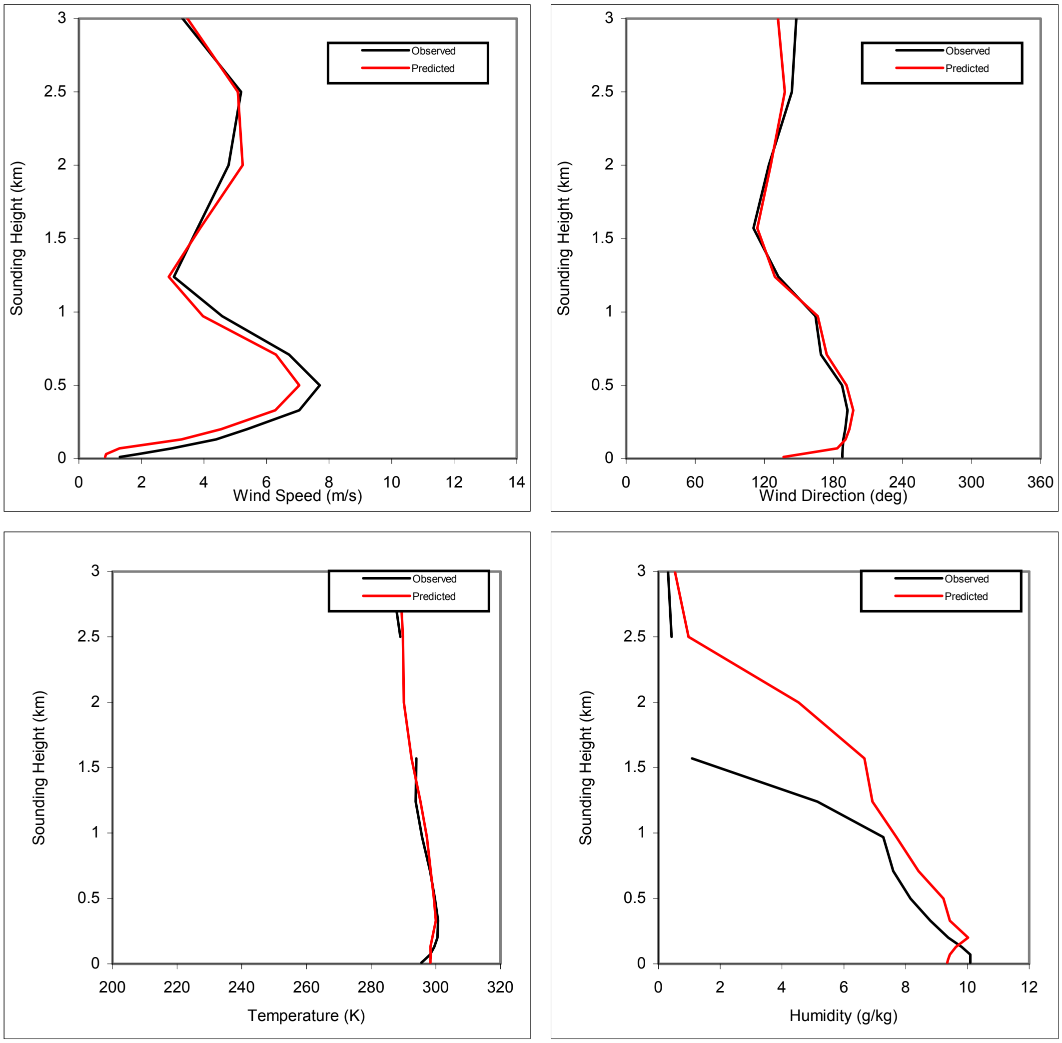

RAOB72249 RAOB72249 1999081718 (run3)

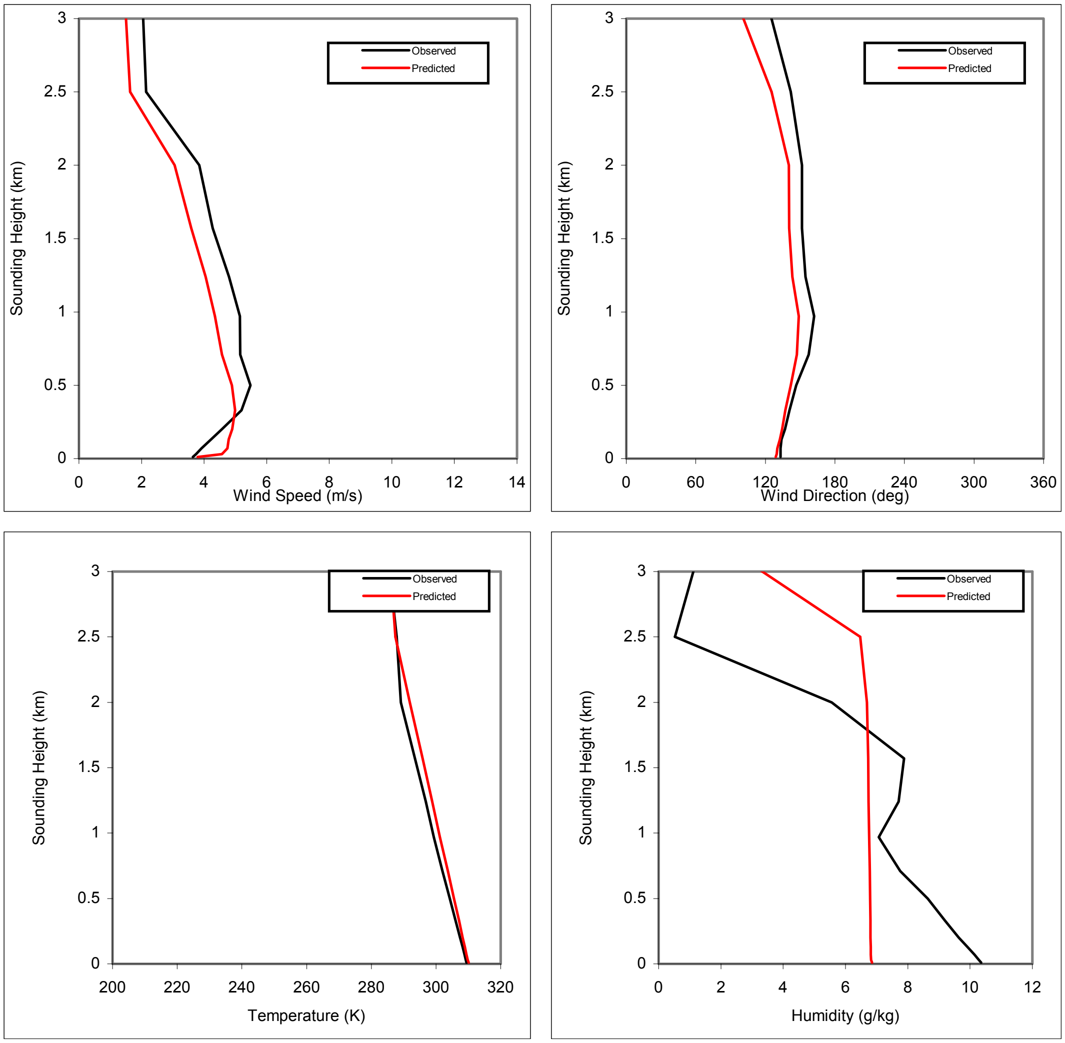

RAOB72249 RAOB72249 1999081806 (run3)

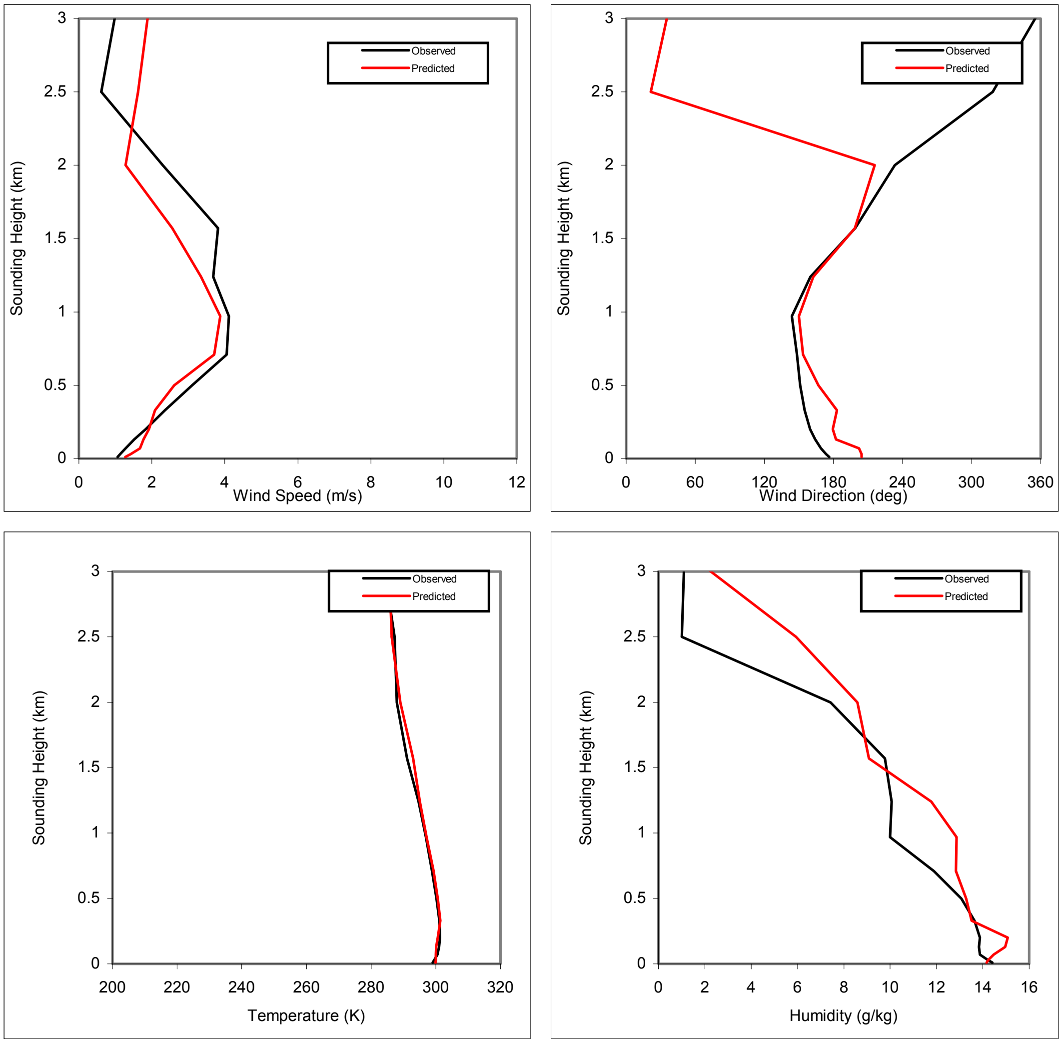

RAOB72249 RAOB72249 1999081818 (run3)

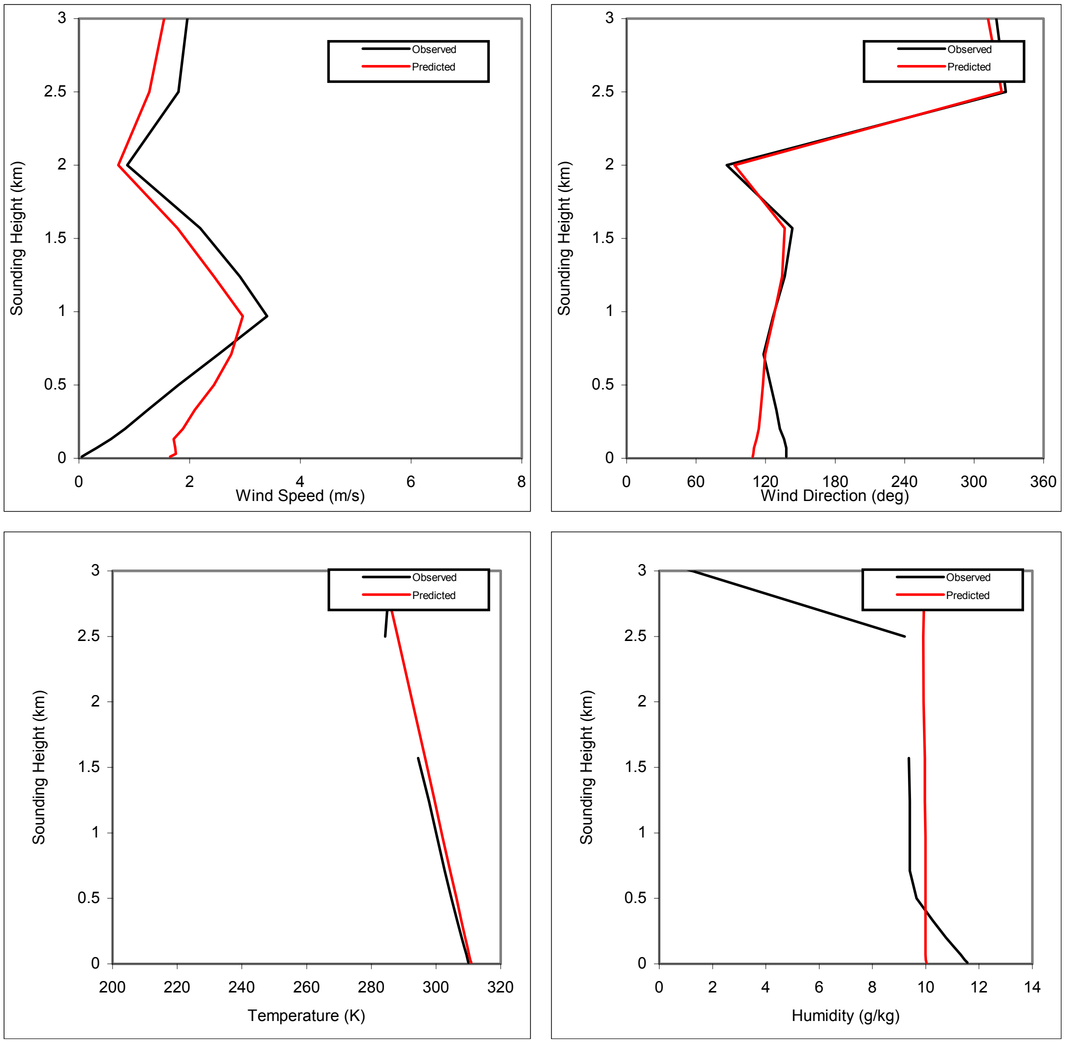

RAOB72249 RAOB72249 1999081906 (run3)

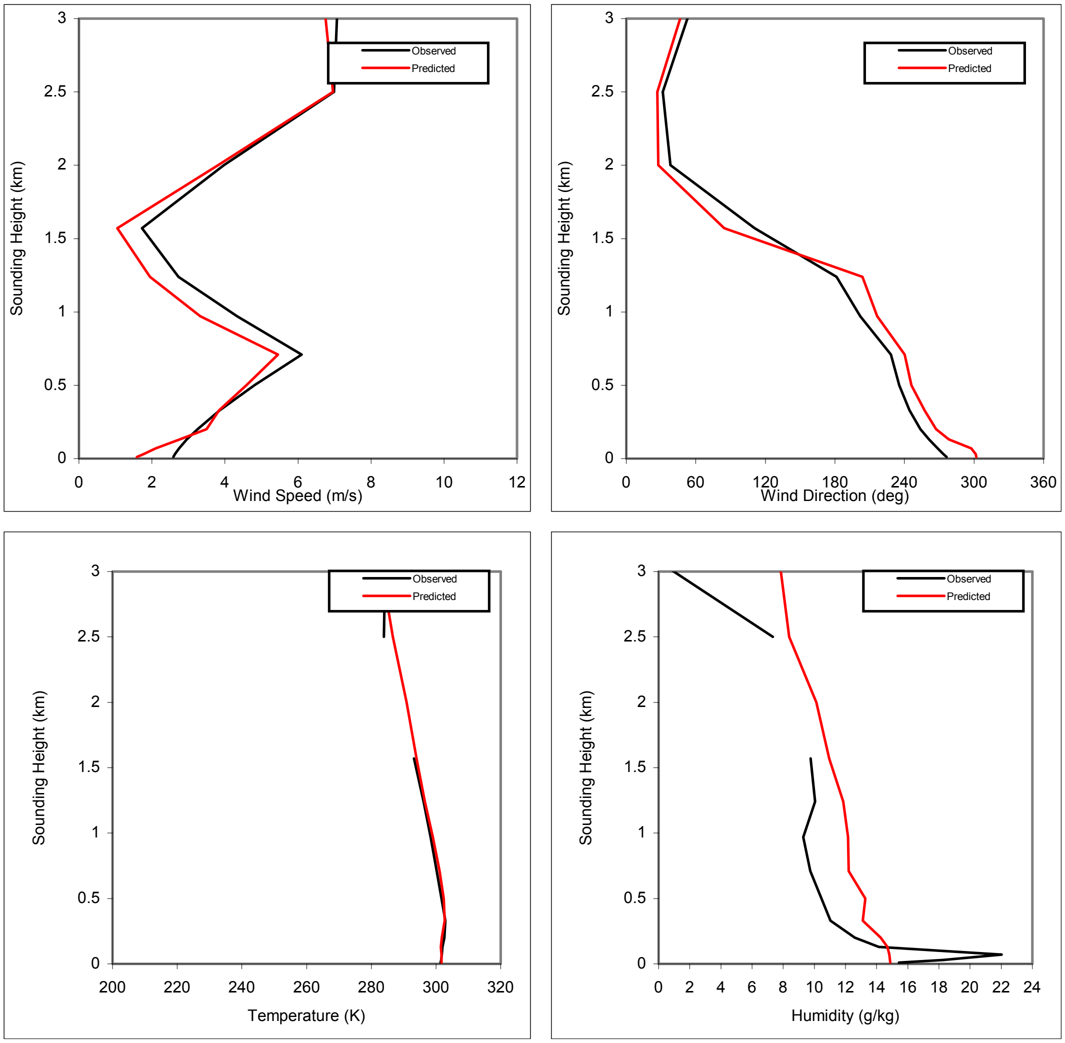

RAOB72249 RAOB72249 1999081918 (run3)

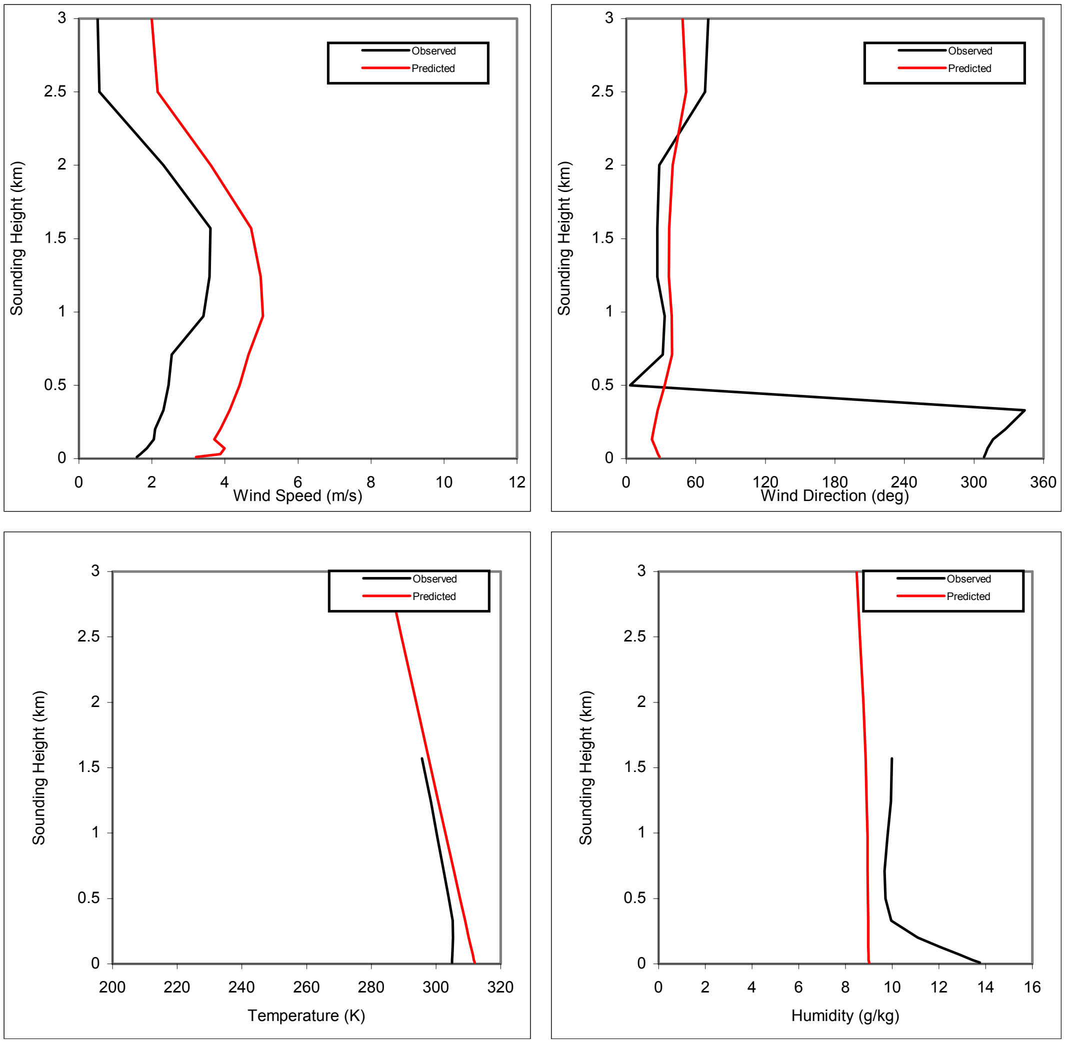

RAOB72249 RAOB72249 1999082006 (run3)

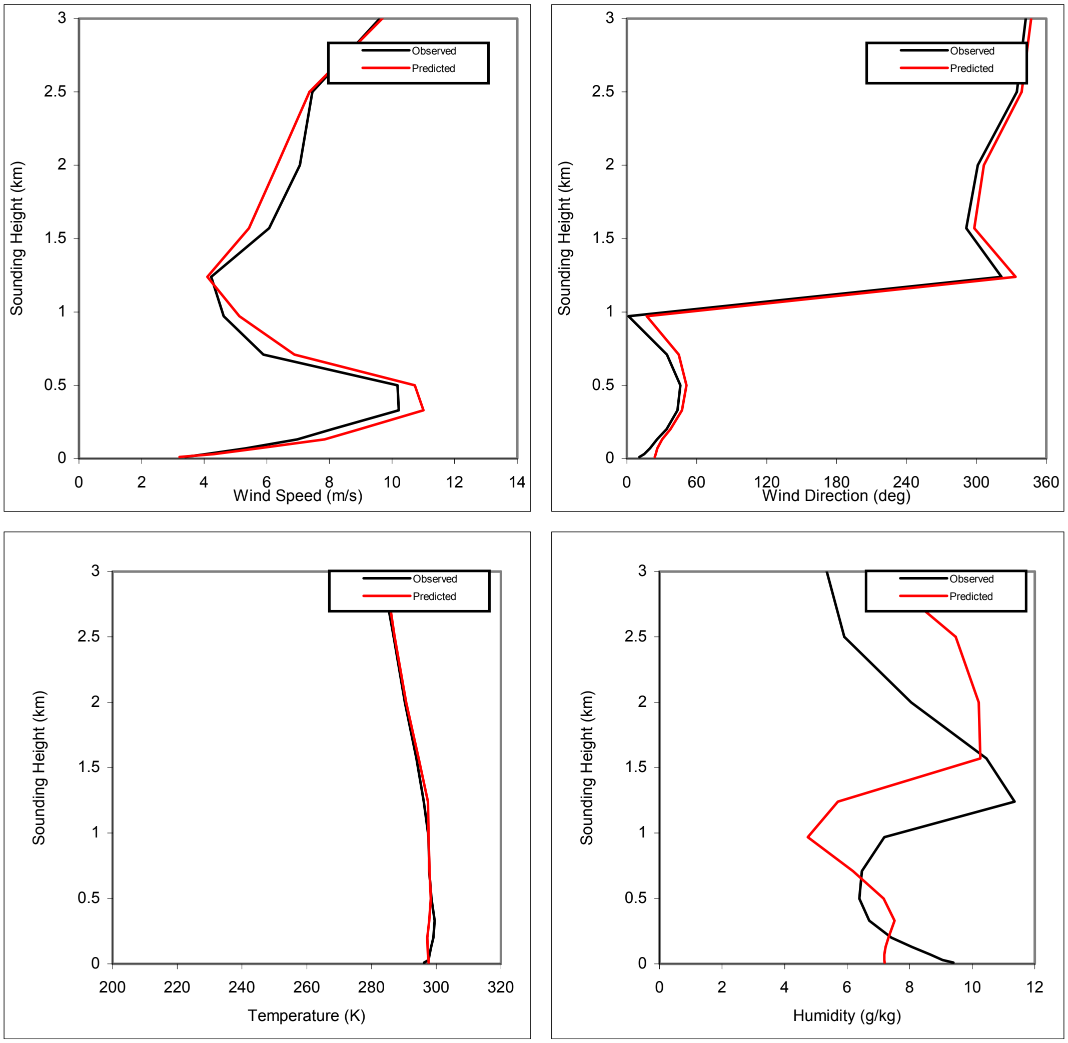

RAOB72249 RAOB72249 1999082018 (run3)

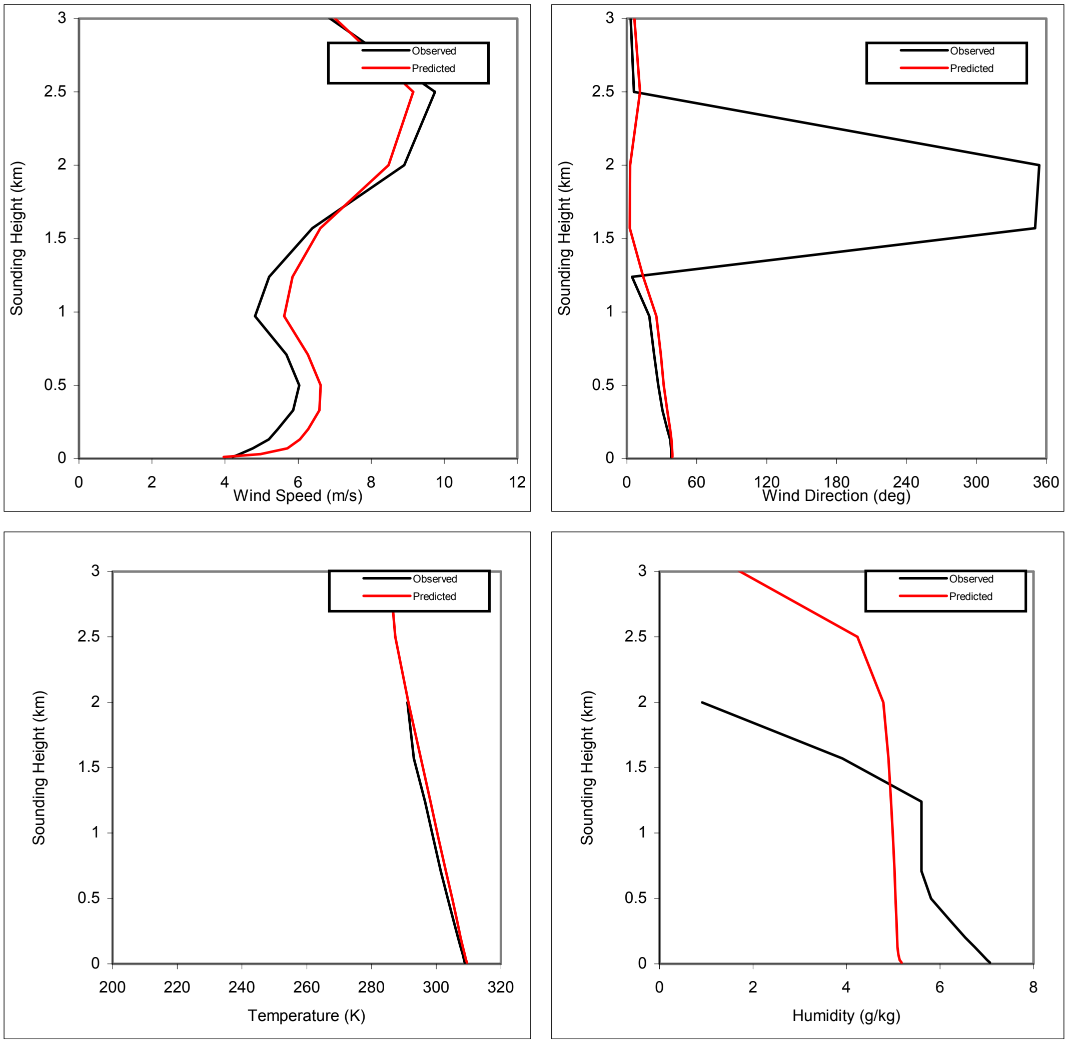

RAOB72249 RAOB72249 1999082106 (run3)

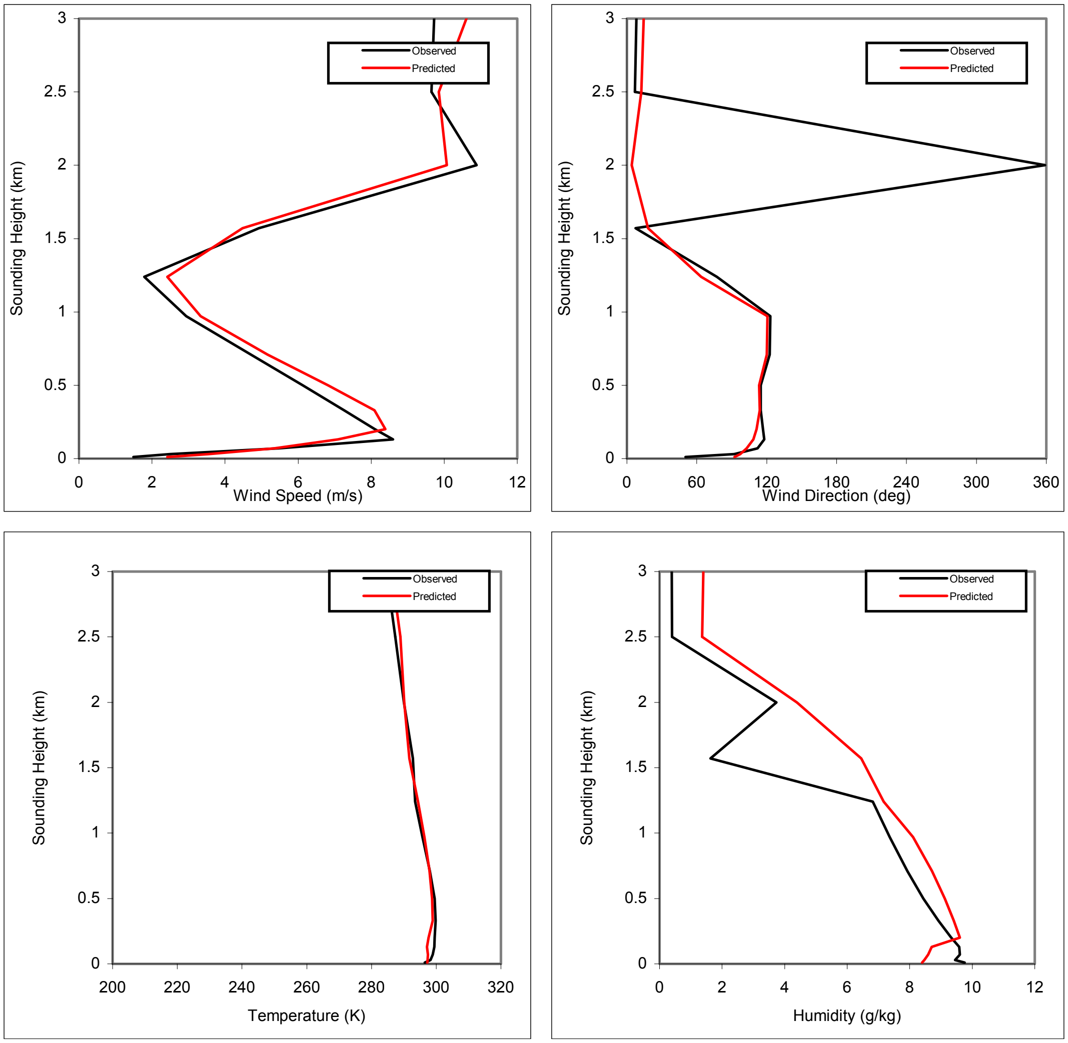

RAOB72249 RAOB72249 1999082118 (run3)

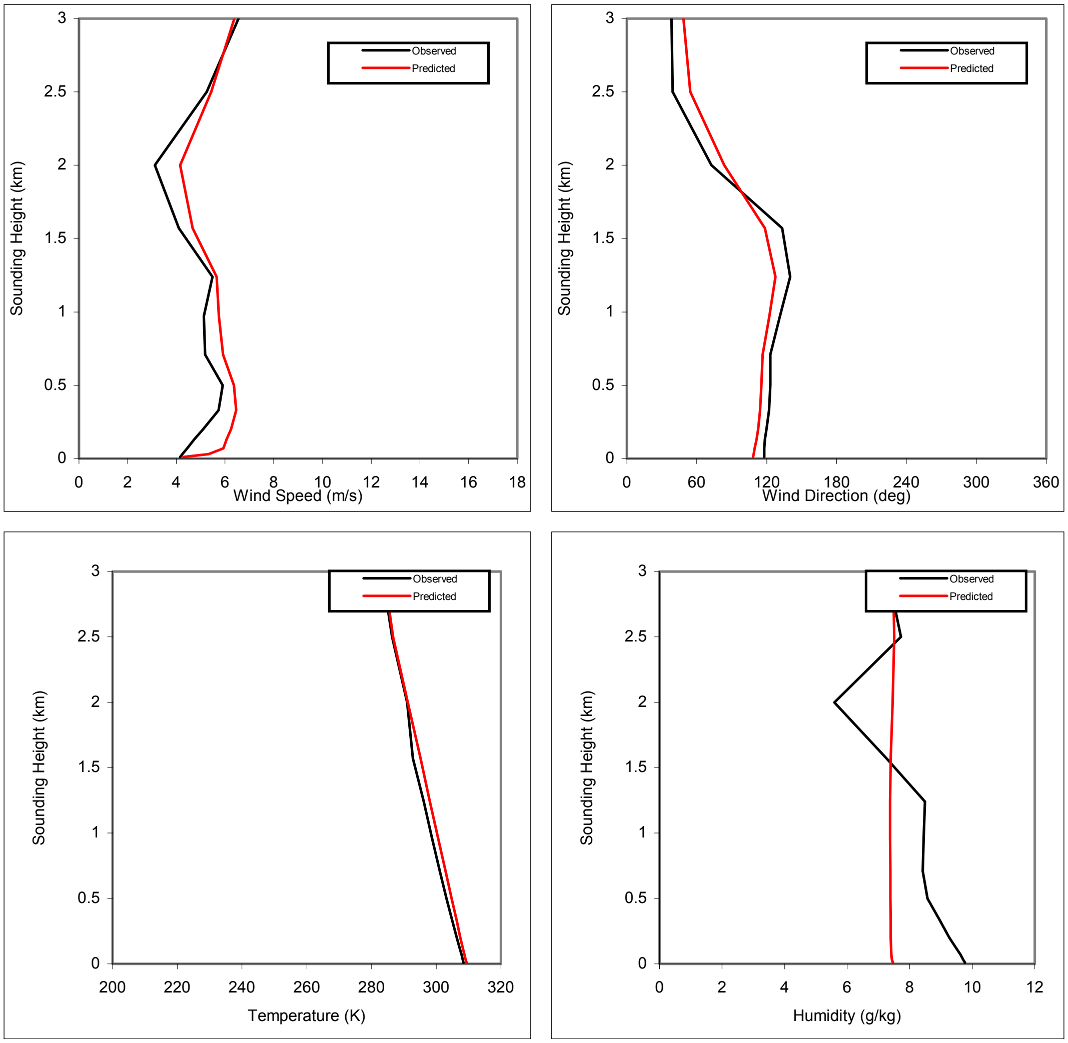

**MM5 Results of Run1**

RAOB72249 RAOB72249 1999081306 (run1)

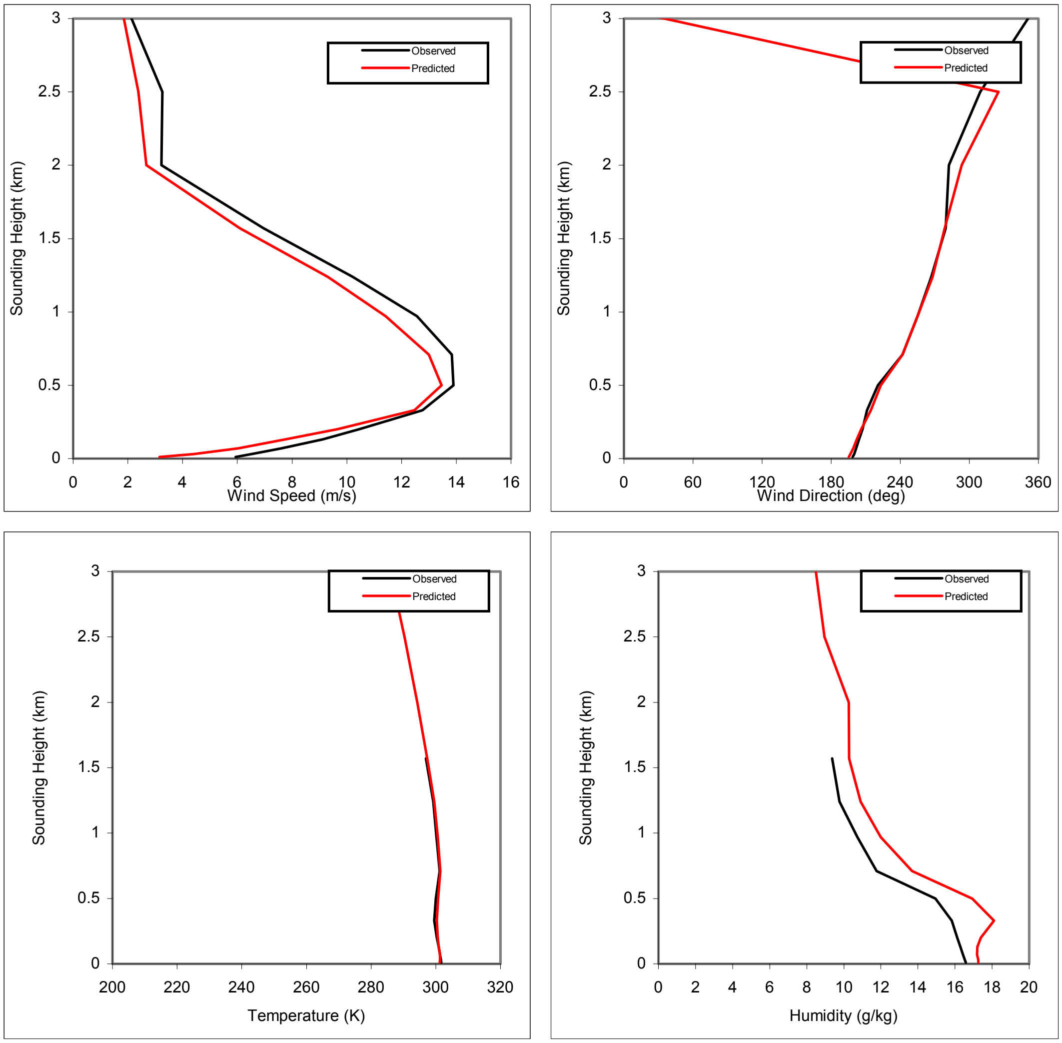

RAOB72249 RAOB72249 1999081318 (run1)

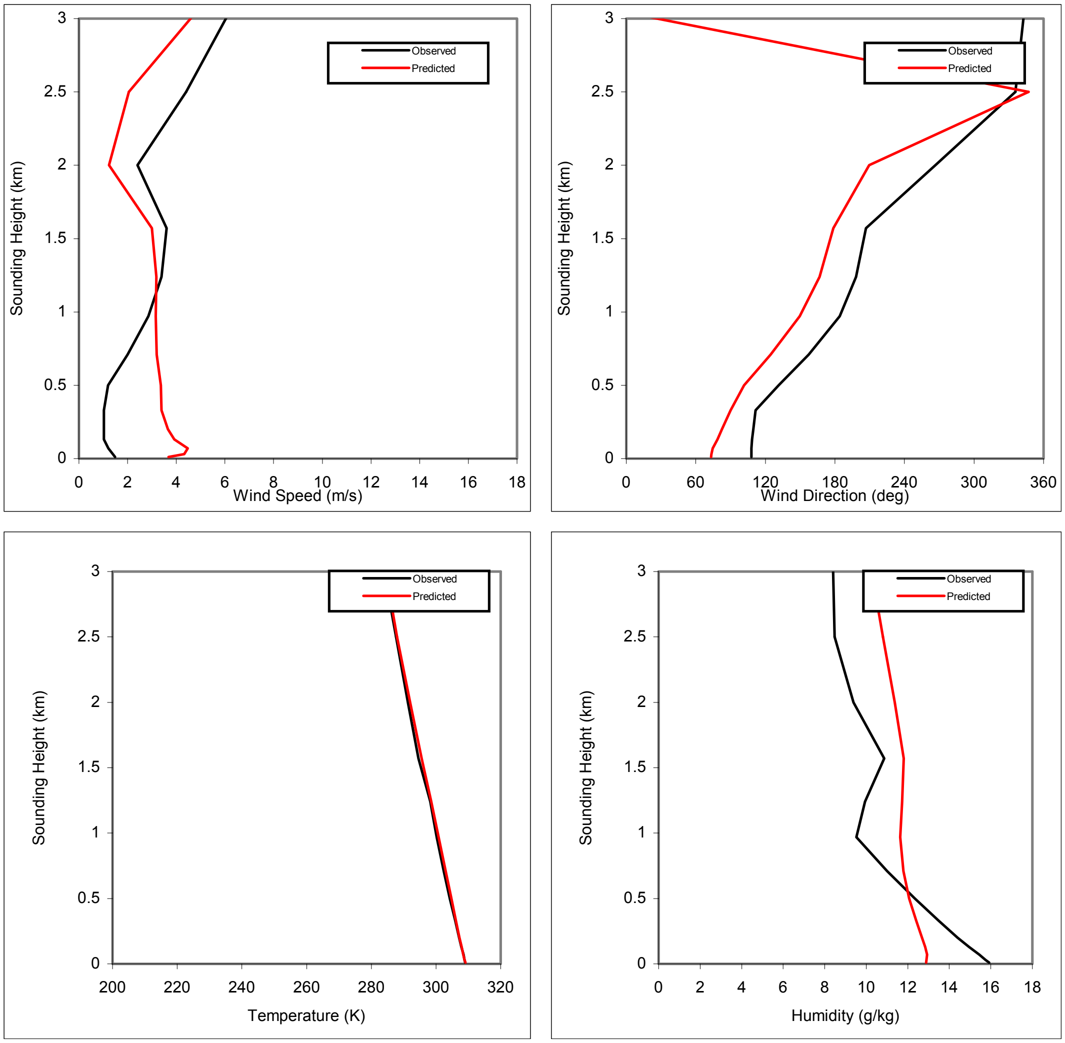

RAOB72249 RAOB72249 1999081406 (run1)

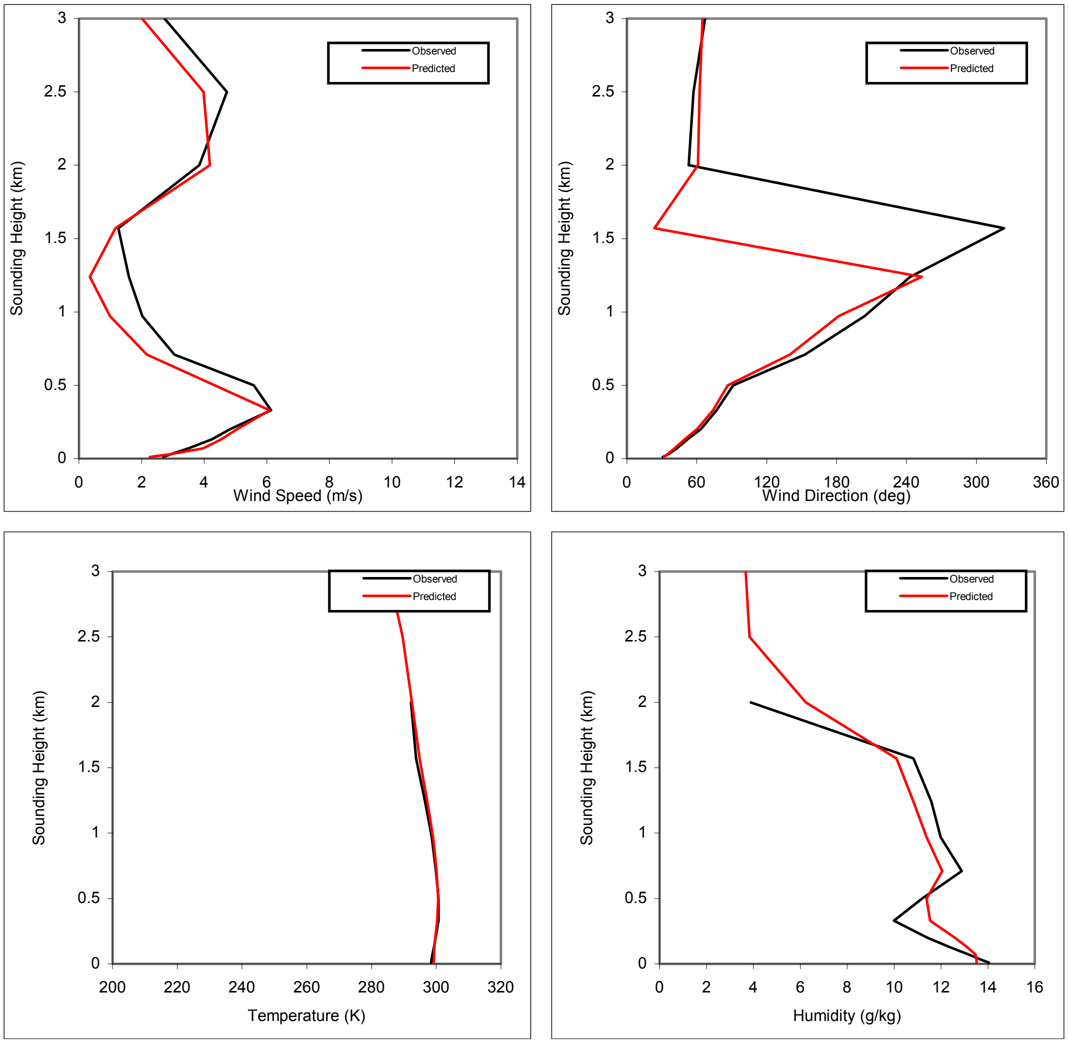

RAOB72249 RAOB72249 1999081418 (run1)

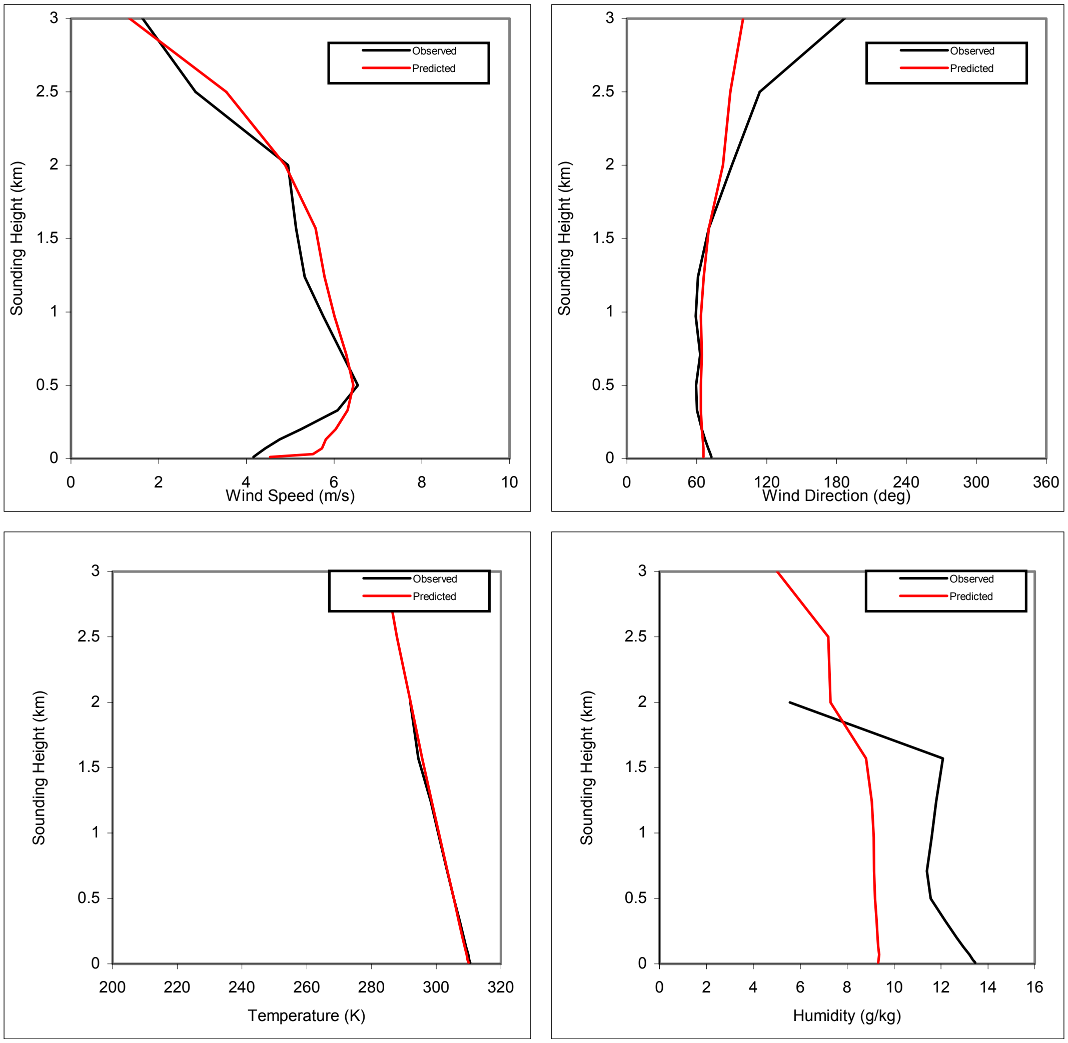

RAOB72249 RAOB72249 1999081506 (run1)

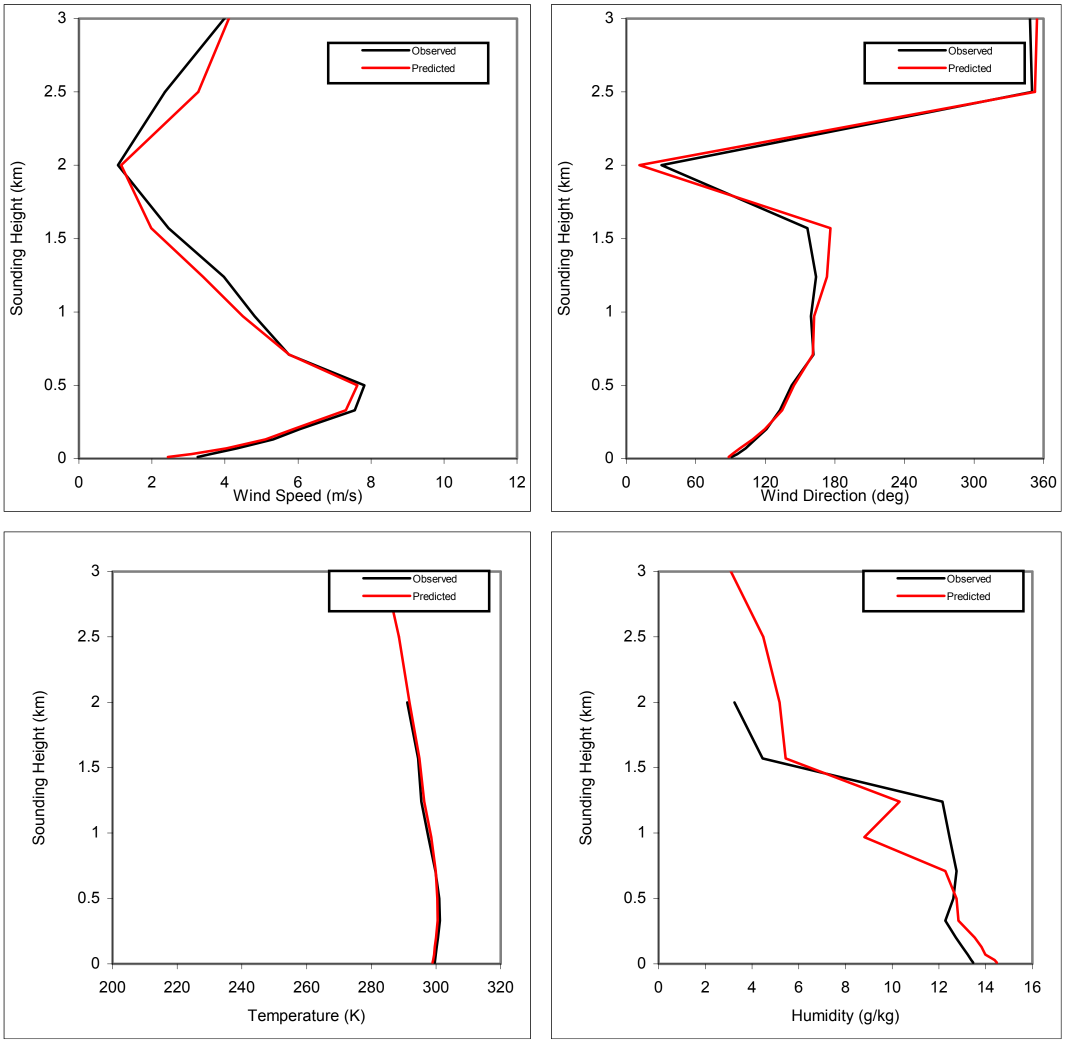

RAOB72249 RAOB72249 1999081518 (run1)

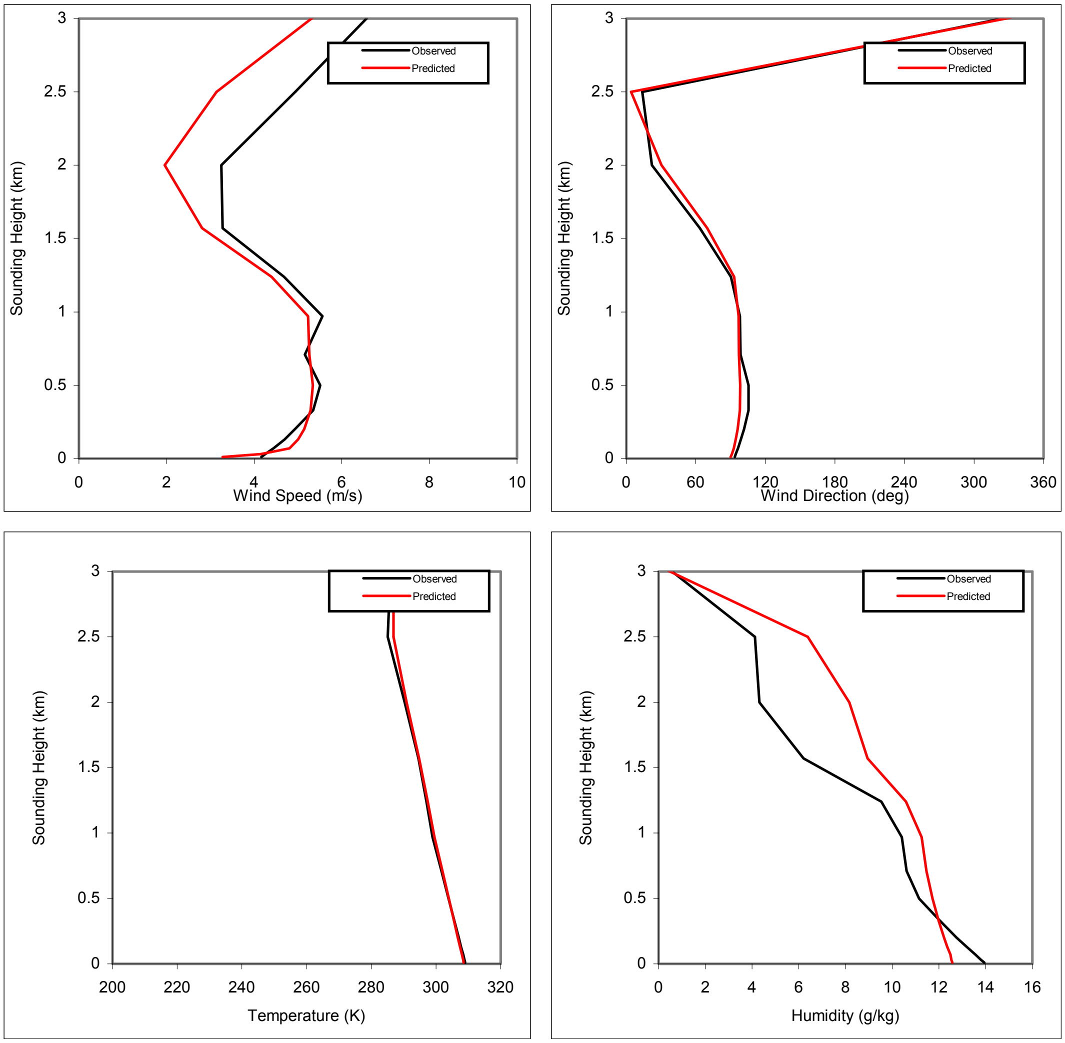

RAOB72249 RAOB72249 1999081606 (run1)

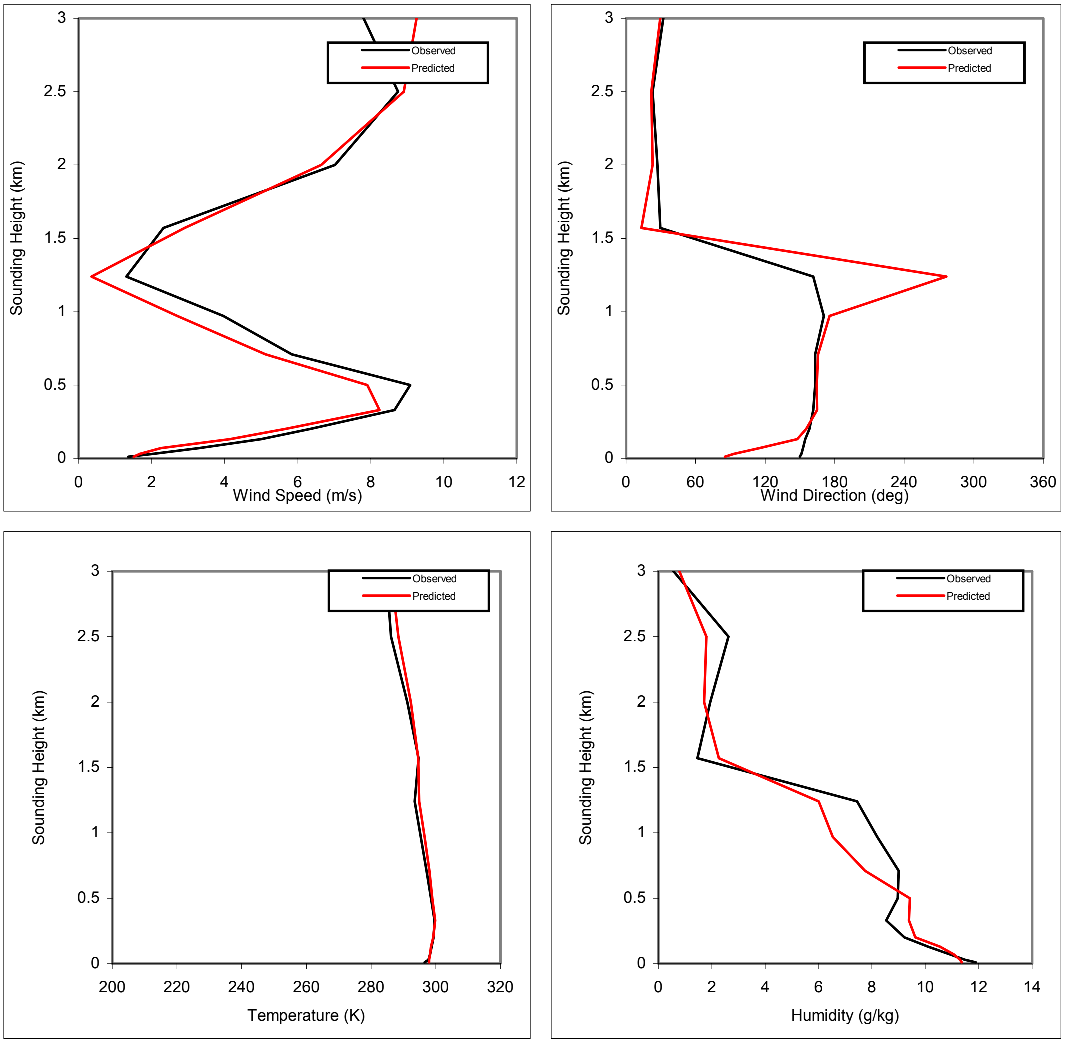

RAOB72249 RAOB72249 1999081618 (run1)

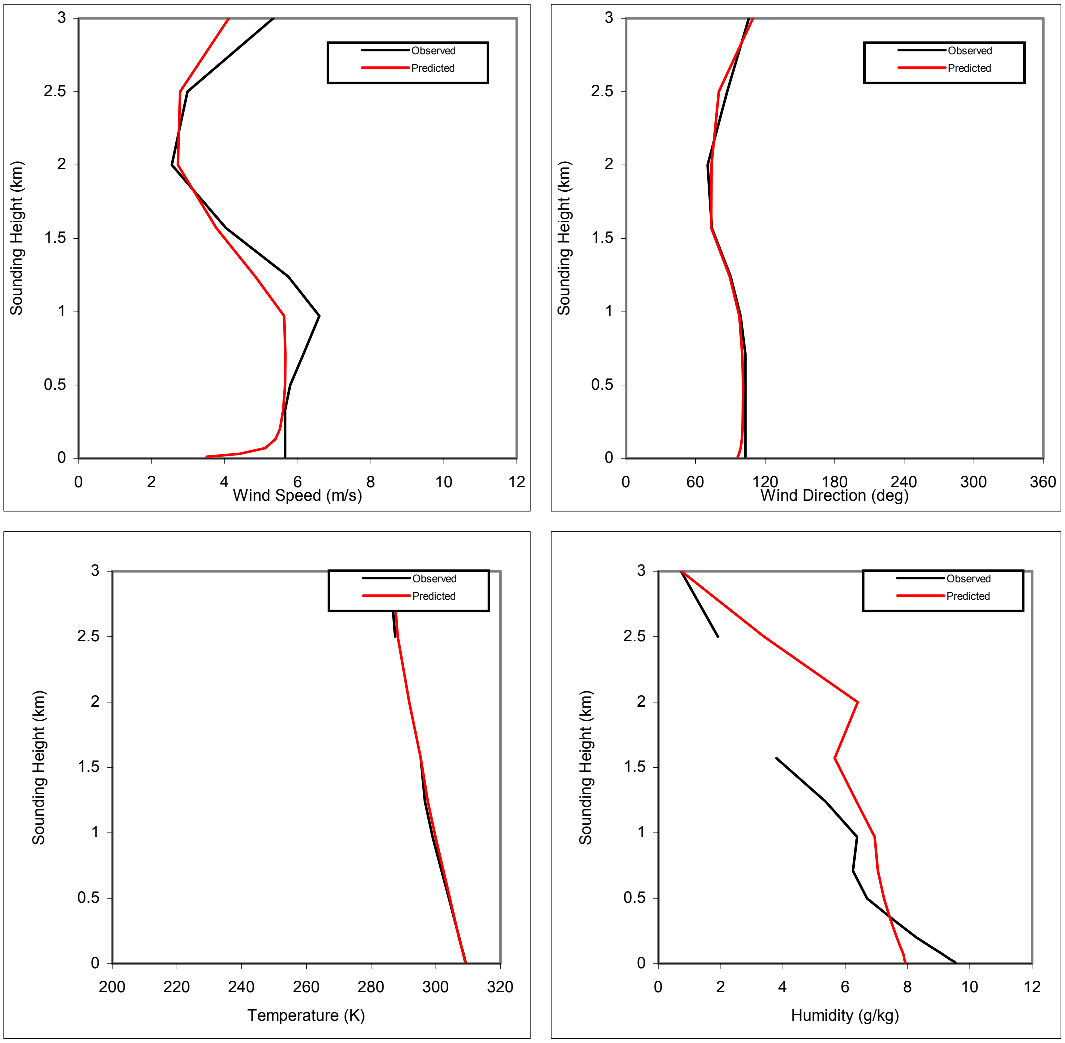

RAOB72249 RAOB72249 1999081706 (run1)

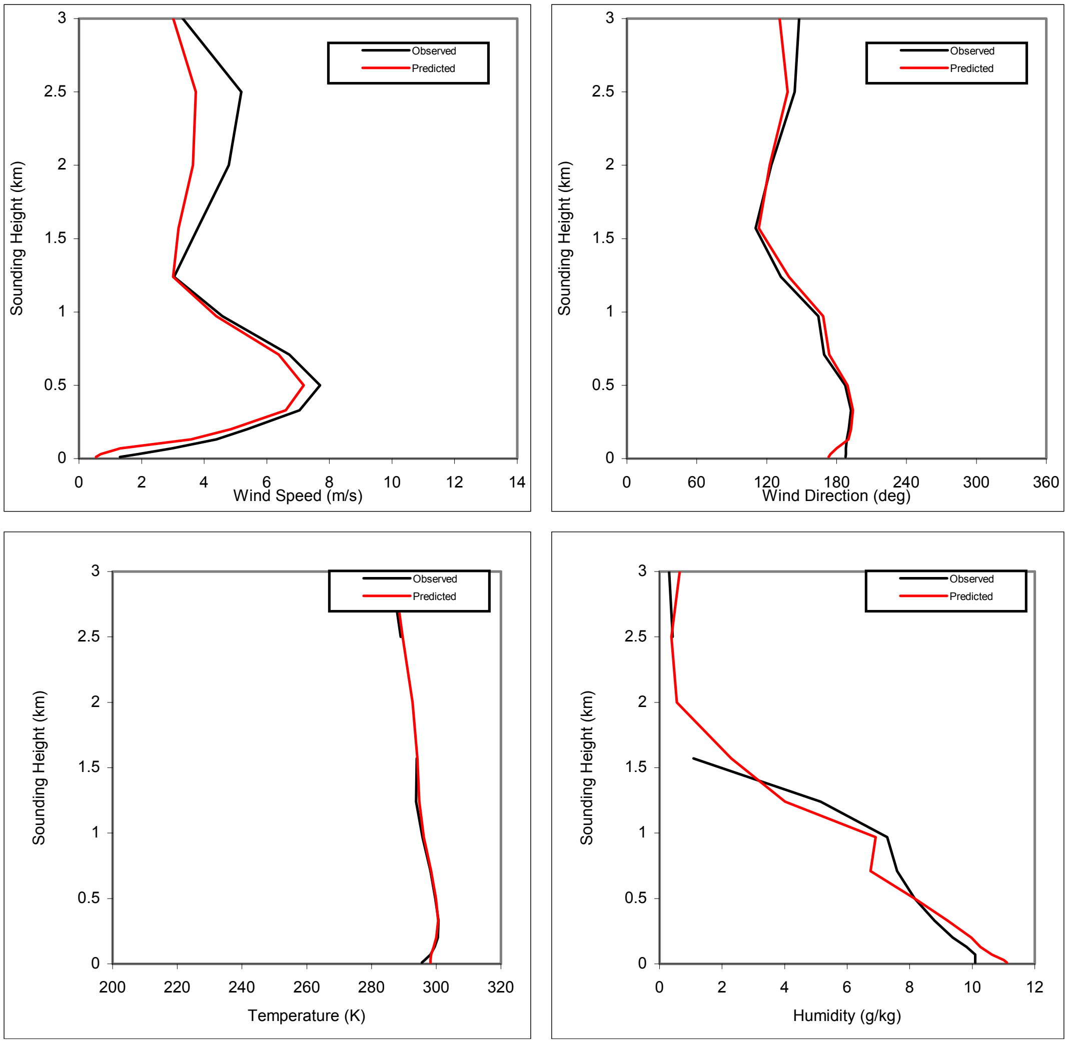

RAOB72249 RAOB72249 1999081718 (run1)

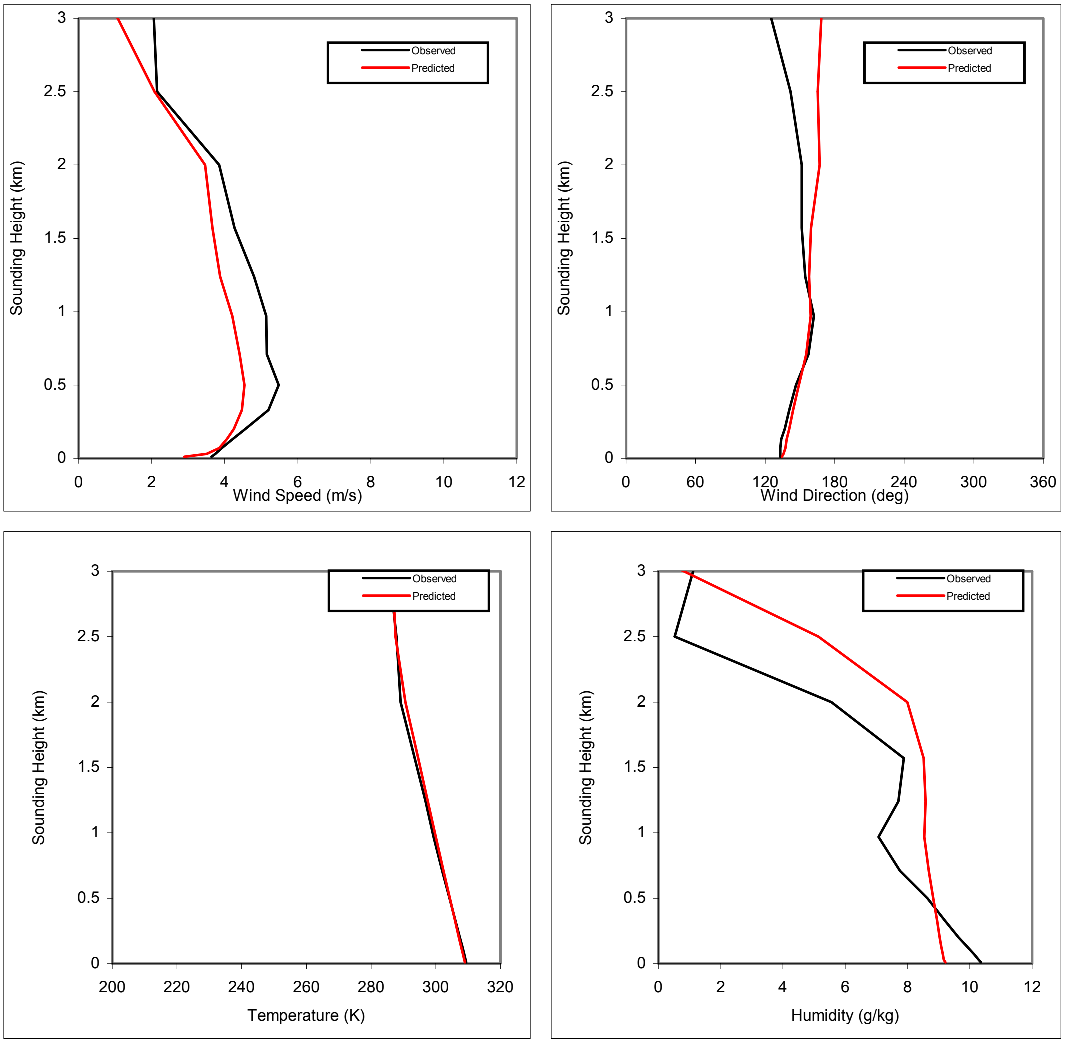

RAOB72249 RAOB72249 1999081806 (run1)

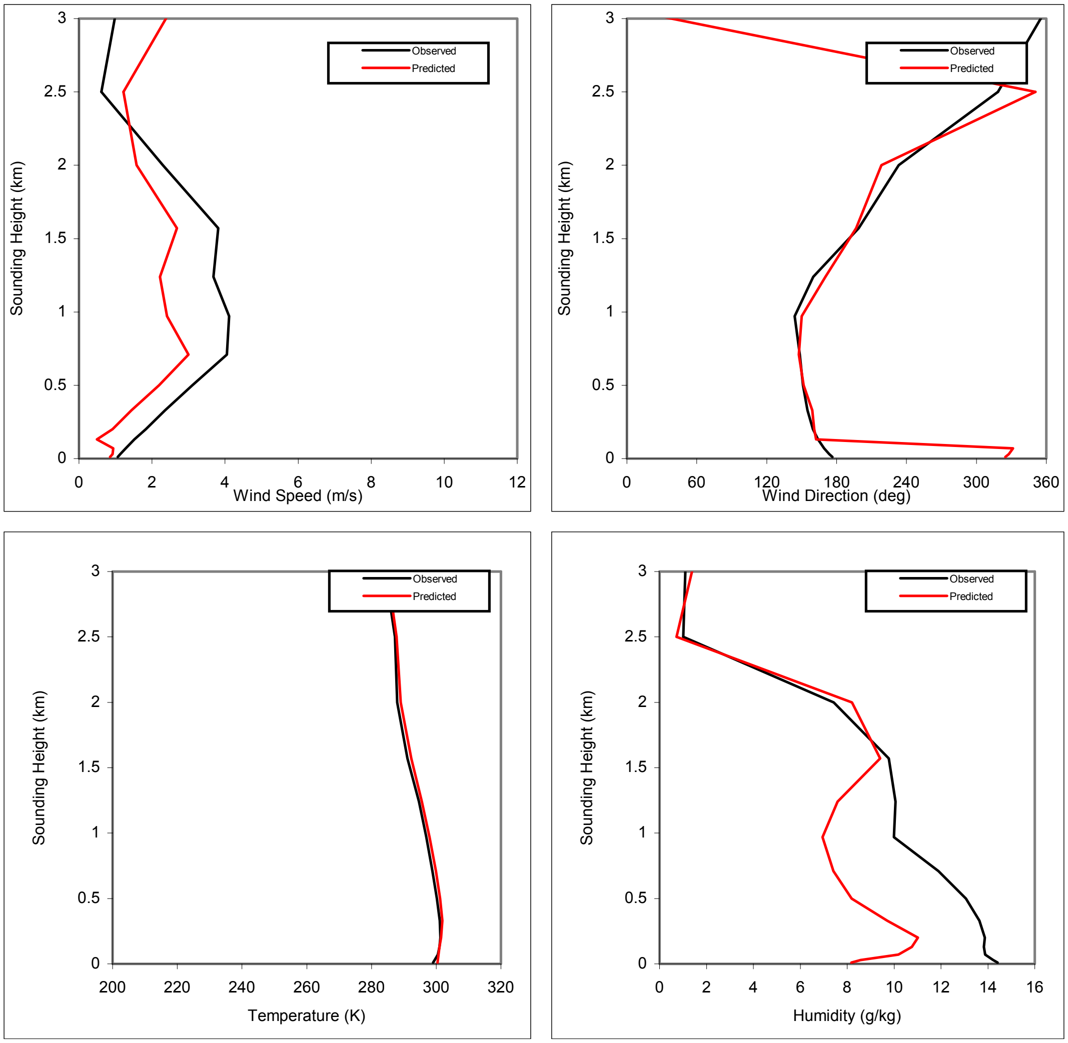

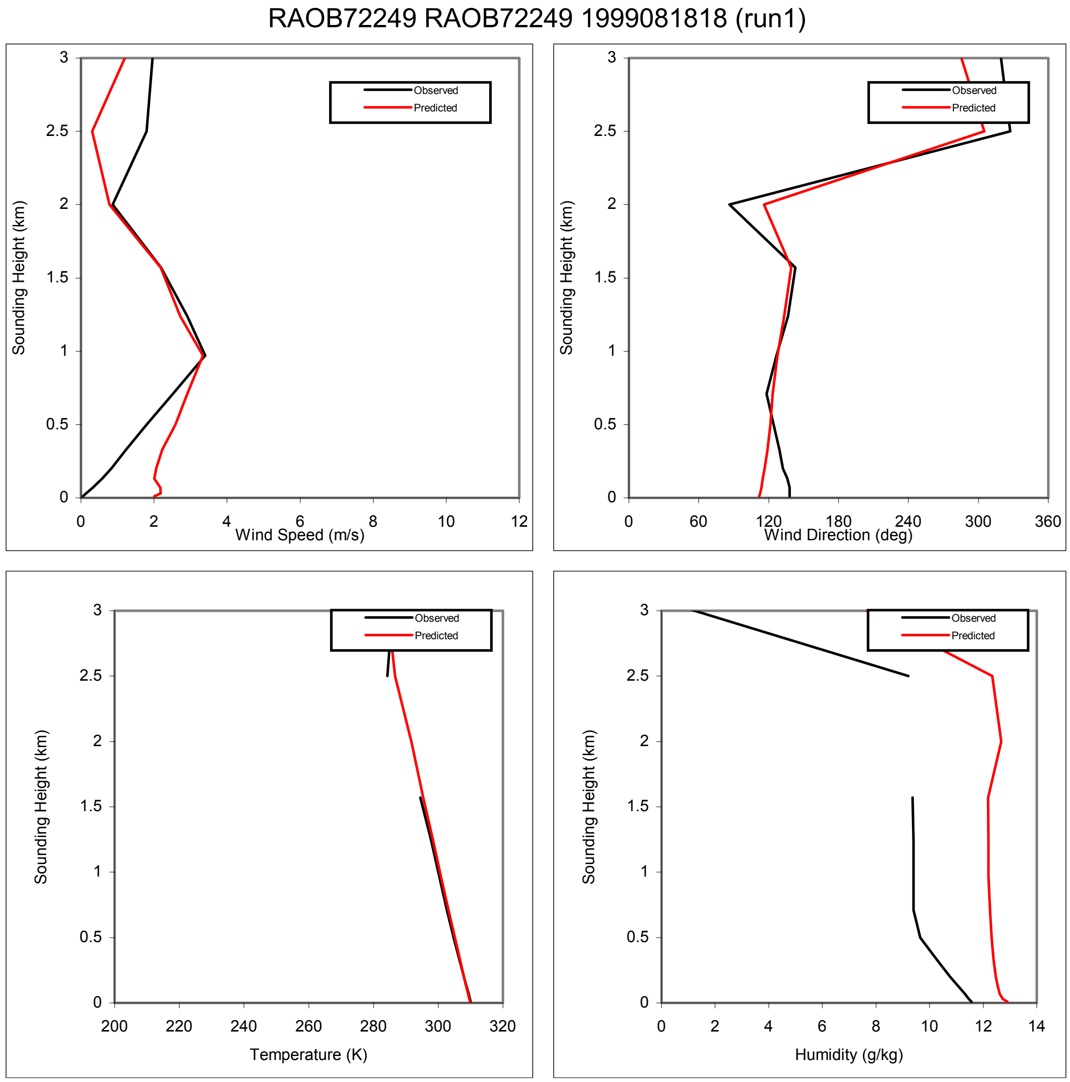
RAOB72249 RAOB72249 1999081818 (run1)
Observed
Predicted
Sounding Height (km)
Wind Speed (m/s)
Wind Direction (deg)
Temperature (K)
Humidity (g/kg)

RAOB72249 RAOB72249 1999081906 (run1)

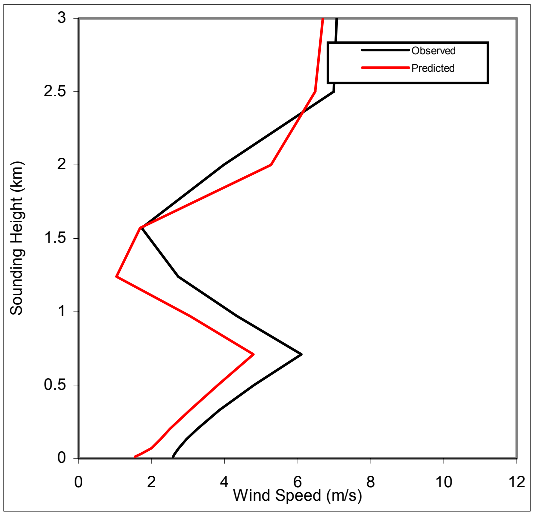


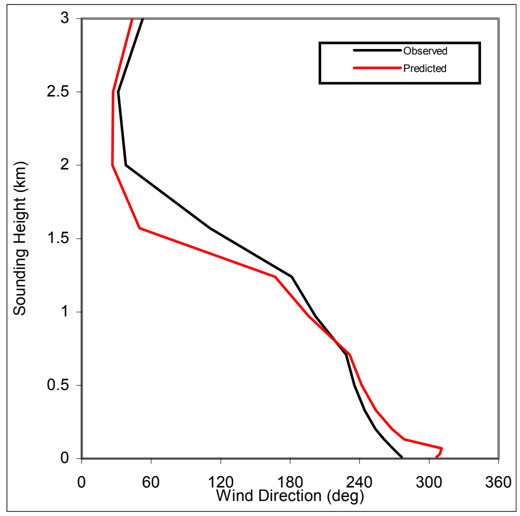


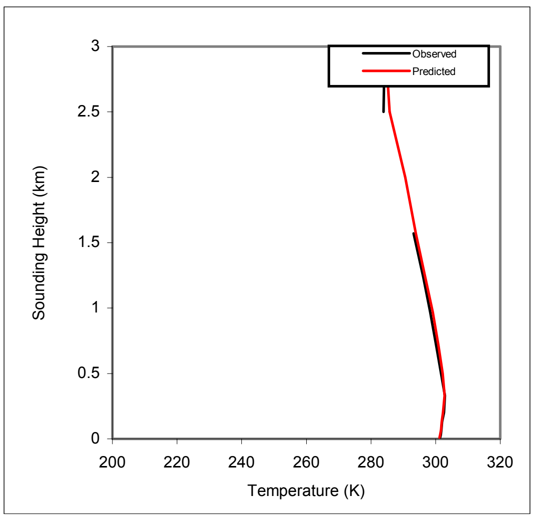


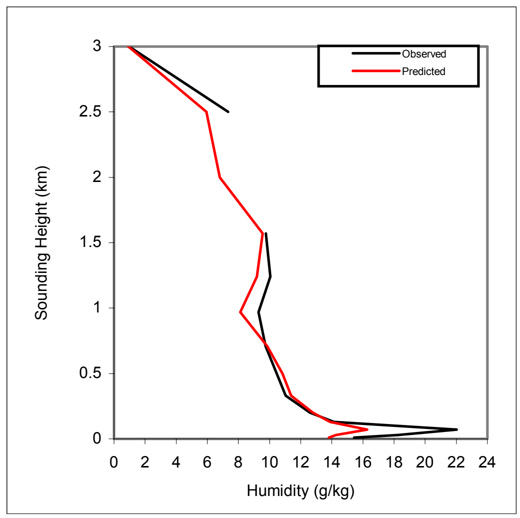

RAOB72249 RAOB72249 1999081918 (run1)

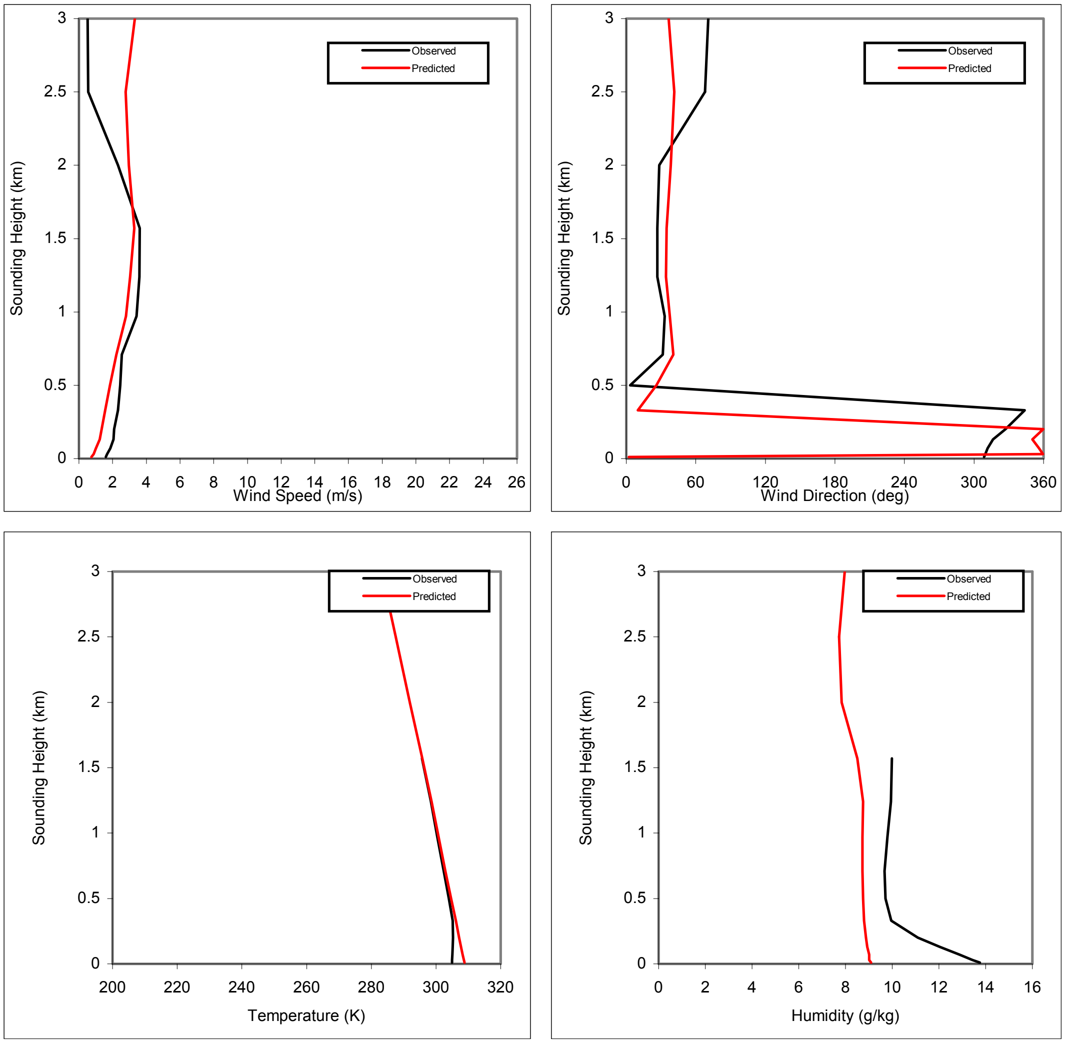

RAOB72249 RAOB72249 1999082006 (run1)

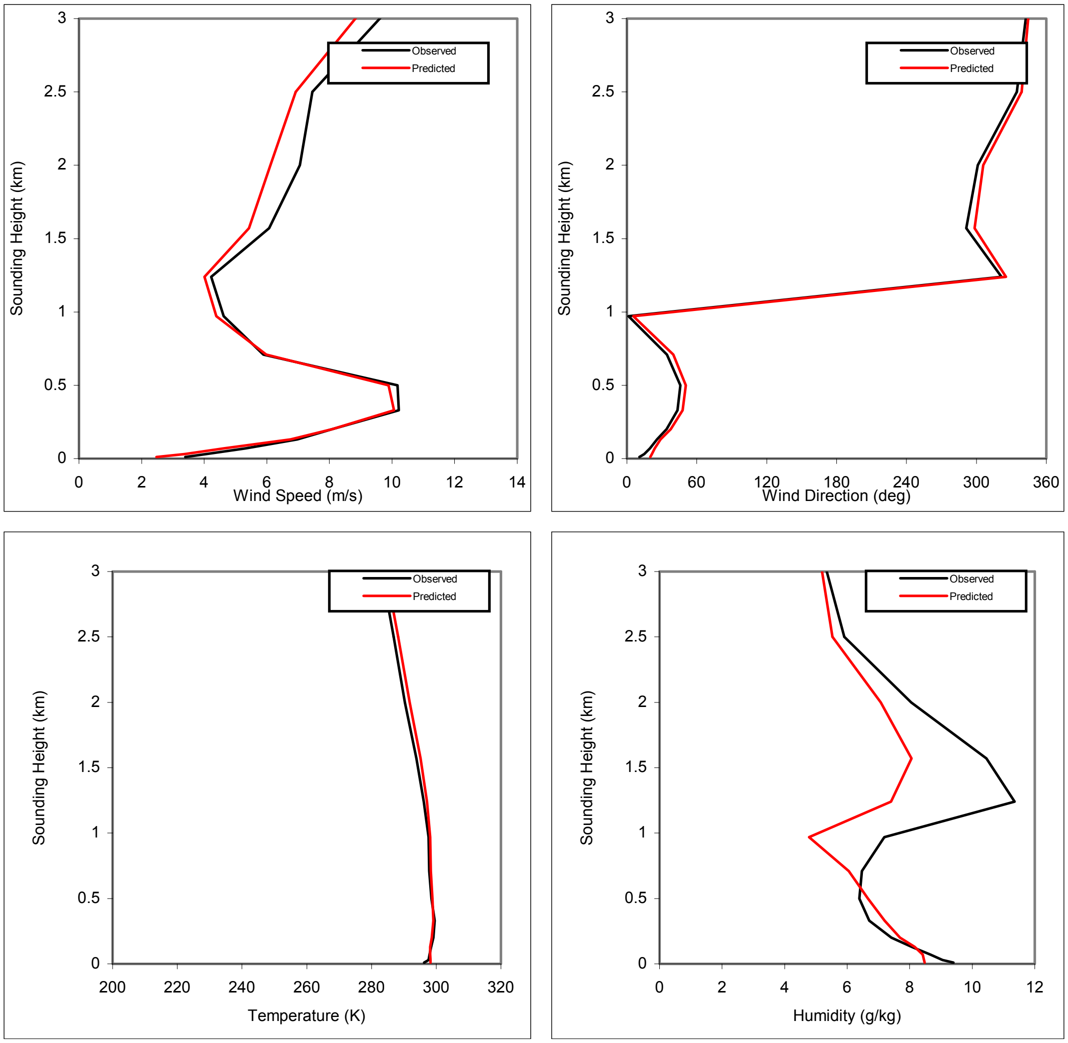

RAOB72249 RAOB72249 1999082018 (run1)

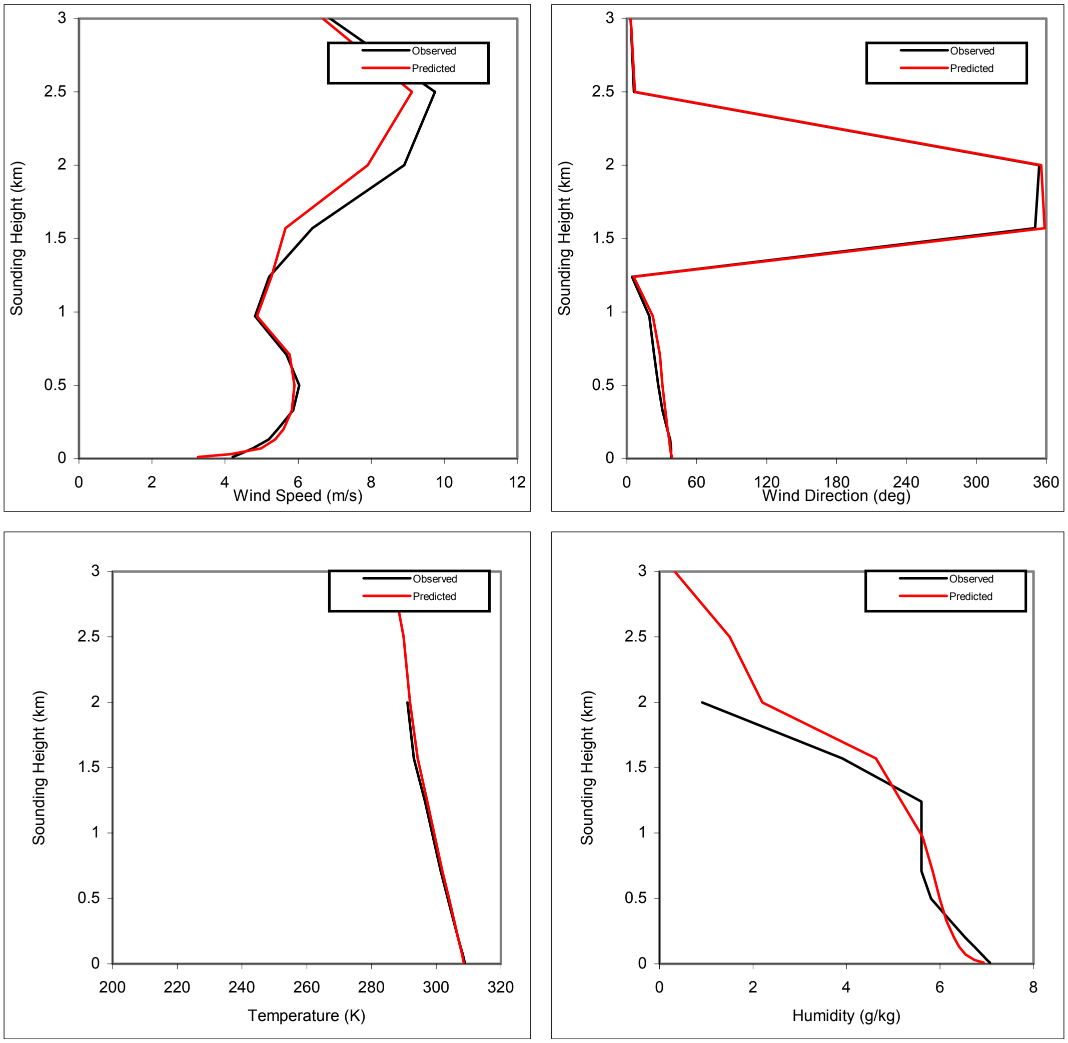

RAOB72249 RAOB72249 1999082106 (run1)

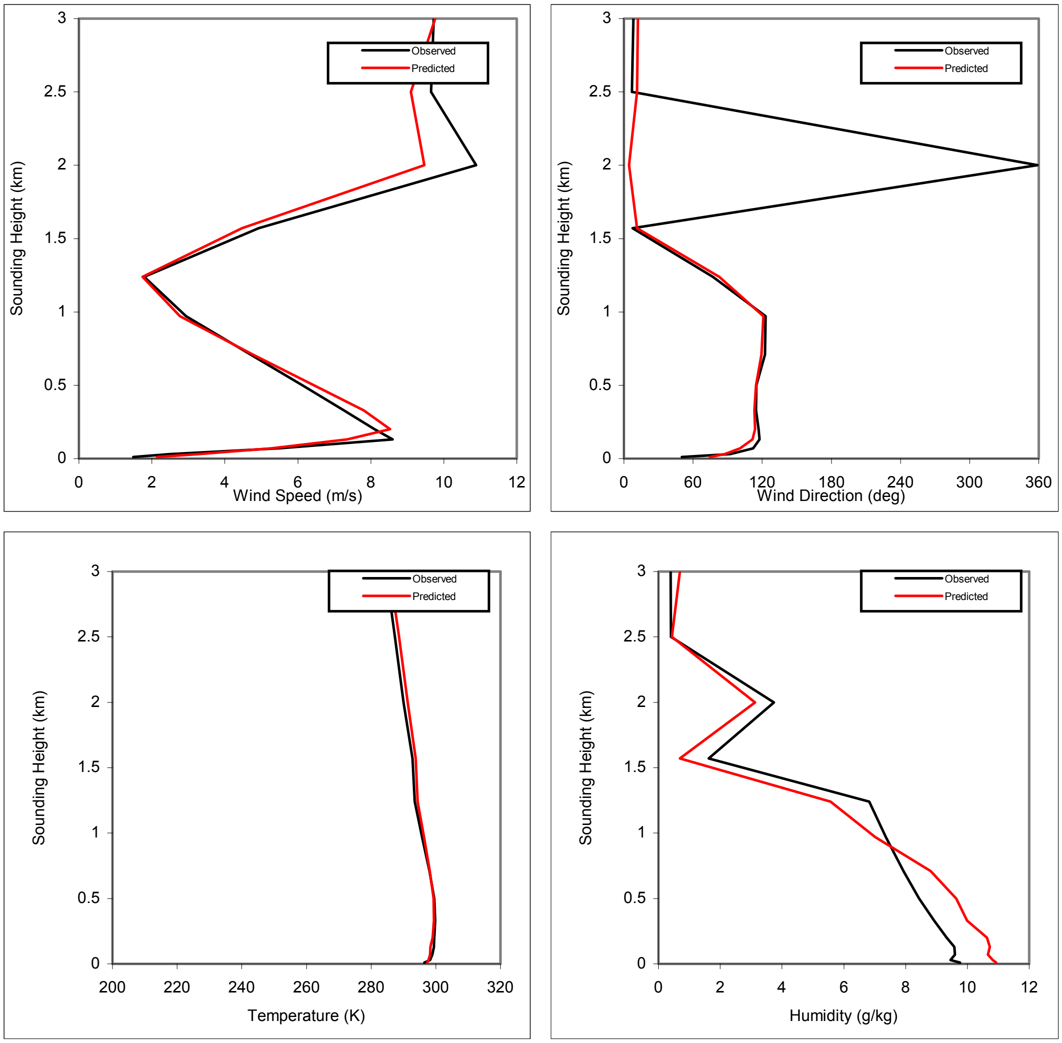

RAOB72249 RAOB72249 1999082118 (run1)

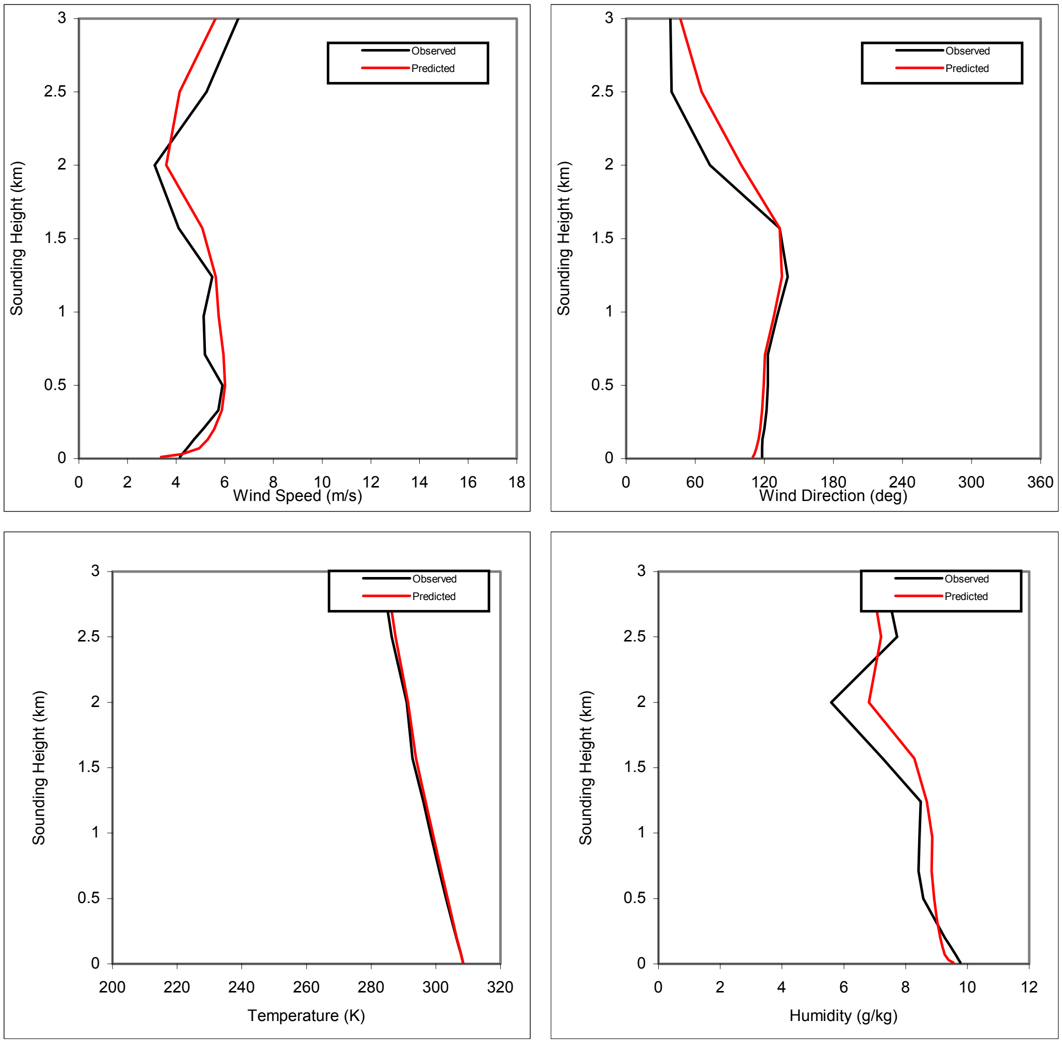

# Appendix C

## Qualitative Assessment of MM5 Results

# Surface Wind and Sea Level Pressure

SIGMA =1.000 SEA PRES (mb ) 1999-08-16_00:00:00 = 1999-08-13_00 + 72.00H SMOOTH= 0
SIGMA =0.999 BARB UV (m/s ) 1999-08-16_00:00:00 = 1999-08-13_00 + 72.00H SMOOTH= 0

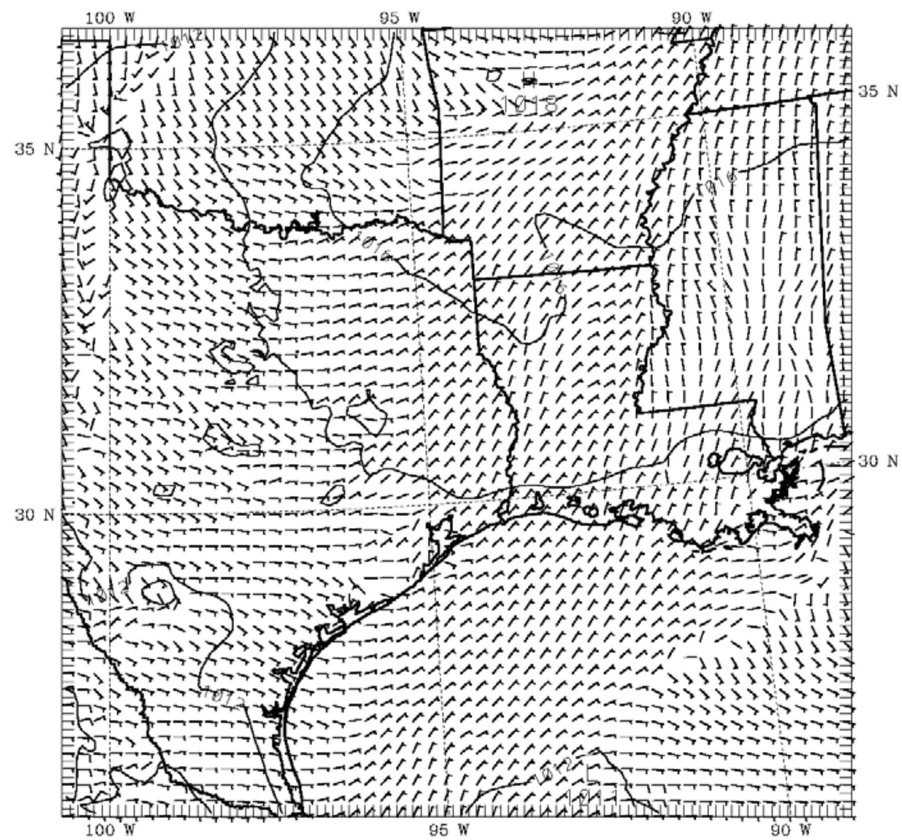


TCEQ DFW, August 13-22, 1999, Run3
CONTOUR FROM 1008.0 TO 1018.0 CONTOUR INTERVAL OF 2.0000 PT(3,3)= 1010.5

SIGMA =1.000 SEA PRES (mb ) 1999-08-17_00:00:00 = 1999-08-13_00 + 96.00H SMOOTH= 0
SIGMA =0.999 BARB UV (m/s ) 1999-08-17_00:00:00 = 1999-08-13_00 + 96.00H SMOOTH= 0

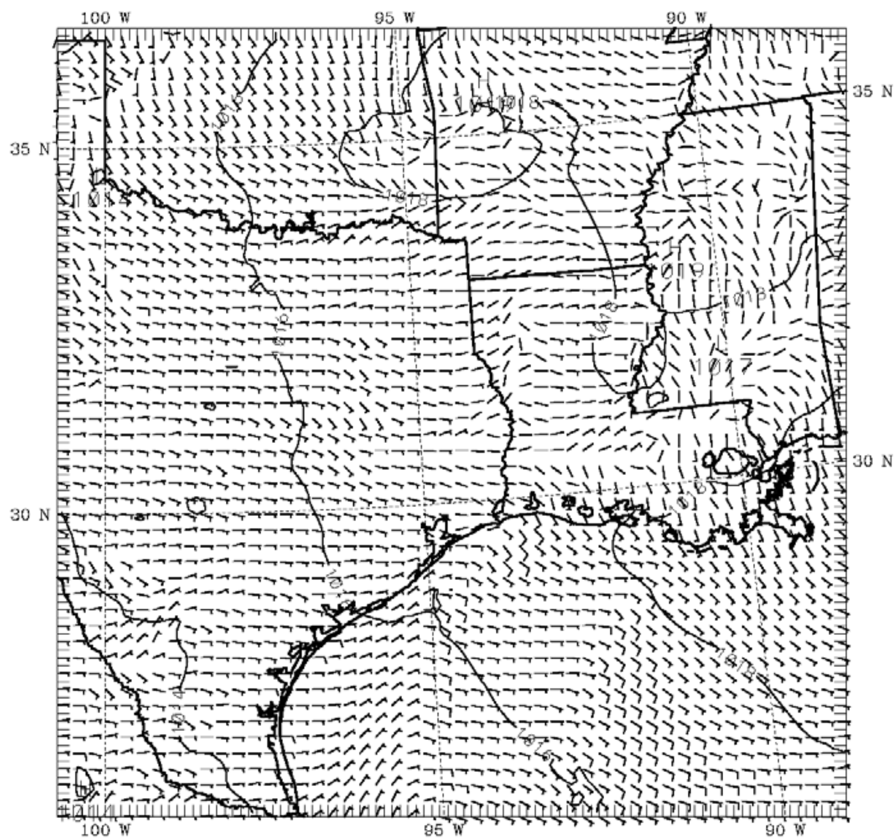


TCEQ DFW, August 13-22, 1999, Run3
CONTOUR FROM 1012.0 TO 1018.0 CONTOUR INTERVAL OF 2.0000 PT(3,3)= 1014.0

SIGMA =1.000 SEA PRES (mb ) 1999-08-18_00:00:00 = 1999-08-13_00 +120.00H SMOOTH= 0
SIGMA =0.999 BARB UV (m/s ) 1999-08-18_00:00:00 = 1999-08-13_00 +120.00H SMOOTH= 0

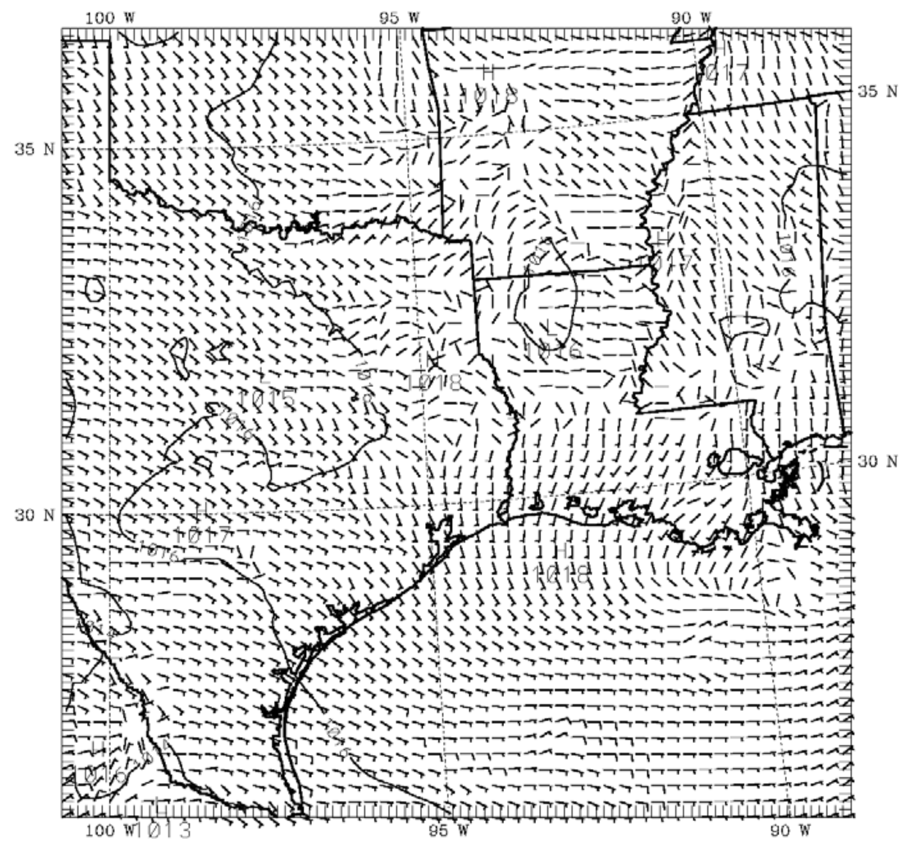


TCEQ DFW, August 13-22, 1999, Run3
CONTOUR FROM 1012.0 TO 1016.0 CONTOUR INTERVAL OF 2.0000 PT(3,3)= 1014.0

SIGMA =1.000 SEA PRES (mb ) 1999-08-19_00:00:00 = 1999-08-13_00 +144.00H SMOOTH= 0
SIGMA =0.999 BARB UV (m/s ) 1999-08-19_00:00:00 = 1999-08-13_00 +144.00H SMOOTH= 0

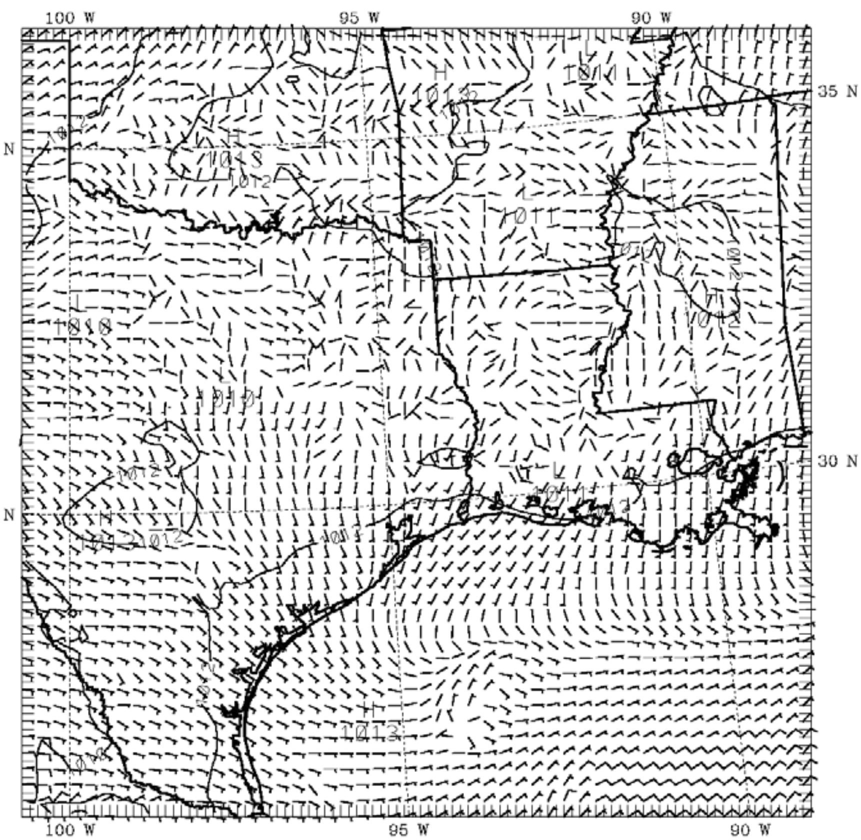


TCEQ DFW, August 13-22, 1999, Run3
CONTOUR FROM 1008.0 TO 1012.0 CONTOUR INTERVAL OF 2.0000 PT(3,3)= 1010.4

SIGMA =1.000 SEA PRES (mb ) 1999-08-20_00:00:00 = 1999-08-13_00 +168.00H SMOOTH= 0
SIGMA =0.999 BARB UV (m/s ) 1999-08-20_00:00:00 = 1999-08-13_00 +168.00H SMOOTH= 0

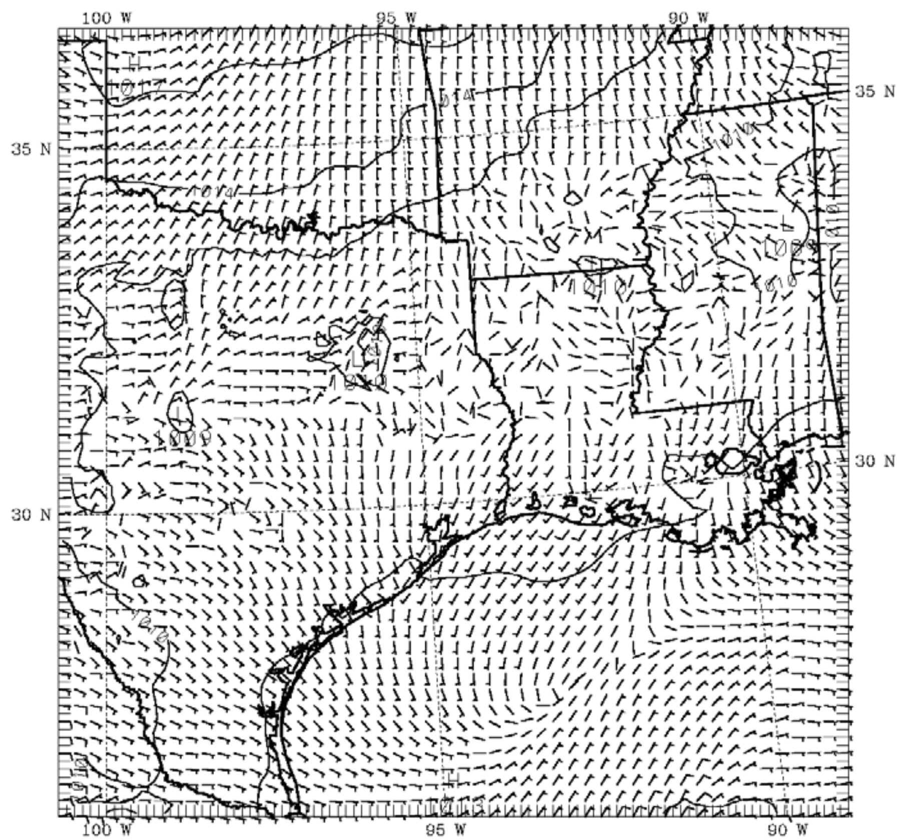


TCEQ DFW, August 13-22, 1999, Run3
CONTOUR FROM 1008.0 TO 1016.0 CONTOUR INTERVAL OF 2.0000 PT(3,3)= 1010.4

SIGMA =1.000 SEA PRES (mb ) 1999-08-21_00:00:00 = 1999-08-13_00 +192.00H SMOOTH= 0
SIGMA =0.999 BARB UV (m/s ) 1999-08-21_00:00:00 = 1999-08-13_00 +192.00H SMOOTH= 0

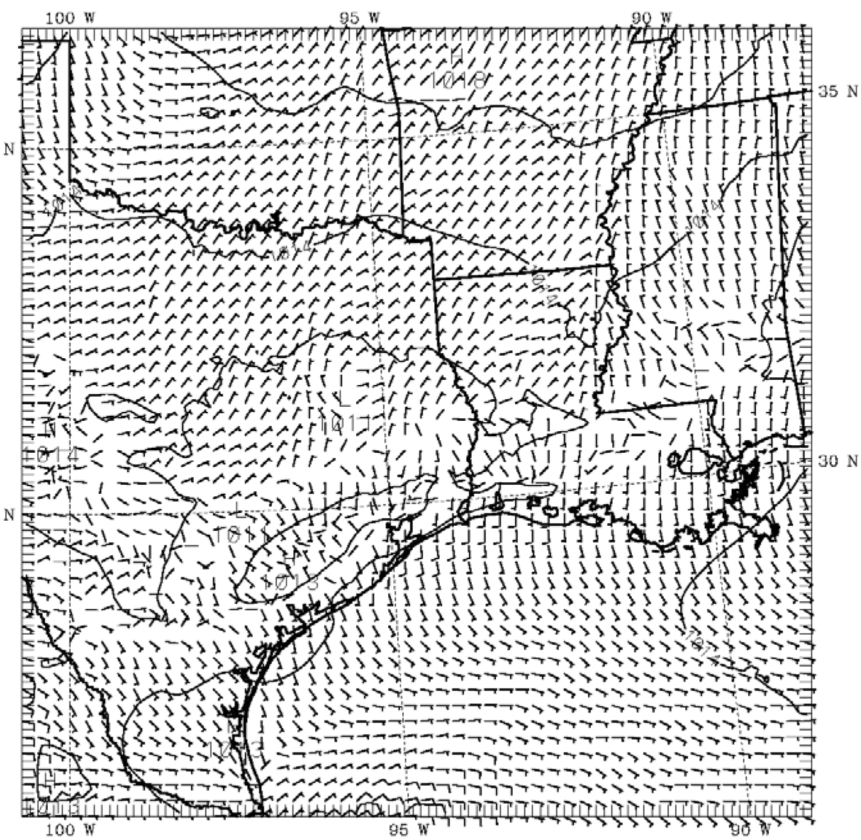


TCEQ DFW, August 13–22, 1999, Run3

CONTOUR FROM 1008.0 TO 1016.0 CONTOUR INTERVAL OF 2.0000 PT(3,3)= 1012.4

**PBL Depth**

# Layer 1 PBL

MM5-based layer 1 PBL field on TCEQ 04-km CAMx grid

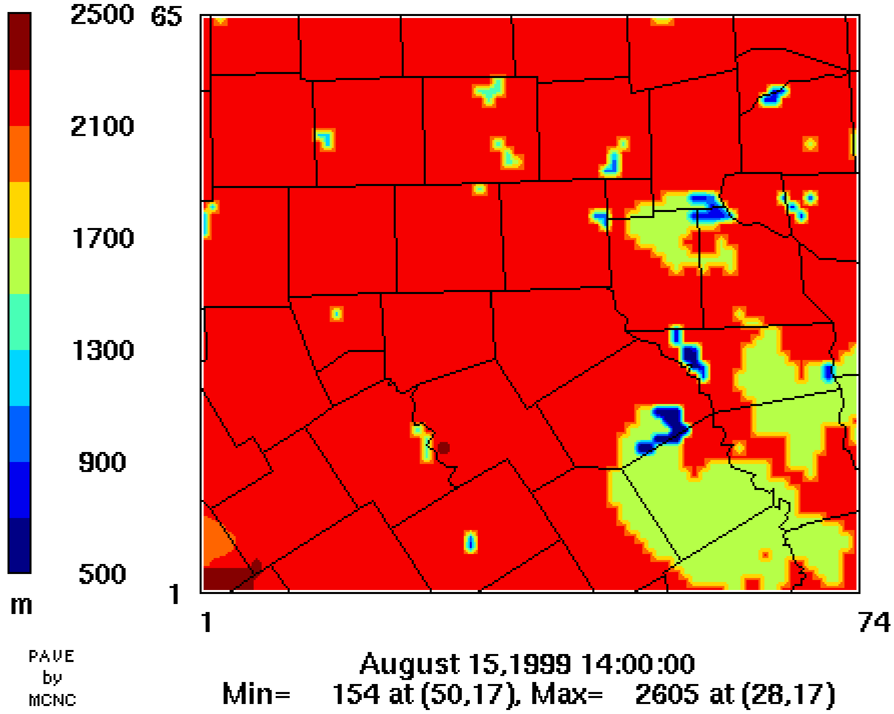


August 15,1999 14:00:00
Min= 154 at (50,17), Max= 2605 at (28,17)

# Layer 1 PBL

MM5-based layer 1 PBL field on TCEQ 04-km CAMx grid

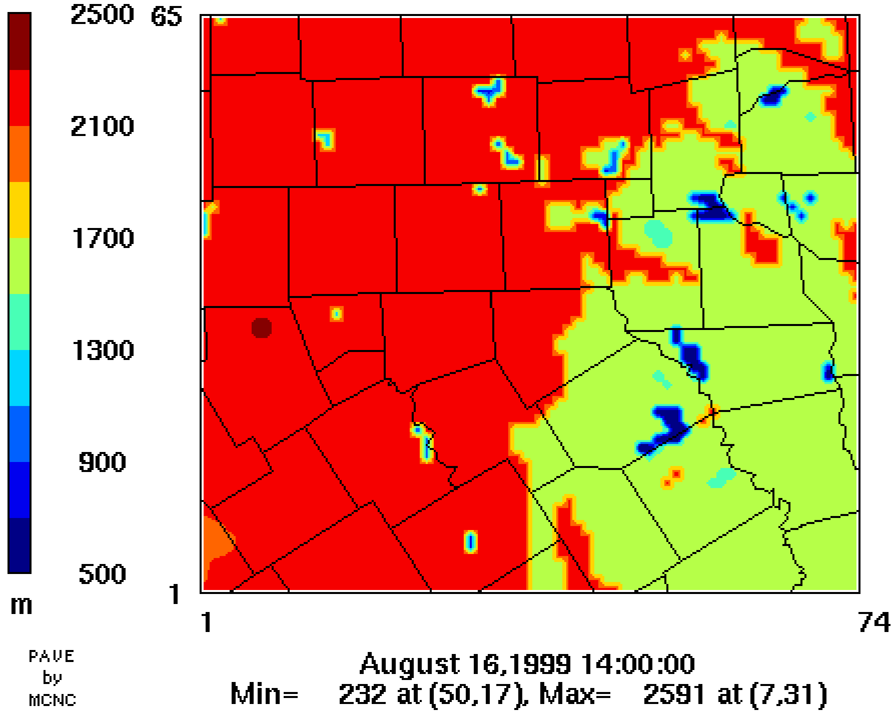

# Layer 1 PBL

MM5-based layer 1 PBL field on TCEQ 04-km CAMx grid

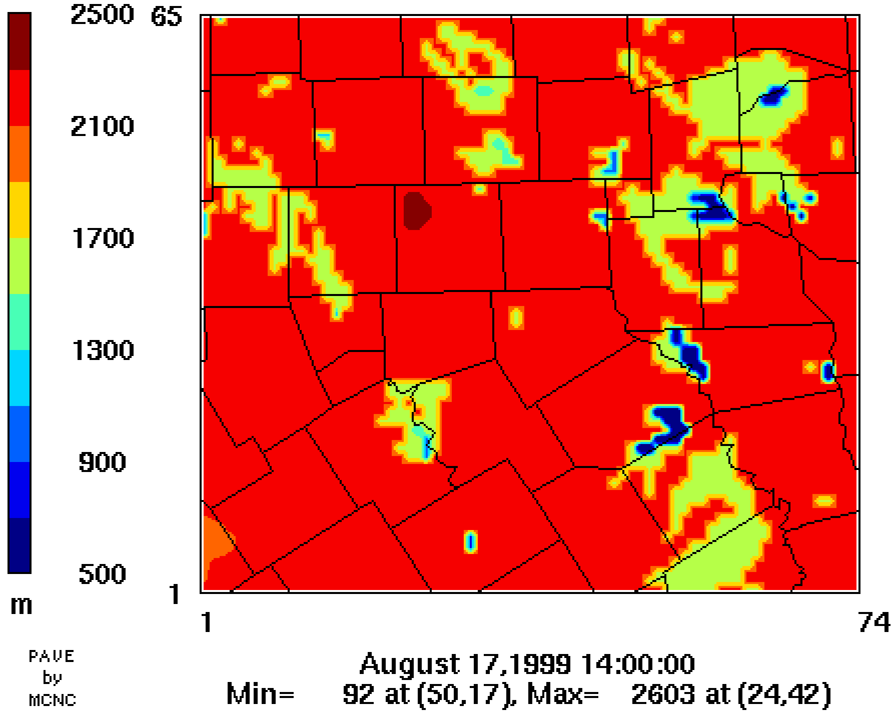


August 17,1999 14:00:00
Min= 92 at (50,17), Max= 2603 at (24,42)

## Layer 1  PBL

MM5-based layer 1 PBL field on TCEQ 04-km CAMx grid

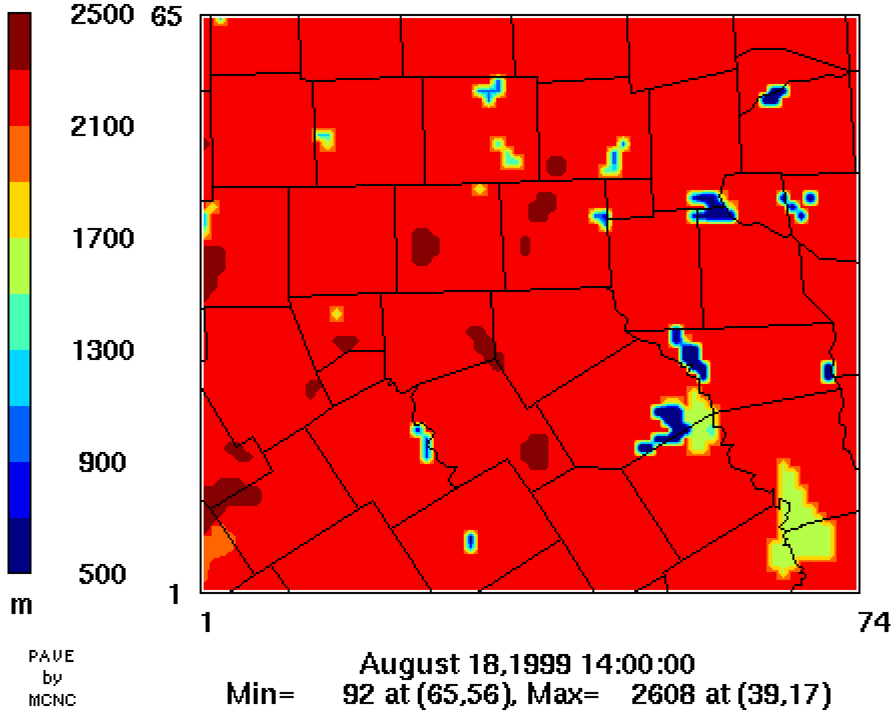


August 18,1999 14:00:00
Min= 92 at (65,56), Max= 2608 at (39,17)

# Layer 1 PBL

MM5-based layer 1 PBL field on TCEQ 04-km CAMx grid

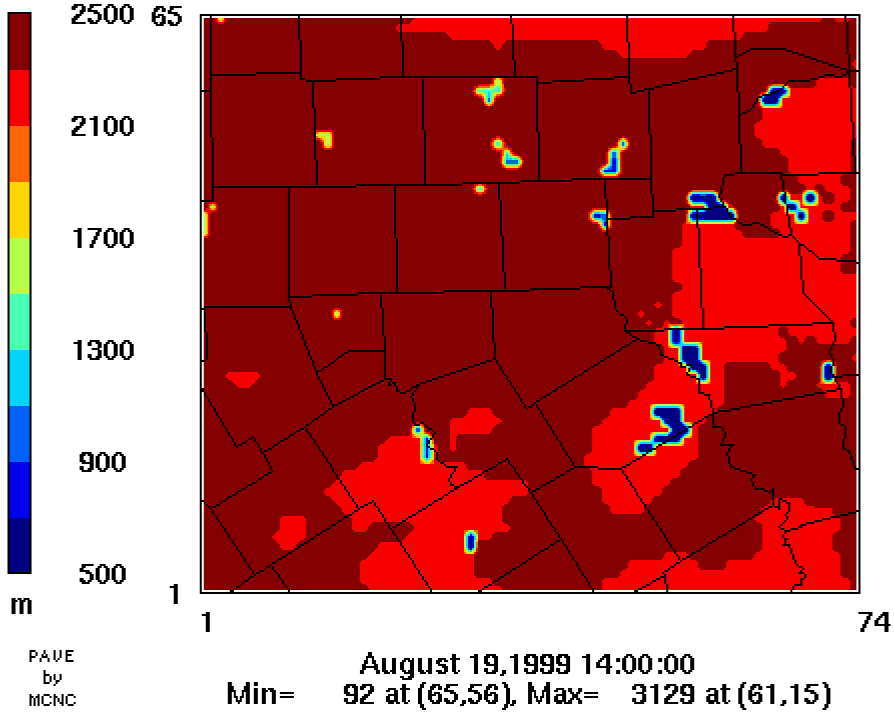


August 19,1999 14:00:00
Min= 92 at (65,56), Max= 3129 at (61,15)

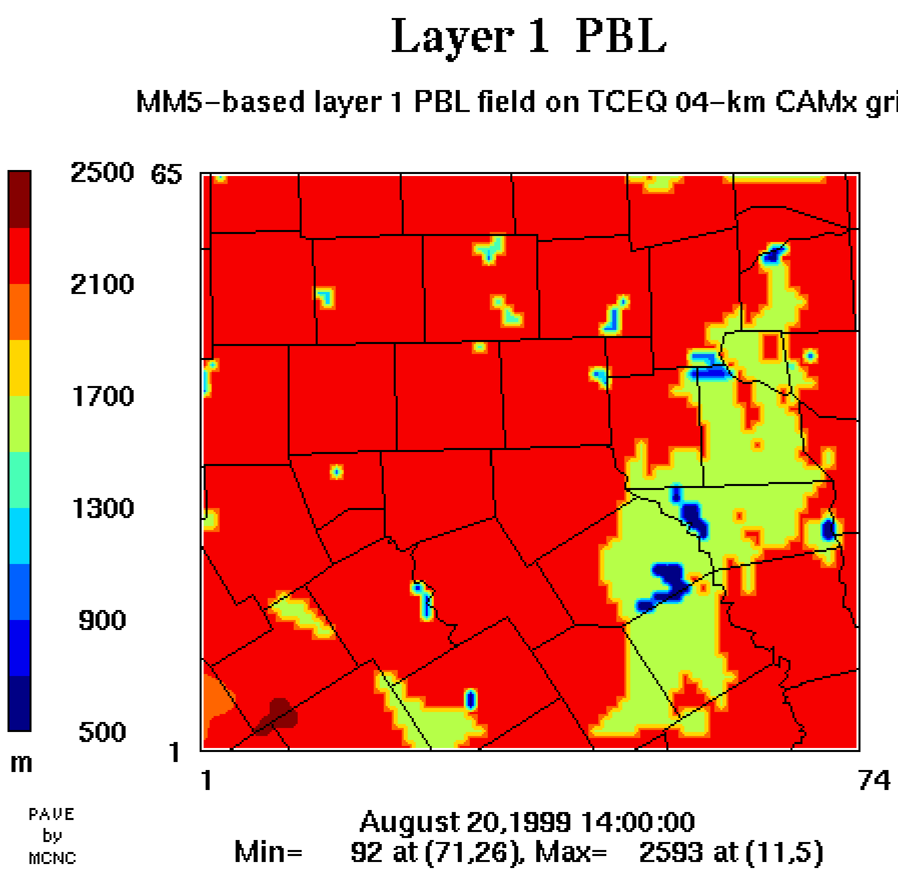

Layer 1 PBL
MM5-based layer 1 PBL field on TCEQ 04-km CAMx grid
2500
2100
1700
1300
900
500
m
65
1
1
74
PAVE
by
MCNC
August 20,1999 14:00:00
Min= 92 at (71,26), Max= 2593 at (11,5)

# Layer 1 PBL

MM5-based layer 1 PBL field on TCEQ 04-km CAMx grid

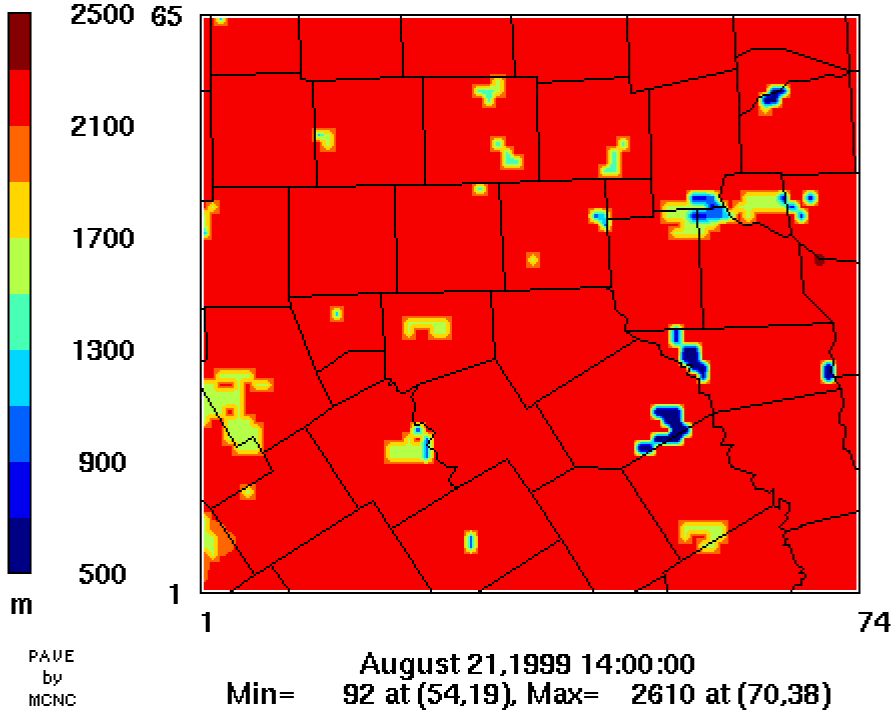


August 21,1999 14:00:00
Min= 92 at (54,19), Max= 2610 at (70,38)

# Layer 1  PBL

MM5-based layer 1 PBL field on TCEQ 04-km CAMx grid

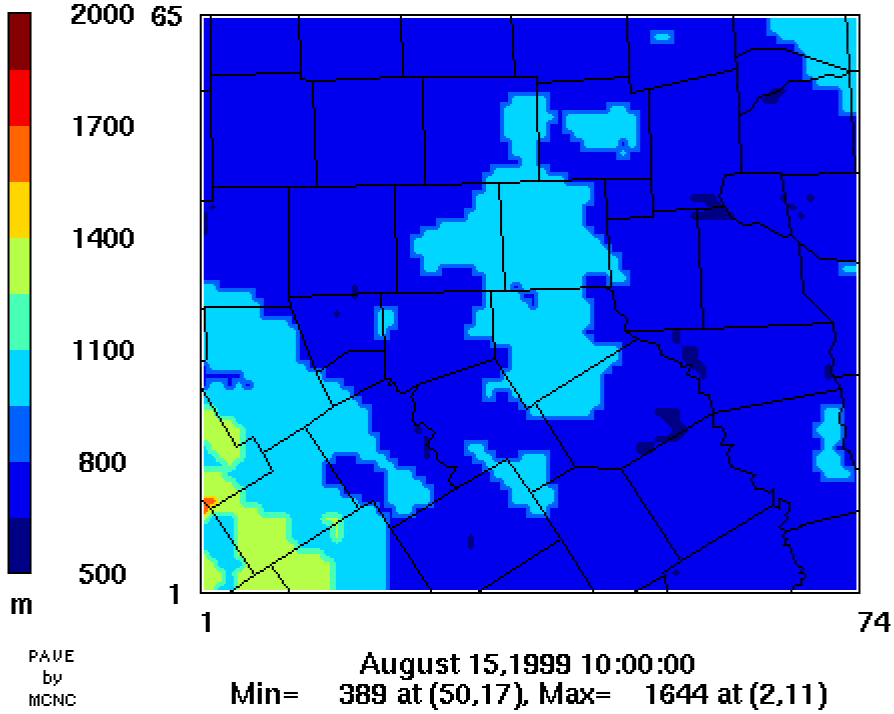


August 15,1999 10:00:00

Min= 389 at (50,17), Max= 1644 at (2,11)

# Layer 1  PBL

MM5-based layer 1 PBL field on TCEQ 04-km CAMx grid

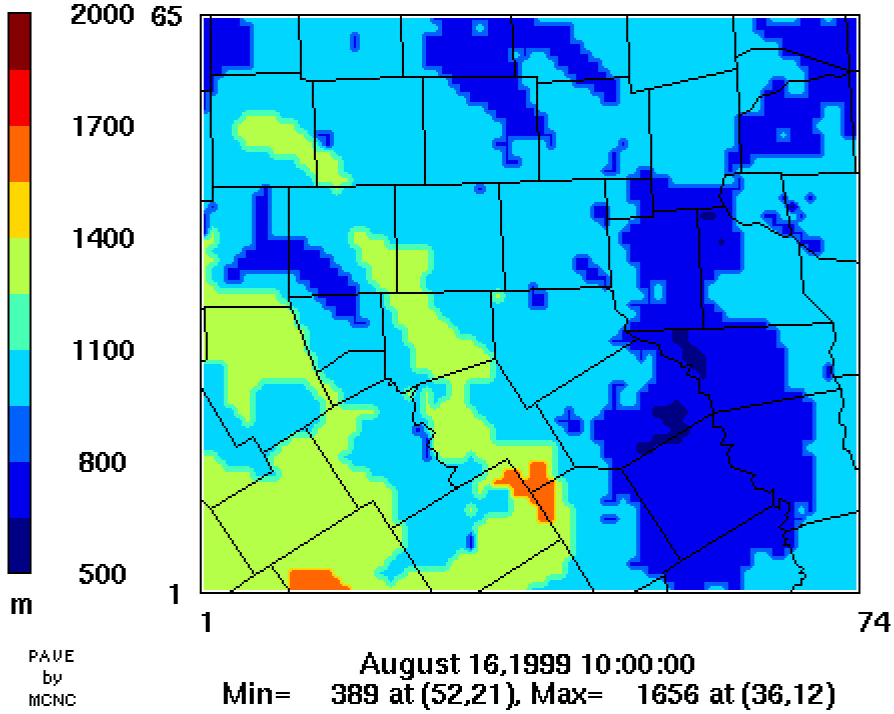


August 16,1999 10:00:00
Min= 389 at (52,21), Max= 1656 at (36,12)

# Layer 1 PBL

MM5-based layer 1 PBL field on TCEQ 04-km CAMx grid

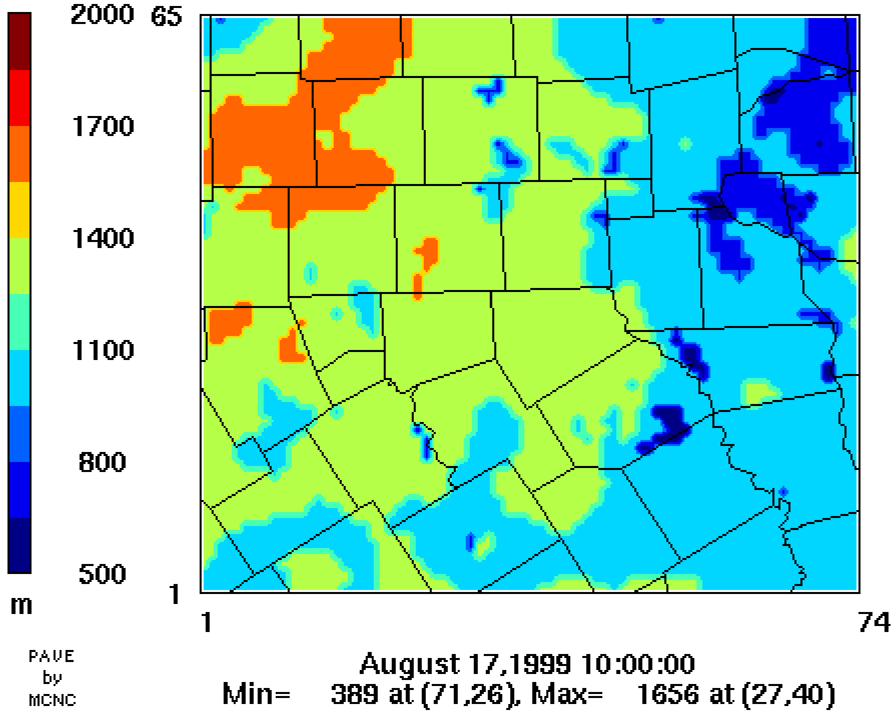


August 17,1999 10:00:00
Min= 389 at (71,26), Max= 1656 at (27,40)

# Layer 1 PBL

MM5-based layer 1 PBL field on TCEQ 04-km CAMx grid

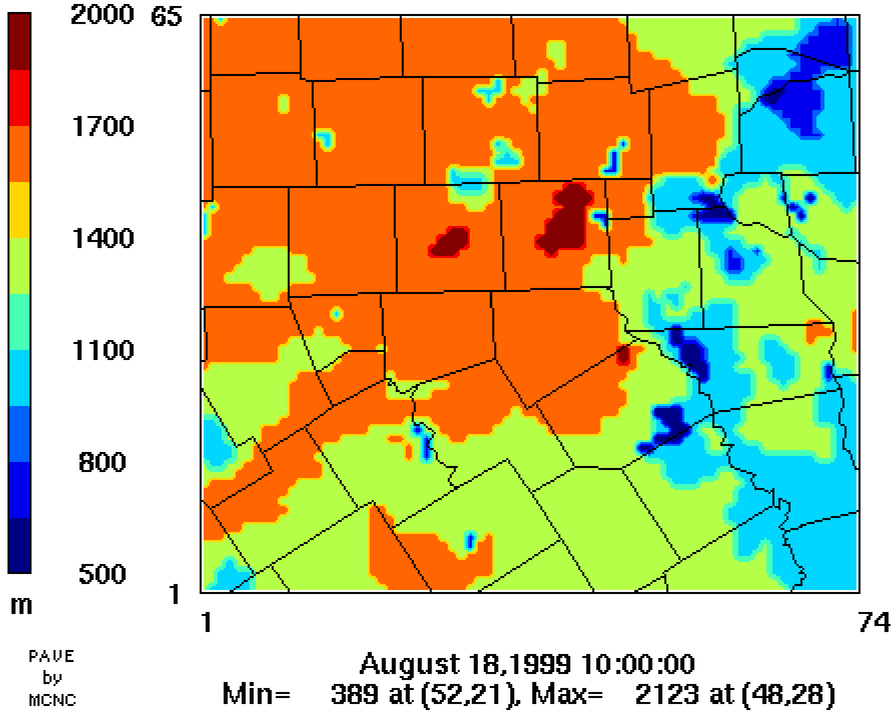

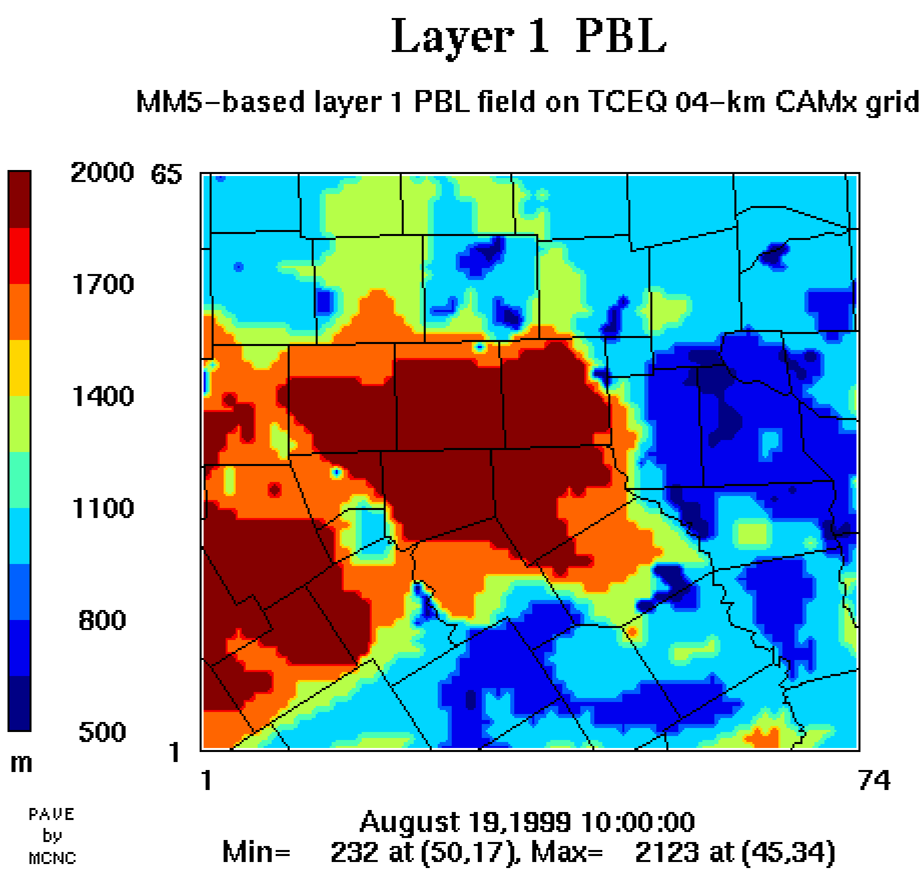
Layer 1 PBL
MM5-based layer 1 PBL field on TCEQ 04-km CAMx grid
2000
1700
1400
1100
800
500
m
65
1
1
74
PAVE
by
MCNC
August 19,1999 10:00:00
Min= 232 at (50,17), Max= 2123 at (45,34)

# Layer 1  PBL

MM5-based layer 1 PBL field on TCEQ 04-km CAMx grid

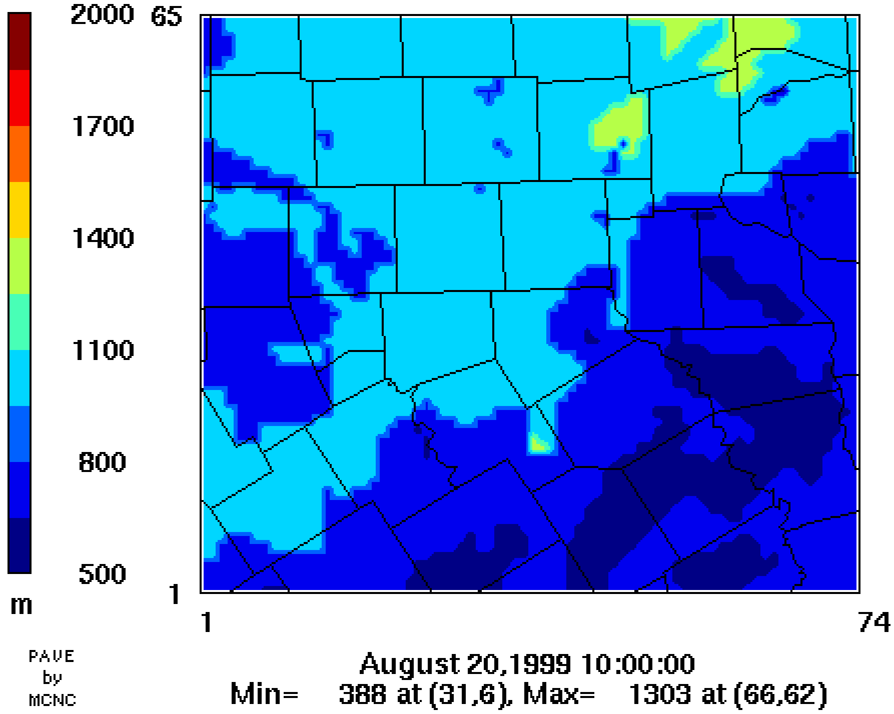


August 20,1999 10:00:00
Min=    388 at (31,6), Max=    1303 at (66,62)

# Layer 1  PBL

MM5-based layer 1 PBL field on TCEQ 04-km CAMx grid

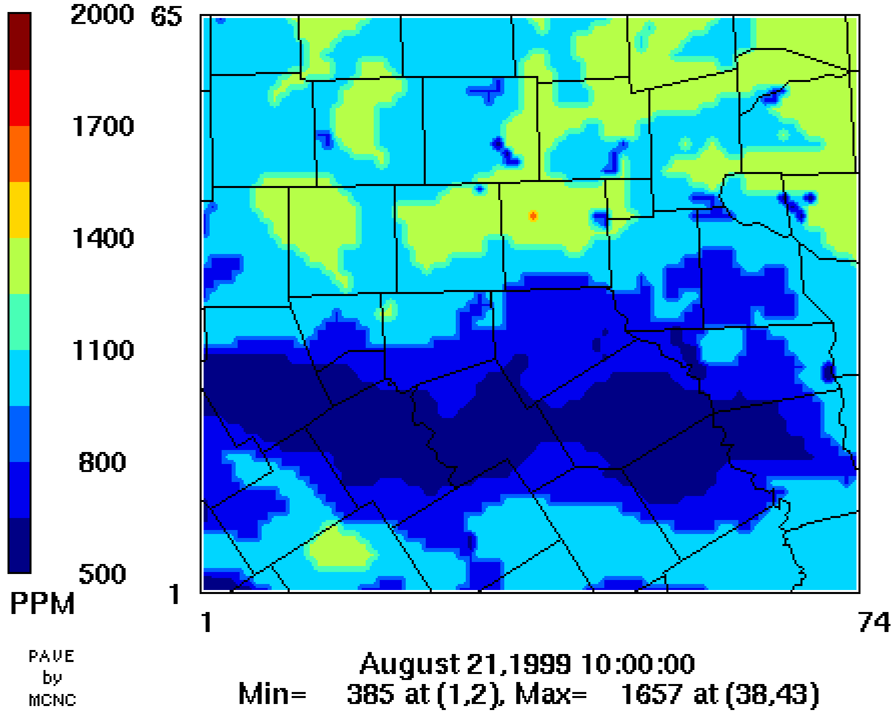


August 21,1999 10:00:00
Min=    385 at (1,2), Max=    1657 at (38,43)

# Appendix D

# Cloud Optical Depth and PAR

# CAMx Cloud Optical Depth

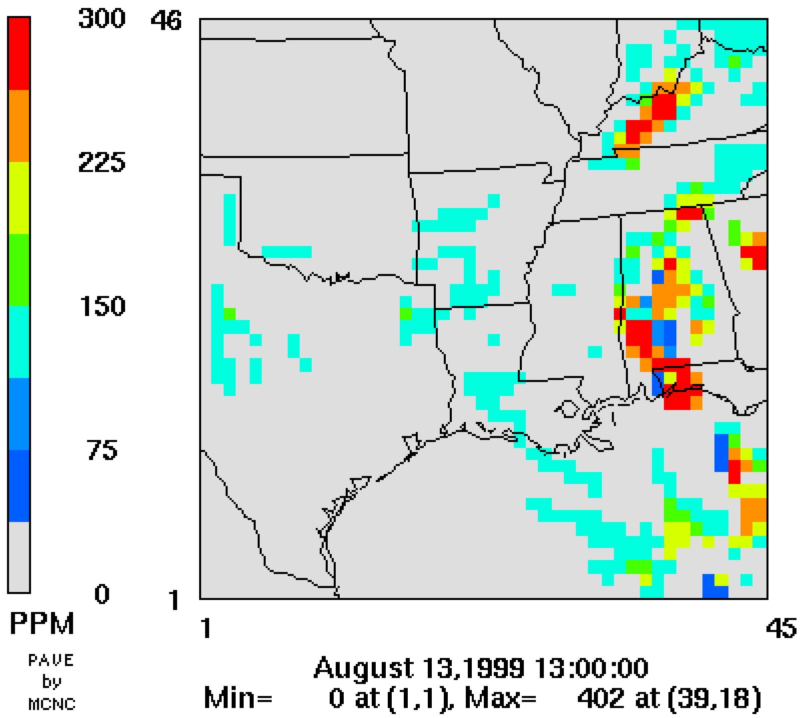


# PAR

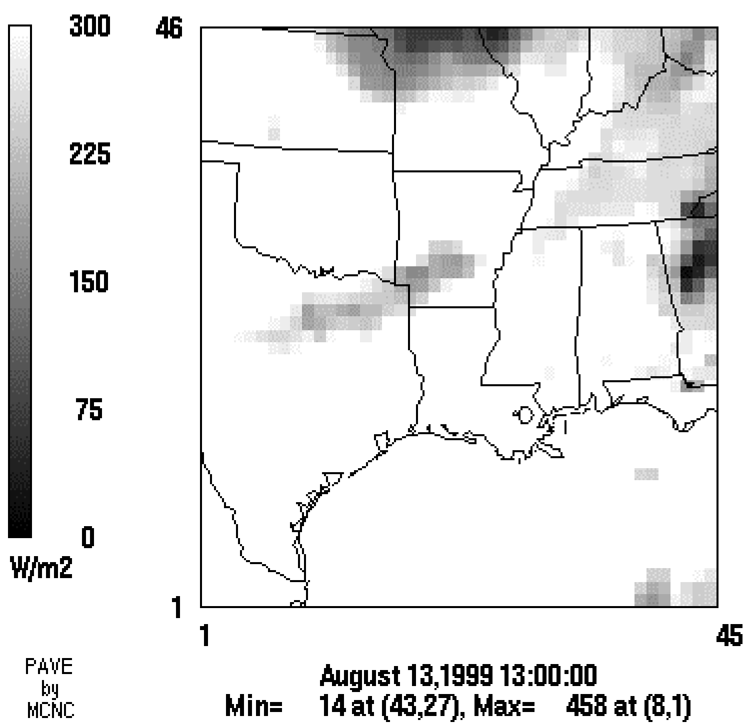


**Figure D-1.** MM5-derived cloud optical depth and satellite-derived PAR on the CAMx 36-km domain on 1300 CST August 13, 1999.

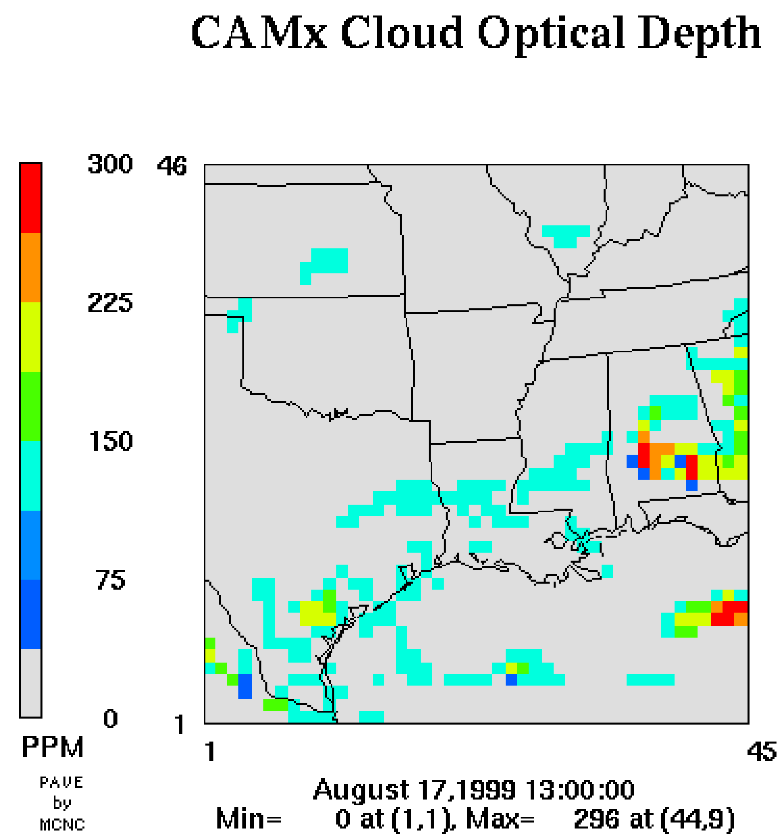


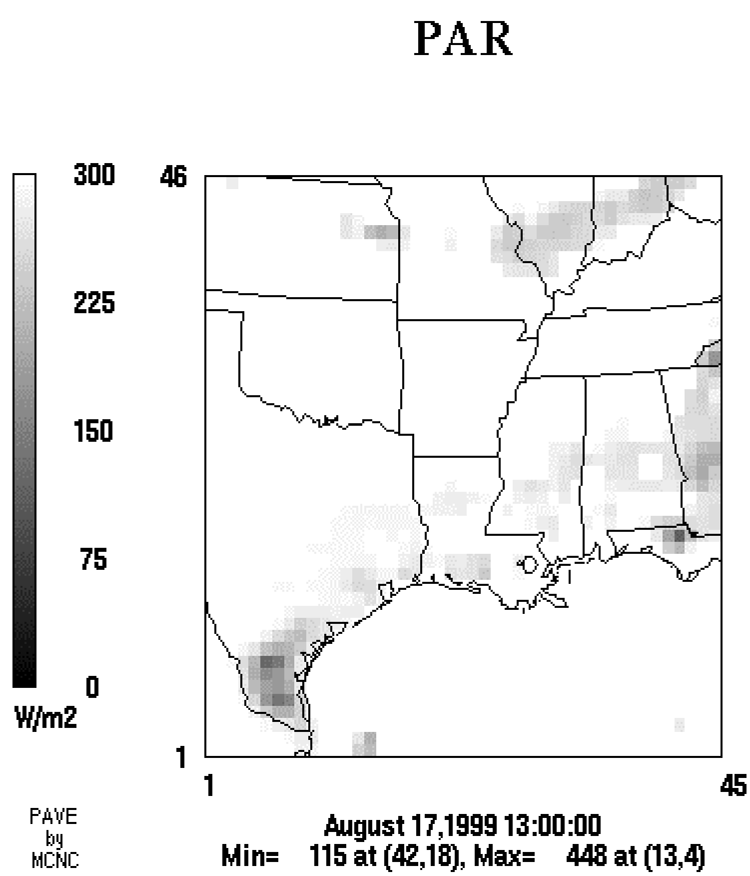


**Figure D-2.** MM5-derived cloud optical depth and satellite-derived PAR on the CAMx 36-km domain on 1300 CST August 17, 1999.

## CAMx Cloud Optical Depth

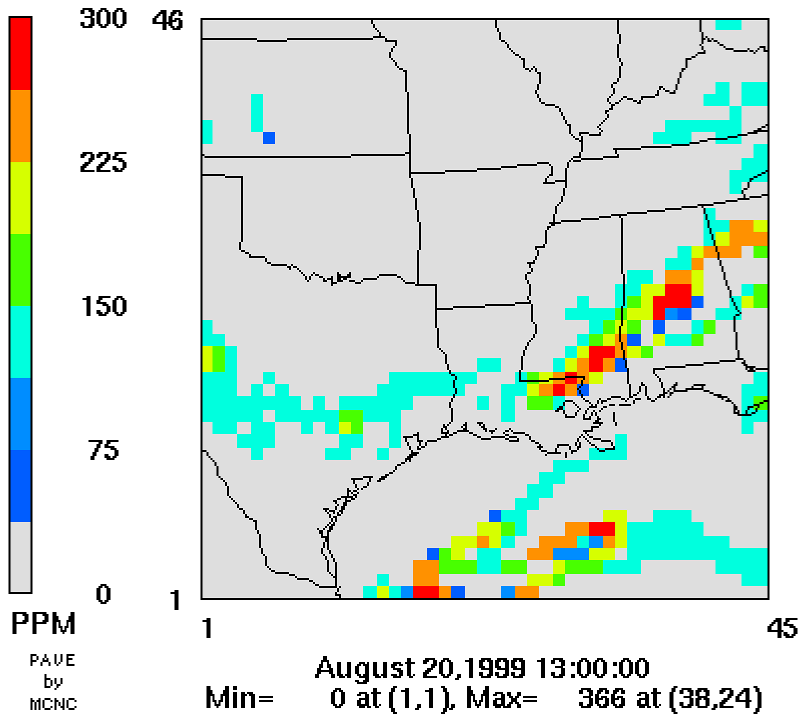


## PAR

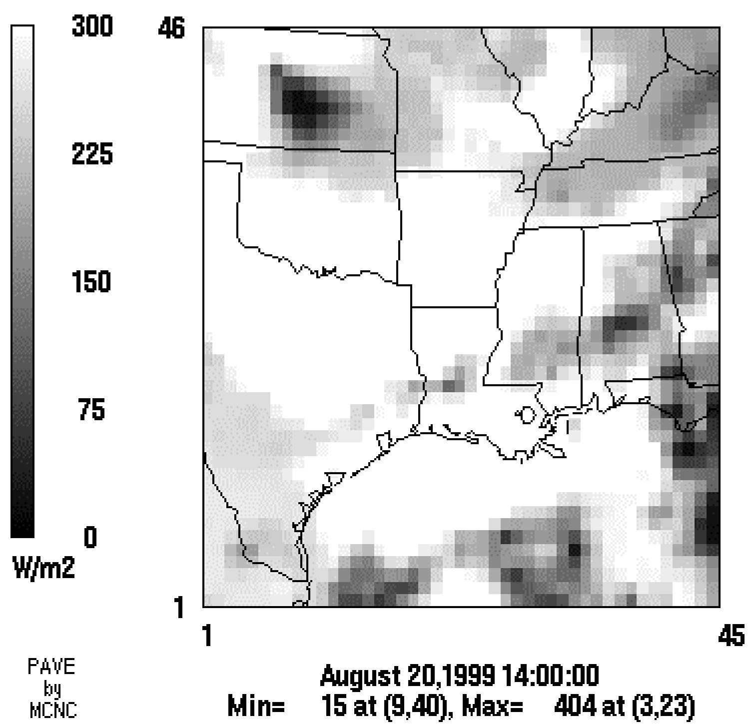


**Figure D-3.** MM5-derived cloud optical depth and satellite-derived PAR on the CAMx 36-km domain on 1300 CST August 20, 1999.

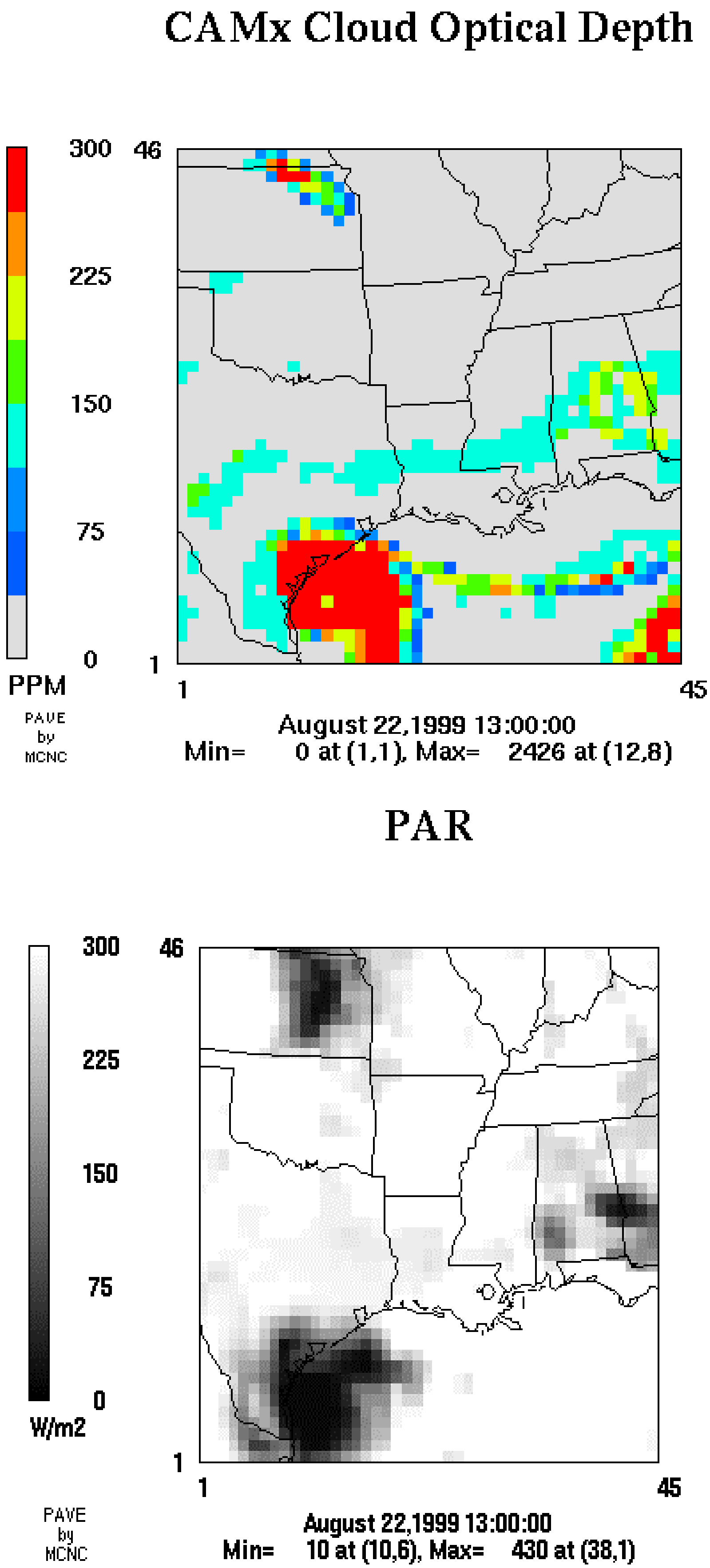


**Figure D-4.** MM5-derived cloud optical depth and satellite-derived PAR on the CAMx 36-km domain on 1300 CST August 22, 1999.